

Attention is drawn to the fact that the copyright of this thesis rests with its author.

This copy of the thesis has been supplied on condition that anyone who consults it is understood to recognise that its copyright rests with its author and that no quotation from the thesis and no information derived from it may be published without the author's prior written consent.

II

Δ 44154/82.

V/ADI N.M.A.

ps

277

434

THE PREPARATION, METAL BINDING ABILITY
AND CATALYTIC ACTIVITY OF POLY ITACONATE COPOLYMERS
WITH PENDANT ETHYLENE AMINE GROUPS

A thesis submitted to the
University of Stirling
for the degree of
Doctor of Philosophy

N M A WADI

Department of Chemistry
April 1982

Graduation - June 1982

ACKNOWLEDGEMENTS

I wish to thank most sincerely my supervisor, Professor J M G Cowie, for his advice, guidance and encouragement.

I also wish to thank all the members of the academic and technical staff in the department for all their help, particularly to Dr I J McEwen for the many stimulating and rewarding discussions in polymer science, to Mr T Forrest for his assistance with the electron microscopy, to Mr G Castle for indefatigably supplying me with liquid and gaseous nitrogen and to Mrs P Brown for a beautifully typed thesis.

Finally, I wish to thank the members of the polymer group at Glasgow University for providing the facilities for thermal volatilization studies.

PREFACE

This thesis is submitted for the degree of Doctor of Philosophy at the University of Stirling, having been submitted for no other degree. It is a record of research undertaken in the Department of Chemistry from February 1979 to March 1982. This work is wholly original except where due reference is made.

N M A Wadi

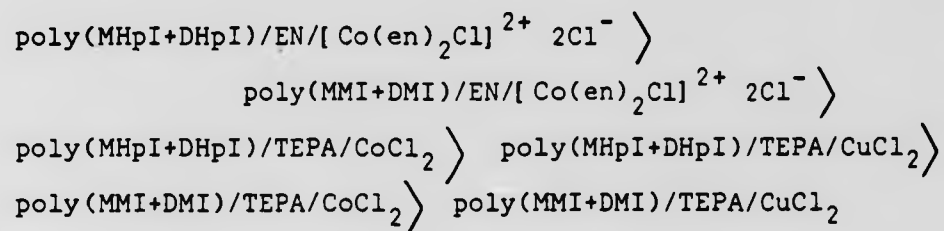
N M A WADI

ABSTRACT

A polymeranalogous reaction in homogeneous medium was carried out to prepare poly itaconate copolymers with pendant ethylene imine groups. Three copolymers, poly(MHpI+DHpI), poly(MBI+DBI) and poly(MMI+DMI) were prepared, characterised and their composition analysed. The acid groups in the monoesters were reacted with ethylenediamine, diethylenetriamine, triethylenetetramine or tetraethylenepentamine in the presence of dicyclohexylcarbodiimide.

Two types of polymer-metal complexes, polymer chelates and pendant-type polymer-metal complexes were prepared. The complexation between the polymeric ligands and cobalt(II) chloride or copper(II) chloride was studied by visible spectroscopy. The electron microscopy study of these polymer-metal complexes shows that the size and the number of the metal ion clusters increases proportionally with the mole percentage of the metal ions.

The catalytic activity of the polymer-metal complexes on the decomposition of hydrogen peroxide has been studied. Graphical and mathematical methods were used to show and compare the catalytic activity of these polymer-metal complexes. It was found that the catalyst efficiencies were in the decreasing order of:



The thermal stability of these modified polymers and polymer-metal complexes confirms that degradation was a random chain scission process and that the thermal stability of the polymer-metal complexes were higher than the polymeric ligands due to crosslinking.

The viscoelasticity study shows that the modulus in the rubbery region increases when the mole percentage of the pendant ethylene amine group was less than 6.3. The glass transition temperature increases and becomes broader and ill-defined as the mole percentage of pendant ethylene amine group increases due to enhanced intermolecular interactions in the system.

CONTENTS

	<u>Page</u>
CHAPTER ONE INTRODUCTION	
1.1 Itaconic acid	1
1.2 Esters of itaconic acid	3
1.3 Homopolymerization and copolymerization of itaconic acid	3
1.4 Homopolymerization and copolymerization of itaconic acid esters	4
1.5 Polymer reactions	7
CHAPTER TWO POLYMER REACTIONS, COMPLEXATION AND PROPERTIES	
2.1 Chemical reactions of polymers	9
2.2 Classification of polymer reactions	9
2.3 Polymeranalogous reactions	10
2.4 Polymer metal complexes	14
2.5 Classification of polymer-metal complexes	16
2.6 Reactions catalysed by polymer-metal complexes	18
2.7 Viscoelastic behaviour	20
2.8 Thermal degradation	22
CHAPTER THREE EXPERIMENTAL	
3.1 Synthesis of monomers	27
3.2 Bulk copolymerization	31
3.3 Copolymerization of mono- and diesters of itaconic acid	32
3.4 Reaction with amines	32
3.5 Reaction with metal halides	44

CONTENTS (cont'd)

	<u>Page</u>
3.6 Reaction with <u>trans</u> [Co(en) ₂ Cl ₂]Cl	49
3.7 Determination of the composition of the copolymers	52
3.8 Decomposition of hydrogen peroxide	54
3.9 Infrared analysis	57
3.10 Visible spectrophotometer	58
3.11 Electron microscopy	60
3.12 Membrane osmometry	62
3.13 Differential scanning calorimetry	65
3.14 Rheovibron	68
3.15 Torsional braid analysis	72
3.16 Thermogravimetric analysis	77
3.17 Thermal volatilization analysis	78
 CHAPTER FOUR PREPARATION OF MONOMERS, COPOLYMERS AND MODIFIED POLYMERS	
4.1 The preparation of monomers	80
4.2 Discussion	81
4.3 Copolymerization and composition of copolymers	83
4.4 Composition of the copolymers	84
4.5 Microanalysis	86
4.6 The preparation of itaconate copolymers with pendant ethylene amine groups	87
 CHAPTER FIVE ION BINDING	
5.1 Metal ion binding	92
5.2 Polymer-metal complexes	92
5.3 Visible spectrophotometry results	99

CONTENTS (Cont'd)

	<u>Page</u>
5.4 Discussion	102
5.5 Electron microscopy results	104
5.6 Discussion	104
 CHAPTER SIX CATALYTIC ACTIVITY	
6.1 Catalytic activity	106
6.2 Results of decomposition of hydrogen peroxide	106
6.3 Discussion	110
6.4 Determination of the rate constant (k)	117
6.5 Discussion	122
 CHAPTER SEVEN VISCOELASTIC STUDIES	
7.1 DSC and TBA analysis	123
7.2 DSC results	124
7.3 Discussion	125
7.4 TBA results	126
7.5 Discussion	127
7.6 DSC results for the modified polymers	129
7.7 Discussion	129
7.8 TBA results for the modified polymers	131
7.9 Discussion	132
7.10 Viscoelasticity	134
7.11 The viscoelastic behaviour of the modified polymers	134
7.12 Discussion	138

CONTENTS (Cont'd)

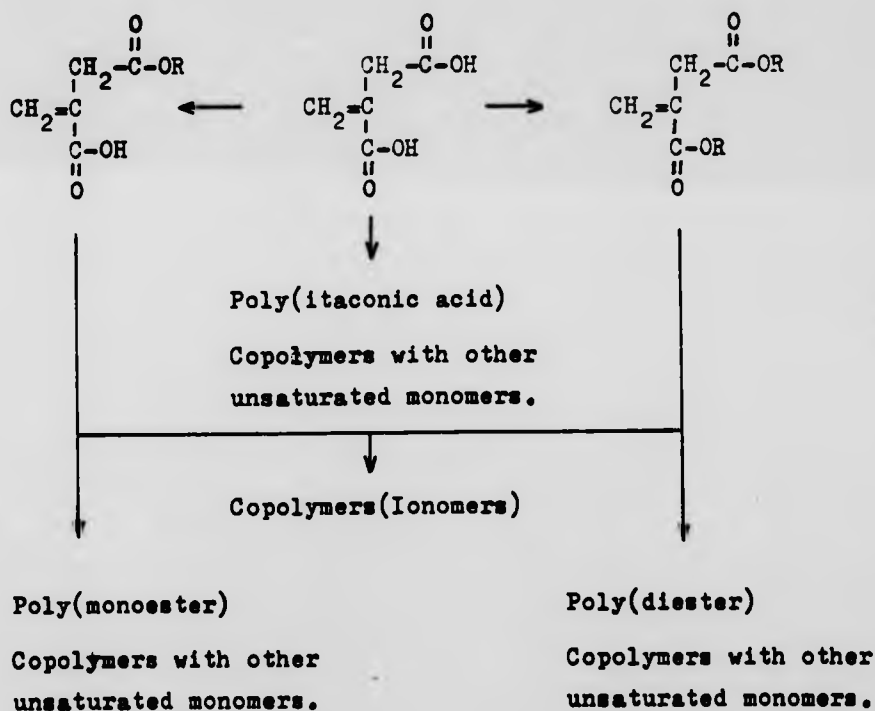
	<u>Page</u>
7.13 The viscoelastic behaviour of polymer-metal complexes	139
7.14 Discussion	140
 CHAPTER EIGHT THERMAL STABILITY	
8.1 Thermal stability studies	142
8.2 Interpretation of TVA trace	142
8.3 Results of TVA studies	144
8.4 Results of TVA of modified polymers	146
8.5 Discussion	148
8.6 TVA result for the polymer-metal complex	150
8.7 Thermogravimetric analysis	152
8.8 TGA results for the parent polymers	152
8.9 Discussion	153
8.10 TGA results of the modified polymers	154
8.11 Discussion	155
8.12 TGA results of polymer-metal complexes	155
8.13 Discussion	156
 CHAPTER NINE GENERAL CONCLUSIONS	
	157
 REFERENCES	
	164
 APPENDIX	
	171

CONTENTS
CHAPTER ONE
CHAPTER TWO
CHAPTER THREE
CHAPTER FOUR
CHAPTER FIVE
CHAPTER SIX
CHAPTER SEVEN
CHAPTER EIGHT
CHAPTER NINE
CHAPTER TEN
CHAPTER ELEVEN
CHAPTER TWELVE
CHAPTER THIRTEEN
CHAPTER FOURTEEN
CHAPTER FIFTEEN
CHAPTER SIXTEEN
CHAPTER SEVENTEEN
CHAPTER EIGHTEEN
CHAPTER NINETEEN
CHAPTER TWENTY
CHAPTER TWENTY-ONE
CHAPTER TWENTY-TWO
CHAPTER TWENTY-THREE
CHAPTER TWENTY-FOUR
CHAPTER TWENTY-FIVE
CHAPTER TWENTY-SIX
CHAPTER TWENTY-SEVEN
CHAPTER TWENTY-EIGHT
CHAPTER TWENTY-NINE
CHAPTER THIRTY
CHAPTER THIRTY-ONE
CHAPTER THIRTY-TWO
CHAPTER THIRTY-THREE
CHAPTER THIRTY-FOUR
CHAPTER THIRTY-FIVE
CHAPTER THIRTY-SIX
CHAPTER THIRTY-SEVEN
CHAPTER THIRTY-EIGHT
CHAPTER THIRTY-NINE
CHAPTER FORTY
CHAPTER FORTY-ONE
CHAPTER FORTY-TWO
CHAPTER FORTY-THREE
CHAPTER FORTY-FOUR
CHAPTER FORTY-FIVE
CHAPTER FORTY-SIX
CHAPTER FORTY-SEVEN
CHAPTER FORTY-EIGHT
CHAPTER FORTY-NINE
CHAPTER FIFTY
CHAPTER FIFTY-ONE
CHAPTER FIFTY-TWO
CHAPTER FIFTY-THREE
CHAPTER FIFTY-FOUR
CHAPTER FIFTY-FIVE
CHAPTER FIFTY-SIX
CHAPTER FIFTY-SEVEN
CHAPTER FIFTY-EIGHT
CHAPTER FIFTY-NINE
CHAPTER SIXTY
CHAPTER SIXTY-ONE
CHAPTER SIXTY-TWO
CHAPTER SIXTY-THREE
CHAPTER SIXTY-FOUR
CHAPTER SIXTY-FIVE
CHAPTER SIXTY-SIX
CHAPTER SIXTY-SEVEN
CHAPTER SIXTY-EIGHT
CHAPTER SIXTY-NINE
CHAPTER SEVENTY
CHAPTER SEVENTY-ONE
CHAPTER SEVENTY-TWO
CHAPTER SEVENTY-THREE
CHAPTER SEVENTY-FOUR
CHAPTER SEVENTY-FIVE
CHAPTER SEVENTY-SIX
CHAPTER SEVENTY-SEVEN
CHAPTER SEVENTY-EIGHT
CHAPTER SEVENTY-NINE
CHAPTER EIGHTY
CHAPTER EIGHTY-ONE
CHAPTER EIGHTY-TWO
CHAPTER EIGHTY-THREE
CHAPTER EIGHTY-FOUR
CHAPTER EIGHTY-FIVE
CHAPTER EIGHTY-SIX
CHAPTER EIGHTY-SEVEN
CHAPTER EIGHTY-EIGHT
CHAPTER EIGHTY-NINE
CHAPTER NINETY
CHAPTER NINETY-ONE
CHAPTER NINETY-TWO
CHAPTER NINETY-THREE
CHAPTER NINETY-FOUR
CHAPTER NINETY-FIVE
CHAPTER NINETY-SIX
CHAPTER NINETY-SEVEN
CHAPTER NINETY-EIGHT
CHAPTER NINETY-NINE
APPENDIX A
APPENDIX B
APPENDIX C
APPENDIX D
APPENDIX E
APPENDIX F
APPENDIX G
APPENDIX H
APPENDIX I
APPENDIX J
APPENDIX K
APPENDIX L
APPENDIX M
APPENDIX N
APPENDIX O
APPENDIX P
APPENDIX Q
APPENDIX R
APPENDIX S
APPENDIX T
APPENDIX U
APPENDIX V
APPENDIX W
APPENDIX X
APPENDIX Y
APPENDIX Z
INDEX
BIBLIOGRAPHY
GLOSSARY
NOTES
REFERENCES

CHAPTER ONE
I N T R O D U C T I O N

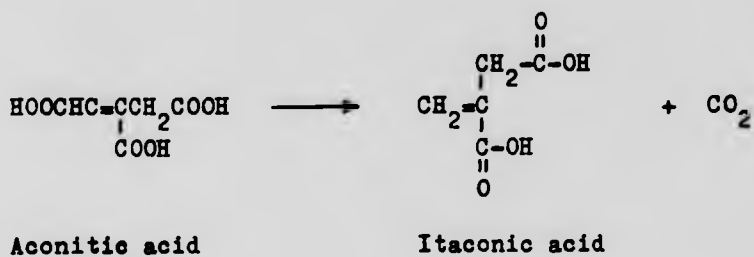
1.1 ITACONIC ACID

Itaconic acid (methylene butanedioic acid), $\text{CH}_2=\text{C}(\text{COOH})\text{CH}_2\text{COOH}$ is an unsaturated dicarboxylic acid. The trifunctionality and readily renewable source of this acid leads to considerable technical application as a comonomer and a polymerisable mono- and diester.



Itaconic acid was first isolated from the pyrolysis of citric acid by Baup¹ in 1836, who characterised this acid by measuring its solubility and melting point. An alternative method for the preparation of itaconic acid from naturally occurring material, based on the decarboxylation of aconitic acid, was reported by Crasso² who also invented

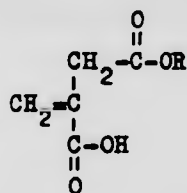
the trivial name itaconic acid as an anagram of the source.



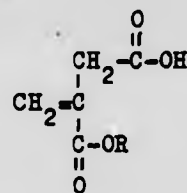
Kinoshita³ in 1929 was the first to identify itaconic acid as a metabolic product of the fermentation of sugar. He isolated a fungus, Aspergillus Itaconicus, from the vinegar made from the juice of Japanese sour plums, which was capable of fermenting sugar to itaconic acid. Smith⁴ in 1935 isolated a strain of Aspergillus Terreus from American cotton yarn and this micro-organism was later found to be a better producer of itaconic acid⁵. Methods have now been developed which lead to high yields of itaconic acid. A less expensive nutrient such as beet or sugar cane molasses was used to lower the cost and the Pfizer Chemical Company developed a large scale fermentation process using Aspergillus Terreus with molasses, which has become commercially viable⁶. The production of itaconic acid from the decarboxylation of alkaline earth aconitates (preferably calcium aconitate) extracted from molasses has been described⁷.

1.2 ESTERS OF ITACONIC ACID

Swarts⁸ in 1876 was the first to report the esterification of itaconic acid. Messina et al⁹ described a method of preparing both dimethyl and monomethyl itaconate from a mixture of itaconic acid and methanol (1:1 mole ratio). Baker et al¹⁰ described how to prepare monoesters under mild conditions in good yields and also established the structure of the monoester as the 4-alkyl itaconate (I) not the 1-alkyl itaconate (II).



(I)



(II)

The simple diesters are prepared by an acid catalysed process in excess of alcohol¹¹.

1.3 HOMOPOLYMERIZATION AND COPOLYMERIZATION OF ITACONIC ACID

It was originally believed that itaconic acid could not be homopolymerized successfully but in 1958 Marvel and Shepherd¹² reported that itaconic acid undergoes homopolymerization in 0.5M hydrochloric acid using potassium persulphate as an initiator at 323K for 48 hours. Subsequently, Nagai and Yoshida¹³ found that itaconic acid

homopolymerizes at 323K with potassium persulphate at various levels of acidity. Poly(itaconic acid) can also be prepared by hydrolysing poly(itaconic anhydride) with water^{14,15}. The structure and the decarboxylation of poly(itaconic acid) has been studied by a number of workers^{16,17} but it is the incorporation of itaconic acid into copolymers which has proved of greater interest than homopolymerization. Copolymerization of itaconic acid with certain unsaturated monomers will give higher molecular weight polymers containing a primary carboxyl group. Copolymers of styrene, ethyl methacrylate and methyl methacrylate with itaconic acid have been prepared and the reactivity ratios of these monomers with itaconic acid have been established¹⁸. Copolymers of aconitic acid, butadiene, acrylonitrile, and acrylamide incorporating up to 30% of itaconic acid, have been prepared⁶. These copolymers find considerable use in the fibre, coating (for film used particularly in packing) and adhesive industries.

1.4 HOMOPOLYMERIZATION AND COPOLYMERIZATION OF ITACONIC ACID ESTERS

It has been noticed that diethyl itaconate, on standing for several years, will form a transparent hard solid. Stobe and Lippold¹⁹ have described what happens when diethyl itaconate is exposed to sunlight; they noticed that a viscous liquid was formed after 65 days and

a brittle glass-like solid was formed after 103 days. Walden²⁰ found that di-n-amyl itaconate formed a glass-like polymer and recorded a change in the optical rotation during polymerization. Knops²¹ reported the polymerization of dimethyl itaconate. The homopolymerization of dimethyl, diethyl, and dibutyl itaconates by solution polymerization and the bulk polymerization of dimethyl, diethyl, di-n-propyl, and di-n-octyl itaconates at 323K using α, α' -azobis-isobutyronitrile (AIBN) as an initiator have been described²². Tate²³, in 1967, studied the kinetics of the polymerization and copolymerization of itaconic acid and some of its esters. He found that the rate of polymerization of itaconic esters was slower and the molecular weight lower than the corresponding methacrylic or acrylic esters. He also found that the rate of polymerization of dimethyl itaconate in dioxane was greater than that of monobutyl itaconate, whilst in benzene, monobutyl itaconate was faster. In bulk, monobutyl itaconate polymerizes at least six times faster than dimethyl itaconate due to the greater viscosity of the monobutyl itaconate. A high molecular weight poly(dimethyl itaconate) was obtained by polymerization of the monomer by γ -irradiation at a temperature where dimethyl itaconate does not polymerize thermally²⁴.

The hydrodynamic properties of some of the poly-(itaconic acid esters) have been studied by Velickovic et al²⁵. The refractive index increment and the Kuhn-Mark-Houwink-Sakurada relationship for poly dimethyl, diethyl,

di-n-propyl, di-n-butyl, di-n-hexyl, di-n-octyl, di-n-decyl and di-n-undecyl itaconates were established in toluene at 298K.

Dicyclohexyl itaconate was polymerized by bulk polymerization and the Kuhn-Mark-Houwink-Sakurada relationship and solubility parameters have been established²⁶. A series of poly(mono-n-alkyl itaconic acid esters) with ester chain lengths ranging from methyl to decyl were prepared by emulsion polymerization and their thermal stability was also studied^{27,28}. Cowie et al²⁹ in 1977, reported the polymerization of a series of diesters with ester chain lengths ranging from methyl to hexyl by both bulk and emulsion polymerization. They studied the thermomechanical, thermostability and other related properties and found that as the ester side chain increased in length the glass transition decreased. Two glass transition temperatures have been observed for di-n-alkyl itaconic acid esters of chain length from heptyl to undecyl due to the independent cooperative relaxation of the alkyl side chain³⁰. Esters with chain lengths of more than eleven carbon atoms display a melting temperature due to crystallization³¹. Poly(itaconic acid esters) containing phenyl and cyclohexyl rings have been synthesised and it was found that the glass transition of the phenyl derivative is lower than the corresponding cyclohexyl derivative^{32,33}.

Tate¹⁸ studied the copolymerization of some dialkyl itaconates with styrene, acrylic acid, and vinyl chloride. He found that lower dialkyl itaconates can undergo ideal

copolymerization. Boudevska et al³⁴ studied the copolymerization of monomethyl itaconate and monobutyl itaconate, and established the reactivity ratios of the copolymer system. Copolymerization of monobutyl itaconate and dibutyl itaconate and their hydrodynamic properties have been studied³⁵. Cowie et al^{36,37} reported the preparation, characterization and thermomechanical properties of six series of copolymers based on mono and dialkyl itaconate.

Ionomers based on copolymers of mono and dialkyl itaconates have been prepared and it was observed that tough, non-tacky materials were obtained after salt formation, due to the ionic crosslinking in the matrix³⁸.

1.5 POLYMER REACTIONS

One of the most rapidly growing areas in modern polymer science is the study of the reactions of macromolecules. Modification of natural and synthetic polymers can be achieved by chemical reaction of the functional group of the polymer.

Marvel and Shepherd¹² reported the reduction of poly(dimethyl itaconate) to poly(2-hydroxyethyl allyl alcohol) using lithium hydride. Poly(dimethyl itaconate) has been prepared from poly(itaconic acid) by the action of diazomethane¹⁵. Yokota et al¹⁵ have described the preparation of poly(dimethyl itaconate) by the esterification

of poly(itaconic acid). Poly(itaconic acid dihydrazide) was prepared by heating poly(itaconic acid) with hydrazine hydrate in boiling water and was found to react with aldehydes or ketones to form polymeric hydrazones³⁹.

The main interest in these polymer reactions was as an alternative synthetic route, and method for characterization.

The aim of the present study is, therefore, to modify polymer based esters of itaconic acid and to study the thermomechanical and other related properties of these modified polymers.

CHAPTER TWO
POLYMER REACTIONS, COMPLEXATION, AND PROPERTIES

2.1 CHEMICAL REACTIONS OF POLYMERS

The term "polymer reaction" encompasses the study of the chemical reactions of an active pendant group on the polymer chain with another polymer or reagent, or a transformation caused by some form of energy, such as radiation or heat. In industry the term "polymer modification" is used to describe changes wrought on the polymer by a manufacturing operation separate from the final moulding, spinning, or formation process which is essential for the production of a useful end product. Chemical modifications of cellulose⁴⁰ and natural rubber⁴¹ have been investigated intensively. Chemical reactions involving vinyl polymers such as hydrolysis of poly(vinyl acetate) to poly(vinyl alcohol), chlorination of poly(ethylene), and sulphonation of poly(styrene) have been applied industrially⁴². The availability and the new chemical and physical properties of the modified polymer, along with economic factors, justify the importance of the polymer modification. Some of these modified polymers have found many applications as catalysts, chelating agents, ion exchangers, reagents for organic synthesis or as analytical methods to characterise the parent polymer^{43,44}.

2.2 CLASSIFICATION OF POLYMER REACTIONS

The reactions of functional groups in polymers can be

divided into two types. The first type is the reaction of the functional group of a polymer with a low molecular weight reagent which is called a "polymeranalogous reaction". The second type is the reaction between the same functional groups in the polymer and is called an "intramolecular reaction".

2.3 POLYMERANALOGOUS REACTIONS

In the case of polymeranalogous reactions it can be assumed that the reactivity of the functional group in a small organic molecule is the same as that of the same group in a polymer chain⁴⁵, but it has been found that the reactivity of functional groups of polymers may be different from that of the low molecular analogues⁴⁶; this is because of the polymer environment. It has been found that reaction rates and conversions are often lower than those of a small organic molecule, but higher reaction rates and conversions are also found in some reactions. Polymer-analogous reactions will occur if the factors which inhibit the reactivity of the functional group are minimised. This means that polymeranalogous reactions will be affected by certain factors arising from the chain structure of the polymer.

2.3.1 THE EFFECT OF NEIGHBOURING GROUPS

The functional group reactivity is independent of the size of the molecule but is dependent on the neighbouring group which is a fundamental feature of a polymer chain⁴⁷. The reactivity of the functional groups attached to the polymer chain will be affected by the neighbouring group and the kinetics and mechanism of the reaction will change due to the interaction of two neighbouring functional groups. A reacted functional group in a polymer chain alters the reactivity of its neighbouring unreacted groups, and the reactivity of a given functional group depends upon whether or not the neighbouring groups have already reacted. One should bear in mind that there are theoretical and mathematical methods now available to describe quantitatively the kinetics of such reactions⁴⁸. The neighbouring group effect can be due to electrostatic interactions between adjacent groups and may lead to inhibition or enhancement of the reaction rates. This effect can be demonstrated by studying the poly(methyl methacrylate) ester hydrolysis⁴⁹. Poly(methyl methacrylate) (syndiotactic) hydrolyses faster than poly(methyl methacrylate) (isotactic) because poly(methyl methacrylate) (isotactic) has neighbouring functional groups in the optimum position for interaction with each other to form the cyclic anhydride intermediate. In many cases the reactivity of an "A" function to yield a "B" function is decreased when the neighbouring groups have already reacted.

This may be due to repelling charges or interaction or even to steric factors.

In conclusion the reactivity of functional groups does not depend on the molecular size but on the nature of the neighbouring groups.

2.3.2 THE EFFECT OF MORPHOLOGY

Morphology is the study of structure in polymers on a macroscale. Polymers which are chemically identical but differ in physical structure exhibit differences in reactivity due to steric hindrance⁴⁰. This is the effect of morphology on the polymer functional groups reactivity and one has to understand the way that a functional group is attached to the polymer main chain. In principle, the functional groups may be⁵⁰:

- (a) Linked to the polymer main chain as a pendant group either directly or with the spacer group of specific length as shown below

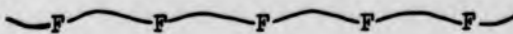


Functional group directly attached to the polymer main chain.



Functional group attached with spacer to the polymer main chain.

- (b) part of the main chain randomly distributed as shown below



- (c) at the end of a low molecular weight polymer chain



These polymers with functional groups can be prepared by replacing an existing group in the high molecular weight polymer with the desired functional group. However, side reactions may lead to chain scission or, in some cases, to cross linking, thus changing the solubility of the starting material and the final reaction product⁵⁰. This may require different reaction conditions to be adopted. Such polymers are active because they contain active centres; these may be hydroxyl or carboxyl groups, halogen atoms, multiple valence bond etc, and the electron cloud distribution surrounding the atoms of the group has a great effect, as do the various induced dipole effects. These influence the chemical reactivity and because the polymer chain contains more than one functional group, steric hindrance may also play a part. This steric hindrance does not arise from any of the above electronic influences but is predominantly physical⁴⁰, and the functional group cannot be reached by the reactants because of the number,

size and close proximity of the other substituents on the molecule. The morphological effect on the reactivity is most frequent and most pronounced in linear semi-crystalline polymers⁴⁰. Only the functional groups in the amorphous region will be available for reaction if the reactions are carried out under conditions such that a portion of the polymer remains crystalline. This is because the functional groups in the crystalline regions will generally be inaccessible to chemical reagents.

In conclusion, one can define a polymeranalogous reaction as the reaction of functional groups with reactants of low molecular weight under conditions minimizing the possibility of exhibiting any of the polymer effects described above. The reaction should best be carried out under homogeneous conditions in a dilute solution with an excess of low molecular weight reactant.

2.4 POLYMER-METAL COMPLEXES

A polymer-metal complex is defined as a complex composed of a polymer ligand and metal ions in which the metal ions are attached to the polymer ligand by a coordinate bond. The polymer ligand containing coordination groups or atoms, (mainly nitrogen, oxygen and sulphur), can be obtained in two ways. The first method is by chemical reaction between a polymer and a low molecular weight

compound having coordinating ability⁵¹. The second method is polymerization of a monomeric metal complex containing a vinyl group, but these monomeric metal complexes are very difficult to prepare⁵². When a monomeric metal complex polymerizes it will give a uniform structure. In the case of the synthetic polymer-metal complexes prepared by mixing polymeric ligand and metal ions, a uniform structure can be obtained if (i) the structures of the complex units existing in the polymer chain are identical in composition and configuration, (ii) the primary structure of the polymer chain or the polymeric ligand is well defined. It is easier to obtain a uniform structure from polymerization of a monomeric metal complex containing a vinyl group than by mixing a polymeric ligand with metal ions.

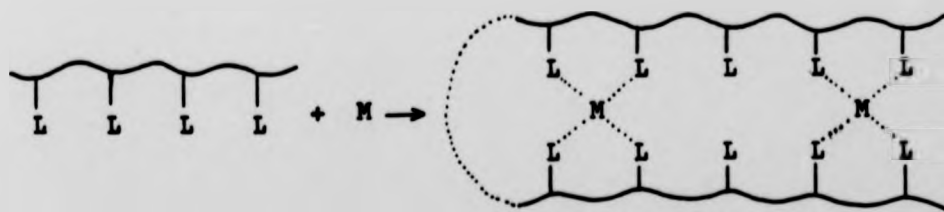
The metal complex bound to the polymer may show a specific type of catalytic behaviour⁵³. Detailed information about the reactivity or catalytic activity can be obtained by studying the structure of these polymeric metal complexes. Many polymer-metal complexes have been reported and have found a wide variety of applications. The study of the thermostability, semiconductivity, clustering of metal ions, biomedical effects, and catalytic activity of polymer-metal complexes has attracted considerable interest in recent years.

2.5 CLASSIFICATION OF POLYMER-METAL COMPLEXES

When a monomeric metal complex containing a vinyl group polymerizes, or a polymeric ligand which contains coordinating groups or atoms is mixed with metal ions, a polymer metal complex will be formed. These polymer-metal complexes can be divided into the two main types⁵⁴ outlined below.

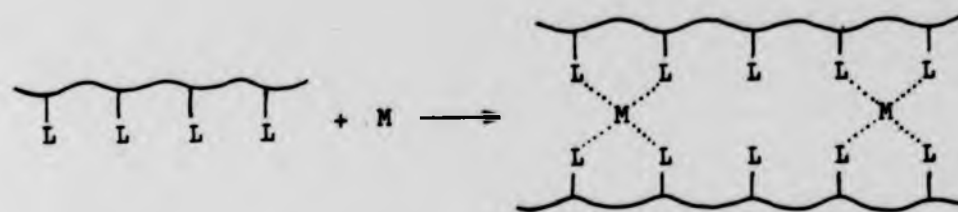
2.5.1 Chelating polymers

When a polymeric ligand containing coordinating groups or atoms is mixed directly with a metal ion which has four or six coordinate bonding sites, a polymer-metal complex will be formed. This polymer-metal complex can be either an intra-polymer chelate or an inter-polymer chelate^{55,56}. Intra-polymer chelates can be represented by Scheme I.



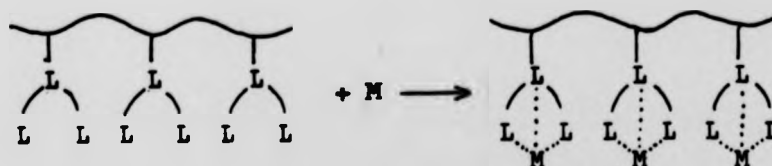
Scheme I

Inter-polymer chelates can be represented in Scheme II



Scheme II

Another type of chelating polymer is formed when a polymer containing a multidentate ligand such as ethylenediamine or aminocarboxylic acid is mixed with a metal ion⁵⁷. Although these chelating polymers take up almost all transition metal ions in high yield, they are not particularly selective towards any metal ion. Scheme III represents this type of chelating polymer.



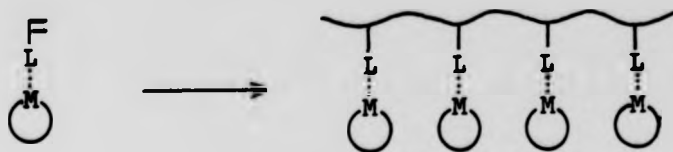
Scheme III

2.5.2 The pendant-type polymer-metal complex.

The pendant-type polymer-metal complex can be prepared by two methods:

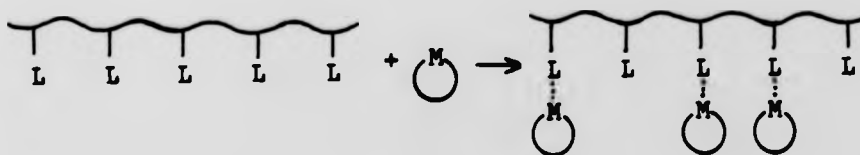
- (i) When a monomeric metal complex containing a vinyl-

group polymerizes⁵², a pendant-type polymer-metal complex with uniform structure will be formed and this is represented in Scheme IV.



Scheme IV

(ii) When a polymer ligand reacts with a stable metal complex which has one coordination site vacant, a pendant polymer-metal complex will be formed⁵⁸. This type is represented in Scheme V.



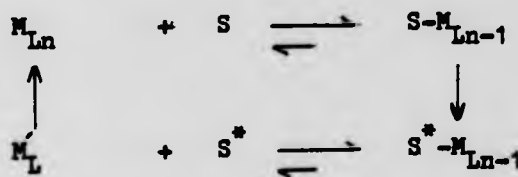
Scheme V

2.6 REACTIONS CATALYSED BY POLYMER-METAL COMPLEXES

Metal complexes catalyse many organic reactions and they have significant importance in the modern petrochemical industry. It is clear that without the use of catalysts many major industrial processes would be uneconomic. Many polymers have been used as supports for some metal complexes

which have catalytic activity to specific organic reactions⁵⁹.

The cycle of a metal complex in the catalysis of a chemical reaction is shown in Scheme VI⁵⁴.



Scheme VI

Where M is the metal ion, L is the ligand, and S is the substrate. In the first step there is the formation of an intermediate (mixed complex LMS) and this will be formed when a substrate S coordinates to a metal catalyst. In the second step the substrate is activated by the metal ion. The third step is the dissociation of the new substrate from the catalyst. The fourth step will be the regeneration of the complex catalyst to the original metal complex after it has accomplished its purpose. The catalytic activity of polymer-metal complexes depends on the nature of the ligand. Some of these ligands inhibit the catalytic activity of the metal ion, others will reduce or increase the catalytic activity⁶⁰.

In this work the catalytic activity of polymeric chelates containing copper(II) or cobalt(III) as metal ion, and the pendant-type polymer-metal complexes containing cobalt(III) as metal ion has been studied. This involves

a comparison of the catalytic activity of polymers with and without metal ions on the decomposition of hydrogen peroxide.

2.7 VISCOELASTIC BEHAVIOUR

An amorphous polymer can be defined as a polymer in which no long-range order over an extensive region occurs and the distribution of the polymer chains in the matrix is completely random. The term "viscoelastic" is used to describe the behaviour of polymeric materials which exhibit the characteristics of both solid and liquid⁶¹. In an amorphous polymer, as the temperature increases, the molecular motions become more and more large-scale until eventually it becomes molten⁶². Typical linear amorphous polymers can have five distinguishable viscoelastic regions. These regions are easily displayed if a parameter such as the elastic modulus, which is a useful parameter to use in characterising polymeric behaviour, is measured over a range of temperatures. The modulus-temperature curve for a typical linear and crossed lined amorphous polymer is shown in Figure 2.1.

(i) The glassy region.

In the glassy region, the cooperative motion along with the chain is frozen and the thermal energy is

insufficient to surmount the potential energy barriers for rotational and translational motion. The polymer responds to strain like an elastic solid and the elastic modulus is normally found to lie between $10^{9.5}$ and 10^9 Nm^{-2} .

(ii) The leathery (or transition) region.

This is the region where the modulus is rapidly falling from about 10^9 to $10^{5.7} \text{ Nm}^{-2}$. The molecular motion becomes greater as the temperature rises and the thermal energy becomes roughly comparable to the potential energy barriers for segment rotation and translation. In this region the glass transition temperature (which is the characteristic temperature at which a rubber-like amorphous polymer becomes glass-like and vice versa) is located⁶².

(iii) The rubbery region.

In the rubbery region the long range co-operative motion will be restricted by the presence of strong local interactions between neighbouring chains in a polymer. Because of this the modulus curve begins to flatten and maintain an approximately constant value from $10^{5.7}$ to $10^{5.4} \text{ Nm}^{-2}$. A linear and lightly crosslinked polymer will show identical viscoelastic responses but as the temperature increases the crosslinked network which is formed by covalent bonding⁶¹ will maintain the plateau modulus as indicated by the broken line in Figure 2.1.

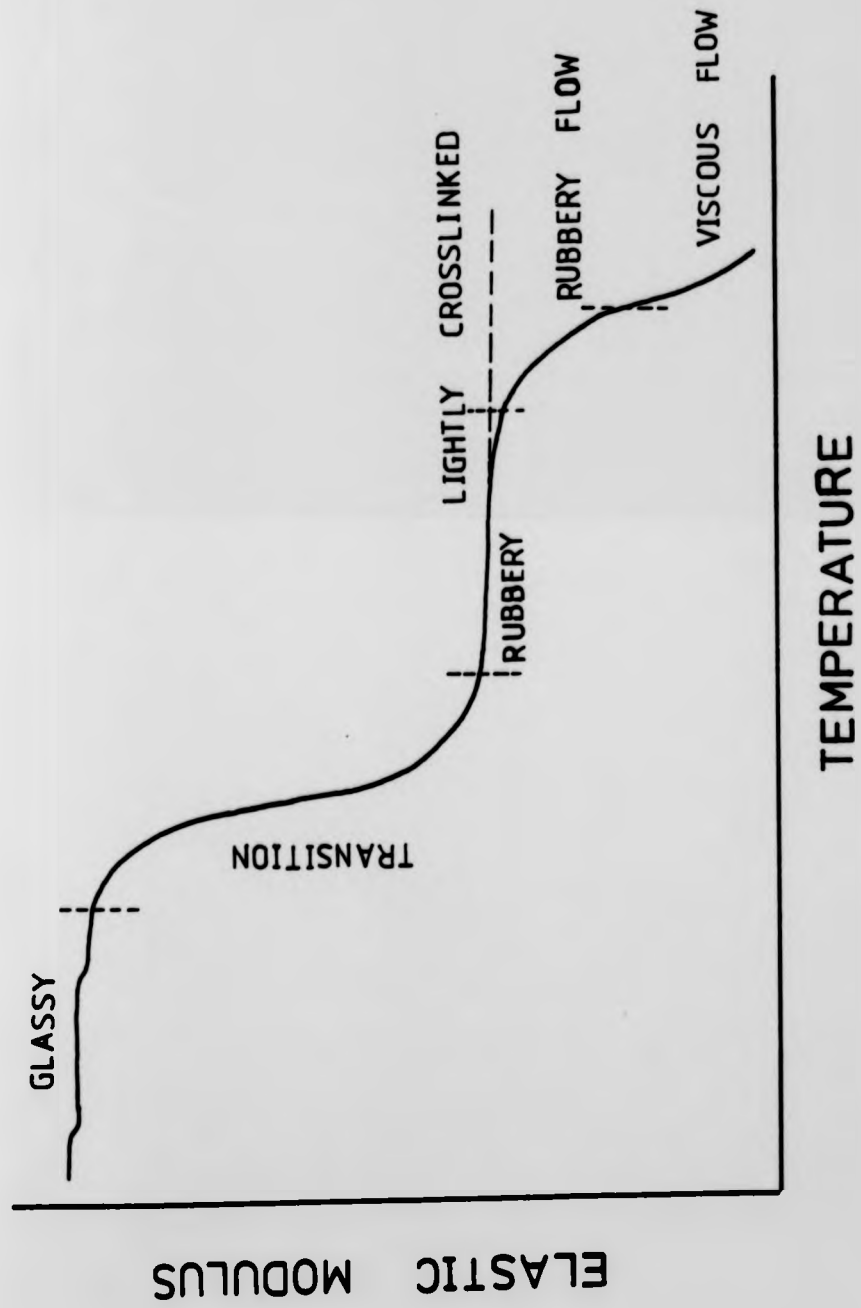


Fig. 2.1 Idealized Modulus-Temperature Curve Showing Various Regions of Viscoelastic Behaviour.

(iv) Rubbery flow region.

In this region the modulus decreases from $10^{5.4}$ to $10^{4.5} \text{ Nm}^{-2}$ and the elastic recovery begins to decrease. This means that the sample will not recover its former length but will relax to a new equilibrium state.

(v) The viscous flow region.

If the temperature increases, local chain interactions no longer have sufficient energy to prevent molecular flow. In this region there is little evidence of any elastic recovery and the modulus decreases from $10^{4.5}$ and continues to decrease. The sample will become a viscous liquid.

2.8 THERMAL DEGRADATION

Thermal degradation of polymers can often be defined by the amount of weight lost by a polymer as a function of temperature in a particular environment⁶³. A comparison of the thermal stability of a set of polymers can be made if one can establish a stability criterion for that set under the same experimental conditions. Because significant property changes can occur without noticeable weight changes great caution must be exercised in drawing conclusions concerning the apparent chemical ramification that the data may suggest.

There are two reasons why polymers degrade; firstly because they are reactive and secondly because they are unstable⁶⁴. To understand the mechanism of polymer

degradation one can study the reaction of low molecular weight analogues. The degradation of high molecular weight polymers can be categorized as affecting the side chain of the polymer or the backbone of the polymer. In some polymer degradations the bonds in the polymer chain break at random⁶³. Other polymers degrade by chain depolymerization and the original monomer is formed which, in some cases, can be recovered in good yield and high purity⁶⁵. Most of the polymers suffer chain cleavage and elimination of a low molecular weight by-product, thereby producing a highly unsaturated carbonaceous residue which is called a char⁶⁴. In thermal degradation there are three regions which can be seen in a normal thermogram⁶³. The first region is the temperature at which gradual degradation commences. Maximum rate of volatilization of degradation product occurs in the second region. The third region is the temperature at which 50% of the polymer remains. The second region often coincides with the third region.

CHAPTER THREE

EXPERIMENTAL

The following abbreviations were used in this chapter:

<u>Abbreviated Name</u>	<u>Detail</u>
Sample No 1	Poly(MHpI+DHpI), mole % of MHpI 0.29
Sample No 2	Poly(MHpI+DHpI), mole % of MHpI 1.42
Sample No 3	Poly(MHpI+DHpI), mole % of MHpI 3.12
Sample No 4	Poly(MHpI+DHpI), mole % of MHpI 4.93
Sample No 5	Poly(MHpI+DHpI), mole % of MHpI 6.3
Sample No 6	Poly(MHpI+DHpI), mole % of MHpI 13.0
Sample No 7	Poly(MHpI+DHpI), mole % of MHpI 23.5
Sample No 8	Poly(MHpI+DHpI), mole % of MHpI 36.53
Sample No 9	Poly(MHpI+DHpI), mole % of MHpI 50.05
Sample No 10	Poly(MBI+DBI), mole % of MBI 33.05
Sample No 11	Poly(MBI+DBI), mole % of MBI 73.0
Sample No 12	Poly(MMI+DMI), mole % of MMI 10.5
Sample No 13	Poly(MHpI+DHpI)/TEPA, mole % of TEPA 0.29
Sample No 14	Poly(MHpI+DHpI)/TEPA, mole % of TEPA 1.42
Sample No 15	Poly(MHpI+DHpI)/TEPA, mole % of TEPA 3.12
Sample No 16	Poly(MHpI+DHpI)/TEPA, mole % of TEPA 4.93
Sample No 17	Poly(MHpI+DHpI)/EN, mole % of EN 6.3
Sample No 18	Poly(MHpI+DHpI)/DETA, mole % of DETA 6.3
Sample No 19	Poly(MHpI+DHpI)/TETA, mole % of TETA 6.3
Sample No 20	Poly(MHpI+DHpI)/TEPA, mole % of TEPA 6.3
Sample No 21	Poly(MHpI+DHpI)/EN, mole % of EN 13.0
Sample No 22	Poly(MHpI+DHpI)/DETA, mole % of DETA 13.0
Sample No 23	Poly(MHpI+DHpI)/TETA, mole % of TETA 13.0
Sample No 24	Poly(MHpI+DHpI)/TEPA, mole % of TEPA 13.0

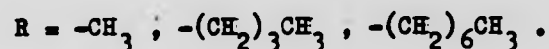
Sample No 25 Poly(MHpI+DHpI)/EN, mole % of EN 23.5
Sample No 26 Poly(MHpI+DHpI)/DETA, mole % of DETA 23.5
Sample No 27 Poly(MHpI+DHpI)/TETA, mole % of TETA 23.5
Sample No 28 Poly(MHpI+DHpI)/TEPA, mole % of TEPA 23.5
Sample No 29 Poly(MHpI+DHpI)/EN, mole % of EN 36.53
Sample No 30 Poly(MHpI+DHpI)/DETA, mole % of DETA 36.53
Sample No 31 Poly(MHpI+DHpI)/TETA, mole % of TETA 36.53
Sample No 32 Poly(MHpI+DHpI)/TEPA, mole % of TEPA 36.53
Sample No 33 Poly(MHpI+DHpI)/EN, mole % of EN 50.05
Sample No 34 Poly(MHpI+DHpI)/DETA, mole % of DETA 50.05
Sample No 35 Poly(MHpI+DHpI)/TETA, mole % of TETA 50.05
Sample No 36 Poly(MHpI+DHpI)/TEPA, mole % of TEPA 50.05
Sample No 37 Poly(MBI+DBI)/EN, mole % of EN 33.05
Sample No 38 Poly(MBI+DBI)/DETA, mole % of DETA 33.05
Sample No 39 Poly(MBI+DBI)/TETA, mole % of TETA 33.05
Sample No 40 Poly(MBI+DBI)/TEPA, mole % of TEPA 33.05
Sample No 41 Poly(MBI+DBI)/EN, mole of EN 73.0
Sample No 42 Poly(MBI+DBI)/DETA, mole % of DETA 73.0
Sample No 43 Poly(MBI+DBI)/TETA, mole % of TETA 73.0
Sample No 44 Poly(MBI+DBI)/TEPA, mole % of TEPA 73.0
Sample No 45 Poly(MMI+DMI)/EN, mole % of EN 10.5
Sample No 46 Poly(MMI+DMI)/DETA, mole % of DETA 10.5
Sample No 47 Poly(MMI+DMI)/TETA, mole % of TETA 10.5
Sample No 48 Poly(MMI+DMI)/TEPA, mole % of TEPA 10.5
Sample No 49 Poly(MHpI+DHpI)/TEPA/CoCl₂, mole % of
TEPA 0.29
Sample No 50 Poly(MHpI+DHpI)/TEPA/CoCl₂, mole % of
TEPA 1.42

Sample No 51	Poly(MHpI+DHpI)/TEPA/CoCl ₂ , mole % of TEPA 3.12
Sample No 52	Poly(MHpI+DHpI)/TEPA/CoCl ₂ , mole % of TEPA 4.93
Sample No 53	Poly(MHpI+DHpI)/TEPA/CoCl ₂ , mole % of TEPA 6.3
Sample No 54	Poly(MHpI+DHpI)/TEPA/CuCl ₂ , mole % of TEPA 6.3
Sample No 55	Poly(MHpI+DHpI)/TEPA/CoCl ₂ , mole % of TEPA 13.0
Sample No 56	Poly(MHpI+DHpI)/TEPA/CuCl ₂ , mole % of TEPA 13.0
Sample No 57	Poly(MHpI+DHpI)/TEPA/CoCl ₂ , mole % of TEPA 23.5
Sample No 58	Poly(MHpI+DHpI)/TEPA/CuCl ₂ , mole % of TEPA 23.5
Sample No 59	Poly(MHpI+DHpI)/TEPA/CoCl ₂ , mole % of TEPA 36.53
Sample No 60	Poly(MHpI+DHpI)/TEPA/CuCl ₂ , mole % of TEPA 36.53
Sample No 61	Poly(MHpI+DHpI)/TEPA/CoCl ₂ , mole of TEPA 50.05
Sample No 62	Poly(MHpI+DHpI)/TEPA/CuCl ₂ , mole % of TEPA 50.05
Sample No 63	Poly(MBI+DBI)/TEPA/CoCl ₂ , mole % of TEPA 33.05
Sample No 64	Poly(MBI+DBI)/TEPA/CuCl ₂ , mole % of TEPA 33.05
Sample No 65	Poly(MBI+DBI)/TEPA/CoCl ₂ , mole % of TEPA 73.0
Sample No 66	Poly(MBI+DBI)/TEPA/CuCl ₂ , mole % of TEPA 73.0
Sample No 67	Poly(MMI+DMI)/TEPA/CoCl ₂ , mole % of TEPA 10.5
Sample No 68	Poly(MMI+DMI)/TEPA/CuCl ₂ , mole % of TEPA 10.5
Sample No 69	Poly(MHpI+DHpI)/EN[Co(en) ₂ Cl] ²⁺ 2Cl ⁻ mole % of EN 13.0
Sample No 70	Poly(MMI+DMI)/EN/[Co(en) ₂ Cl] ²⁺ 2Cl ⁻ mole % of EN 10.5

3.1 SYNTHESIS OF MONOMERS

3.1.1 Mono-n-Alkyl Itaconates

Monomethyl, mono-n-butyl and mono-n-heptyl itaconates were prepared by a method described by Baker et al¹⁰.



A mixture of itaconic acid and alcohol (1:4 mole ratio) was refluxed for 10-20 minutes in the presence of a catalytic amount of acetyl chloride. The unreacted alcohol was removed under reduced pressure and the monoester was isolated by fractional distillation. The monoester was purified by vacuum distillation and recrystallized from benzene/petroleum ether solution. The product was identified by i.r., n.m.r. and melting point.

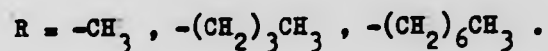
The amount of reagents used in the preparation of these monoesters, the boiling range and distillation pressure of the pure monoesters, and the melting points are shown in Table 3.1.

TABLE 3.1 Preparation of mono-n-alkyl itaconates

Ester	Acid (Moles)	Alcohol (Moles)	Acetyl chloride (cm ³)	Boiling Temp. (K)	Range pressure (Torr)	Melting point (K)
Monomethyl itaconate	1	4	3	395-440	25-20	341-342
Mono-n-butyl itaconate	1	4	3	442-448	8-10	314-315
Mono-n-heptyl itaconate	1	4	3	453-457	0.6-0.5	323-324

3.1.2 Di-n-Alkyl Itaconates

Dimethyl, di-n-butyl and di-n-heptyl itaconates were prepared by an acid catalysed process using an excess of alcohol¹¹.



A mixture of itaconic acid and alcohol (1:4 mole ratio) in benzene was refluxed for seven hours using sulphuric acid as a catalyst. After cooling, the benzene layer was isolated and washed with water until the washings become neutral to litmus paper. The benzene layer which contains the diester was dried overnight with potassium sulphate followed by filtration and removal of benzene. The crude diester was distilled twice under vacuum and the pure diester was then identified by i.r. and n.m.r.

The amount of itaconic acid and alcohols used in the preparation of the diesters, the boiling range, the distillation pressure of the pure diesters, and refractive index are shown in Table 3.2

TABLE 3.2 Preparation of di-n-alkyl itaconates

Ester	Acid (Moles)	Alcohol (Moles)	Benzene (cm ³)	H ₂ SO ₄ (cm ³)	Boiling Range Temp. pressure (K) (Torr)	Refractive Index
Dimethyl itaconate	1	4	400	35	363-368 1-1.2	1.4412
Di-n-butyl itaconate	1	4	400	35	395-403 0.3-0.1	1.4419
Di-n-heptyl itaconate	1	4	500	35	461-463 0.3-0.2	1.4497

3.2 BULK COPOLYMERIZATION

The simplest way to carry out a copolymerization is to place the required amounts of monomers and radical initiator into a round bottom flask and to subject the mixture to a temperature at which polymerization proceeds. This simple procedure is known as bulk polymerization. The required amounts of each monomer and initiator (α, α' -azobisisobutyronitrile, BDH), which was recrystallised from ethanol and characterised by its i.r., n.m.r. and melting point, were weighed out into a 100 cm³ round bottom flask. The air in the flask was flushed out with oxygen-free-nitrogen (OFN) for 10-20 minutes then sealed and placed in a thermostatted oil bath controlled to $\pm 0.1K$ for the required reaction time. The percentage conversion was limited to less than 15%. The crude copolymer was isolated by dissolving it in 5-10 cm³ of suitable solvent. This solution was added to a stirred, twenty fold, excess of suitable precipitant and the copolymer was purified by several further reprecipitations until the infrared spectrum of the copolymer was free from monomer (no C=C absorption). The copolymer was dried for 24 hours at room temperature under vacuum prior to subsequent use. The composition of the copolymer formed was determined as described in section 3.7.

3.3 COPOLYMERIZATION OF MONO- AND DIESTERS OF ITACONIC ACID

Three series of copolymers were prepared by bulk polymerization using α, α' -azobisisobutyronitrile (AIBN) as initiator. These were:

- 1 Poly(MHpI+DHpI) : Copolymer of mono-n-heptyl itaconate and di-n-heptyl itaconate.
- 2 Poly(MBI+DBI) : Copolymer of mono-n-butyl itaconate and di-n-butyl itaconate.
- 3 Poly(MMI+DMI) : Copolymer of monomethyl itaconate and dimethyl itaconate.

The monomer feed ratios, amount of initiator, reaction time and temperature for each of the above series of copolymers are shown in Tables 3.3, 3.4 and 3.5 respectively.

3.4 REACTION WITH AMINES

An attempt to react itaconic acid with amines such as ethylenediamine to form a monomer with pendant amine groups was not successful¹⁸. Amines such as ethylenediamine, diethylenetriamine triethylenetetramine and tetraethylenepentamine are very attractive and useful chelates, but tend to add across the vinyl double bond by

TABLE 3.3 Copolymerization of mono-n-heptyl and di-n-heptyl itaconate

Sample Number	Wt of MhipI in feed (g)	Wt %	Mole %	Wt of DhipI in feed (g)	Wt %	Mole %	Wt of AIBN (g)	Oil Bath Temp. (K)	Reaction Time (hr)
1	0.075	0.375	0.53	19.925	99.63	99.46	0.06	328	6
2	0.25	1.25	1.78	19.75	98.75	98.22	0.06	328	6
3	0.5	2.5	3.54	19.5	97.5	96.46	0.06	328	6
4	0.75	3.75	5.28	19.25	96.25	94.72	0.06	328	6
5	1.0	4.95	7.0	19.2	95.05	93.07	0.0505	343	6.1
6	2.0	10.0	13.71	18.0	90.0	86.29	0.06	328	6.0

(cont'd)

TABLE 3.3 (cont'd)

Sample Number	Wt of MHPi in feed (g)	Wt %	Mole %	Wt of DHPi in feed (g)	Wt %	Mole %	Wt of AIBN (g)	Oil Bath Temp (K)	Reaction Time (hr)
7	3.2	15.38	20.64	17.6	84.62	79.36	0.0561	343	4.0
8	5.0	25.0	32.28	15.0	75.0	67.72	0.06	356	3.2
9	7.0	33.98	42.4	13.6	66.02	57.6	0.0535	356	20.0

Solvent: Chloroform

Precipitant: Cold (273K) methanol

TABLE 3.4 Copolymerization of mono-n-butyl and di-n-butyl itaconate

Sample Number	Wt of MBI in feed (g)	Wt %	Mole %	Wt of DBI in feed (g)	Wt %	Mole %	Wt of AIBN (g)	Oil Bath Temp (K)	Reaction Time (hr)
10	2.8	12.67	15.88	19.3	87.33	84.12	0.0707	323	4.6
11	5.5	55.0	61.40	4.5	45.0	38.60	0.032	323	2.3

Solvent : Chloroform

Precipitant : Petroleum ether

TABLE 3.5 Copolymerization of monomethyl and dimethyl itaconate

Sample Number	Wt of MMI in feed (g)	Wt %	Mole %	Wt of DMI in feed (g)	Wt %	Mole %	Wt of AIBN (g)	Oil Bath Temp (K)	Reaction Time (hr)
12	1	10	10.87	9	90	89.13	0.0524	353	5

Solvent : Chloroform

Precipitant : Methanol

a Michaelis addition, when free monomer is used¹⁸. To obtain polymers containing this type of chelate, the acid groups of the monoesters in the copolymer were reacted with these amines in the presence of dicyclohexylcarbodiimide. Dicyclohexylcarbodiimide is a very reactive agent and useful for peptide synthesis⁶⁶.

In this work ethylenediamine (EN) $\text{H}_2\text{NCH}_2\text{CH}_2\text{NH}_2$ was purified by fractional distillation prior to use.

Diethylenetriamine (DETA) $\text{H}_2\text{NCH}_2\text{CH}_2\text{NHCH}_2\text{CH}_2\text{NH}_2$,

triethylenetetramine (TETA) $\text{H}_2\text{NHCH}_2\text{CH}_2\text{NHCH}_2\text{CH}_2\text{NHCH}_2\text{CH}_2\text{NH}_2$,

tetraethylenepentamine (TEPA) $\text{H}_2\text{NHCH}_2\text{CH}_2\text{NHCH}_2\text{CH}_2\text{NHCH}_2\text{CH}_2\text{NHCH}_2\text{CH}_2\text{NH}_2$,

dicyclohexylcarbodiimide (DCC) $\text{C}_6\text{H}_{11}\text{N}=\text{C}=\text{NC}_6\text{H}_{11}$, were distilled under vacuum.

A weighed amount of the copolymers prepared in section 3.3, of known mole percentage of the monoester, was placed in a round bottom flask (100 cm^3), and was dissolved in 75 cm^3 of distilled chloroform. To the dilute polymer solution a weighed amount of DCC was added, followed by the addition of a calculated amount of the amine. Both DCC and amine were used in excess. The reaction mixture was stirred for 48 hours at room temperature, filtered, then the volume of the solvent was reduced by flashing air inside the flask. The contents of the flask were added to about 500 cm^3 of distilled methanol while agitating with a glass rod. The precipitate which formed was separated and washed with methanol several times. The modified polymer was dissolved in a minimum amount of chloroform and

reprecipitated in methanol three times.

3.4.1 Poly(MHpI+DHpI)

(i) The first four copolymers of poly(MHpI+DHpI) samples, numbers 1, 2, 3 and 4, were reacted with TEPA only, in the presence of DCC. The mole percentage of the monoester in the feed and the copolymer, and the amount of the copolymer, TEPA and DCC used are shown in Table 3.6.

(ii) Each of the remaining copolymers of mono-n-heptyl itaconate and di-n-heptyl itaconate samples, numbers 5, 6, 7, 8 and 9 were reacted with EN, DETA, TETA and TEPA in the presence of DCC. Reaction conditions are shown in Table 3.7.

3.4.2 Poly(MBI+DBI)

Both poly(MBI+DBI) samples, numbers 10 and 11, were reacted with EN, DETA, TETA and TEPA in the presence of DCC. The mole percentage of the mono-n-butyl itaconate in the feed and in the copolymer, the amount of amines and DCC used are shown in Table 3.8.

3.4.3 Poly(MMI+DMI)

The acid group in the monomethyl itaconate was reacted with EN, DETA, TETA and TEPA in the presence of DCC. The mole percentage of the monomethyl itaconate in the feed and copolymer, amines and DCC are shown in Table 3.9.

TABLE 3.6 Preparation of poly(itaconate copolymers) with pendant ethylene amine groups using poly(MHpI+DHpI) systems

Sample Number	Wt of copolymer used/(g)	Wt% of MHpI in feed	Mole% of MHpI in feed	Wt% of MHpI in copolymer	Mole% of MHpI in copolymer	DCC (g)	TEPA (g)
13	4.0	0.375	0.53	0.2	0.29	0.04	0.07
14	4.0	1.25	1.78	1.0	1.42	0.18	0.33
15	4.0	2.5	3.54	2.2	3.12	0.4	0.73
16	4.0	3.75	5.28	3.5	4.93	0.63	1.16

TABLE 3.7 Preparation of poly(itaconate copolymers) with pendant ethylene amine groups, using poly(MHpI+DHpI) systems

Sample Number	Wt of copolymer taken (g)	Wt % of MhpI in feed	Mole % of MhpI in feed	Wt % of MhpI in copolymer	Mole % of MhpI in copolymer	DCC (g)	Amine used (g)
17	4.0	5.0	7.0	4.95	6.3	0.89	EN/0.52
18	4.0	5.0	7.0	4.95	6.3	0.89	DETA/1.12
19	4.0	5.0	7.0	4.95	6.3	0.89	TETA/1.26
20	4.0	5.0	7.0	4.95	6.3	0.89	TEPA/1.64
21	2.0	10.0	13.71	9.48	13.0	0.85	EN/0.49
22	2.0	10.0	13.71	9.48	13.0	0.85	DETA/1.08
23	2.0	10.0	13.71	9.48	13.0	0.85	TETA/1.21
24	2.0	10.0	13.71	9.48	13.0	0.85	TEPA/1.57
25	2.0	15.4	20.6	17.7	23.5	1.59	EN/0.93

(cont'd)

TABLE 3.7 Preparation of poly(itaconate copolymers) with pendant ethylene amine groups, using poly(MHpI+DHpI) systems

Sample Number	Wt of copolymer taken (g)	Wt % of MhpI in feed	Mole % of MhpI in feed	Wt % of MhpI in copolymer	Mole % of MhpI in copolymer	DCC (g)	Amine used (g)
17	4.0	5.0	7.0	4.95	6.3	0.89	EN/0.52
18	4.0	5.0	7.0	4.95	6.3	0.89	DETA/1.12
19	4.0	5.0	7.0	4.95	6.3	0.89	TETA/1.26
20	4.0	5.0	7.0	4.95	6.3	0.89	TEPA/1.64
21	2.0	10.0	13.71	9.48	13.0	0.85	EN/0.49
22	2.0	10.0	13.71	9.48	13.0	0.85	DETA/1.08
23	2.0	10.0	13.71	9.48	13.0	0.85	TETA/1.21
24	2.0	10.0	13.71	9.48	13.0	0.85	TEPA/1.57
25	2.0	15.4	20.6	17.7	23.5	1.59	EN/0.93

(cont'd)

TABLE 3.7 (cont'd)

Sample Number	Wt of copolymer taken (g)	Wt % of MHPi in feed	Mole % of MHPi in feed	Wt % of MHPi in copolymer	Mole % of MHPi in copolymer	DCC (g)	Amine used (g)
26	2.0	15.4	20.6	17.7	23.5	1.59	DETA/2.01
27	2.0	15.4	20.6	17.7	23.5	1.59	TETA/2.26
28	2.0	15.4	20.6	17.7	23.5	1.59	TEPA/2.93
29	1.5	25.0	32.3	28.7	36.53	1.95	EN/1.14
30	1.5	25.0	32.3	28.7	36.53	1.95	DETA/2.47
31	1.5	25.0	32.3	28.7	36.53	1.95	TETA/2.77
32	1.5	25.0	32.3	28.7	36.53	1.95	TEPA/3.59
33	1.0	34.0	42.4	41.2	50.05	1.85	EN/1.07
34	1.0	34.0	42.4	41.2	50.05	1.85	DETA/2.33
35	1.0	34.0	42.4	41.2	50.05	1.85	TETA/2.62
36	1.0	34.0	42.4	41.2	50.05	1.85	TEPA/3.39

TABLE 3.8 Preparation of poly(itaconate copolymers) with pendant ethylene amine groups, using poly(MBI+DBI) systems

Sample Number	Wt of copolymer taken (g)	Wt % of MBI in feed	Mole % of MBI in feed	Wt % of MBI in copolymer	Mole % of MBI in copolymer	DCC (g)	Amines (g)
37	1.0	12.7	27.4	27.5	33.05	1.51	EN/0.88
38	1.0	12.7	27.4	27.5	33.05	1.51	DETA/1.91
39	1.0	12.7	27.4	27.5	33.05	1.51	TETA/2.15
40	1.0	12.7	27.4	27.5	33.05	1.51	TEPA/2.78
41	0.5	55.0	61.4	67.5	73.0	1.86	EN/1.08
42	0.5	55.0	61.4	67.5	73.0	1.86	DETA/2.35
43	0.5	55.0	61.4	67.5	73.0	1.86	TETA/2.65
44	0.5	55.0	61.4	67.5	73.0	1.86	TEPA/3.43

TABLE 3.9 Preparation of poly(itaconate copolymers) with pendant ethylene amine groups, using poly(MMI+DMI) systems.

Sample Number	Wt of copolymer used (g)	Wt % of MMI in feed	Mole % of MMI in feed	Wt % of MMI in copolymer	Mole % of MMI in copolymer	DCC (g)	Amines (g)
45	2.0	10.0	10.87	9.66	10.5	1.38	EN/0.8
46	2.0	10.0	10.87	9.66	10.5	1.38	DETA/1.74
47	2.0	10.0	10.87	9.66	10.5	1.38	TETA/1.96
48	2.0	10.0	10.87	9.66	10.5	1.38	TEPA/2.53

3.5 REACTION WITH METAL HALIDES

The modified polymers prepared in section 3.4 contain a chelate group capable of forming a coordinate bond with metal ions. The polymers which contain TEPA in the side chain were reacted with different metal halides. This leads to the formation of polymer-metal complexes as described in section 2.4.

A weighed amount of the copolymer, containing TEPA as a side chain, was placed in a round bottom flask (100 cm³) and dissolved in distilled chloroform 75 cm³. The metal halides were first dissolved in a mixture of 1:1 volume ratio chloroform to methanol added to the polymer solution and the reaction mixture was stirred for 24 hours. A change in the colour of the polymer solution after the addition of the metal halide solution was noticed. The volume of the solvent was reduced by flashing air inside the flask and the contents of the flask were added with stirring to about 500 cm³ of distilled methanol. The precipitated polymer-metal complexes were washed with methanol several times then dissolved in a minimum amount of chloroform and reprecipitated in methanol three times.

3.5.1 Poly(MHpI+DHpI)/TEPA

(i) The first four modified polymers, sample numbers 13, 14, 15 and 16, of mono-n-heptyl and di-n-heptyl itaconate in which the acid group in the mono-n-heptyl

itaconate was substituted with TEPA, were reacted with cobalt(II) chloride (CoCl_2) only. The mole percentage of the monoester in the copolymer, the amount of cobalt(II) chloride and solvent used are shown in Table 3.10.

(ii) The remaining samples of poly(MHpI+DHpI), sample numbers 20, 24, 28, 32 and 36, which contain different mole percentages of the mono-n-heptyl itaconate were reacted with TEPA in the presence of DCC. These modified polymers were reacted with cobalt(II) chloride, and copper(II) chloride only. The mole percentage of the mono-n-heptyl itaconate in the copolymer, the amount of polymeric ligand, cobalt(II) chloride, copper(II) chloride and solvent used are shown in Table 3.11.

3.5.2 Poly(MBI+DBI)/TEPA

Poly(MBI+DBI), sample numbers 40 and 44, with the acid group in the mono-n-butyl itaconate converted with TEPA, were reacted with cobalt(II) chloride and copper(II) chloride. The mole percentage of the monoester in the copolymer, the amount of polymeric ligand, cobalt(II) chloride, copper(II) chloride and solvent used are shown in Table 3.12.

3.5.3 Poly(MMI+DMI)/TEPA

Poly(MMI+DMI), sample number 48, containing TEPA in the side chain was reacted with cobalt(II) chloride and copper(II) chloride. The mole percentage of the monomethyl itaconate in the copolymer, the amount of the polymeric

TABLE 3.10 Preparation of polymer chelates of cobalt(II) chloride using modified poly(MHpI+DHpI)

Sample Number	Wt of the polymeric ligand taken (g)	Mole % of the MHpI in copolymer (equivalent to the side chain concentration)	CoCl ₂ (g)	Solvent CHCl ₃ :MeOH (cm ³)	Reaction Time (hr)
49	3.0	0.29	0.0019	2:2	24
50	3.0	1.42	0.0097	2:2	24
51	3.0	3.12	0.0214	2:2	24
52	3.0	4.93	0.0341	2:2	24

TABLE 3.11 Preparation of polymer chelates of cobalt(II) chloride or copper(II) chloride, using modified poly (MHP1+DHP1)

Sample Number	Wt of polymeric Ligand used (g)	Mol % of MHP1 in copolymer (equivalent to the side chain)	CHCl ₃ cm ³	Metal halides used (g)	Solvent CHCl ₃ :MeOH cm ³	Reaction Time (hr)
53	2.0	6.3	75	CoCl ₂ /0.0322	2:2	24
54	2.0	6.3	75	CuCl ₂ /0.0333	2:2	24
55	2.0	13.0	75	CoCl ₂ /0.0616	2:2	24
56	2.0	13.0	75	CuCl ₂ /0.0638	2:2	24
57	1.5	23.5	75	CoCl ₂ /0.0863	2:2	24
58	1.5	23.5	75	CuCl ₂ /0.0894	2:2	24
59	1.0	36.53	75	CoCl ₂ /0.0933	2:2	24
60	1.0	36.53	75	CuCl ₂ /0.0967	2:2	24
61	0.5	50.05	75	CoCl ₂ /0.0670	2:2	24
62	0.5	50.05	75	CuCl ₂ /0.0694	2:2	24

TABLE 3.12 Preparation of polymer chelates of cobalt(II) chloride or copper(II) chloride, using modified poly(MBI+DBI)

Sample Number	Wt of polymeric ligand taken (g)	Mol % of MBI in copolymer (equivalent to the side chain)	CHCl ₃ cm ³	Metal halide used (g)	Solvent CHCl ₃ :MeOH cm ³	Reaction Time (hr)
63	1.0	33.05	75	CoCl ₂ /0.1	2:2	24
64	1.0	33.05	75	CuCl ₂ /0.1035	2:2	24
65	0.5	73.0	75	CoCl ₂ /0.1227	2:2	24
66	0.5	73.0	75	CuCl ₂ /0.1271	2:2	24

ligand, cobalt(II) chloride, copper(II) chloride and solvent used are shown in Table 3.13.

3.6 REACTION WITH trans[Co(en)₂Cl₂]Cl

The modified polymers (polymeric ligands) prepared in section 3.4 contain a ligand capable of forming a pendant-type polymer-metal complex. Modified polymers containing EN in the side chain were reacted with a stable preformed metal complex having elimination ligand (weak ligand) (such as trans[Co(en)₂Cl₂]Cl) to form a pendant-type polymer metal complex similar to that described in section 2.4.

A weighed amount of the modified polymer which contains EN as ligand was placed in a round bottom flask (100 cm³) and was dissolved in distilled chloroform 75 cm³. A calculated amount of trans [Co(en)₂Cl₂]Cl was dissolved in a 1:1 mixture of chloroform and methanol. The metal complex solution was added to the polymer solution and a change in the colour was detected. The reaction mixture was stirred for 24 hours. The volume of the solvent was reduced and the contents of the flask were added to about 500 cm³ distilled methanol to precipitate the pendant-type polymer-metal complex, which was then reprecipitated three times. The mole percentage of the mono-ester in the feed and copolymer, the amount of the polymeric ligand, trans[Co(en)₂Cl₂]Cl and solvent used are shown in Table 3.14.

TABLE 3.13 Preparation of polymer chelates of cobalt(II) chloride or copper(II) chloride, using modified poly(MMI+DMI)

Sample Number	Wt of polymeric ligand used (19)	Mol % of MMI in copolymer (equivalent to the side chain)	CHCl ₃ cm ³	Metal halides used (g)	Solvent CHCl ₃ :MeOH cm ³	Reaction Time (hr)
67	1.5	10.87	75	CoCl ₂ /0.0597	2:2	24
68	1.5	10.87	75	CuCl ₂ /0.0618	2:2	24

TABLE 3.14 Preparation of pendant-type polymer metal complexes

Sample Number	Polymeric ligand used	Wt taken (g)	CHCl ₃ cm ³	Amount of <u>transl</u> Co(en) ₂ Cl ₂ Cl used (g)	Solvent CHCl ₃ :MeOH (cm ³)	Reaction Time (hr)
69	poly(MHpI+DHPi)/EN	1.5	75	0.1461	2:2	24
70	poly(MMI+DMI)/EN	1.5	75	0.2161	2:2	24

3.7 DETERMINATION OF THE COMPOSITION OF THE COPOLYMERS

Two methods were used to determine the composition of a copolymer. The first method involved using a non-aqueous potentiometric titration technique and the second method was microanalysis. The mole percentage of the monoester in the copolymer can be calculated from data obtained from each method. The non-aqueous potentiometric titration was carried out in the following way:

The copolymer 0.2-0.4g was weighed into a 25 cm³ volumetric flask, dissolved in a suitable solvent mixture (see Table 3.15) and made up to 25 cm³ with the solvent mixture. Sodium hydroxide (0.1 M) was prepared by using CVS (BDH) solution. A suitable solvent mixture was used to prepare the base solution (see Table 3.15) which was titrated against standard 0.1 M hydrochloric acid solution to determine its molarity. A pH meter (Corning-EEL Model 7) connected to a Heathkit 10 mV recorder was used. A 5 cm³ aliquot of the copolymer solution was titrated against the base solution whilst monitoring the pH value on the meter. The titration was carried out at 298K. The volume of the base solution used was measured as a function of pH until there was no further change in the pH meter reading and this can be best achieved by using a recorder. The end point is then related to the amount of the acid group that had been

TABLE 3.15 The base solution and solvent used in the non-aqueous potentiometric titration

Copolymer system	Solvent mixture used to dissolve the copolymer	Base solution
poly(MBI+DBI)	EtOH	10% aq. 0.1 M NaOH + 90% EtOH
poly(MHpI+DHpI)	50% n-BuOH + 50% EtOH	10% aq. 0.1 M NaOH + 45% EtOH + 45% n-BuOH

neutralized. The acid group in the copolymer is simply referred to as the monoester in the copolymer.

The second method used to determine the composition of the copolymer was microanalysis. A Carloerba, Elemental Analyser Model 1106 was used to analyse polymer samples. The mole percentage of the monoester in the copolymer was calculated from the percentage of carbon, hydrogen and oxygen in the copolymer.

3.8 DECOMPOSITION OF HYDROGEN PEROXIDE

The catalytic activities of the polymer-metal complexes were examined by measuring the rate of decomposition of hydrogen peroxide⁶⁷. This was done by calculating the rate of decomposition of hydrogen peroxide in the presence and absence of the polymer-metal complexes. The following procedure was used:

3.8.1 Preparation of solutions

The following solutions were prepared:

- (i) 0.02 M KMnO_4 . This was prepared by dissolving 3.1608 g KMnO_4 in 1000 cm^3 distilled water.
- (ii) Hydrogen peroxide solution. This was prepared by diluting 1 cm^3 of 30 W/V hydrogen peroxide with 100 cm^3 distilled water.
- (iii) 1:2 H_2SO_4 solution. This was prepared by diluting 10 cm^3 of concentrated sulphuric acid with 20 cm^3 distilled water.

3.8.2 Standardization of KMnO_4 .

The 0.02 M KMnO_4 solution was standardized by using sodium oxalate. About 0.2 g of A.R. sodium oxalate was dried for two hours in an oven at 378K. From this dried sodium oxalate, 1.7 g was weighed accurately and transferred to a volumetric flask and made up to 250 cm^3 with distilled water. From the sodium oxalate solution 25 cm^3 was pipetted into a 250 cm^3 conical flask and to it 150 cm^3 of 2 M H_2SO_4 solution were added. The burette contained the KMnO_4 solution and titration was carried out at room temperature. When the faint pink colour appeared the solution was warmed to 320-330K until the solution became colourless. More KMnO_4 solution was added until the faint pink colour was permanent. Once the volume of sodium oxalate and KMnO_4 solution are known, one can calculate the molarity of KMnO_4 .

3.8.3 Measurement of the rate of decomposition of hydrogen peroxide.

(a) In a 250 cm^3 round bottom flask, 75 cm^3 of the hydrogen peroxide solution were placed. The flask was kept inside a thermostat at 313K. Distilled water 25 cm^3 was added to the hydrogen peroxide solution, and 5 cm^3 of this solution were pipetted into a 250 cm^3 conical flask. To the solution in the conical flask 5 cm^3 of 1:2 H_2SO_4 solution were added and this was titrated against the standardized KMnO_4 solution until a permanent faint pink colour appeared. The volume of the

KMnO_4 solution used was recorded, and the titration repeated as a function of time. From this information one can plot the log of the volume of added KMnO_4 solution (which is proportional to the concentration of the hydrogen peroxide remaining) as a function of time.

(b) The same procedure was used for the reaction involving metal halides, metal complex, polymeric ligands and polymer-metal complexes. A polymer-metal complex which contained a known number of moles of the metal ion was added to the hydrogen peroxide solution, followed by addition of distilled water using the same procedure as described above. The catalytic activity for each of the following materials was measured:

- 1 0.05 g of poly(MHpI+DHpI)/TEPA.
- 2 0.05 g of poly(MHpI+DHpI)/EN.
- 3 4.649×10^{-5} mole of cobalt(II) as CoCl_2 .
- 4 4.649×10^{-5} mole of cobalt(III) as $\text{trans}[\text{Co}(\text{en})_2\text{Cl}_2]\text{Cl}$.
- 5 4.649×10^{-5} mole of copper(II) as CuCl_2 .
- 6 4.649×10^{-5} mole of cobalt(III) as poly(MHpI+DHpI)/TEPA/ CoCl_2 .
- 7 4.649×10^{-5} mole of cobalt(III) as poly(MMI+DMI)/TEPA/ CoCl_2 .
- 8 4.649×10^{-5} mole of cobalt(III) as poly(MHpI+DHpI)/EN/ $[\text{Co}(\text{en})_2\text{Cl}]^{2+} 2\text{Cl}^-$.
- 9 4.649×10^{-5} mole of copper(II) as poly(MHpI+DHpI)/TEPA/ CuCl_2 .
- 10 4.649×10^{-5} mole of copper(II) as poly(MMI+DMI)/TEPA/ CuCl_2 .
11. 4.649×10^{-5} mole of cobalt(III) as poly(MMI+DMI)/EN/ $[\text{Co}(\text{en})_2\text{Cl}]^{2+} 2\text{Cl}^-$.

3.9 INFRARED ANALYSIS

3.9.1 Introduction:

A Perkin Elmer Infrared Spectrophotometer 577 was used in this study. Infrared is a useful technique in identifying characteristic frequencies in polymers. The various groups present in the polymers used here (C-C, C=C, C-O, C=O, O-H, NH etc) have different vibrational frequencies and can be distinguished using this technique. Infrared spectroscopy for polymers was achieved by casting a 5-10 W/V solution onto a sodium chloride plate. The film which was formed on the plate was dried using an IR radiant lamp.

3.9.2 Infrared Study.

Monomers of itaconic acid derivatives were readily identified; both the monoesters and the diesters of itaconic acid show characteristic bands at 1640 and 1750 cm^{-1} . The infrared spectrum was used to ensure that the copolymers of mono and diester of itaconic acid were free from any residual monomer after reprecipitation. The characteristic absorption of the C=C bond is an indication of the presence of monomers in the copolymer. Infrared spectra for the modified polymers which contain pendant amine groups in the side chain have also been studied.

3.10 VISIBLE SPECTROPHOTOMETER

3.10.1 Introduction.

A Beckman Spectrophotometer Model 24 was used in this study. The visible region in the spectrophotometer proved to be most useful for measuring the absorption of coloured metal ions and to study the formation and the structure of the metal complexes. In this work the visible region was used to study the absorption of the coloured metal halides (cobalt(II) chloride and copper(II) chloride). The intensity of the colour was proportional to the concentration of the metal halide solutions. All the modified polymers which contain tetraethylene-pentamine in the side chain were colourless and they do not show any absorption in the visible region. Using the visible region in the spectrophotometer one can measure the absorption as a function of concentration or time. The formation and the structure of the polymer-metal complexes also can be studied.

3.10.2 Visible Spectrophotometer Study.

The reaction between the metal halides (cobalt(II) chloride and copper(II) chloride) with the modified polymers (which contain tetraethylenepentamine in the side chain) was followed by visible spectrophotometry. Two different methods were used. In the first method, the spectrum of the solvent (chloroform:methanol) used to dissolve the

metal halides (cobalt(II) chloride and copper(II) chloride) was run first. No absorption was detected in the visible region. An accurate amount by weight of the modified polymer was placed in a 250 cm³ round bottom flask and was dissolved in chloroform. The spectrum of this modified polymer solution again showed no absorption in the visible region. Knowing the mole percentage of the side chain in the polymer, an equivalent molar solution of the metal halide was prepared and this solution was found to absorb quite strongly in the visible region. The metal halide solution was then added to the polymer solution and a change in the colour was detected, which was reflected in a change in the absorption in the visible region.

In the second method, a series of known concentrations of metal halide (cobalt(II) chloride and copper(II) chloride) was prepared in 25 cm³ volumetric flasks, using a mixture of 10:1 ratio of chloroform to ethanol as solvent and the absorptions of these were measured. An accurate amount of each metal halide was added to the polymer solution of known concentration and the colourless polymer solution became coloured. The absorption spectrum of this complex was recorded and was measured as a function of the amount of metal halide added. The same procedure as above was carried out, but in this case the absorption was measured as a function of time. A change in the original colour of the metal ion solution indicates a

change in the coordination.

3.11 ELECTRON MICROSCOPY

3.11.1 Introduction.

Electron microscopy (EM) has been used to examine the morphology of polymers containing metal ions. Electron microscopy is a technique analogous to that of visible light microscopy and has been proved to be a powerful tool for studying polymer internal micromorphology, polymer lattices, polymer networks, pore size distribution and block copolymer structure⁶⁸. In electron microscopy an electron beam and electrostatic and/or electromagnetic lenses are used instead of a light beam and the usual glass lenses. The microscope column which contains the electron gun and the fluorescent screen is under vacuum ($\sim 10^{-5}$ torr) to reduce the scattering of electrons by air. The electron microscope consists of the following parts⁶⁸:

(i) The electron gun.

The electron gun produces thermal electrons and is usually made of a tungsten filament. The electron beam is focussed on the sample with the aid of a series of electrostatic and/or electromagnetic lenses after having been accelerated by applying a high voltage.

(ii) The sample.

The sample is placed in a special holder known as

a specimen support grid. The size of the polymer film is limited to a few thousand ångstroms in thickness and to 2 mm or less in diameter.

(iii) The fluorescent screen.

Two or more additional electrostatic and/or electromagnetic lenses are used to form the image and this is observed on a fluorescent screen or recorded photographically.

3.11.2 Sample preparation.

Polymer films were prepared by a compression moulding technique using a hot press as described in section 3.14.3. The lowest possible temperature and pressure were used in order to minimise damage to the polymer structure. Polymer films (0.5-0.2 mm thick) were prepared by this technique. From these, sections of ca 100-150 μm thick were cut by an L.K.B. Ultratome III, following standard procedures. Copper grids containing 200-300 mesh per inch were used as supports for these sections.

3.11.3 Electron microscopy study.

A Jeol JEM 100 C transmission electron microscope was used in this study with a 200,000 x magnification and 0.014 resolution. The electron plates were enlarged photographically to the required scales.

3.12 MEMBRANE OSMOMETRY

3.12.1 Introduction.

A Knauer membrane osmometer and detecting bridge (K.G.Dr.Ing.H.Knauer & Co. GmbH, I Berlin 37, "West" Holstweg 18) was used to measure the number average molecular weight of a given polymer. The instrument consists of two cells, one for pure solvent the other for the polymer solution, separated by a semipermeable membrane. The principle of the technique is based on measuring the osmotic pressure which is detected as a pressure change in the lower chamber by a pressure sensitive diaphragm.

3.12.2 Theory.

In membrane osmometry the pressure difference between a solution and pure solvent is measured for the case where the solvent is separated from the solution by a semi-permeable membrane, permeable only to the solvent molecules. In order to reach equilibrium the solvent molecules will pass through the membrane into the solution because the chemical potential μ of the solvent in the solution is lower than that of the pure solvent μ° .⁶⁹ The difference in chemical potential of the solvent $\Delta\mu$ and the partial molar volume \bar{V}_1^m can be related by

$$-\Delta\mu = -(\mu - \mu^{\circ}) = \pi \bar{V}_1^m \quad (3.1)$$

In very dilute polymer solutions the chemical potential can be replaced by the solvent activity a_1 and equation (3.1)

can be written as

$$\pi \bar{V}_1^m = -RT \ln a_1 \quad (3.2)$$

Equation (3.2) can also be written in terms of mole fractions of solvent X_1 and solute (polymer X_2).

$$\pi \bar{V}_1^m = -RT \ln X_1 = -RT \ln (1-X_2) \quad (3.3)$$

$$\pi \bar{V}_1^m = RT X_2 \quad (3.4)$$

The mole fraction of the solute (polymer X_2) in very dilute solution where $n_2 \ll n_1$ and $v_2 \ll v_1$ is given by equation (3.5)

$$X_2 = \bar{V}_1^m C_2 / M_2 \quad (3.5)$$

$$C_2 = M_2 / v_2 + v_1 \quad (3.6)$$

$$\bar{V}_1^m = v_1 / n_1 \quad (3.7)$$

where \bar{V}_1^m is the molar volume of the solvent, C_2 is the concentration of the solute (polymer), M_2 is the molecular weight of the solute (polymer), v_1 and v_2 are the volume of solvent and solute respectively, and n_1 and n_2 are the number of moles of solvent and solute respectively. For infinite dilution where $\bar{V}_1^m = v_1^m$, the van't Hoff equation as a limiting law is given by:

$$\lim_{c \rightarrow 0} \frac{\pi}{C_2} = \frac{RT}{M_2} \quad (3.8)$$

Experimentally a series of four or five concentrations were prepared and the osmotic pressure for each was measured.

The results were plotted using the virial equation:

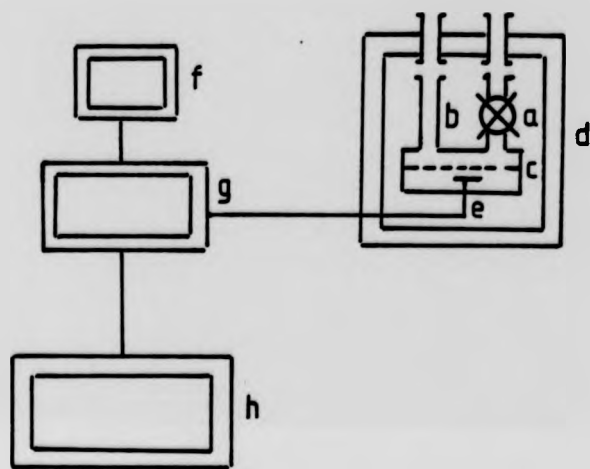


Fig. 3.1 Schematic diagram of membrane osmometer.

- a = outlet valve
- b = inlet tube
- c = membrane
- d = thermostatted chamber
- e = pressure detecting membrane
- f = osmotic pressure dial
- g = wheatstone bridge circuit
- h = recorder

$$\pi / C = RT / \bar{M}_n + Bc + Cc^2 + \dots \quad (3.9)$$

where B and C are the second and third virial coefficients respectively. If the solution concentrations are sufficiently dilute the third virial coefficient can be neglected and a plot of (π/C) versus the concentration (C) is normally linear. The intercept is equal to RT/\bar{M}_n and the slope is equal to the second virial coefficient.

3.12.3 Experimental.

The instrument was first calibrated by applying a known external pressure to the inlet tube and then balancing this electrically with solvent both below and above the semipermeable membrane. These membranes should be protected against bacteriological damage and conditioned to water or organic solvent prior to use. A schematic diagram of the instrument is shown in Figure 3.1. A series of four to five polymer solutions with concentrations in the range $0-11 \text{ g.dm}^{-3}$ were prepared. The osmotic pressure of each solution was measured, the one with the lowest concentration being measured first. This was done by the addition of the polymer solution to the upper chamber. The solvent molecules will diffuse upwards through the semipermeable membrane, causing a pressure change in the lower chamber. This change in the pressure is detected by the diaphragm which will bring about a resistance change. The out-of-balance signal which will appear on the recorder is proportional to the pressure change.

3.13 DIFFERENTIAL SCANNING CALORIMETER

3.13.1 Introduction.

Differential scanning calorimetry (DSC) is a technique of non-equilibrium calorimetry which records the energy necessary to establish zero temperature difference between a sample and an inert reference as a function of either time or temperature. Both sample and reference are subject to identical temperature conditions by altering the electric heating current to the sample and reference chambers. Watson et al⁷⁰ and O'Neill⁷¹ described and analysed the performance of a differential scanning calorimeter in 1964. Differential scanning calorimetry measures the thermal response of a solid or liquid sample. A Perkin-Elmer differential scanning calorimeter (DSC-2) fitted with a scanning autozero and a low temperature accessory was used in this study and a block diagram of a DSC instrument is shown in Figure 3.2.

3.13.2 Theory.

Muller and co-workers⁷² developed the mathematical description which neglects the temperature gradient within the sample. The heat flow into the sample holder can be approximated by:

$$dQ / dT = K (T_b - T) \quad (3.10)$$

Where K is the geometry-dependent thermal conductivity of

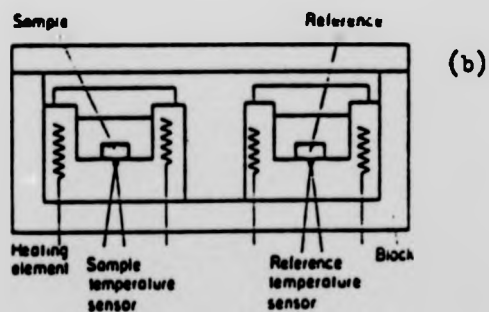
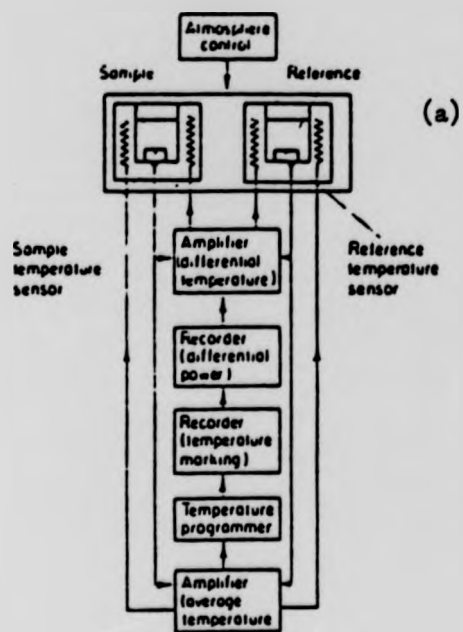


Fig. 3.2 Differential scanning calorimeter (DSC):
 (a) Block diagram of a DSC instrument.
 (b) Essential elements of the DSC cell.

the thermal resistance layer around the sample, T_b is the programmed block temperature and T is the sample temperature. The programmed block temperature T_b changes at constant rate q :

$$T_b = T_o + qt \quad (3.11)$$

where q is the heating rate. The heat flow into the reference holder can be represented by a relation similar to equation (3.10).

$$dQ_{\text{ref}} / dt = K (T_b - T_{\text{ref}}) \quad (3.12)$$

At constant heat capacity C_p the heat absorbed on heating between T_o and T is in this case

$$Q = C_p (T - T_o) \quad (3.13)$$

The differential equation for the heat flow can be obtained from the combination of equations (3.10), (3.11) and (3.13).

$$dQ / dt = K (-Q / C_p + qt) \quad (3.14)$$

The initial conditions are:

$$t = 0, T_b = T = T_o = 0 \text{ and } Q = 0.$$

The solution of equation (3.14) can be written as:

$$T_b - T = \frac{dT}{dt} \frac{C_p}{K} \quad (3.15)$$

The heat capacity of the reference C_p' can be expressed by the equation

$$T_b - T_{\text{ref}} = \frac{dT_{\text{ref}}}{dt} \frac{C_p'}{K} \quad (3.16)$$

The heat capacity is proportional to the temperature difference between sample and block at a steady state which can be reached after a sufficiently long time and,

$$\Delta T = \frac{q(C_p' - C_p)}{K} \quad (3.17)$$

where ΔT is the temperature difference between reference and sample.

3.13.3 Experimental.

The instrument is capable of measurement in the temperature range 100 - 1000 K at scan rates of up to 320 K min⁻¹. Helium was used as a purge gas when samples were examined at temperatures below 200 K. Above 200 K oxygen-free-nitrogen (OFN) was used as the purge gas for sample and reference chambers. The instrument was calibrated by using metal standards with known melting points. Polymer samples (10-25 mg) were dried for at least one day in a vacuum oven at room temperature and were encapsulated in standard aluminium sample pans. Thermograms were measured between 100 and 500 K usually at scan rates of up to 40 K min⁻¹.

3.13.4 Data analysis.

The DSC thermogram was displayed on a chart recorder. The glass transition temperature (T_g) was identified as a base-line shift on the thermogram and it was estimated as

the point of intersection of the base-line with the extrapolation of the sloping portion of the curve.

3.14 RHEOVIBRON

3.14.1 Introduction.

The Rheovibron viscoelastometer is a device to measure the complex modulus E^* , dynamic storage modulus E' , dynamic loss modulus E'' and dynamic loss tangent $\tan \delta$ of polymers in the form of films or filaments at specific selected frequencies (3.5, 11, 35 and 110 Hz) of strain input as a function of temperature. A Rheovibron direct reading dynamic viscoelastometer model II C supplied by Toyo Baldwin Co Ltd, Japan, was used in this study and was first developed by Takayanagi⁷³. The principle of the technique is based on measuring a sinusoidal tensile stress generated at one end of polymer strip due to a small sinusoidal tensile strain imposed on the other end of the strip. The device uses two transducers for detection of the phase angle between strain and stress and the complex dynamic modulus. A block diagram of the Rheovibron is shown in Figure 3.3. The instrument was kept inside a perspex dry box to reduce the effect of moisture when samples were being tested at subambient temperatures and to maintain high accuracy measurement.

3.14.2 Theory.

If a small sinusoidal tensile strain is applied on one end of the polymer strip then a sinusoidal tensile stress can be measured at the other end. The resulting sinusoidal stress which is generated may be out of phase with the strain. The sinusoidal elongation strain (γ) of small amplitude at time (t) is given by the equation:

$$\gamma = \gamma_0 \sin \omega t \quad (3.18)$$

Where γ is the sinusoidal elongation strain, γ_0 is the maximum value of the strain and ω is the frequency. The stress (S) is given by the equation:

$$S = S_0 \sin (\omega t + \delta) \quad (3.19)$$

where S_0 is the maximum value of the stress and δ is the phase angle difference. Equation (3.19) can be expanded to give:

$$S = S_0 \sin \omega t \cos \delta + S_0 \cos \omega t \sin \delta \quad (3.20)$$

The relation between stress and strain as a function of time is shown in Figure 3.4. The peak stress can be resolved into a component $S_0 \cos \delta$ which is the storage modulus (E') (defined as the ratio of the applied strain to the in phase component of the resulting stress), and a component $S_0 \sin \delta$ which is the loss modulus (E'') (defined as the ratio of the applied strain to the stress 90° out of phase). Thus these two elastic moduli can be

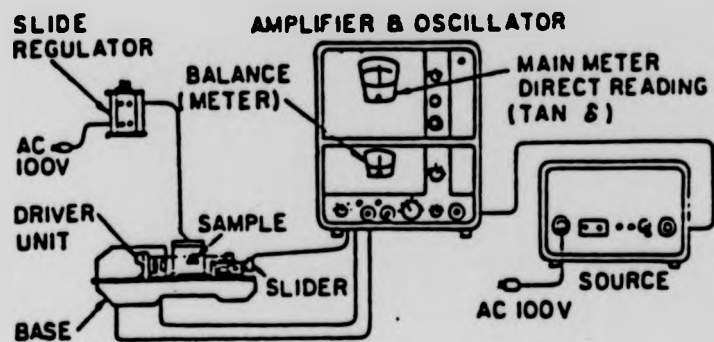


Fig. 3.3 Drawing of Rheovibron.

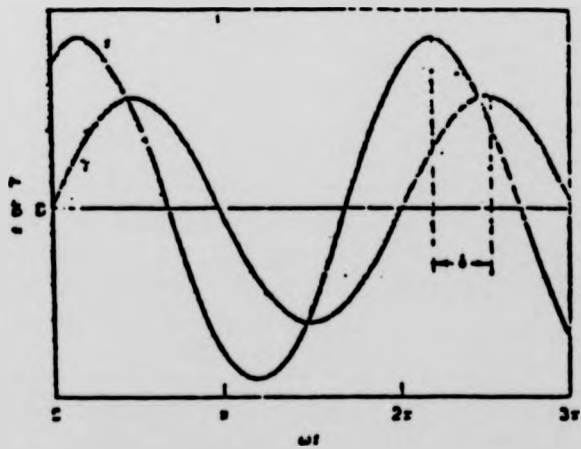


Fig. 3.4 Stress and strain as a function of time in the application of a sinusoidal strain to a viscoelastic specimen.

defined as⁷⁴:

$$E' = (S_0 / \gamma_0) \cos \delta \quad (3.21)$$

Where E' is the amount of stored energy per cycle, and

$$E'' = (S_0 / \gamma_0) \sin \delta \quad (3.22)$$

where E'' is the amount of energy dissipated by the material as heat during one cycle. The ratio of the two is given by the equation:

$$\tan \delta = E'' / E' \quad (3.23)$$

$\tan \delta$ is the amount of damping in the system or the energy loss per cycle. From these two quantities, the imaginary part (E'') and the real part (E'), the complex elastic modulus (E^*) can be calculated from the equation:

$$E^* = E' + i E'' \quad (3.24)$$

The absolute value of the complex elastic modulus (E^*) is given by the equation:

$$E^* = (E'^2 + E''^2)^{1/2} \quad (3.25)$$

The Rheovibron will measure the complex elastic modulus (E^*) and $\tan \delta$.

3.14.3 Experimental.

Polymer samples were analyzed in the form of rectangular strips. These films were prepared by a compression molding technique using a hot press. The

polymer was placed in between two PTFE (polytetrafluoroethylene) 0.25 cm thick plates and a small pressure was applied. The sample was heated to the required temperature, and the required pressure needed to form polymer film was applied for two hours. From the pressed film a rectangular strip was cut (using single strokes of a sharp razor) and the length, the thickness and the breadth of the polymer film were measured by micrometer. The polymer strip was mounted in the metal chucks of the instrument and the oven lid was closed. Cooling of the sample was achieved by passing oxygen-free-nitrogen (OFN) through a cooling coil immersed in liquid nitrogen and then the instrument heating block. To avoid breaking the film during cooling the tension on the film was constantly monitored. Heating of the sample was achieved by continuously varying the input voltage to the heating block and the output was monitored by a copper-constantan thermocouple and displayed on a digital voltmeter reading to ± 0.01 mV.

3.14.4 Data analysis.

The values of the oven temperature were monitored by the output of a copper-constantan thermocouple using a calibrated "Schnader" digital voltmeter reading to ± 0.01 mV. These values were converted to the corresponding temperature using a calibration curve. The complex elastic modulus can be expressed by:

$$E^* = (2l / F.D.A.) \times 10^8 \quad (3.26)$$

Where l is the length of the strip in (cm), D is the dynamic force instrument setting, F is the amplitude factor obtained from a specific table⁷⁵, and A is the cross section area in cm^2 . The cross section area of the strip can be obtained from the equation:

$$A = txd \quad (3.27)$$

where t is the thickness of the polymer film and d is the breadth of the polymer film. From equation (3.26) the value of the complex elastic modulus (E^*) can be calculated at minute intervals in Nm^{-2} . Log-linear graph paper was used to plot the value of $\tan \delta$ and E^* as a function of temperature.

3.15 TORSIONAL BRAID ANALYSIS

3.15.1 Introduction.

Torsional braid analysis (TBA) is an extension of the pendulum method for examining the dynamic mechanical behaviour of a polymer. A torsional braid analyser model 100-B 1 (Chemical Instrument Corporation of New York) was used in this study. The torsional braid analyser differs from the torsional pendulum mainly in that the sample specimen is a composite of a multifilamented glass fibre substrate and the polymer which is to be tested.

Torsional braid analysis was developed by J K Gillham⁷⁶ and a schematic diagram of the instrument is shown in Figure 3.5. It consists of a cylindrical column constructed so as to enclose the mass of the torsional pendulum. Suspended on the end of the braid is a circular glass disc for which a linear relationship exists between intensity of the transmitted light and its angular displacement. The specimen is kept in a controlled atmosphere. The specimen is prepared by impregnating a multifilament glass fibre braid, which acts as a support for a mechanically weak sample, with a solution of less than 100 mg of polymer. The mechanical oscillation is initiated at the top of the pendulum while a transducer senses the oscillation electrically. Typical strip-chart records of damping waves are shown in Figure 3.6.

3.15.2 Theory.

From the damped wave of a homogeneous rod undergoing free torsional oscillations, two parameters can be measured. The first parameter is the complex shear modulus (G^*) which consists of the component (G') the real part and (G'') the imaginary part, so that

$$G^* = G' + i G'' \quad (3.28)$$

The second parameter is the logarithmic decrement (Δ) which is obtained from successive amplitudes (A_n, A_{n+1}) of a decaying wave and is given by the equation:

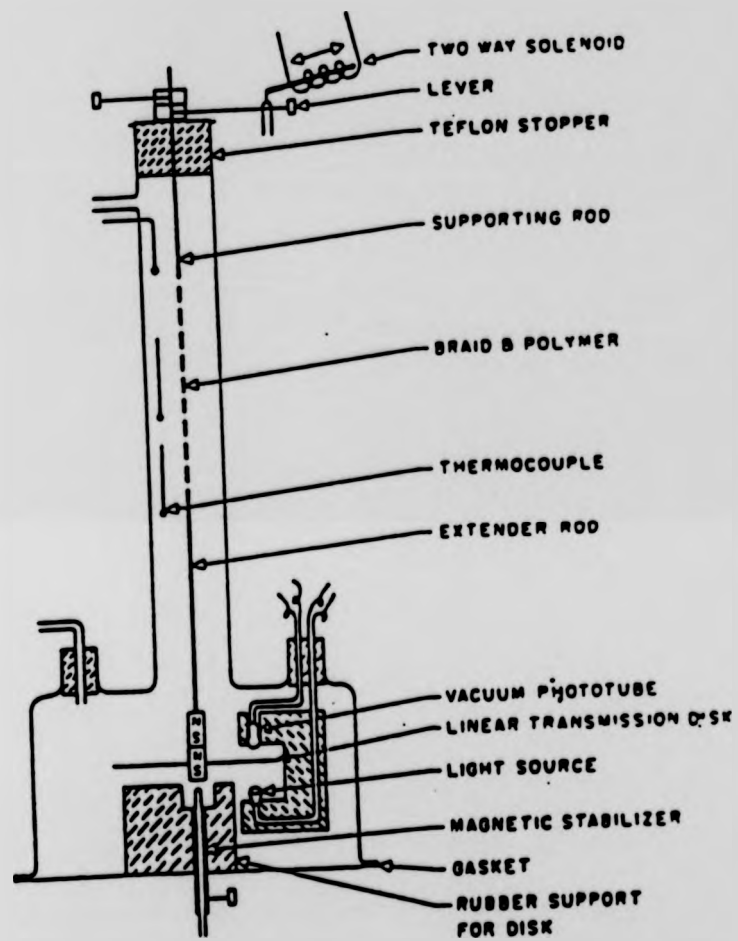


Fig. 3.5 Torsional braid apparatus (schematic).

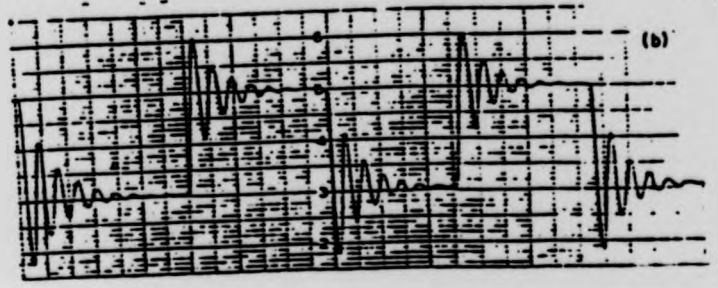
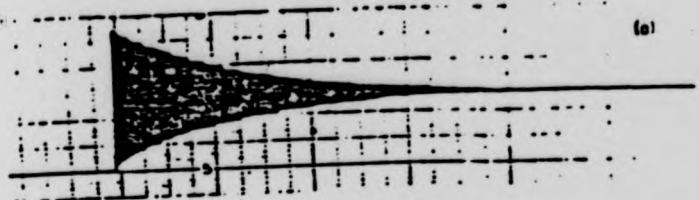


Fig. 3.6 Characteristic output of T.B.A. instrument: (a) glassy state, (b) approach to transition, (c) transition region. (note drift of neutral position).

$$\Delta = \ln \frac{A_n}{A_{n+1}} \quad (3.29)$$

The real component (G') of the complex shear modulus (G^*) is directly proportional to the energy stored in the deformed sample and is given by the equation⁷⁷:

$$G' = \frac{2Ll}{\pi r^4} \omega^2 (4\pi^2 + \Delta^2) \quad (3.30)$$

where ω is the frequency of the damped wave, I is the moment of inertia, Δ is the logarithmic decrement given by equation (3.29), r is the radius of the specimen and L is the length of the specimen. The logarithmic decrement (Δ) is related to the real component (G') and the imaginary component (G'') of the complex shear modulus (G^*) by the approximate relation.

$$\Delta = \pi \frac{G''}{G'} \quad (3.31)$$

The real component of the shear complex modulus and the logarithmic decrement, represent the storage and the loss of energy on cyclic deformation and they can be plotted as a function of time or temperature. In TBA the measurement will be relative rather than absolute because the specimen consists of the polymer and the braid and it is difficult to define the polymer dimensions accurately. In torsional braid analysis the relative rigidity parameter, $1/p^2$ where p is the period of oscillation, is used as a measure of the modulus and is simply ω . This expression implicitly assumes that any changing contribution from both damping

characteristics and dimensional changes to $1/p^2$ are dominated by changes in the modulus of the polymer. The mechanical damping index ($1/n$), where n is the number of oscillations between two arbitrary but fixed boundary conditions in a series of waves, is directly proportional to the logarithmic decrement. These parameters, relative rigidity ($1/p^2$) and the mechanical damping index ($1/n$), which refer to the composite specimen can be interpreted in terms of physical or chemical changes in the polymer.

3.15.3 Experimental.

The braid was first cleaned in order to remove unwanted surface coatings on the glass fibres which interfere with measurement. This was achieved by immersion of the braid in chromic acid for seven days followed by repeated washing in hot distilled water, then drying at 380K. The specimen was prepared by impregnating a multi-filament glass fibre with a solution of less than 100 mg of polymer. The braid was dried under tension (70 g) for at least one day in vacuum at room temperature to form a polymer-braid composite which was then placed in the centre stainless steel tube of the TBA as shown in Figure 3.5. Adjustment of the extension rods, magnetic stabilizer, and optical transducer were made as described in the manufacturer's instruction manual. The sample chamber was continually flushed by oxygen-free-nitrogen (OFN). Cooling was achieved by passing OFN first through a cooling coil immersed in liquid nitrogen and then the instrument at a

flow rate of $20 \text{ dm}^3 \text{ min}^{-1}$. The sample was then allowed to stabilise at the starting temperature (normally 83K) for 20 minutes⁷⁸. The CIC (TBA) apparatus may be operated over the temperature range 83 K - 573 K. The temperature was allowed to rise slowly by gradually reducing the flow rate of the cooling gas until it reached the ambient temperature. A Hewlett Packard 220 linear temperature programmer was used to control further increases in temperature. The damped oscillations of the polymer/braid composites were initiated at 2.5 min. intervals and the temperature was recorded on a Bryans 10 mV. chart recorder as the output of the centre iron-constantan thermocouple.

3.15.4 Data analysis.

The output of the centre iron-constantan thermocouple which was recorded on the chart paper was converted to the corresponding temperature by using a specific table⁸⁰. Typical damped waves for a polymer sample are shown in Figure 3.6. The mechanical damping index ($1/n$), where n is the number of oscillations occurring between two arbitrarily chosen boundary amplitudes in the decay wave was plotted as $\log (1/n)$ against temperature.

3.16 THERMOGRAVIMETRIC ANALYSIS (TGS)

3.16.1 Introduction

Thermogravimetric analysis is a dynamic technique which measures the weight loss of a polymer as a function of temperature. Honda⁸⁰ in 1915 was the first to build a thermobalance to record the change in the weight of a sample when it is exposed to heat and this was called isothermal thermogravimetry. The non-isothermal or dynamic thermal thermogravimetry will record the change in the weight of sample as a function of both temperature and time. Thermogravimetric analysis has been used chiefly to study the thermal decomposition and stability of polymers. There are two main types of thermobalance, a vertical and a horizontal, as shown in Figure 3.7. A thermogravimetric system model TGS-2 (Perkin-Elmer U.S.A.) was used in this study. It consists of the following independently packaged units : the electronic balance control, the heater control unit, the thermobalance analyser, the temperature program controller, the first derivative computer and recorder.

3.16.2 Experimental.

The balance was zeroed by using the coarse and the fine zero, and the instrument was settled. A well dried (90-95 mg) sample was placed in the pan and the thermal degradation was carried out in an atmosphere of OFN at constant flow rate.

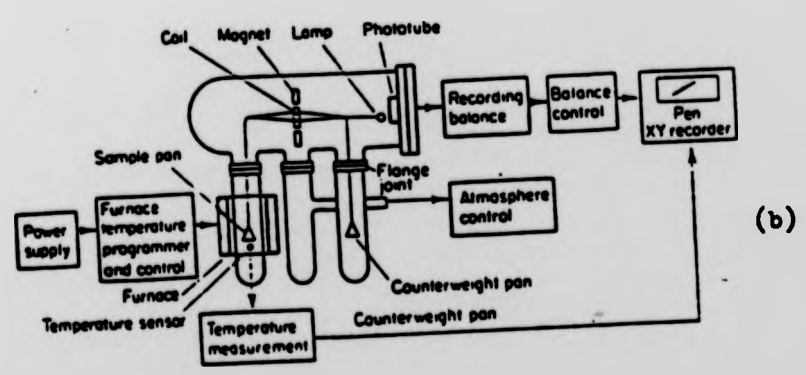
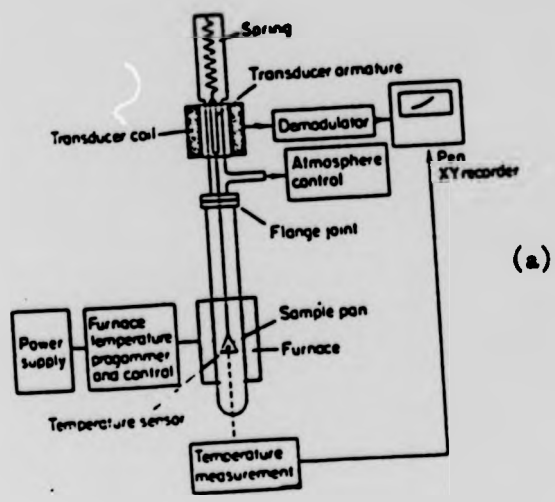


Fig. 3.7 Thermobalance: (a) schematic representation of a vertical balance, (b) schematic representation of a horizontal balance.

3.16.3 Data analysis.

The weight loss is detected by measuring the difference in the weight of sample and reference. These are amplified and displayed on the Y-axis of a chart recorder with the X-axis representing the temperature. The weight loss of a sample was plotted as a function of temperature.

3.17 THERMAL VOLATILIZATION ANALYSIS (TVA)

3.17.1 Introduction.

Thermal volatilization analysis (TVA) is a technique described and developed by McNeil⁸¹. It is used for characterization of polymers and the study of the thermal degradation processes. A number of papers discussing studies of polymer degradation have been published^{82,83}. The equipment required for (TVA) is simple and the quantity of information obtained from this technique makes it a very useful thermo-analytical technique. A diagram for a four line differential condensation thermal volatilization analysis system is shown in Figure 3.8. The problems of sample shape and atmosphere effects are minimized in thermal volatilization by the use of a relatively large sample area and high vacuum conditions.

3.17.2 Experimental.

The polymer sample (25-50 mg) is placed in the flat bottom tube and the apparatus pumped down to the best vacuum

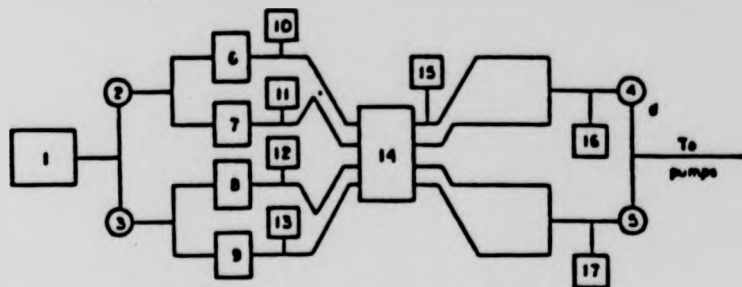


Fig. 3.8 Four line differential condensation TVA system.

1 = heated sample, 2, 3, 4, 5 = stopcocks (large bore, right angle type), 6, 7, 8, 9 = initial cold traps, 10, 11, 12, 13 = Pirani gauge heads, 14 = main cold trap, 15 = exhaust pirani gauge head, 16, 17 = product collection points.

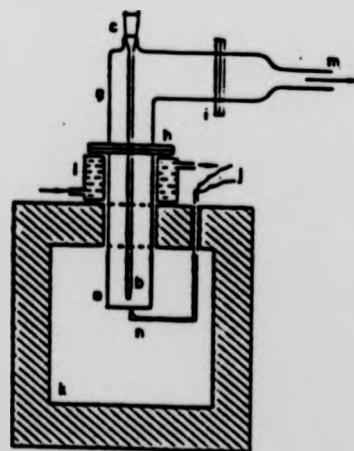


Fig. 3.9 TVA oven, sample tube, lid assembly.

a = sample tube, b = inlet tube; c = ground joint, g = lid, h, i = flange joints, j = thermocouple leads, k = oven, l = water jacket, m = outlet to trap system and pumps, n = thermocouple junction.

without coolant on the initial trap but with the main trap at 77 K. The sample is heated at a linear rate, increasing from room temperature to the required final temperature usually from 298 K to 773 K at a rate of 10 K min^{-1} . Figure 3.9 shows the thermal volatilization oven. Coolant is placed in the initial traps and the zero adjustments are then made on the pirani gauge. A pirani gauge measures the pressure in the system at the same point intermediate between the sample and the trap. The four initial traps (6, 7, 8 and 9) are at different temperatures 273, 228, 198 K and 73 K. The stopcocks 4 and 5 are then closed and the sample is heated. The pirani gauge output is recorded as a function of temperature or time. Mass spectrometer and infrared analysis were carried out on the volatile and non-volatile materials emanating from the decomposition process.

CHAPTER FOUR

PREPARATION OF MONOMERS, COPOLYMERS
AND MODIFIED POLYMERS

RESULTS AND DISCUSSION

4.1 THE PREPARATION OF MONOMERS

4.1.1 Preparation of monoesters

Three monoesters (monomethyl, mono-n-butyl and mono-n-heptyl itaconates) were prepared by the method described in section 3.1.1. The percentage yield of each monoester is shown in Table 4.1.

TABLE 4.1 Mono-n-alkyl itaconates yields

Ester	Yield (%)
Monomethyl itaconate	60
Mono-n-butyl itaconate	65
Mono-n-heptyl itaconate	60

The n.m.r. spectra of these monoesters were studied as 5-10 W/V solution in deuterated chloroform. A Hitachi-Perkin Elmer R 24 High Resolution NMR Spectrometer was used in this study. The n.m.r. spectra of these monoesters are shown in Figure 4.1. The i.r. spectra of these monoesters are shown in Figure 4.2.

4.1.2 Preparation of diesters

Three diesters (dimethyl, di-n-butyl and di-n-heptyl itaconates) were prepared by an acid catalysed method described in section 3.1.2. The percentage yields of these diesters are shown in Table 4.2.

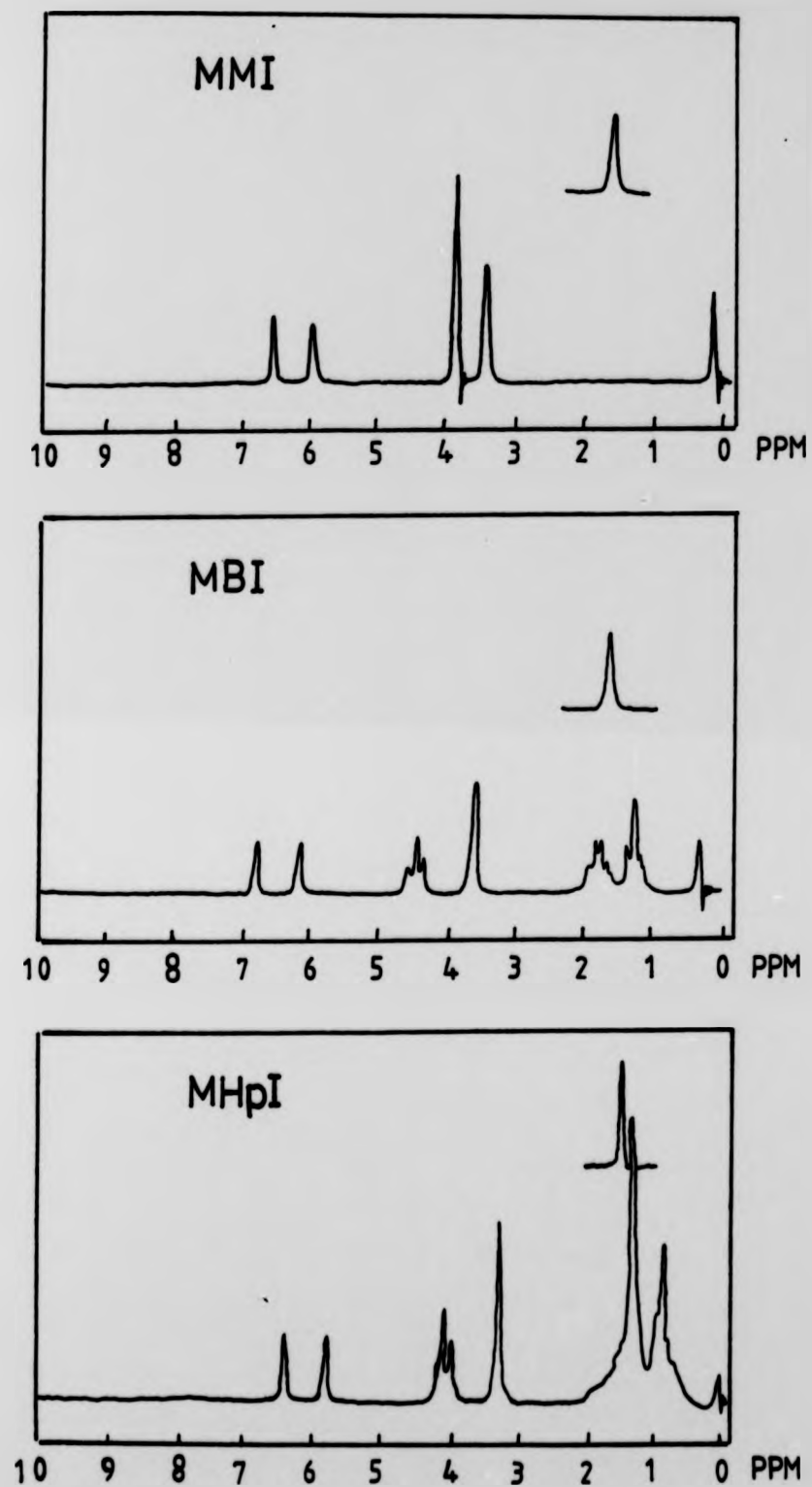


Fig. 4.1 NMR of indicated mono-n-alkyl itaconic acid esters.

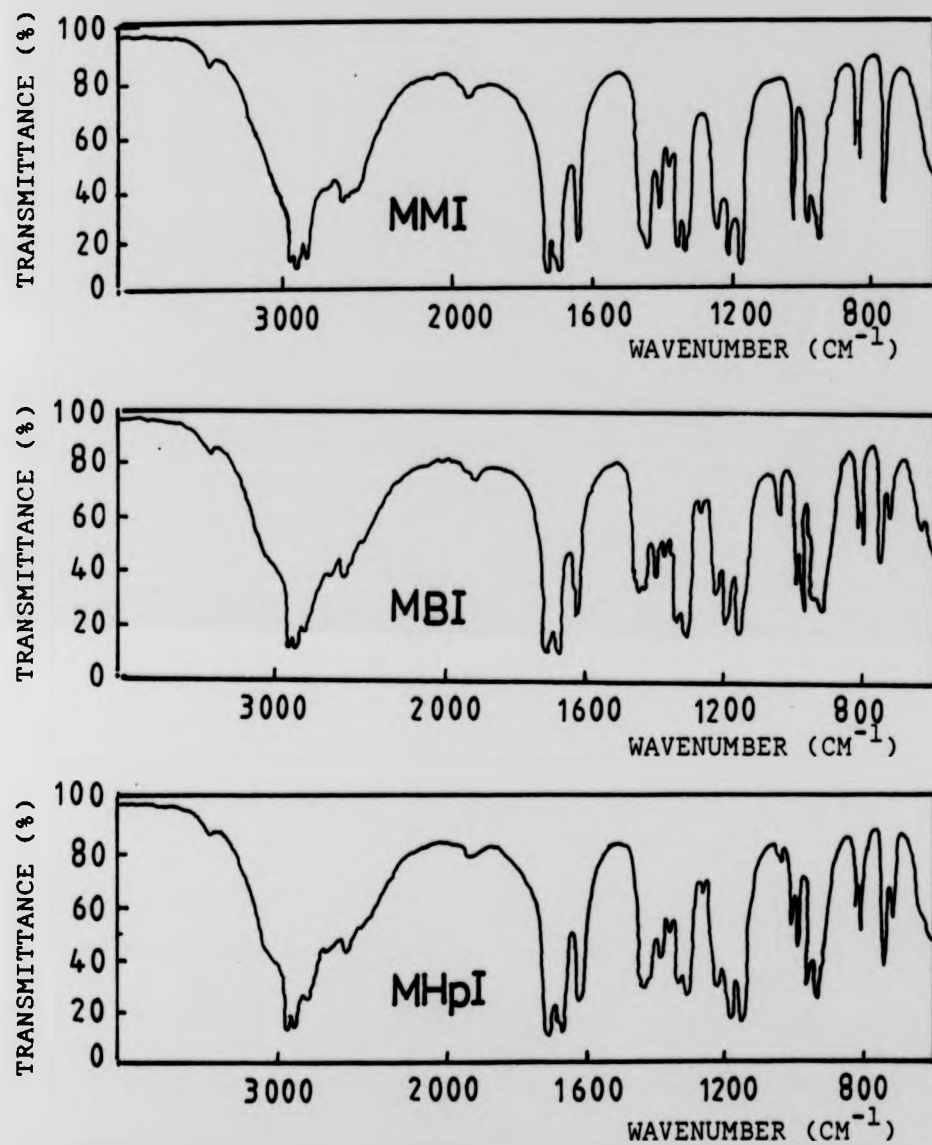


Fig. 4.2 Infrared spectra of indicated mono-n-alkyl itaconic acid esters.

TABLE 4.2 Di-n-alkyl itaconates yields

Ester	Yield (%)
Dimethyl itaconate	70
Di-n-butyl itaconate	70
Di-n-heptyl itaconate	70

The n.m.r. spectra and the i.r. spectra of these diesters are shown in Figures 4.3 and 4.4 respectively.

4.2 DISCUSSION

The main impurities in the preparation of the monoesters were unreacted itaconic acid, unreacted alcohol, itaconic anhydride and diester. Fractional distillation and recrystallization steps must be undertaken to ensure complete removal of these impurities. In order to increase the percentage yields of these monoesters and to reduce contamination, the following steps were implemented.

(i) The acetyl chloride, which was used as catalyst, should be distilled and added dropwise to the warm reaction mixture of alcohol and itaconic acid.

(ii) Stirring the warm reaction mixture during the addition of acetyl chloride will help to increase the percentage yield of the monoester.

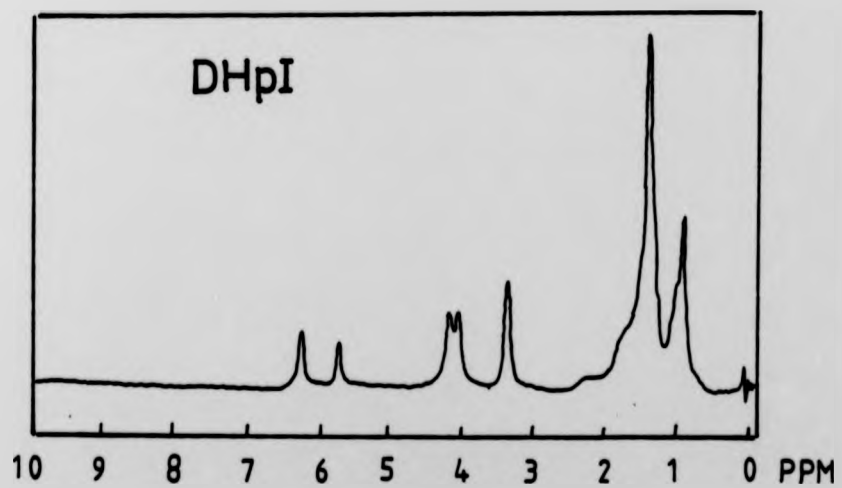
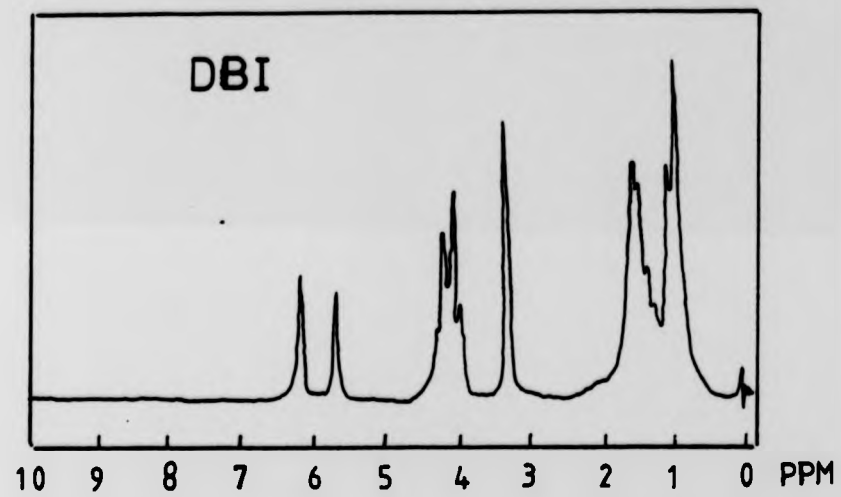
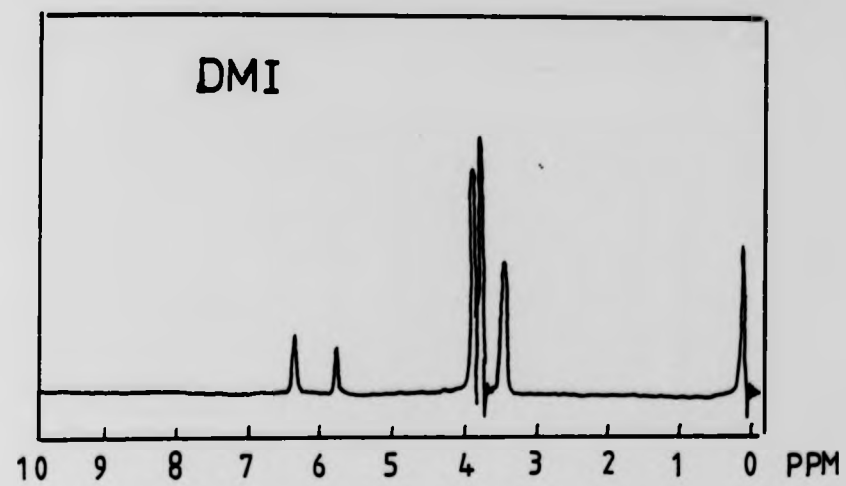


Fig. 4.3 NMR of indicated di-n-alkyl itaconic acid esters.

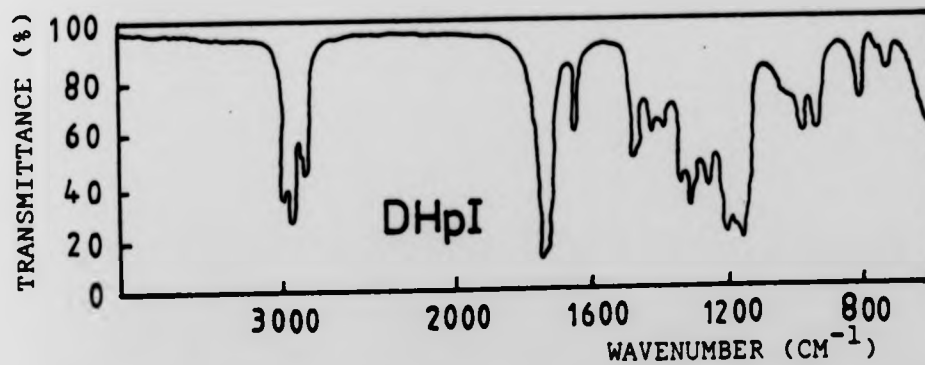
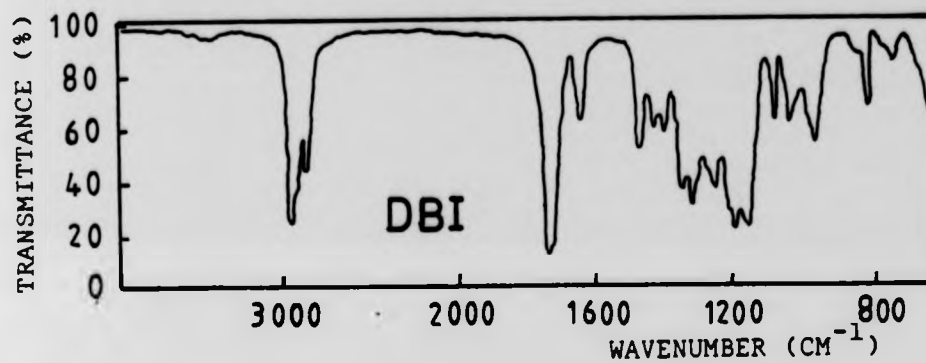
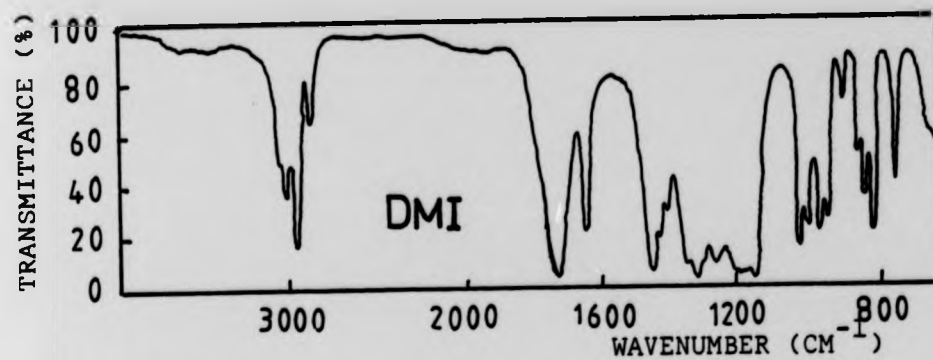


Fig. 4.4 Infrared spectra of indicated di-n-alkyl itaconic acid esters.

(iii) Recrystallization using a benzene/petroleum mixture (1:1) was carried out to ensure complete removal of impurities.

The main impurities in the preparation of the diesters were unreacted itaconic acid, unreacted alcohol and itaconic anhydride. Fractional distillation of the crude product followed by vacuum distillation of the pure product must be undertaken to ensure the removal of these impurities and to obtain pure diester. In order to increase the percentage yield and to reduce impurities the following steps were implemented.

(i) The use of 35 cm³ concentrated sulphuric acid was essential to increase the percentage yield of the diester. Sulphuric acid acted as catalyst and absorbed water which is the side product of the esterification.

(ii) The benzene layer which contains the diester should be dried carefully. Any trace of water may hydrolyse the diester.

(iii) The reaction time should be more than five hours in order to increase the percentage yield of the diester. However, a very long time will not increase the percentage yield because esterification is an equilibrium reaction. The rate of esterification depends on the structure of the acid and the alcohol⁸⁴.

4.3 COPOLYMERIZATION AND COMPOSITION OF COPOLYMERS

4.3.1 Copolymerization.

A bulk copolymerization technique was used to copolymerize mono with diesters of itaconic acid and this is described in section 3.2. This technique proved to be easy, quick and give satisfactory results. The following important steps had to be carried out in order to copolymerize the monomers and to obtain a pure copolymer:

- (i) The solid monoester was dissolved in the diester before the addition of the radical initiator.
- (ii) Monomers and radical initiator were distilled or recrystallised and characterised before copolymerization to ensure there were no impurities in the monomers and the radical initiator.
- (iii) The copolymer was purified by three precipitations to ensure that there were no monomers trapped in the copolymer. This was achieved by checking the i.r. spectrum after each precipitation.

4.3.2 The i.r. spectra of the copolymers

Representative i.r. spectra are shown in Figure 4.5. The i.r. spectra of these copolymers show a characteristic absorption at the region ($\sim 1735 \text{ cm}^{-1}$). This is due to the C=O stretch. The region ($\sim 1600 \text{ cm}^{-1}$) is clear from any absorption which confirms that the copolymer is clean and no residual monomer is trapped.

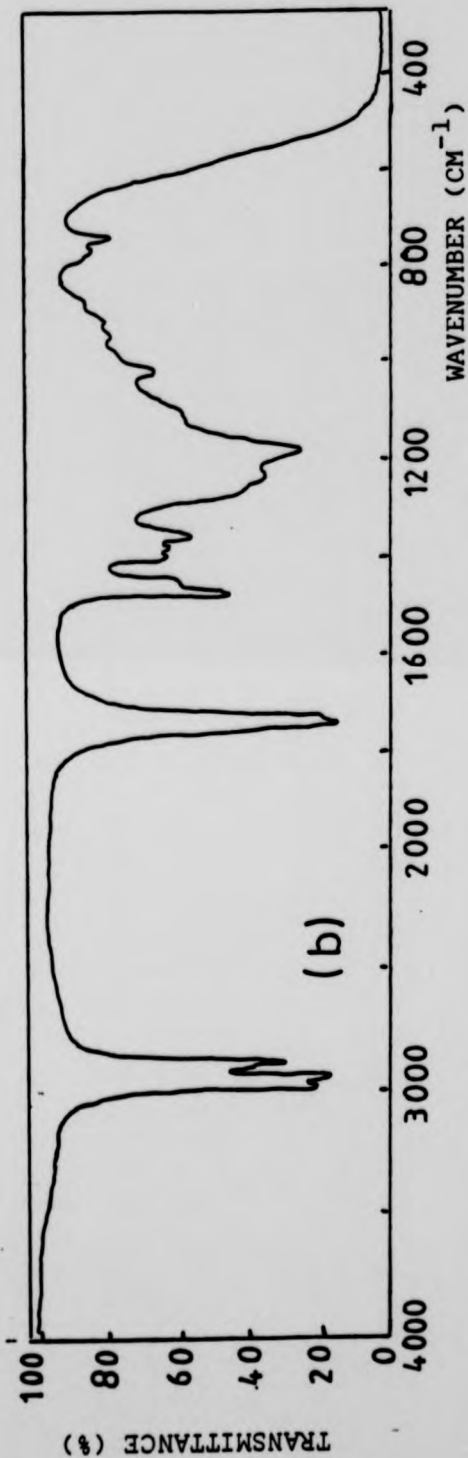
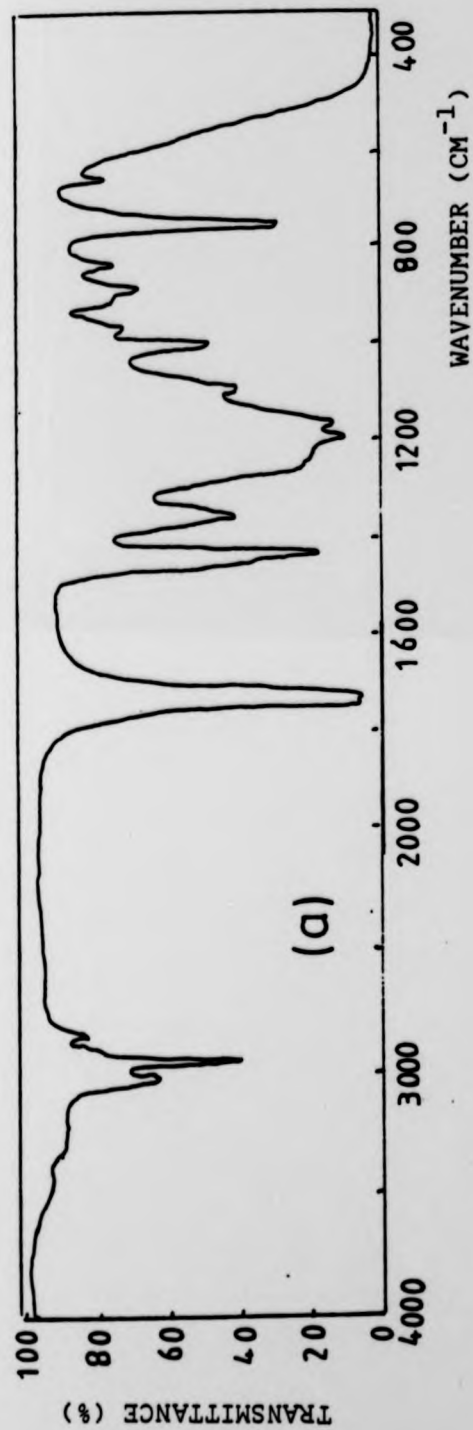


Fig. 4.5 Infrared spectra for (a) poly(MMI+DMI), with mole % of MMI 10.5
 (b) poly(MHpI+DHpI), with mole % of MHpI 4.93.

4.3.3 Discussion.

A bulk copolymerization technique was used because it is convenient and the isolation of the copolymers is a relatively easy task. The conversion was kept to less than 15% in order to avoid composition drift which will result in an uneven distribution of the two comonomers. The copolymer should be dried under vacuum at room temperature without heating. Heating may lead to the formation of the anhydride.

4.4 COMPOSITION OF THE COPOLYMERS

The composition of the copolymers prepared in section 3.3 were analysed by means of the two methods described in section 3.7. The first method was a non-aqueous potentiometric titration of the carboxyl group of the monoester in the copolymer systems, poly(MHpI+DHpI) and poly(MBI+DBI). In this method each pendant acid group (-COOH) corresponds to one monoester unit and titration of the weak acid with a strong base was carried out to determine the amount of the monoester in the copolymer⁸⁵. The weight percentage of the monoester in the copolymer can be obtained if the weight of the copolymer taken is known and the amount of the base solution which is required to neutralise all of the carboxylic acid groups in the copolymer is measured. From a plot of the pH values against volume of the base solution

used, the end point can be obtained. The end point is the point on the titration curve at which a tangent to the curve has a maximum slope and Figure 4.6 shows typical titration curves. From this method the mole percentage of the monester in the copolymer can be calculated.

4.4.1 Copolymer compositions.

The mole percentage of the monester in some of the copolymers is shown in Table 4.3.

TABLE 4.3 Determination of the mole percentage of monoester in the copolymer

Sample No.	Copolymer System	Mol % of monoester in feed	Mol % of monoester in copolymer
10	Poly(MBI+DBI)	15.9	33.05
11	Poly(MBI+DBI)	61.4	73.0
5	Poly(MHpI+DHpI)	7.0	6.3
9	Poly(MHpI+DHpI)	42.4	50.05

4.4.2 Discussion

A non aqueous medium was used owing to the insolubility of the copolymers in water. From Table 4.3 it can be seen that the mole percentage of the monoester in the feed differs from that in the copolymer and this is due to the difference in reactivity between the mono- and diester⁸⁵. It has been found that poly(MHpI+DHpI) systems are not ideal and there is a composition drift in favour of MHpI, whilst the poly(MBI+DBI) systems are more ideal in that the growing

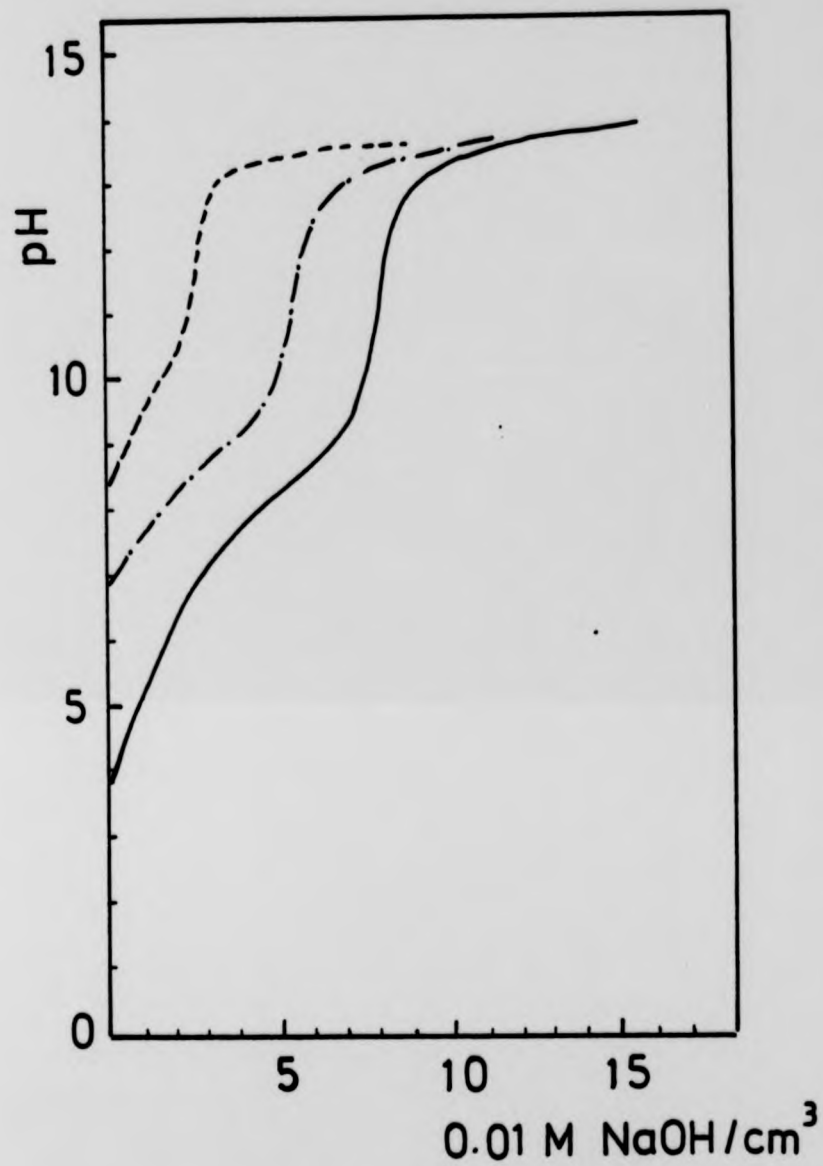
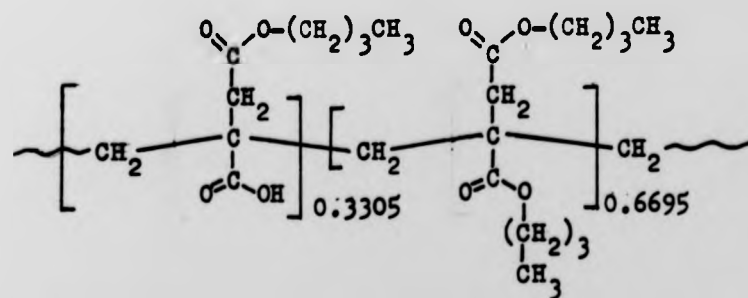


Fig. 4.6 Titration curves for the poly(MHpI+DHpI) copolymers.

chain radical adds preferentially to the other monomer faster than to its own⁸⁵.

4.5 MICROANALYSIS

The second method used to determine the composition of the copolymer was microanalysis and this method proved to be useful for analysing the modified polymers prepared in section 3.4 and polymer-metal complexes prepared in section 3.5. To calculate the mole percentage of the monoester in copolymer, the following method was used: Suppose we want to know the mole percentage of MBI in poly(MBI+DBI) prepared in section 3.3. If we assume that the mole percentage of MBI in the copolymer is 33.06, then



1 Calculate the total molecular weight:

$$(9 \times 12.01115)0.3305 + (13 \times 12.01115)0.6695 + (4 \times 15.9994)0.3305 + (4 \times 15.9994)0.6695 + (14 \times 1.00797)0.3305 + (22 \times 1.00797)0.6695 = 223.77 \text{ g.mol}^{-1}.$$

2 Calculate the percentage of each element:

$$\%C = (140.26621/223.77408) \times 100 = 62.68$$

$$\%O = (63.9976/223.77408) \times 100 = 28.59$$

$$\%H = (19.510267/223.77408) \times 100 = 8.71$$

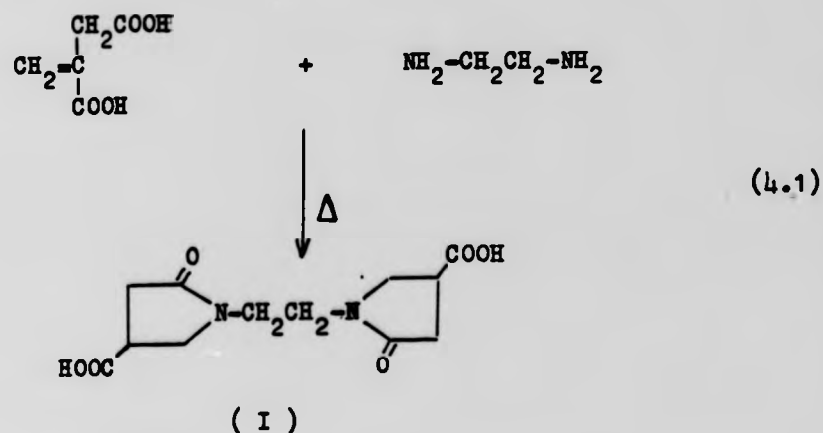
3 Compare the calculated values with the values obtained from the microanalysis:

%C	%H	
62.68	8.71	Cal.
62.80	8.82	Found

4 If the mole percentage of MBI in the copolymer was higher or lower, different values will be obtained for the elemental analysis.

4.6 THE PREPARATION OF ITACONATE COPOLYMERS WITH PENDANT ETHYLENE AMINE GROUPS

A polymeranalogous reaction was carried out between itaconate copolymers containing carboxyl groups and EN, DETA, TETA or TEPA in the presence of DCC as described in section 3.4. It was reported that the preparation of monomers of itaconic acid with pendant groups like EN was not successful¹⁸. The reaction between ethylenediamine and itaconic acid or its esters will give a cyclic product¹⁸.



A Michaelis type of addition occurs when itaconic acid is reacted with ethylenediamine which leads to the formation of 1,1-ethylene bis(5-oxo-3-pyrrolidine carboxylic acid) (I). A polymeranalogous reaction was the only easy way to prepare a copolymer of itaconic acid containing pendant ethylene imine groups. This was achieved by the use of DCC which proved to be a useful reagent in these polymer-analogous reactions^{86,87}.

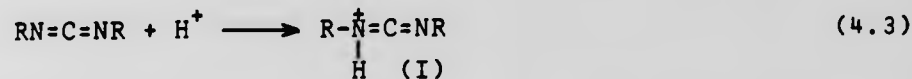
4.6.1 Mechanism of the reaction.

Dicyclohexylcarbodiimide has been used in peptide synthesis⁸⁸ and an amide linkage will be formed when carboxylic acid is reacted with amine in the presence of DCC.

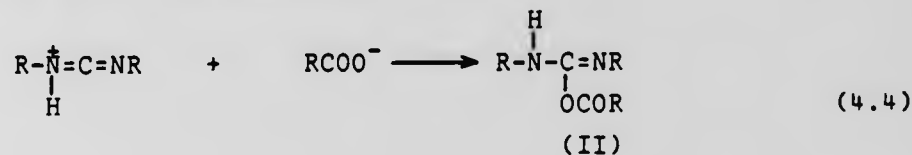


The mechanism of the amide formation under the influence of DCC has been studied by several workers⁸⁹. The initial

step was the protonation of the DCC to form the intermediate (I).



This intermediate (I) was attacked by a carboxylate anion to form the O-acylurea (II).



The O-acylurea (II) is the reactive intermediate and will react with amine to form the peptide linkage



4.6.2 I.r. spectra of the modified polymers.

The modified polymers show two characteristic absorption, the first one is in the region of $\sim 3400 \text{ cm}^{-1}$, due to the (N-H) stretch and the second absorption is in the region of $\sim 1600 \text{ cm}^{-1}$ due to the (N-H) bending vibration⁹⁰. Figure 4.7 shows the i.r. spectra of poly(MHpI+DHpI), where the mole percentage of mono-n-heptyl itaconate is 13.0, before and after the reaction with TEPA. The two characteristic absorptions are observed. Figure 4.8 shows the i.r. spectra of poly(MHpI+DHpI), where the mole percentage of the mono-n-heptyl itaconate is 13.0, after reaction with EN and TETA. The intensity of the absorption in the region $\sim 1600 \text{ cm}^{-1}$

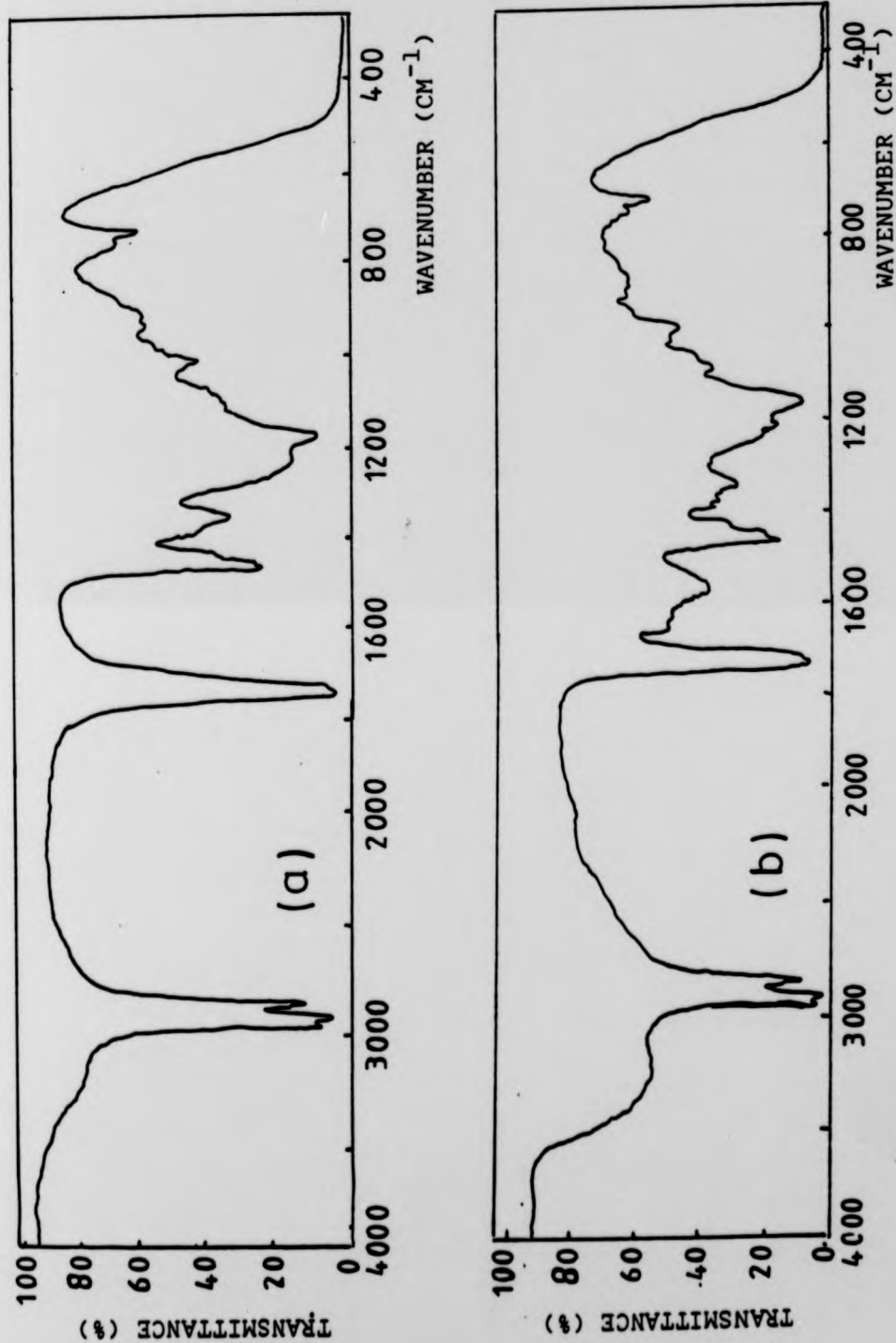


Fig. 4.7 Infrared spectra for (a) poly(MHpI+DHPi), with mole % of MHPi 13.0
 (b) poly(MHpI+DHPi)/TEPA, with mole % of TEPA 13.0.

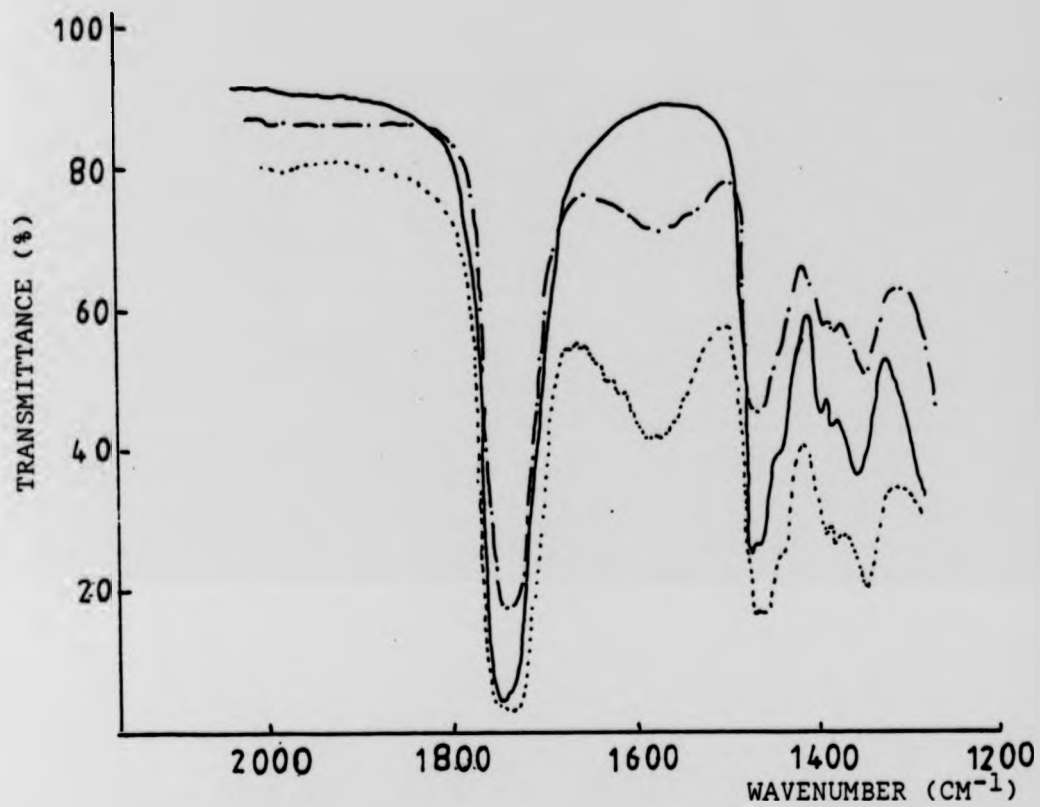


Fig. 4.8 Infrared spectra for (—) poly(MHpI+DHpI) mole percentage of MHPi 13.0, (---) poly(MHpI+DHpI)/EN, mole percentage of EN 13.0, (.....) poly(MHpI+DHpI)/TETA, mole percentage of TETA 13.0.

increases when the side chain becomes TETA, due to the increase in the number of secondary amines.

4.6.3 Discussion

A polymeranalogous reaction was carried out to prepare copolymers of itaconic acid containing a pendant ethylene amine group because monomers of itaconic acid will give a cyclic product as shown in equation 4.1. This polymeranalogous reaction was carried out under homogeneous conditions and the following steps were followed during the preparation of the modified polymers:

- 1 The copolymer should be completely dissolved in the solvent and a clear solution should be obtained before the addition of reactants. A low concentration of copolymer solution was used to open the coil structure of polymer and to allow the reactant to move freely and to avoid a high viscosity during the reaction.
- 2 The DCC was melted, weighed and added to the copolymer solution, followed by the addition of amine. The reaction mixture was heated to a temperature below the boiling point of the solvent for a short period to encourage the reaction then left stirring for 24 hours.
- 3 Both DCC and amine were used in excess.
- 4 Filtration was carried out to ensure the removal of any side product and three precipitations were

carried out to ensure the removal of unreacted DCC and amine.

- 5 These modified polymers are very reactive; heating under vacuum will lead to chemical reaction and evolution of gases. Care must be taken in drying and storing these polymers.

The i.r. spectra of these modified polymers show that the absorption in the region 3400 cm^{-1} is broad and this is because of hydrogen bonding⁹¹. The second absorption which is due to the (N-H) bonding is also broad appearing in the range from 1640 to 1560 cm^{-1} . It was confirmed that as the number of nitrogens in the side chain increases the intensity of the absorption in the region 1640 to 1560 cm^{-1} increases.


CHAPTER FIVE
ION BINDING
RESULTS AND DISCUSSION

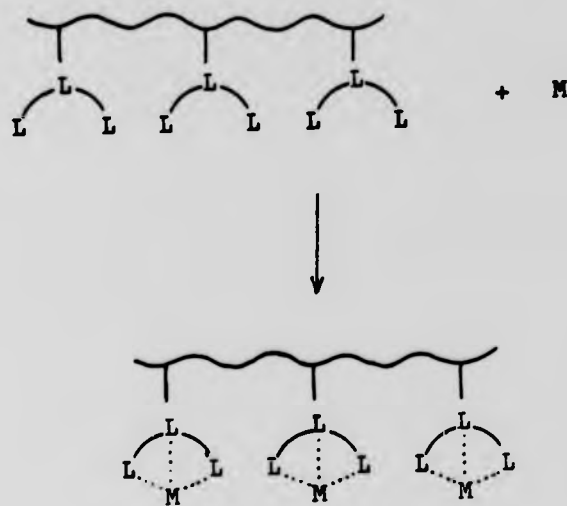
5.1 METAL ION BINDING

Copolymers which contain TEPA in the side chain were reacted with metal halides as described in section 3.5. Tetraethylenepentamine is a multidentate ligand and the complexation of this ligand with some metal halides has been studied.⁹² The binding between the modified polymers which contains TEPA in the side chain and metal halides was carried out in non-aqueous media. A visible region spectrophotometer was used to follow the complex formation. Two types of polymer-metal complexes have been prepared in this work.

5.2 POLYMER-METAL COMPLEXES

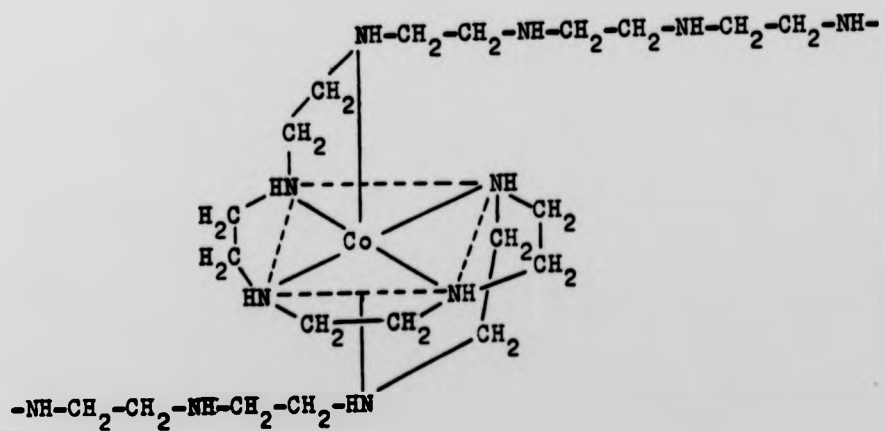
5.2.1 Polymer chelates.

A chelate was formed when a modified polymer, which contained a multidentate ligand (TEPA) in the side chain, was reacted with metal halides (Cobalt(II) chloride or copper(II) chloride) as shown in Scheme 1, where  represents TEPA and M is the cobalt(II) chloride or copper(II) chloride. It is difficult to define the structure and to study the complexation of these polymer chelates⁵⁴. The reaction between polyethyleneimine PEI (which is polymeric substance characterized by high coordinating power) and cobalt(III) compounds has been

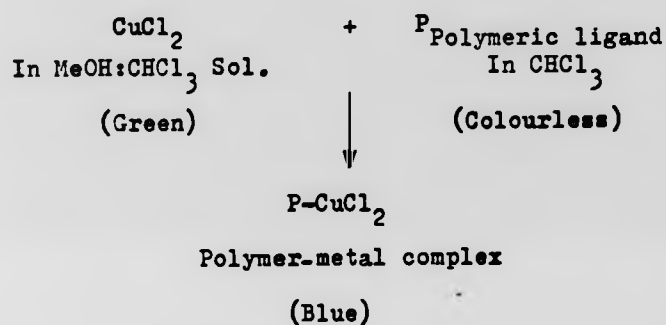


Scheme 1

reported⁹³. It was found that cobalt(III) is six coordinate with the nitrogen and the compound will have the following structure:

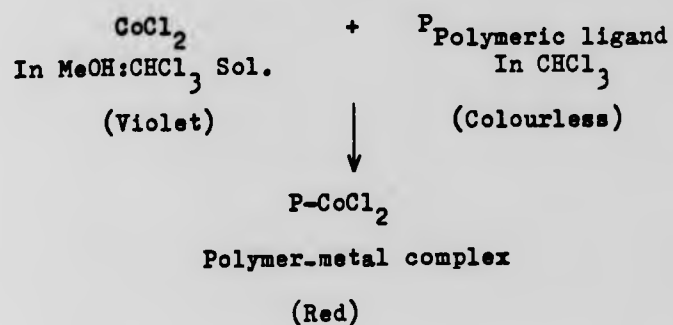


In this work the binding between the modified polymer (polymeric ligand) which contain TEPA in the side chain and cobalt(II) chloride or copper(II) chloride was carried out in non-aqueous media because the polymeric ligand was not soluble in water. The following equation simplifies the complex formation:



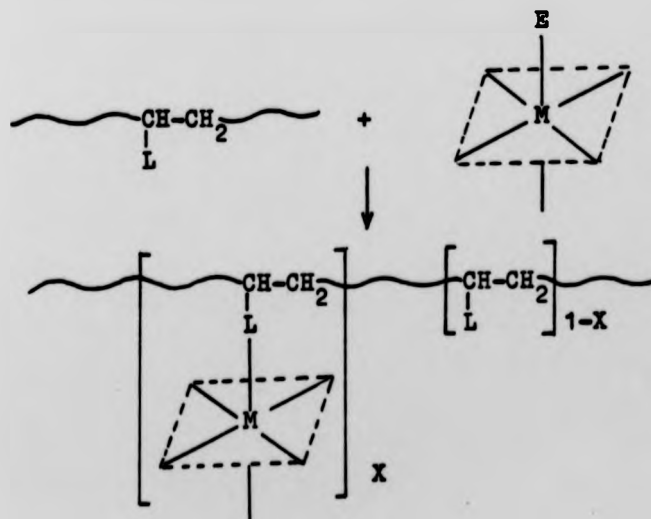
The colour of copper(II) chloride solution changes from green to blue (see figure 5.1) confirming the change in the substituent in the coordination sphere of copper(II) ion⁹⁴. The position of the new absorption band at $\sim 650\text{nm}$ is consistent with the formation of copper complex with nitrogen donors. The chloride ion (Cl^-) can be either coordinated chloride or ionic chloride.

In the case of cobalt(II) chloride solution the colour changes from violet to red, when it reacts with the polymeric ligand (the modified polymer which contains TEPA in the side chain). This confirms the change in the substituent in the coordination sphere⁹⁴ and the following equation simplifies the complex formation:



5.2.2 Pendant-type polymer-metal complexes

Two pendant polymer-metal complexes were prepared in this work and these are poly(MMI+DMI)/EN/[Co(en)₂Cl]²⁺2Cl⁻ and poly(MHpI+MHpI)/EN/[Co(en)₂Cl]²⁺2Cl⁻. The reaction between the modified polymer containing ethylenediamine in the side chain and a stable complex containing a weak ligand will give a pendant-type polymer-metal complex (Scheme II simplifies this reaction).

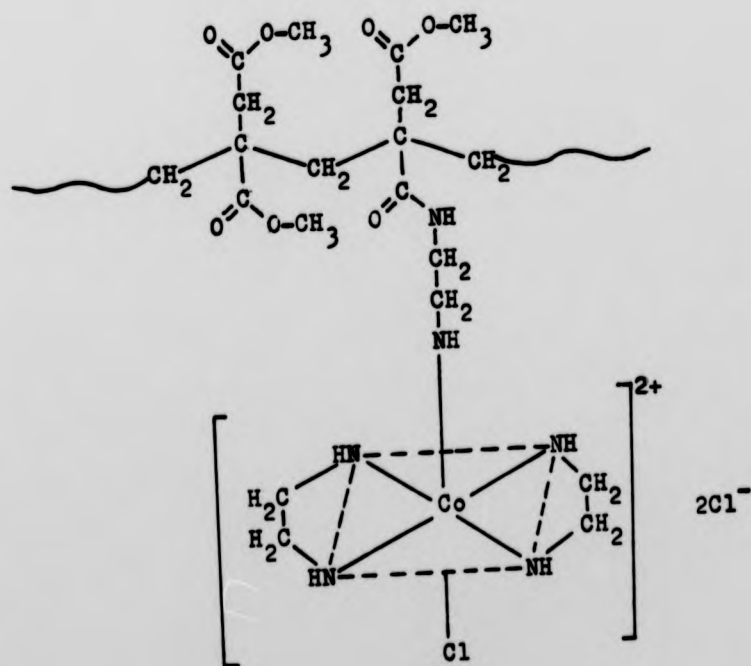
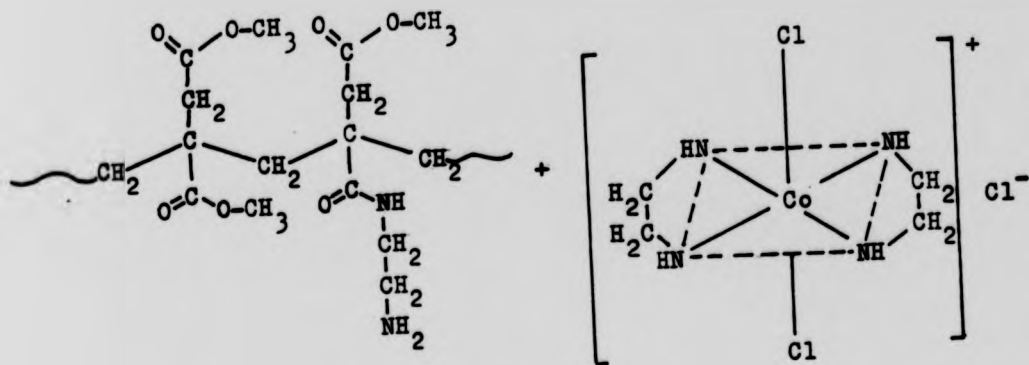


Scheme II

Where E is an elimination-ligand (weak ligand) and X is the degree of coordination. The degree of coordination can be defined as the molar ratio [metal complex/repeating unit of polymeric ligand]. If all the ligands in the polymer are coordinated to the metal complex, the value of (X) becomes 1⁵⁴. Tsuchida et al⁹⁵ reported the preparation of polymeric cobalt(III) complexes and found that the degree of coordination (X) reached a constant value of 0.65. It has been found that the degree of coordination is a function of time; as the time increases the degree of coordination increases until it reaches a constant value⁹⁵.

In this work trans[Co(en)₂Cl]Cl was used as a stable metal complex.

Poly(MMI+DMI)/EN/[Co(en)₂Cl]²⁺ 2Cl⁻ was prepared by a substitution reaction between the polymeric ligand poly-(MMI+DMI)/EN and trans[Co(en)₂Cl₂]Cl which contained an elimination ligand (weak ligand) as shown in Scheme III. In the case of trans[Co(en)₂Cl₂]Cl the colour changes from green to pink. This confirmed that only one chlorine atom was substituted⁹⁶. The elemental analysis for these two pendant-type polymer metal complexes, poly(MHpI+DHpI)/EN/[Co(en)₂Cl]²⁺ 2Cl⁻ is shown in Table 5.1. The degree of coordination (X) in the case of poly(MMI+DMI)/EN/[Co(en)₂Cl]²⁺ 2Cl⁻ is higher than that of poly(MHpI+DHpI)/EN/[Co(en)₂Cl]²⁺ 2Cl⁻, this is presumably because of the greater steric hindrance from the longer heptyl side groups.



Scheme III

TABLE 5.1 Elemental analysis of polymer with pendant metal complex.

Sample Number	Polymer	C	H	N	Cl	Co	Degree of coordination (X)
70	poly(MMI+DMI)/EN/ [Co(en) ₂ Cl] ²⁺ 2Cl ⁻	Found	47.70	6.0	5.38	5.10	2.80
		Cal.	47.79	6.01	5.41	5.13	2.84
69	poly(MHpI+DHpI)/EN/ [Co(en) ₂ Cl] ²⁺ 2Cl ⁻	Found	68.55	10.20	0.80	0.50	0.3
		Cal.	68.61	10.22	0.74	0.52	0.29
45	poly(MMI+DMI)/EN	Found	52.48	6.50	3.10	/	/
		Cal.	52.50	6.49	3.12	/	/
21	poly(MHpI+DHpI)/EN	Found	69.20	10.26	0.50	/	/
		Cal.	69.21	10.30	0.46	/	/

5.3 VISIBLE SPECTROPHOTOMETRY RESULTS

The reaction between the modified polymers which contain TEPA in the side chain and metal halides was followed by visible spectrophotometry. All the modified polymers were colourless and did not show any absorption in the visible region. The solvent system, chloroform: methanol, which was used to dissolve the metal halides and chloroform which was used to dissolve the modified polymers (polymeric ligands) show no absorption in the visible region. The metal halides, cobalt(II) chloride and copper(II) chloride, were dissolved in chloroform: methanol and showed a characteristic absorption in the visible region. Cobalt(II) chloride gives a violet colour whilst copper(II) chloride gives a green colour. Table 5.2 shows the relationship between the colour of the light absorbed by a compound and the observed colour of the compound⁹⁷.

Figure 5.1 shows the visible spectra of poly(MHpI+ DHpI)/TEPA/CuCl₂, where the mole percentage of the original monoester is 13.0. The concentration of the modified polymer (polymeric ligand) which contains TEPA in the side chain was 0.0325M. No absorption was observed for both the polymeric ligand solution and solvent. The concentration of the copper(II) chloride solution was 0.0325M. An absorption in the region ~700nm was recorded for the copper(II) chloride solution and the green colour

TABLE 5.2 The relationship between the colour of light absorbed by a compound and the observed colour

Colour of light absorbed	Wavelength of light absorbed (nm)	Observed colour
Violet	400	Yellow
Blue	450	Orange
Blue-green	500	Red
Yellow-green	530	Red-violet
Yellow	550	Violet
Orange-red	600	Blue-green
Red	700	Green

colour was noticeable. After mixing the copper(II) chloride solution (green) with the colourless polymeric ligand poly(MHpI+DHpI)/TEPA, the colour became blue and an absorption was recorded in the region $\sim 600\text{nm}$. This was due to the change in the substituent in the coordination sphere of copper(II) and proved qualitatively the formation of the polymer metal complex. Figure 5.1, also shows the absorption of the polymer metal complex 50% of the ligands (TEPA) were reacted with copper(II) chloride solution and the absorption after all the ligands in the polymer side chain reacted with copper(II) chloride. A slight shift of the peak was observed. This was proved by the addition of excess of copper(II) chloride solution which changed the colour to greenish blue. This confirms that there were unreacted copper(II) chloride solution.

Figure 5.2 shows the visible spectra of poly(MHpI+DHpI)/TEPA/ CuCl_2 , where the original mole percentage of the monoester is 6.3. The concentration of the polymeric ligand poly(MHpI+DHpI)/TEPA was 0.01M. The concentration of copper(II) chloride solution was 0.01M. From Figure 5.2, it can be seen that the gradual addition of copper(II) chloride solution to the polymeric ligand solution increased the absorption. This is because the absorption is directly proportional to concentration.

Figure 5.3 shows the visible spectra of poly(MHpI+DHpI)/TEPA/ CoCl_2 , where the original mole percentage of the monoester is 13.0. The concentration of the cobalt(II)

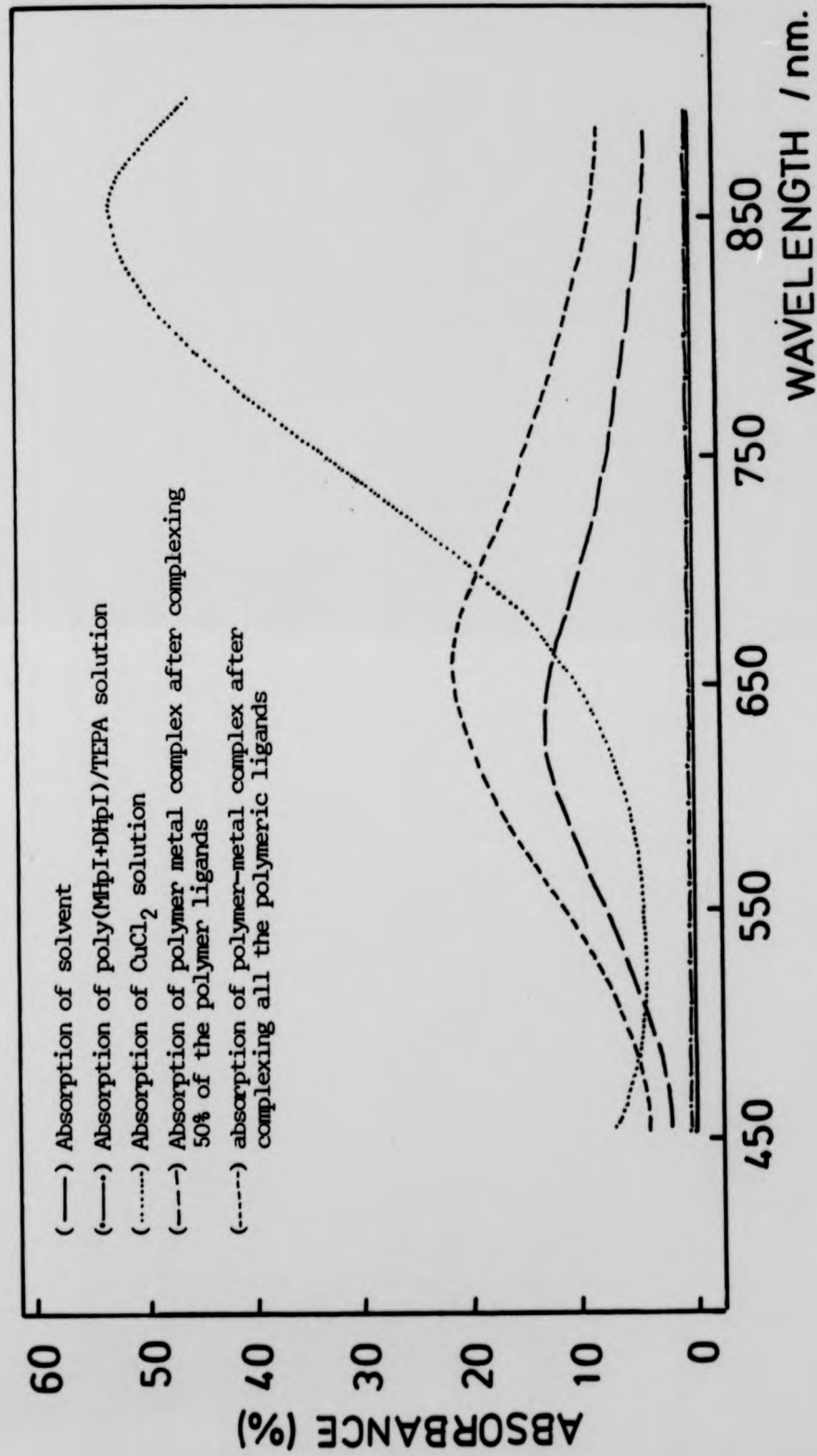


Fig. 5.1 Visible spectrum for poly(MHpI+DHpI)/TEPA/CuCl₂, sample No 56.

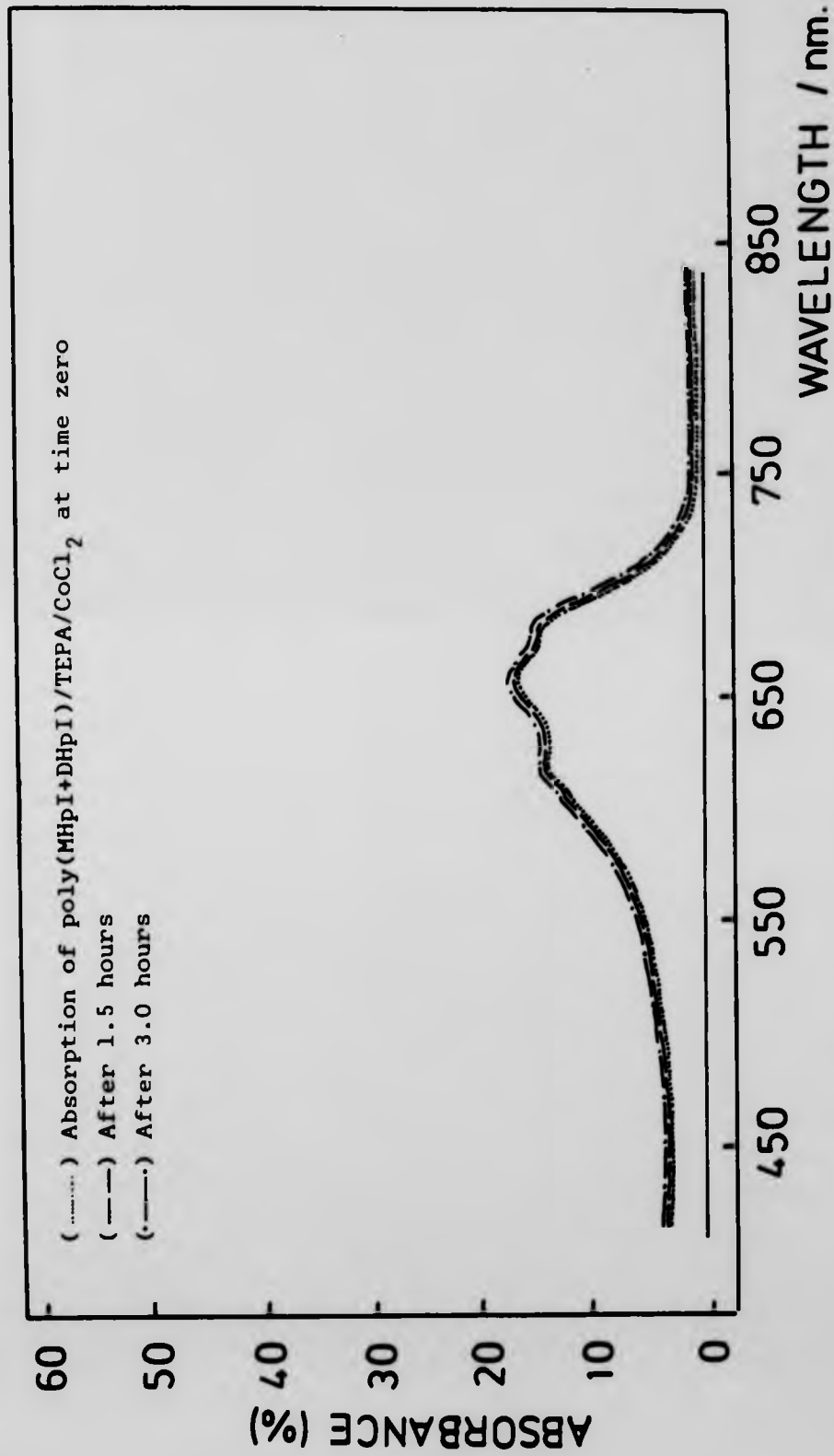


Fig. 5.3 Visible spectra for poly(MHpI+DHpI)/TEPA/CoCl₂ mole % of TEPA 13.0, fully reacted with CoCl₂ solution.

chloride solution was 0.0325M. The concentration of the polymeric ligand, poly(MHpI+DHpI)/TEPA was 0.0325M. The colour of the cobalt(II) chloride solution changed from violet to red, after it had reacted with the polymeric ligand. All the ligands were reacted and the absorption was measured as a function of time. From Figure 5.3, it can be seen that there was no significant change in the absorption after 1.5 hours and after 3.0 hours.

5.4 DISCUSSION

The visible spectrophotometer proved to be a useful technique to study qualitatively the reaction of the modified polymers (polymeric ligands) which contain TEPA in the side chain and metal halides. The changing of the colour of the metal halides solution after the reaction with the polymeric ligands proved that this reaction is a method for analysing the polymer. The parent polymers did not give the same results because they did not contain TEPA in the side chain. Non-aqueous media were used in the complexation because the polymeric ligands were not soluble in water. The visible spectra confirms the change of substituent in the coordination sphere. These polymer metal complexes are too complicated to be discussed quantitatively due to the non-uniformity of their structure and this is due to the following reasons⁵⁴:

(i) It is difficult to determine precisely the structure of the polymeric ligand especially in the copolymer system. In order to define the polymer metal complex structure, the primary structure of the polymeric ligand should be known.

(ii) The effect of the polymer ligand that exists outside the coordination sphere will be affected by the reactivity of the polymer ligands.

(iii) The steric effect. When cobalt(III) chelates coordinate with poly(vinyl pyridine) one of four pyridine units must remain uncoordinated to avoid steric hindrance between the cobalt(III) chelates. This steric hindrance may affect the structure of the complex.

(iv) The reactivity in some cases is strongly affected by the polymer ligands that exist outside the coordination sphere and surround the metal complex.

In conclusion, the visible spectra of these polymer metal complexes confirm the change in the substituent in the coordination sphere of the metal ion when the polymeric ligand reacted with metal halides. This polymer chelates formation proved that the polymer complexation can be used as a method for analysing polymers. Polymers which do not contain a multidentate ligand in the side chain will not give the same results as those obtained from polymers which contain a multidentate ligand.

5.5 ELECTRON MICROSCOPY RESULTS

Electron microscopy was carried out on the modified polymers and polymer-metal complexes, which originally contained 13.0 mole percentage of the monoester in the parent copolymer. Four polymer-metal complexes, which contain different mole percentage of the metal ions were prepared. Samples were viewed and photographed at 200,000 x magnification. The mole percentage of the metal ions and the micrograph plate numbers are shown in Table 5.3.

TABLE 5.3 Micrograph number and mole percentage of metal ion for the following polymers

Polymer	Mol % of cobalt	Micrograph plate number
Poly(MHpI+DHpI)	/	1
Poly(MHpI+DHpI)/TEPA	/	2
Poly(MHpI+DHpI)/TEPA/CoCl ₂	10	3
Poly(MHpI+DHpI)/TEPA/CoCl ₂	25	4
Poly(MHpI+DHpI)/TEPA/CoCl ₂	50	5
Poly(MHpI+DHpI)/TEPA/CoCl ₂	100	6

5.6 DISCUSSION

Plates 1 and 2 show the micrographs of the parent polymer before and after replacing the acid group in the mono-n-heptyl itaconate by TEPA. It is difficult to draw a conclusion from these two micrographs. There is a slight

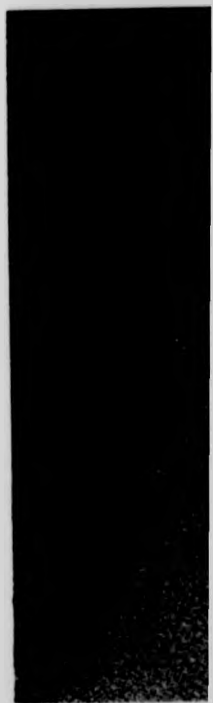


Plate 2

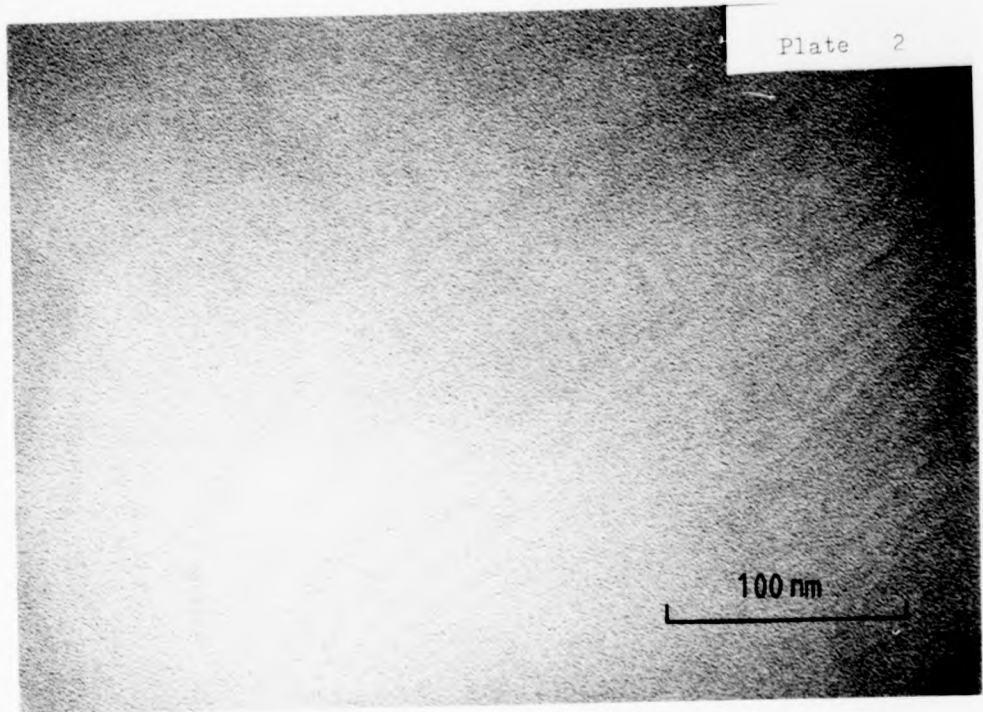
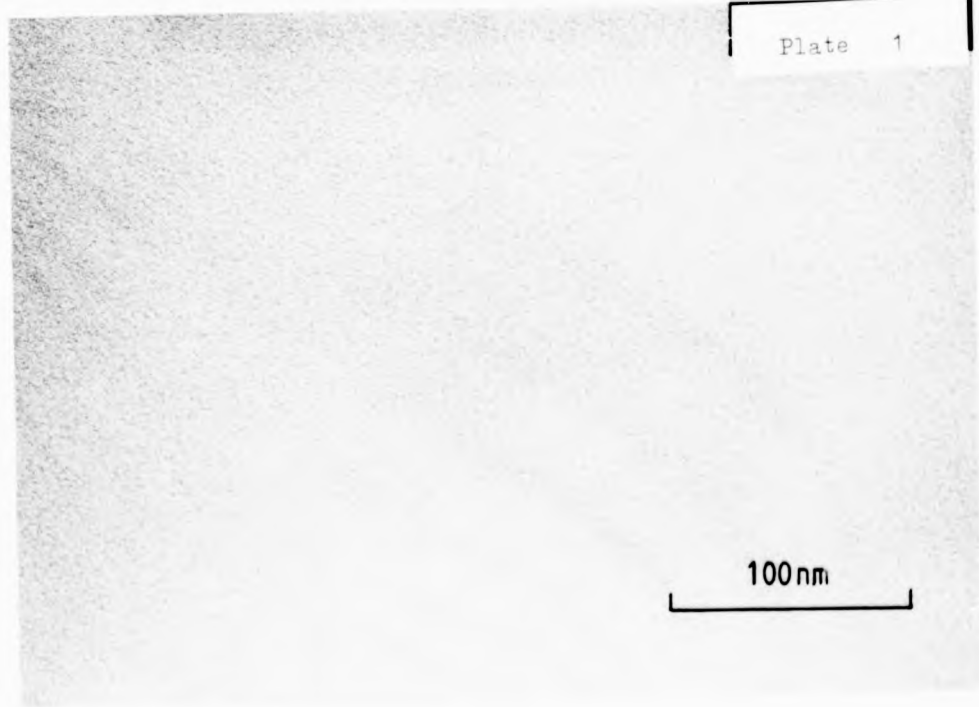


Plate 1



change in the appearance, but it is difficult to find two well defined regions, dark and light areas in both micrographs.

Plates 3 and 4 show the micrographs of the polymer metal complexes. In these polymer metal complexes the side chain TEPA was reacted with cobalt(II) chloride. Due to the complex formation and the presence of metal ions, a change in pattern should appear. Dark areas appear when the metal complexes are examined⁹⁸. These dark areas are believed to indicate clustering of the metal ions in the polymer matrix and these clusters are randomly distributed. The size and the number of these metal ion clusters increase as the mole percentage of the metal ion increases.

The micrograph of poly(MHpI+DHpI)/TEPA/CoCl₂, which contained 50% and 100% of the cobalt(III) ion are shown in plates 5 and 6 respectively. The size of the dark areas increases due to the increase in the mole percentage of the metal ion. The diameter of these metal ion clusters increase from 15 to 64 nm.

In conclusion, the micrographs of the polymer metal complexes show a gradual increase in the size of regions between two metal ion clusters and proved that electron microscopy is a good technique to study qualitatively the complexation and the distribution of the metal ion clusters in the polymer matrix.

Plate 4

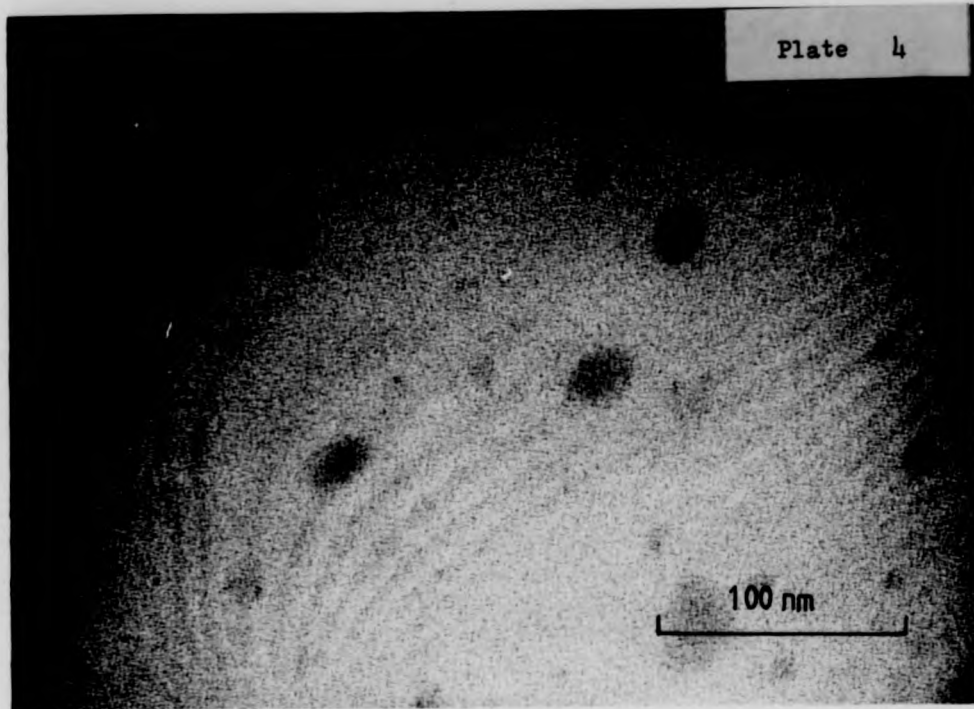
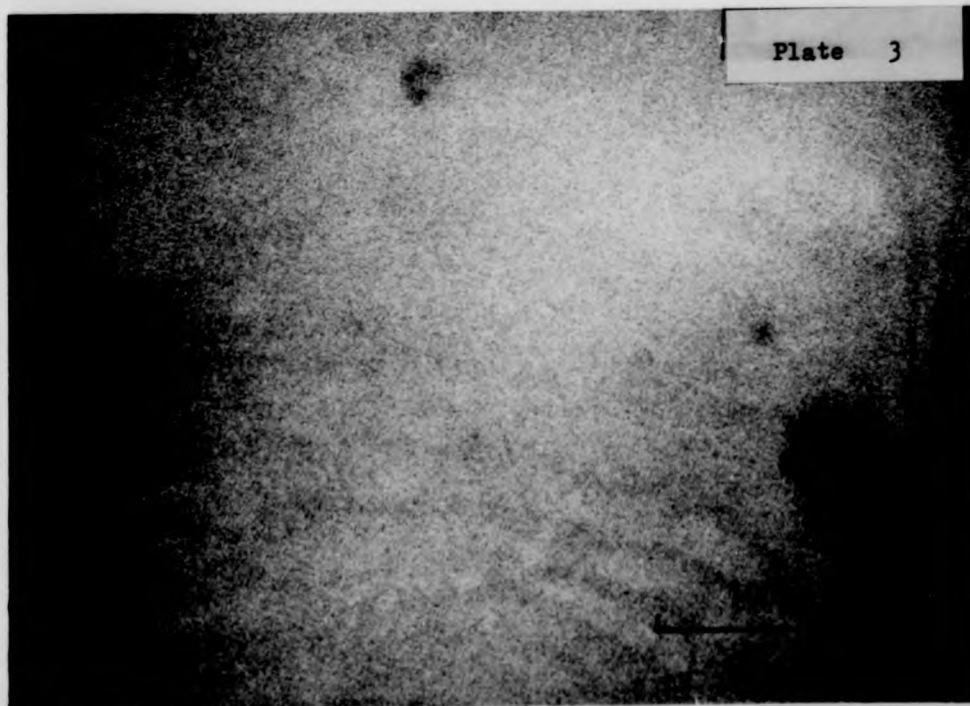


Plate 3



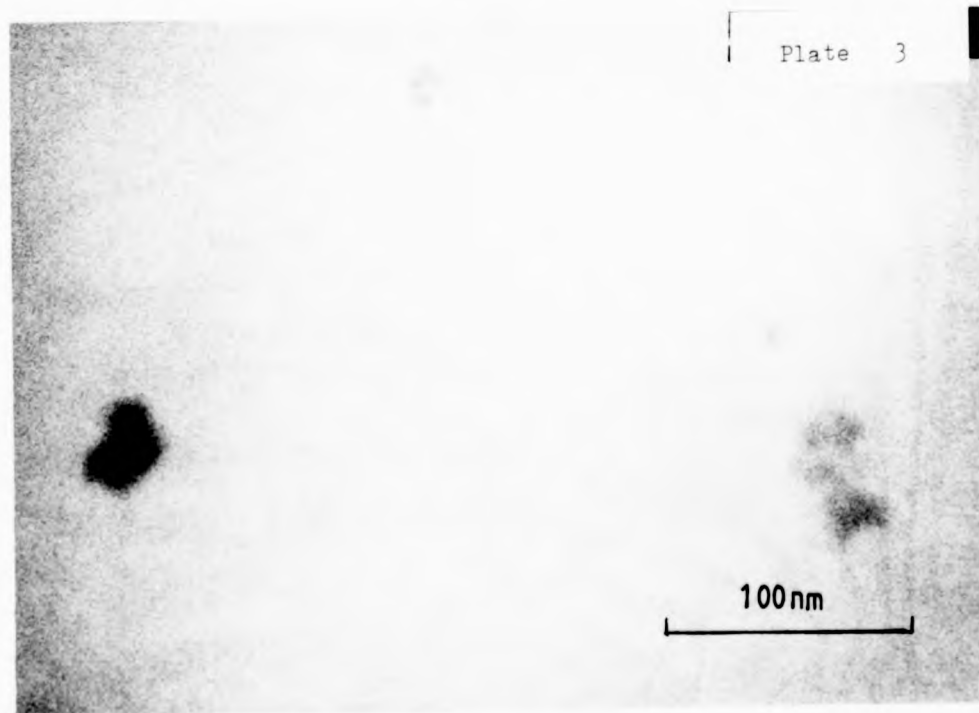
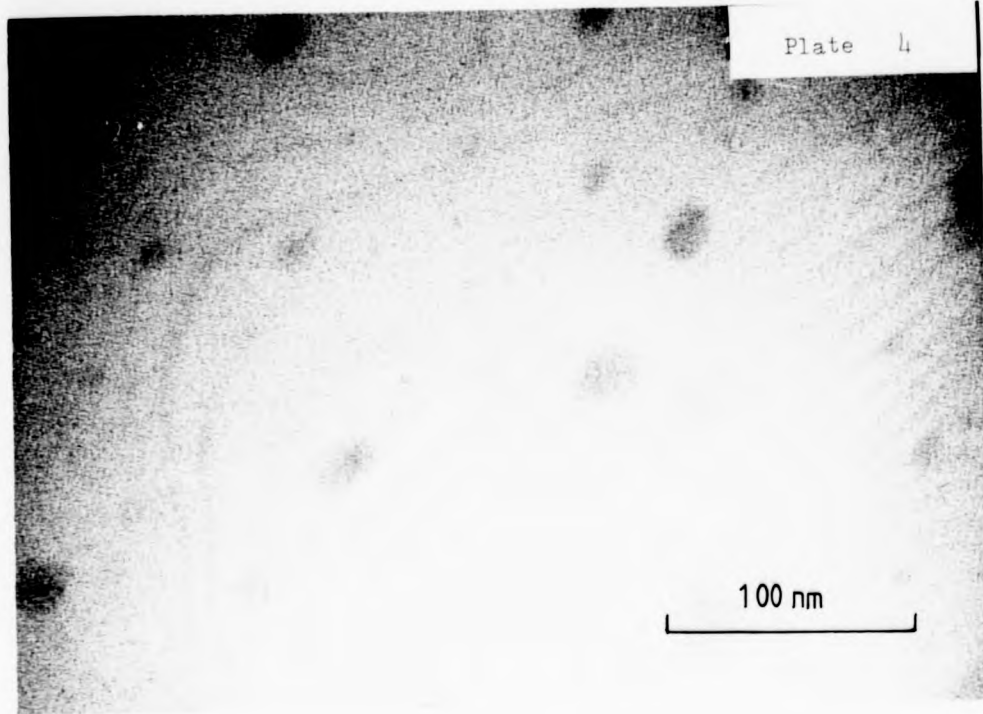


Plate 6

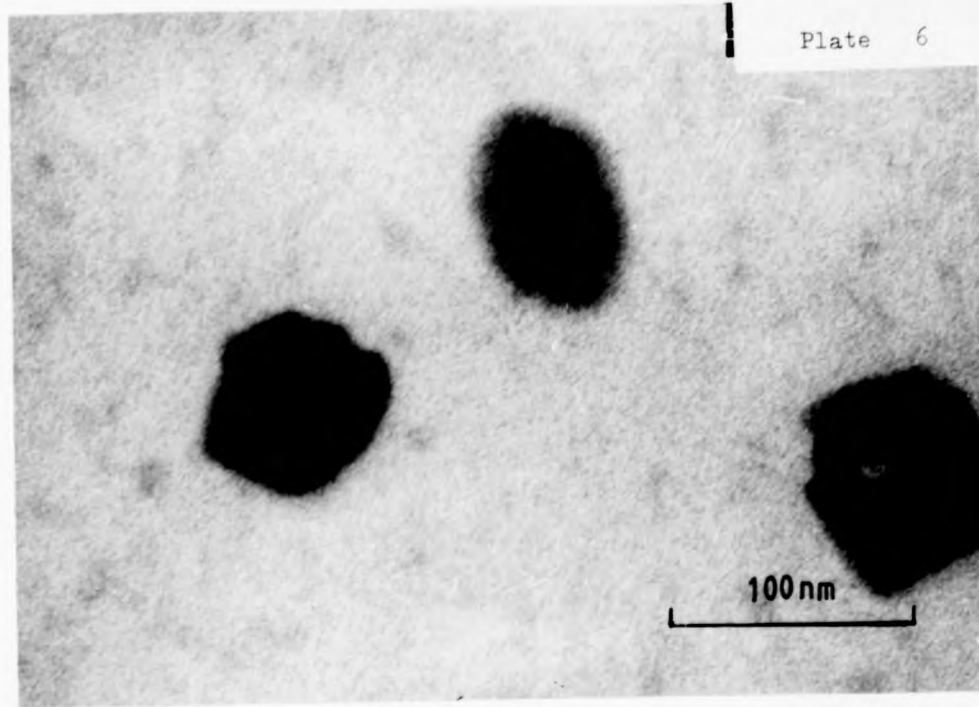


Plate 5

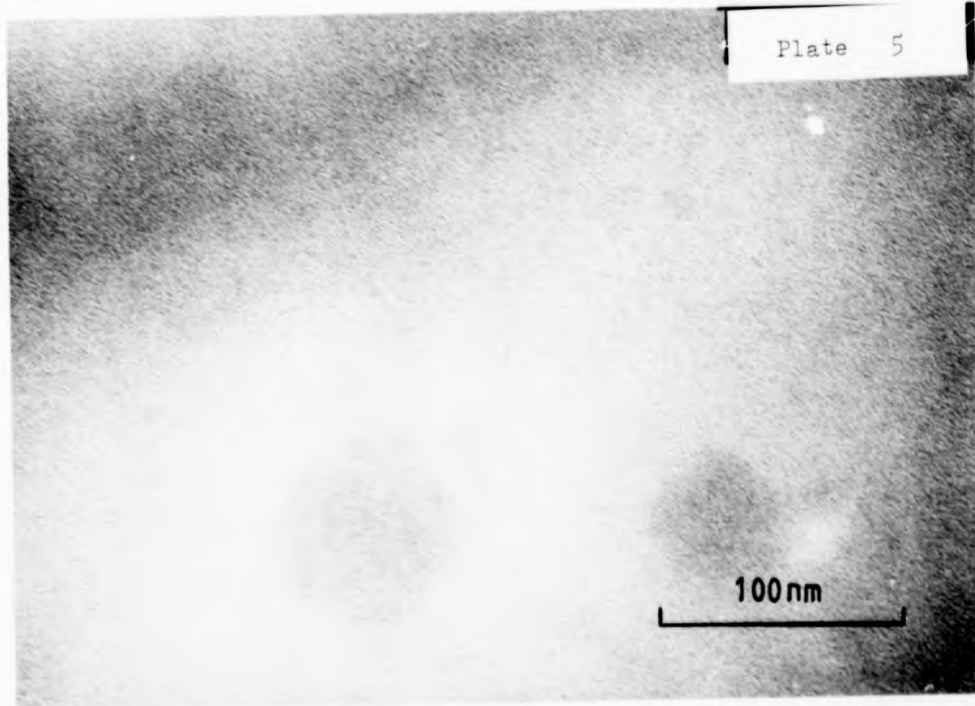


Plate 6

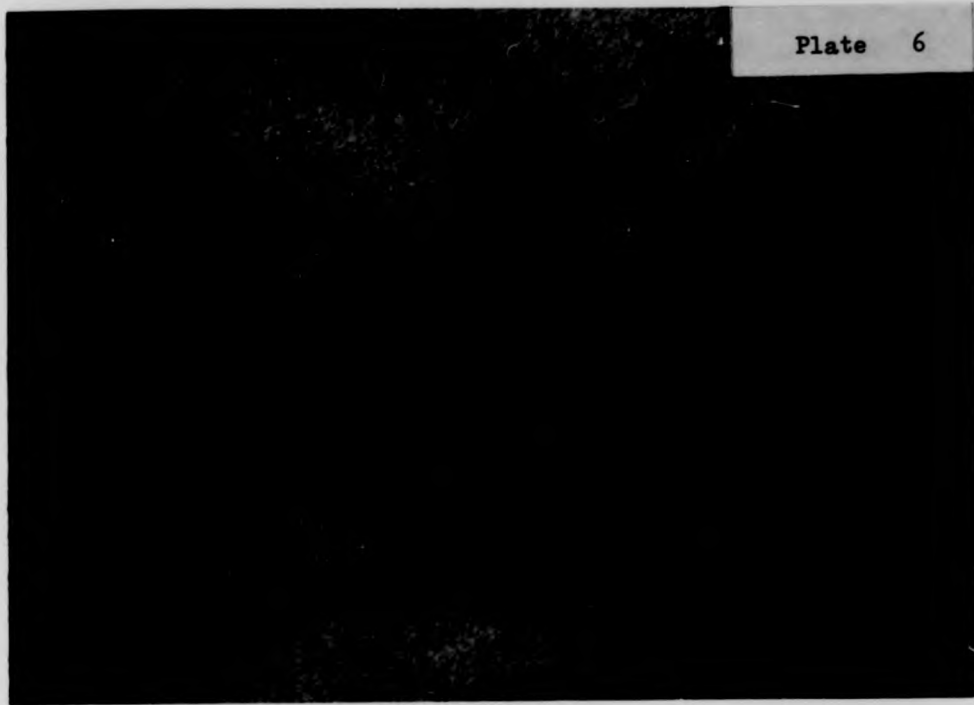
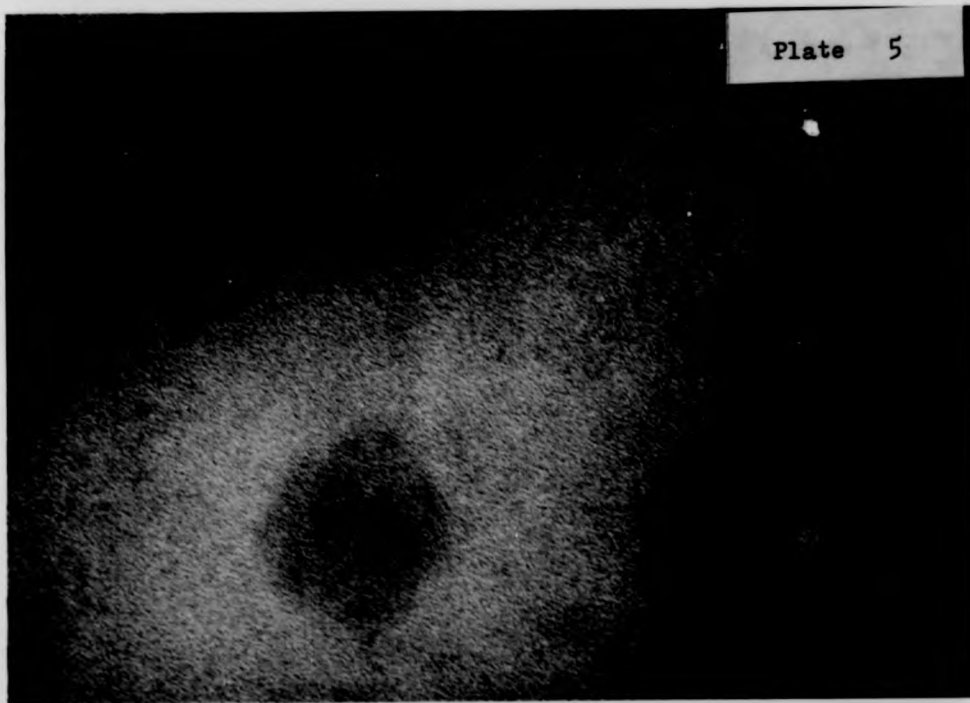


Plate 5



CHAPTER SIX
CATALYTIC ACTIVITY
RESULTS AND DISCUSSION

6.1 CATALYTIC ACTIVITY

The catalytic activity of the polymeric ligands such as poly(MHpI+DHpI)/EN, poly(MHpI+DHpI)/TEPA and polymer chelates like poly(MHpI+DHpI)/TEPA/CuCl₂, poly(MHpI+DHpI)/TEPA/CuCl₂, poly(MMI+DMI)/TEPA/CuCl₂, poly(MMI+DMI)/TEPA/CuCl₂ and pendant-type polymer metal complexes like poly(MHpI+DHpI)/EN/[Co(en)₂Cl]²⁺ 2Cl⁻ and poly(MMI+DMI)/EN/[Co(en)₂Cl]²⁺ 2Cl⁻, has been studied. This involves a comparison of the catalytic activity of these materials on the decomposition of hydrogen peroxide. The measurements were carried out at 313K and the concentration of hydrogen peroxide was 4.0 x 10⁻⁴M. The same number of moles (4.649 x 10⁻⁵M) of metal ion were used. In order to explain the method of calculation, the catalytic activity of poly(MMI+DMI)/EN/[Co(en)₂Cl]²⁺ Cl⁻ on the decomposition of hydrogen peroxide, is detailed in the following section.

6.2 RESULTS OF DECOMPOSITION OF HYDROGEN PEROXIDE

6.2.1 Hydrogen peroxide alone.

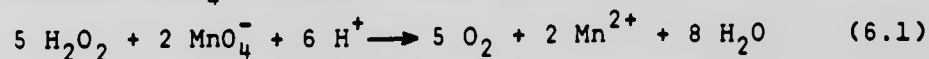
The rate of decomposition of hydrogen peroxide at 313K was measured as a function of time. To show the catalytic activity of polymer-metal complexes, a comparison of the rate of decomposition of hydrogen peroxide with and without a polymer-metal complex was made. The result of

the decomposition of hydrogen peroxide without metal complex, polymeric ligand and polymer-metal complex is shown in Table 6.1.

TABLE 6.1 The decomposition of hydrogen peroxide at 313K. The concentration used $4.0 \times 10^{-4}M$.

Time (hr)	KMnO ₄ solution (cm ³)	Residual H ₂ O ₂ (%)
0.0	8.06	100.0
1.0	8.06	100.0
2.0	8.05	99.87
3.0	8.05	99.87
4.0	8.04	99.75
5.0	8.04	99.75
6.0	8.02	99.50
7.0	8.01	99.37
8.0	8.0	99.25
9.0	8.0	99.25

The residual percentage of hydrogen peroxide was determined by titrating aliquots of the reaction mixture with standardized KMnO₄ solution. The reaction is:



The residual hydrogen peroxide can be calculated from the following equation:

$$R_t (\%) = (V_t/V_o) 100 \quad (6.2)$$

Where $R_t(\%)$ is the percentage of residual hydrogen peroxide

at time= t , V_t is the volume of KMnO_4 solution in cm^3 used at time= t and V_0 is the volume of KMnO_4 solution in cm^3 used at time= 0 . At $t=0$ there was no decomposition and as the time increases the amount of KMnO_4 solution used decreases. This is because the amount of KMnO_4 solution used is proportional to the concentration of hydrogen peroxide remaining at time= t .

The residual hydrogen peroxide percentage was plotted against time as shown in Figure 6.1.

6.2.2 Result of decomposition of hydrogen peroxide in the presences of trans $[\text{Co}(\text{en})_2\text{Cl}_2]\text{Cl}$.

The catalytic activity of trans $[\text{Co}(\text{en})_2\text{Cl}_2]\text{Cl}$ on the decomposition of hydrogen peroxide was measured at 313K, the concentration of cobalt(III) was $4.649 \times 10^{-5}\text{M}$ and Table 6.2 shows the amount of decomposition of hydrogen peroxide in the presence of trans $[\text{Co}(\text{en})_2\text{Cl}_2]\text{Cl}$.

The residual hydrogen peroxide percentage was plotted against time as shown in Figure 6.1.

6.2.3 Result of decomposition of hydrogen peroxide in the presence of poly(MMI+DMI)/EN/ $[\text{Co}(\text{en})_2\text{Cl}]^{2+} 2\text{Cl}^-$.

The catalytic activity of poly(MMI+DMI)/EN/ $[\text{Co}(\text{en})_2\text{Cl}]^{2+} 2\text{Cl}^-$ which is a pendant-type polymer-metal complex on the decomposition of hydrogen peroxide was measured at 313K and the same method of calculation was carried out. The decomposition of hydrogen peroxide in the presence of

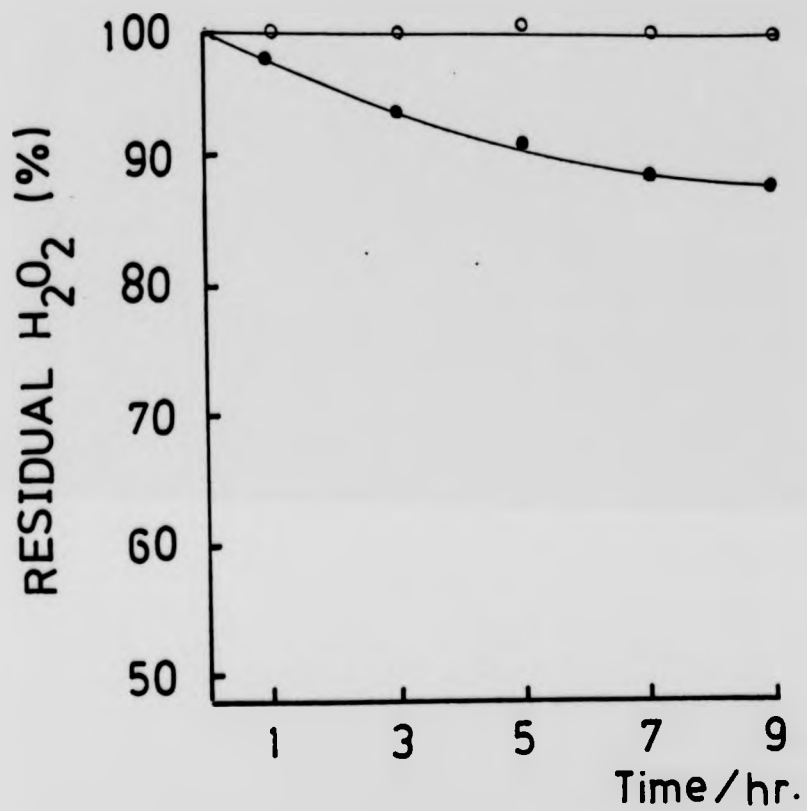


Fig. 6.1 Decomposition of 4.0×10^{-4} mole of hydrogen peroxide in the presence of (●) 4.649×10^{-5} mole of cobalt(III) as $\text{trans}[\text{Co}(\text{en})_2\text{Cl}_2]\text{Cl}$ and (○) hydrogen peroxide alone.

TABLE 6.2 Decomposition of 4.0×10^{-4} M hydrogen peroxide in the presence of 4.649×10^{-5} M cobalt(III) ion as trans[Co(en)₂Cl₂]Cl (Homogeneous Catalyst).

Time (hr)	KMnO ₄ solution (cm ³)	Residual H ₂ O ₂ (%)
0.0	8.06	100.0
1.0	7.86	97.51
2.0	7.66	95.03
3.0	7.52	93.30
4.0	7.34	91.06
5.0	7.30	90.57
6.0	7.22	89.57
7.0	7.12	88.33
8.0	7.10	88.08
9.0	7.06	87.59

poly(MMI+DMI)/EN/[Co(en)₂Cl]²⁺ 2Cl⁻, which is a heterogeneous catalyst, is shown in Table 6.3.

TABLE 6.3 Decomposition of 4.0×10^{-4} M hydrogen peroxide in the presence of 4.649×10^{-5} M of cobalt(III) as poly-(MMI+DMI)/EN/[Co(en)₂Cl]²⁺ 2Cl⁻ (Heterogeneous catalyst).

Time (hr)	KMnO ₄ solution (cm ³)	Residual H ₂ O ₂ (%)
0.0	8.06	100.0
1.0	7.78	96.52
2.0	7.58	93.30
3.0	7.40	91.81
4.0	7.24	89.82
5.0	7.10	88.08

(cont'd)

TABLE 6.3 (cont'd)

Time (hr)	KMnO ₄ solution (cm ³)	Residual H ₂ O ₂ (%)
6.0	7.0	86.84
7.0	6.94	86.10
8.0	6.85	84.98
9.0	6.80	84.36

The residual hydrogen peroxide percentage was plotted against time as shown in Figure 6.2. To show the catalytic activity of poly(MMI+DMI)/EN/[Co(en)₂Cl]²⁺ 2Cl⁻, the results from sections 6.2.1, 6.2.2 and 6.2.3 were plotted together as shown in Figure 6.2 and this demonstrates the catalytic activity of the polymer-metal complex on the decomposition of hydrogen peroxide.

The same procedure was carried out for the rest of the polymer-metal complexes and polymeric ligands and the data for these are shown in the appendix.

6.3 DISCUSSION

6.3.1 The mechanism of the decomposition of hydrogen peroxide.

In this work the catalytic activity of homogeneous and heterogeneous catalysts on the decomposition reaction of hydrogen peroxide has been studied. Homogeneous catalysis occurs when the catalyst is in the same phase as

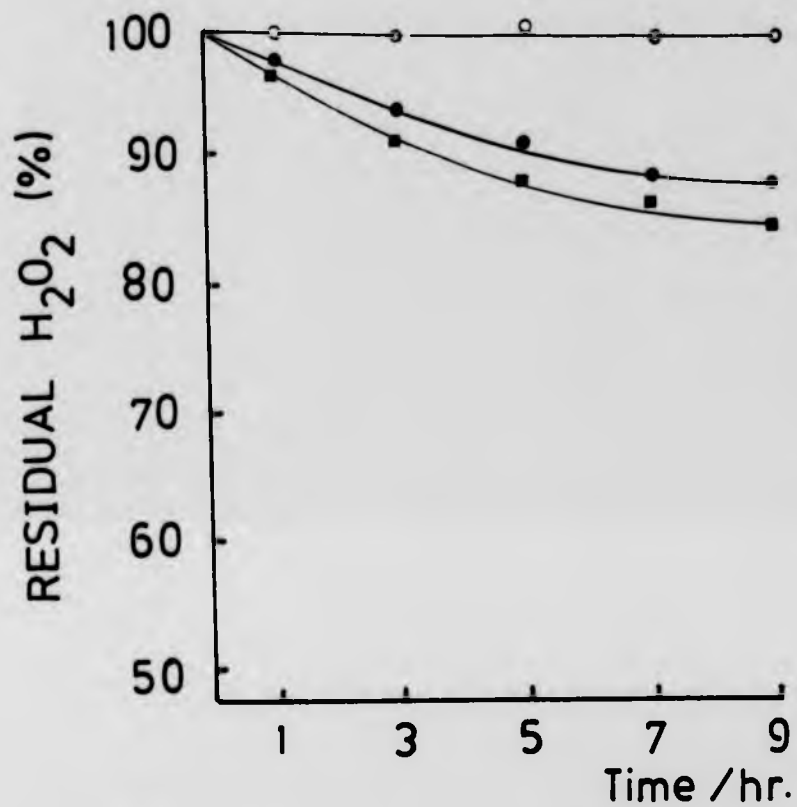


Fig. 6.2 Decomposition of 4.0×10^{-4} mole of hydrogen peroxide in the presence of (●) 4.649×10^{-5} mole of cobalt(III) as $\text{trans}[\text{Co}(\text{en})_2\text{Cl}_2]\text{Cl}$, (■) 4.649×10^{-5} mole of cobalt(III) as $\text{poly}(\text{MMI}+\text{DMI})\text{EN}/[\text{Co}(\text{en})_2\text{Cl}]^{2+} 2\text{Cl}^-$ and (○) hydrogen peroxide alone.

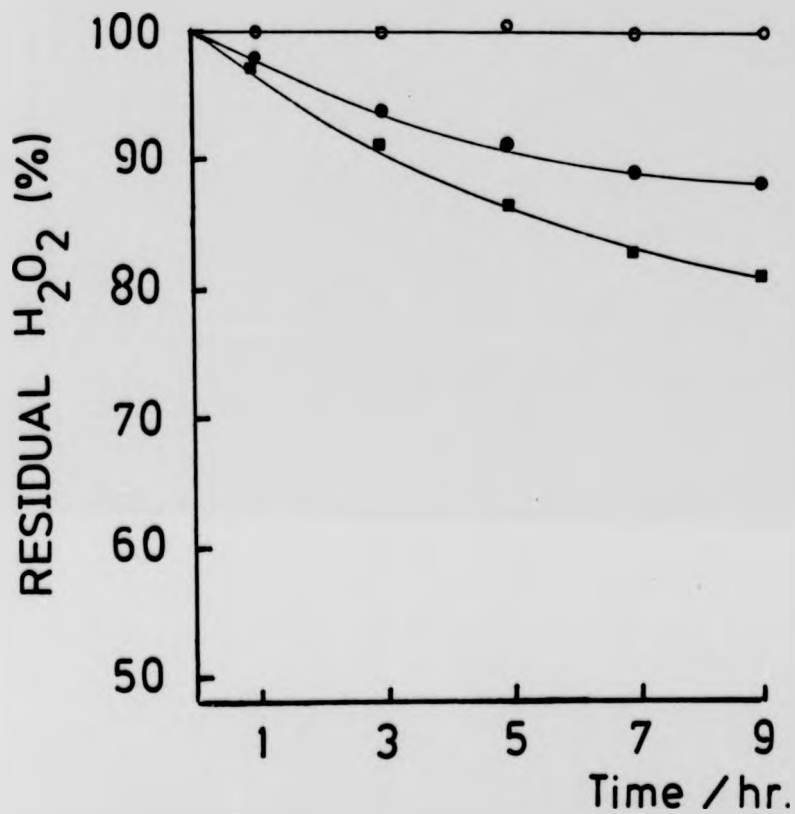


Fig. 6.3 Decomposition of 4.0×10^{-4} mole of hydrogen peroxide in the presence of (●) 4.649×10^{-5} mole of cobalt(III) as $\text{trans}[\text{Co}(\text{en})_2\text{Cl}_2]\text{Cl}$, (■) 4.649×10^{-5} mole of cobalt(III) as $\text{poly}(\text{MHP}I + \text{DHP}I)/\text{EN}/[\text{Co}(\text{en})_2\text{Cl}]^{2+} 2\text{Cl}^-$ and (○) hydrogen peroxide alone.

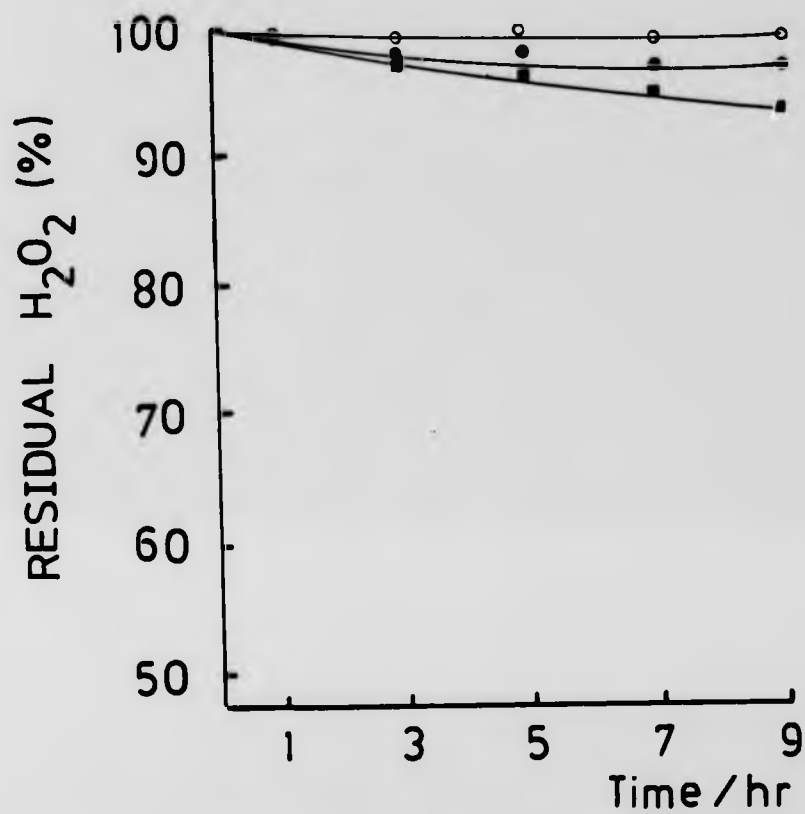


Fig. 6.4 Decomposition of 4.0×10^{-4} mole of hydrogen peroxide in the presence of (●) 4.649×10^{-5} mole of cobalt as CoCl_2 , (■) 4.649×10^{-5} mole of cobalt as poly(MMI+DMI)/TEPA/ CoCl_2 and (○) hydrogen peroxide alone.

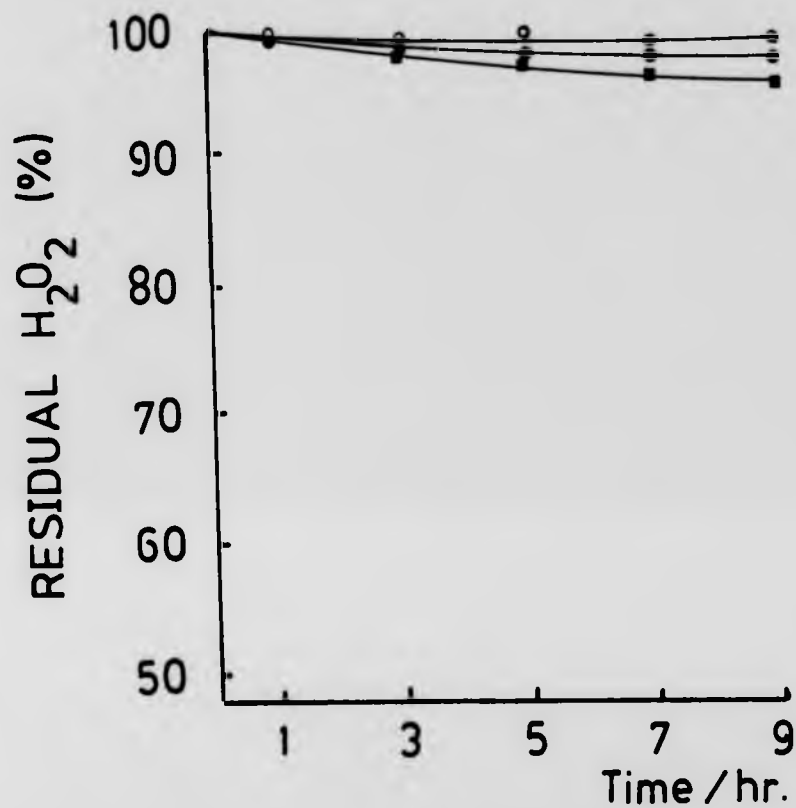


Fig. 6.5 Decomposition of 4.0×10^{-4} mole of hydrogen peroxide in the presence of (●) 4.649×10^{-5} mole of copper as CuCl_2 , (■) 4.649×10^{-5} mole of copper as poly(MMI+DMI)/TEPA/ CuCl_2 and (○) hydrogen peroxide alone.

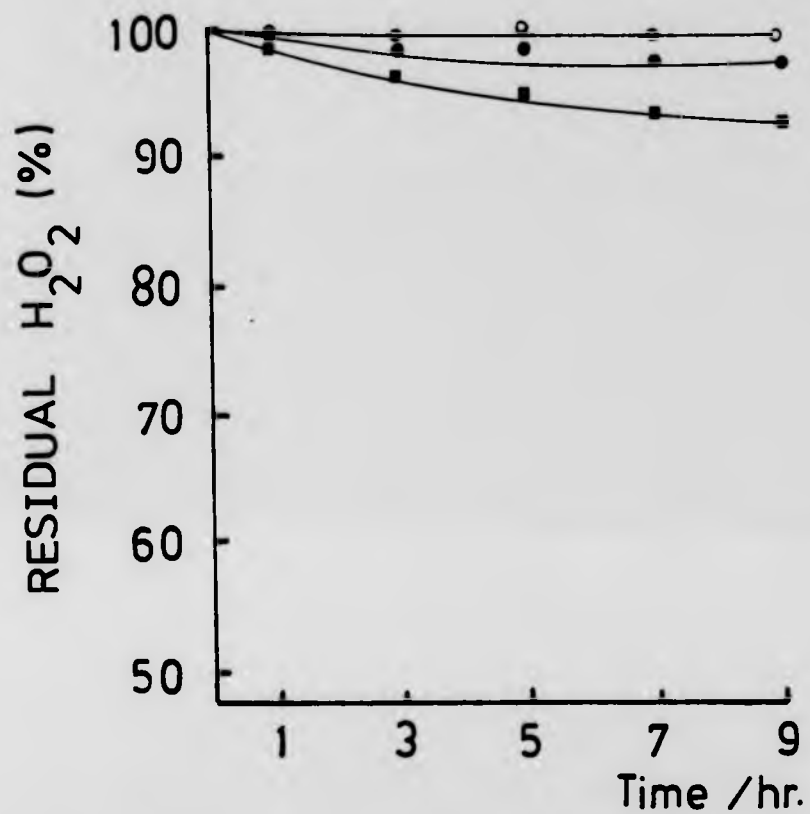


Fig. 6.6 Decomposition of 4.0×10^{-4} mole of hydrogen peroxide in the presence of (●) 4.649×10^{-5} mole of cobalt as CoCl_2 , (■) 4.649×10^{-5} mole of cobalt as poly(MHpI+DHpI)/TEPA/ CoCl_2 and (○) hydrogen peroxide alone.

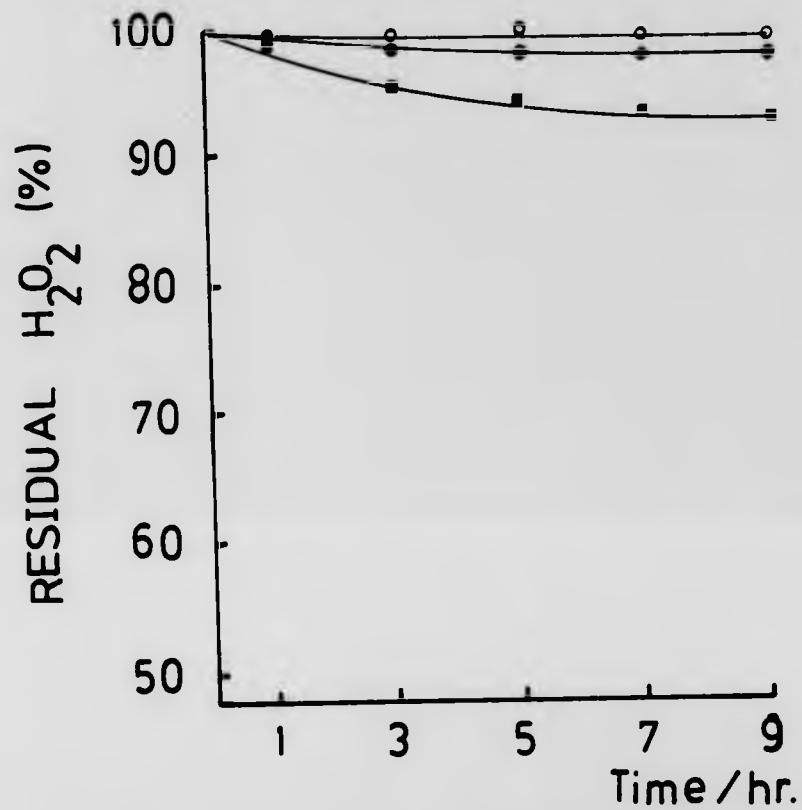
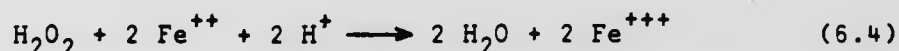
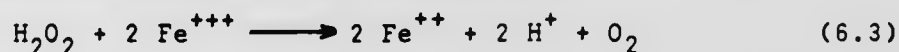
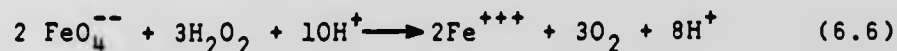
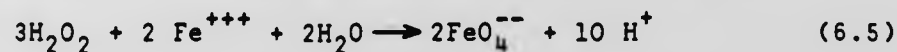


Fig. 6.7 Decomposition of 4.0×10^{-4} mole of hydrogen peroxide in the presence of (●) 4.649×10^{-5} mole of copper as CuCl_2 , (■) 4.649×10^{-5} mole of copper as poly(MHpI+DHpI)/TEPA/ CuCl_2 and (○) hydrogen peroxide alone.

the reactants and no phase boundary exists (as in the case of cobalt(II) chloride solution, copper(II) chloride solution and trans[Co(en)₂Cl₂]Cl solution. Heterogeneous catalysis occurs when a phase boundary does separate the catalyst from the reactants (as in the case of the polymeric ligands and polymer-metal complexes). In homogeneous catalysis the catalyst somehow takes part directly in the sequence of elementary decomposition steps although its overall concentration does not change in the course of the decomposition. The decomposition of hydrogen peroxide in the presence of metal halides has been studied by several workers. Von Bertalan⁹⁹, suggested that the following reactions should take place when hydrogen peroxide is decomposed by a ferric salt:



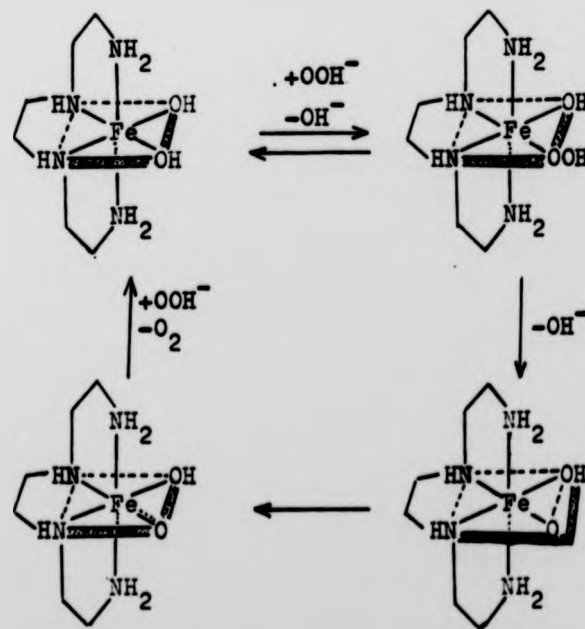
It has been shown experimentally that ferrate ion is formed during the decomposition of hydrogen peroxide by ferric salts¹⁰⁰. The following reactions take place:



The ferric salt catalyses the decomposition by providing an alternative reaction mechanism that changes the rate, usually by altering the activation energy. Haber and Weiss¹⁰¹, proposed that the reaction proceeds through a

chain mechanism, with an HO_2° radical or an HO_2^- ion as chain carrier. Wang¹⁰² reported the decomposition of hydrogen peroxide by $\text{Fe}(\text{trien})(\text{OH})_2^+$ and has devised a synthetic system which illustrates the importance of strain in catalysis. This strain weakens and breaks the O-O bond as shown in Scheme I.

In this mechanism the ferric complex must have two coordination sites open for the substrate to coordinate to ferric ion in the complex. The ferric complex works by interacting with one of the reactants, enlarges the number of coordinates and thereby permits a path from reactants to products with a different barrier height than that of the uncatalysed reaction.



Scheme I

Sasaki and Matsunaga¹⁰³ prepared polymeric complexes [CoX(DH)₂ P-4VP] (where DH₂ is dimethylglyoxime, P-4VP is poly-4-vinylpyridine and X is CN or Cl) and found that they showed good catalytic activity in the decomposition of hydrogen peroxide. They did not propose a mechanism for the reaction. The cobalt complexes have six coordination sites and all were occupied, therefore it was wrong to accept the mechanism in Scheme I.

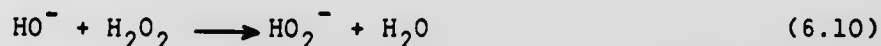
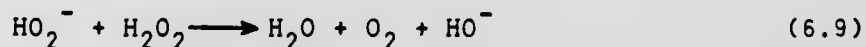
Haber and Willstatter¹⁰⁴, proposed the following mechanism for the decomposition of hydrogen peroxide by catalase. A catalase is an iron-containing enzyme that catalyses the decomposition of peroxides.

Initiation:



The catalase initiated a chain decomposition in hydrogen peroxide.

Propagations:



The reaction between hydrogen peroxide and ferrous ion in solution produces hydroxyl radicals⁴⁷.



The free radical (HO[°]) is formed in a reaction which can be thought of as an electron transfer. These hydroxyl radicals can initiate polymerization (redox polymerization), but in the absence of a suitable monomer the hydrogen peroxide may be catalytically decomposed by a chain process.

6.3.2 The effect of using polymer metal complexes.

It has been reported that the catalytic activity of metal complex on the decomposition of hydrogen peroxide increased when these metal complexes are supported on polymers¹⁰³. Polymeric complexes were synthesized and the catalytic effects of their polymer chelates on the decomposition of hydrogen peroxide were measured and compared with that of monomeric complexes of the same structure. Some of these polymer-metal complexes behave like heterogeneous catalysts. Many chemical reactions occur in the presence of certain surfaces, that do not at all, or do so only very slowly, in the absence of such a surface¹⁰⁵. The catalytic decomposition of hydrogen peroxide by polymer-metal complex is due to the following reasons:

1. Some polymer-metal complexes exhibit high efficiency in catalysing the decomposition, incomplete complexes due to steric hindrance, and this contributes to their activity.
2. The coordination bond between polymeric ligands and metal ions is relatively weak in some polymer-metal complexes and this allows the substrate to coordinate with high frequency.
3. Because the catalytic sites are locally enhanced in polymer-metal complex systems, the chain decomposition of hydrogen peroxide proceeds rapidly.

The polymeric ligand poly(MMI+DMI)/EN, was synthesised and the catalytic activity of its cobalt(III) complex, poly(MMI+DMI)/EN/[Co(en)₂Cl]²⁺ 2Cl⁻ on the decomposition of hydrogen peroxide was measured and compared with that of the monomeric metal complex trans[Co(en)₂Cl]Cl as shown in Figure 6.2. This graphical method shows that in the presence of poly(MMI+DMI)/EN/[Co(en)₂Cl]²⁺ 2Cl⁻ more hydrogen peroxide was decomposed. After 9 hours 84.36% of the hydrogen peroxide was left, whilst 87.59% of hydrogen peroxide was left when trans[Co(en)₂Cl]Cl was used. Figure 6.3 shows the catalytic activity of poly(MHpI+DHpI)/EN/[Co(en)₂Cl]²⁺ 2Cl⁻. In this case 80.39% of hydrogen peroxide was left undecomposed after 9 hours, meaning that the catalytic efficiency of poly(MHpI+DHpI)/EN/[Co(en)₂Cl]²⁺ 2Cl⁻ is higher than that of poly(MMI+DMI)/EN/[Co(en)₂Cl]²⁺ 2Cl⁻. Neither poly(MHpI+DHpI)/EN nor poly(MHpI+DHpI)/TEPA catalyse the decomposition of hydrogen peroxide. The catalytic activity of a metal ion depends substantially on the nature of the ligand; some ligands induce an increase in catalytic activity whilst others inhibit the catalytic activity. Poly(MHpI+DHpI)/TEPA/CoCl₂, poly(MHpI+DHpI)/TEPA/CuCl₂, poly(MMI+DMI)/TEPA/CoCl₂ and poly(MMI+DMI)/TEPA/CuCl catalysed the decomposition of hydrogen peroxide because they contain an incomplete complex and the catalytic sites are locally enhanced. The catalytic efficiency of poly(MHpI/DHpI)/TEPA/CoCl₂ is higher than that of poly(MMI+DMI)/TEPA/CoCl₂. This is because of steric

hindrance. The ester side chains in the case of poly(MHpI+DHpI)/TEPA/CoCl₂ contain a heptyl group whilst in the case of poly(MMI+DMI)/TEPA/CoCl₂ there is only a pendant methyl group. It was also observed that the catalytic efficiency of poly(MHpI+DHpI)/TEPA/CoCl₂ is higher than that of poly(MHpI+DHpI)/TEPA/CuCl₂. It has been found that the stability of copper chelates in an aqueous solution is sufficient to make them difficult to hydrolyze, whilst cobalt chelates are less stable in an aqueous solution⁵⁴. The weaker the interaction between the metal ion and the ligand, the higher the catalytic activity¹⁰³. However, the formation constant of the complexation involving a polymeric ligand is not easily estimated. The catalytic efficiency of poly(MMI+DMI)/EN/[Co(en)₂Cl]²⁺ 2Cl⁻ is found to be higher than that of poly(MHpI+DHpI)/TEPA/CoCl₂, and it is thought that this is because the catalytic sites are locally enhanced in the case of poly(MMI+DMI)/EN/[Co(en)₂Cl]²⁺ 2Cl⁻. Thus the catalyst efficiencies are in the decreasing order of:

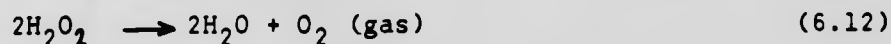
$$\begin{array}{l} \text{Poly(MHpI+DHpI)/EN/[Co(en)}_2\text{Cl]}^{2+} \text{ 2Cl}^{-} \rangle \text{ poly(MMI+DMI)} \\ \text{/EN/[Co(en)}_2\text{Cl]}^{2+} \text{ 2Cl}^{-} \rangle \text{ poly(MHpI+DHpI)/TEPA/CoCl}_2 \rangle \\ \text{poly(MHpI+DHpI)/TEPA/CuCl}_2 \rangle \text{ poly(MMI+DMI)/TEPA/CoCl}_2 \rangle \\ \text{poly(MMI+DMI)/TEPA/CuCl}_2. \end{array}$$

The catalytic activities of poly(MMI+DMI)/TEPA/CoCl₂, poly(MMI+DMI)/TEPA/CuCl₂, poly(MHpI+DHpI)/TEPA/CoCl₂ and poly(MHpI+DHpI)/TEPA/CuCl₂ are shown in Figures 6.4, 6.5, 6.6 and 6.7 respectively.

In conclusion, the decomposition of hydrogen peroxide is clearly catalysed by these polymer-metal complexes. A transient intermediate may be formed between the hydrogen peroxide and the metal catalyst, at least in the initial step of the reaction, but the reaction is also thought to proceed through chain decomposition. It is worthwhile emphasising here that the catalytic mechanism has not been elucidated. The decomposition of hydrogen peroxide is often employed as a standard reaction to determine and compare the catalytic activity of polymer complexes, because the experimental technique used to follow the reaction is simple and the reaction takes place even if the catalyst is insoluble in the reaction solvent.

6.4 Determination of the rate constant (k)

Hydrogen peroxide undergoes decomposition according to the equation:



The kinetics of this reaction can be studied either by measuring the rate of oxygen gas evolution at the same constant pressure¹⁰⁵, or by titrating aliquots of the mixture with a standard solution of potassium permanganate as described in section 3.8.3. The rate expression is¹⁰⁶:

$$\frac{-d[\text{H}_2\text{O}_2]}{dt} = k [\text{H}_2\text{O}_2] \quad (6.13)$$

Equation (6.13) can be rearranged to

$$\frac{-d[\text{H}_2\text{O}_2]}{[\text{H}_2\text{O}_2]} = -d \log_e [\text{H}_2\text{O}_2] \quad (6.14)$$

$$-d \log_e [\text{H}_2\text{O}_2] = k dt \quad (6.15)$$

The decomposition of hydrogen peroxide is a first order reaction under the present experimental conditions. If the initial concentration $[\text{H}_2\text{O}_2]_0$ is reduced to $[\text{H}_2\text{O}_2]_t$ after t seconds then:

$$-\int_{[\text{H}_2\text{O}_2]_0}^{[\text{H}_2\text{O}_2]_t} d \log_e [\text{H}_2\text{O}_2] = k \int_0^t dt \quad (6.16)$$

$$\int d \log_e [\text{H}_2\text{O}_2] = \log_e [\text{H}_2\text{O}_2] + \text{const.} \quad (6.17)$$

Equation 6.16 will become:

$$-\log_e [\text{H}_2\text{O}_2]_t + \log_e [\text{H}_2\text{O}_2]_0 = \log \frac{[\text{H}_2\text{O}_2]_0}{[\text{H}_2\text{O}_2]_t} = kt \quad (6.18)$$

whence

$$k = \frac{1}{t} \log_e \frac{[\text{H}_2\text{O}_2]_0}{[\text{H}_2\text{O}_2]_t} \quad (6.19)$$

$$k = \frac{2.303}{t} \log_{10} \frac{[\text{H}_2\text{O}_2]_0}{[\text{H}_2\text{O}_2]_t} \quad (6.20)$$

A plot of $\log [\text{H}_2\text{O}_2]_t$ versus t will give the slope (s) and by substituting the value of the slope (s) in equation (6.21), the rate constant (k) can be calculated.

$$k = -S \times 2.303 \quad (6.21)$$

6.4.1 Calculation of the rate of decomposition of hydrogen peroxide.

In order to calculate the rate of decomposition of hydrogen peroxide at 313K, $\log(a-x)$ where a is the initial concentration of the reactant and $(a-x)$ is the concentration at time= t , was plotted against time. Table 6.4 shows the values of $\log(a-x)$ which are the concentrations of the peroxide remaining at time t .

TABLE 6.4 Decomposition of 4.0×10^{-4} M hydrogen peroxide at 313K.

Time (hr)	KMnO ₄ solution (cm ³)	$\log(a-x)$	Cal.
0.0	8.06	0.9063	0.9067
1.0	8.06	0.9063	0.9063
2.0	8.05	0.9057	0.9059
3.0	8.05	0.9057	0.9054
4.0	8.04	0.9052	0.9050
5.0	8.04	0.9052	0.9046
6.0	8.02	0.9041	0.9042
7.0	8.01	0.9036	0.9038
8.0	8.00	0.9030	0.9034
9.0	8.00	0.9030	0.9030

The best straight line through the points was obtained by the least squares method. The calculated $\log(a-x)$ is plotted as a function of time. The linear relationship confirms that the decomposition of hydrogen peroxide is a first order reaction. The value of the slope was obtained

from the computer calculation. The rate of the decomposition can be calculated from equation 6.21. The value of the slope is -0.00040975 (from the computer)

$$k = -(-0.00040975) \times 2.303$$

$$k = 9.43 \times 10^{-4} \text{ hr}^{-1}$$

6.4.2 Calculation of the rate of decomposition of hydrogen peroxide in the presence of polymer ligands and polymer-metal complexes.

The same method of calculation was carried out to determine the rate of decomposition of hydrogen peroxide in the presence of metal halides, modified polymers contain EN or TEPA in the side chain, and polymer metal complexes containing cobalt or copper as the metal ion. The rate constant values are listed in Table 6.5

TABLE 6.5 Rates of decomposition (4.0×10^{-4} mole hydrogen peroxide at 313K) in the presence of polymeric ligands, and polymer-metal complexes.

Sample Number	Polymer	Type of Catalyst	k/hr^{-1}
21	Poly(MHpI+DHpI)/EN	Heterogeneous	9.43×10^{-4}
28	Poly(MHpI+DHpI)/TEPA	Heterogeneous	9.43×10^{-4}
54	Poly(MHpI+DHpI)/TEPA/ CuCl_2	Heterogeneous	8.22×10^{-3}
55	Poly(MHpI+DHpI)/TEPA/ CoCl_2	Heterogeneous	8.85×10^{-3}
69	Poly(MHpI+DHpI)/EN/ $[\text{Co}(\text{en})\text{Cl}]^{2+} 2\text{Cl}^-$	Heterogeneous	2.49×10^{-2}
66	Poly(MMI+DMI)/TEPA/ CuCl_2	Heterogeneous	5.91×10^{-3}
67	Poly(MMI+DMI)/TEPA/ CoCl_2	Heterogeneous	6.67×10^{-3}
70	Poly(MMI+DMI)/EN/ $[\text{Co}(\text{en})_2\text{Cl}]^{2+} 2\text{Cl}^-$	Heterogeneous	1.84×10^{-2}
/	CuCl_2 solution	Homogeneous	2.40×10^{-3}
/	CoCl_2 solution	Homogeneous	3.59×10^{-3}
/	<u>Trans</u> $[\text{Co}(\text{en})_2\text{Cl}_2]\text{Cl}$	Homogeneous	1.45×10^{-2}

6.5 DISCUSSION

The course of decomposition of hydrogen peroxide was followed by titration aliquots of the mixture with a standard solution of potassium permanganate at various intervals of time. The potassium permanganate will react with the residual hydrogen peroxide according to the equation :



Acid was used to stop any further decomposition of hydrogen peroxide during titration. A stable pink colour is the end point. The amount of potassium permanganate used is a function of the residual hydrogen peroxide which is a function of time. In the presence of a catalyst the rate of both forward and reverse reactions will increase. This means less hydrogen peroxide will remain. The efficiency of a catalyst for a specific reaction will differ from other catalysts for different reasons. Table 6.5 shows the value of the rate constants corresponding to each catalyst. It shows that poly(MHpI+DHpI)/EN/[Co(en)₂Cl]²⁺ 2Cl⁻ has the highest rate constant and so is the most efficient of the catalysts studied here. As the value of the rate increases the efficiency of the catalyst increases.

CHAPTER SEVEN
VISCOELASTIC STUDIES
RESULTS AND DISCUSSION

7.1 DSC AND TBA ANALYSIS

The DSC thermograms were obtained at a scan of 40K min^{-1} over a temperature range of 140 to 400K, and the results are displayed with the relative specific heat (C_p) as the ordinate and the temperature as the abscissa. The glass transition temperature was located as the point of intersection of the baseline with the extrapolated sloping portion of the thermogram resulting from the baseline shift which is experienced during this transition.

A torsional braid analyser was used to obtain the mechanical response of a polymer at a nominal frequency of 1 Hz, over a temperature range 80 to 500K. The TBA thermograms have the temperature as the abscissa and the mechanical damping index as the ordinate. The mechanical damping index scale ($-\log 1/n$) was not marked, but the intervals indicated correspond to a change of 0.5 arbitrary units in the damping. The data obtained from the torsional braid analyser were not absolute because of the nature of the composite sample which does not allow precise measurement of its geometry.

7.2 DSC RESULTS

7.2.1 Poly(MHpI+DHpI)

The DSC thermograms of poly(MHpI+DHpI) systems, where the mole percentage of mon-n-heptyl itaconate is 0.29 and 4.93 are shown in Figures 7.1 and 7.2 respectively. Two distinct inflexions are observed in this system corresponding to two glass transition temperatures.

The glass transition temperatures and the mole percentage of the mono-n-heptyl itaconate in these copolymers are shown in Table 7.1.

TABLE 7.1 The glass transition temperatures of some poly(MHpI+DHpI) systems

Sample Number	Polymer	Mole % of MHpI	Tg/K	Tg ₂ /K
1	poly(MHpI+DHpI)	0.29	178	247
2	poly(MHpI+DHpI)	1.42	179	248
3	poly(MHpI+DHpI)	3.12	180	249
4	poly(MHpI+DHpI)	4.93	182	251

7.2.2 Poly(MMI+DMI)

The DSC thermogram of the poly(MMI+DMI) system, where the mole percentage of the monomethyl itaconate = 10.5, is shown in Figure 7.3. In the case of poly(MMI+DMI) the glass transition temperature was recorded at 261K for a copolymer of this composition.

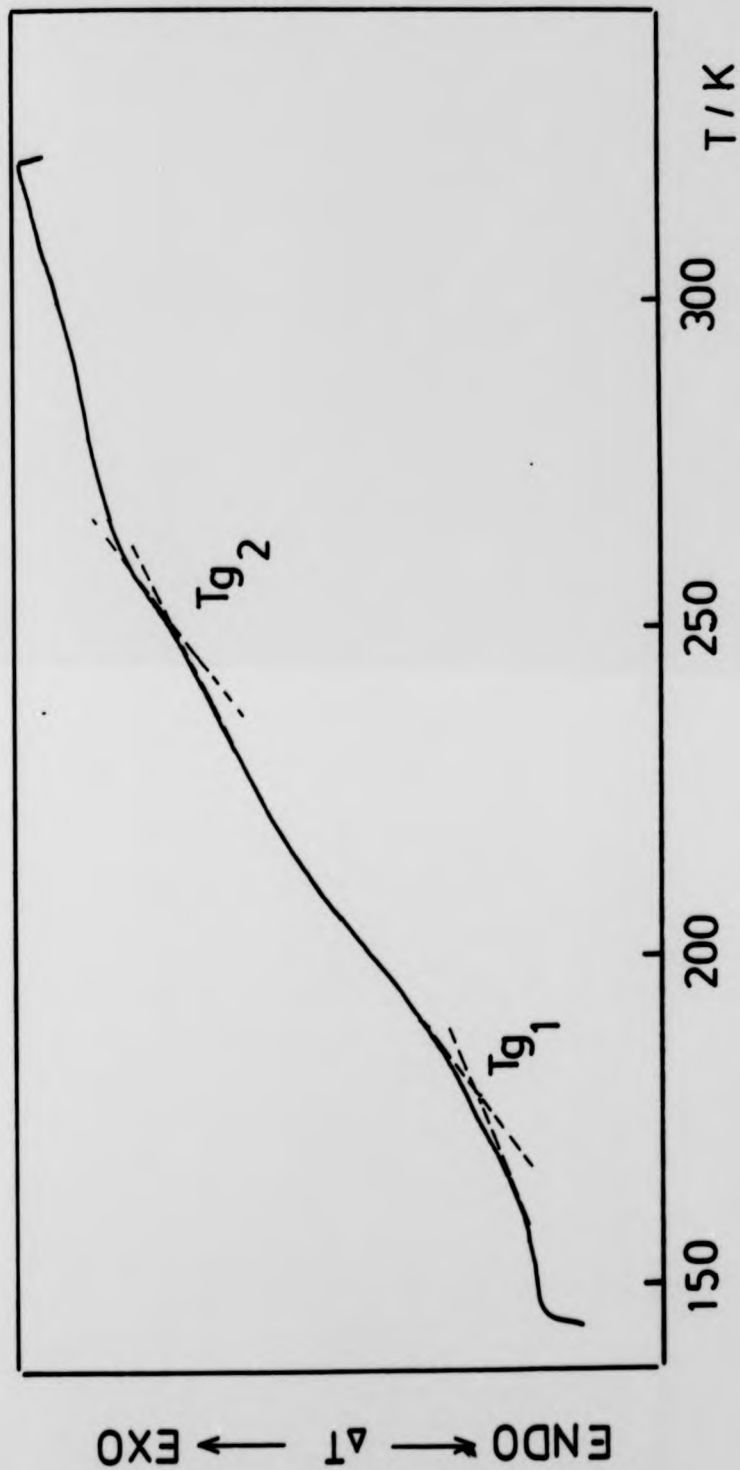


Fig. 7.1 DSC thermogram for poly(MHpI+DHpI), mole % of MHpI = 0.29.

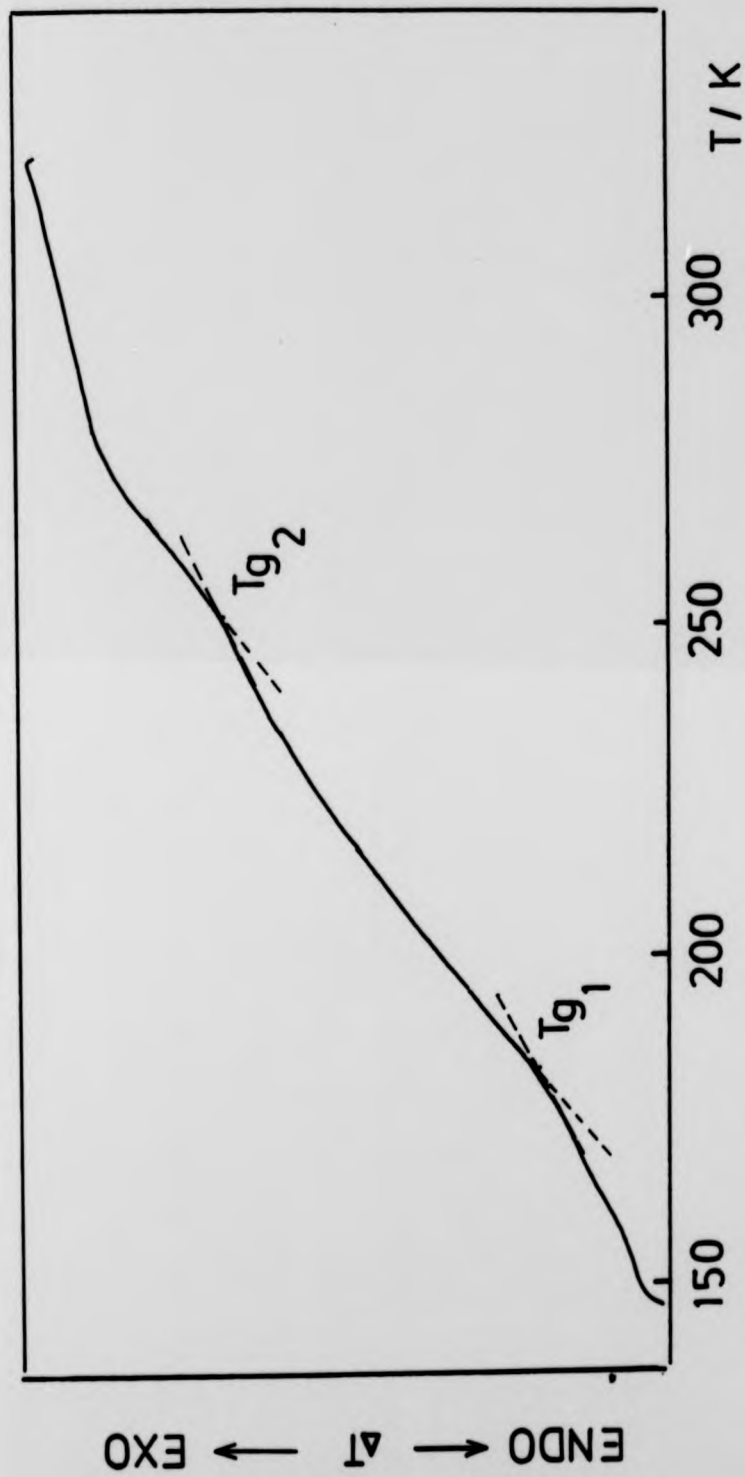


Fig. 7.2 DSC thermogram for poly(MHpI+DHpI), mole % of MHpI = 4.93.

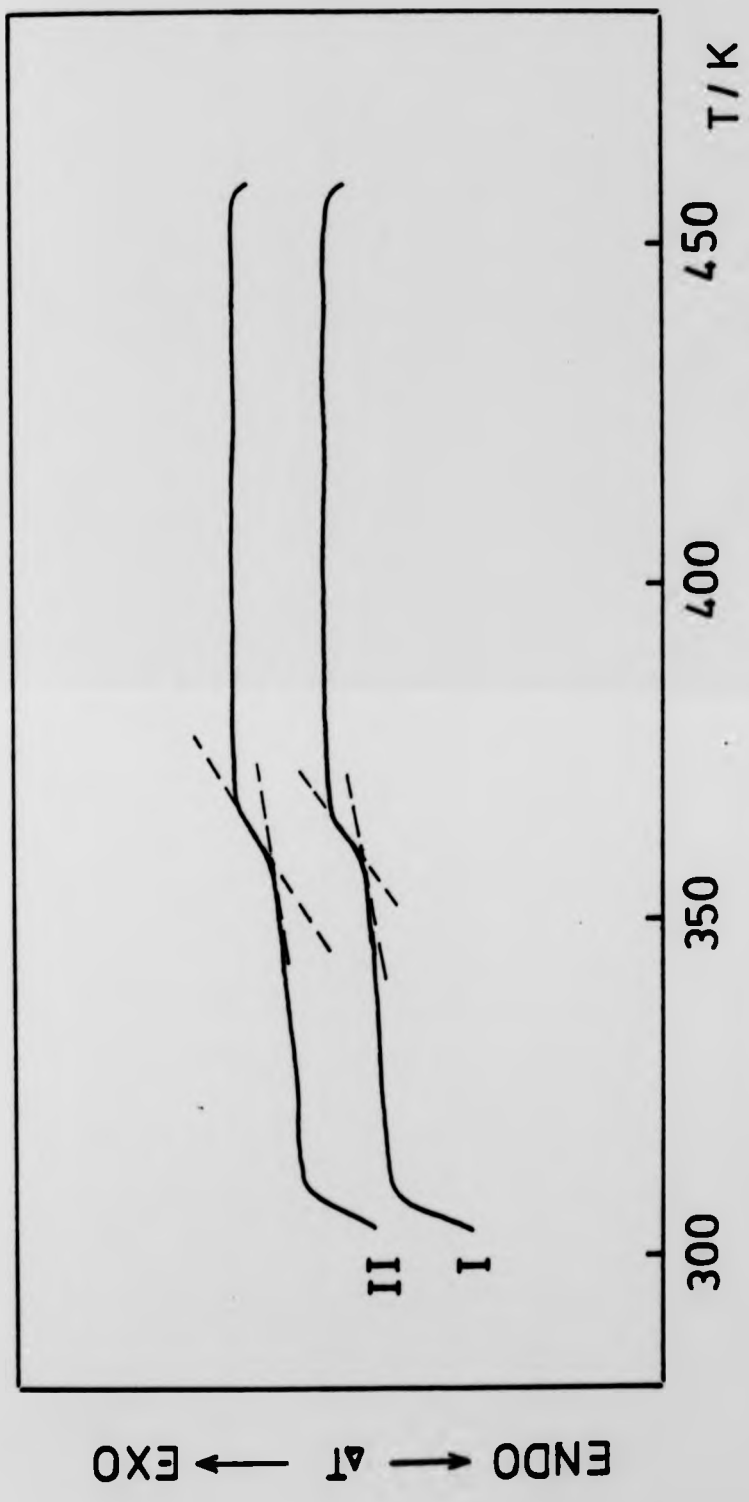


Fig. 7.3 DSC thermogram for poly(MMI+DMI), mole % MMI = 10.5.

7.3 DISCUSSION

Two glass transition temperatures were observed in agreement with previous results which showed that two glass transitions were detected in poly(di-n-alkyl itaconates) with seven to eleven carbons in the side chain³⁰. The first glass transition temperature, occurring in the region 178-182K, is due to the independent cooperative relaxation of the alkyl side chains. The second glass transition temperature, occurring in the region 247-251K, is associated with long-range cooperative motion of the whole molecule including the backbone chain. The first glass transition temperature was observed because the side chains are long enough to act independently of the main chain. It was difficult to detect the glass transition temperatures of poly(MHpI+DHpI) systems or poly(MBI+DBI) systems, with a high mole percentage of the monoesters. This is because a chemical reaction between two adjacent acid groups will take place to form an anhydride structure (see section 8.3.2) and this may shift the glass transition temperature to higher temperatures. Also, the expected glass transition temperatures of these copolymers are believed to lie above the temperature of dehydration.

In conclusion, the side chains relax independently of the main chain and exhibit a separate glass transition temperature process at lower temperatures than that reflecting the glass-rubber transition of the main chain.

7.4 TBA RESULTS

7.4.1 Poly(MHpI+DHpI)

The mole percentage of the mono-n-heptyl itaconate in the copolymer and the glass transition temperatures assigned as described below, of the poly(MHpI+DHpI) system are shown in Table 7.2. The TBA thermograms of these copolymers are shown in Figure 7.4.

TABLE 7.2 The glass transition temperatures of some poly(MHpI+DHpI) systems

Sample Number	Polymer	Mole % of MHpI	Tg/K
5	poly(MHpI+DHpI)	6.3	252-255
6	poly(MHpI+DHpI)	13.0	256-260
7	poly(MHpI+DHpI)	23.5	277-280
8	poly(MHpI+DHpI)	36.53	285-290
9	poly(MHpI+DHpI)	50.05	310-315

7.4.2 Poly(MBI+DBI)

The TBA thermograms of these copolymers are shown in Figure 7.5. The mole percentages of the mono-n-butyl itaconate in the copolymer and the glass transition temperatures are shown in Table 7.3.

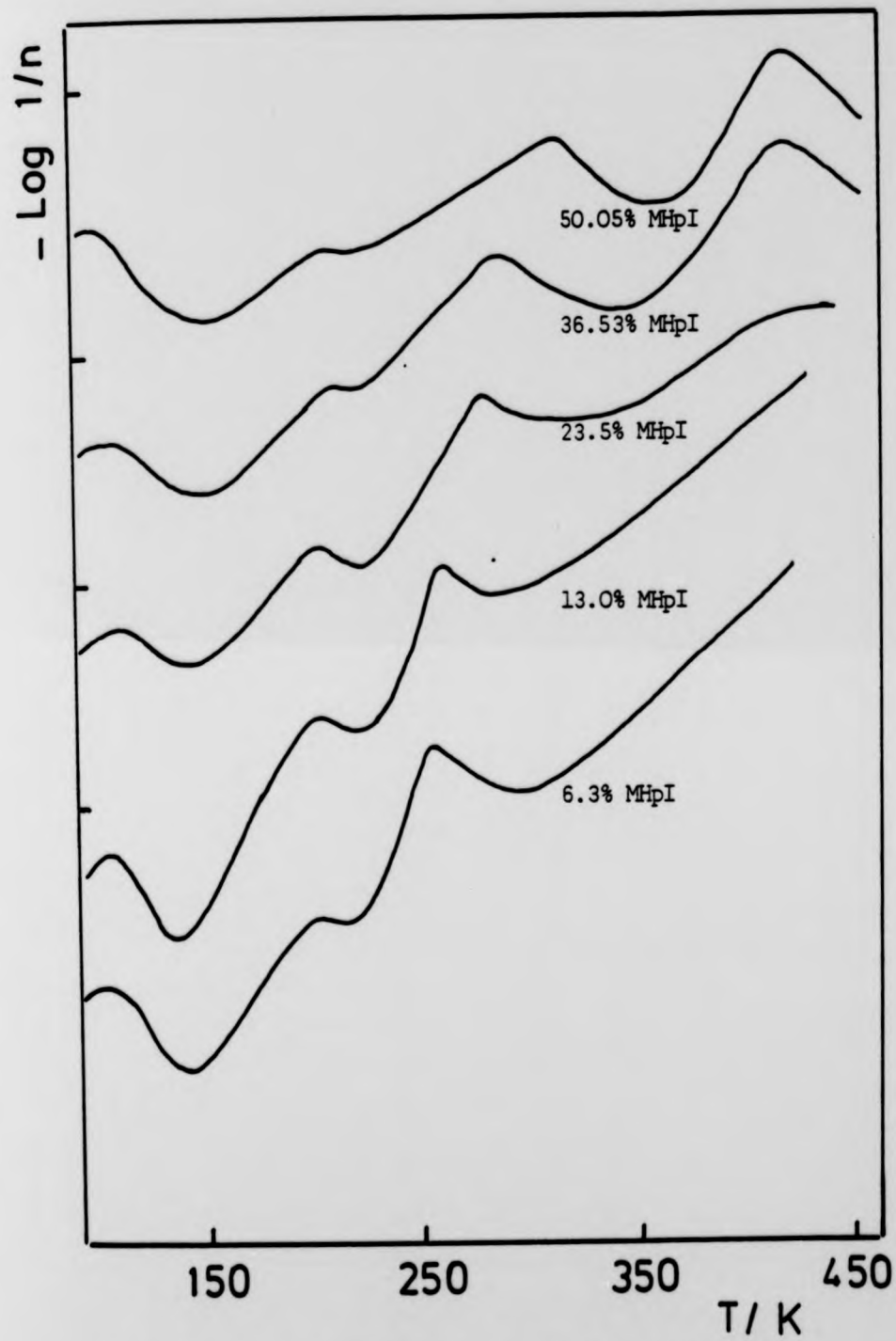


Fig. 7.4 TBA thermogram for the poly(MHpI+DHpI) system.

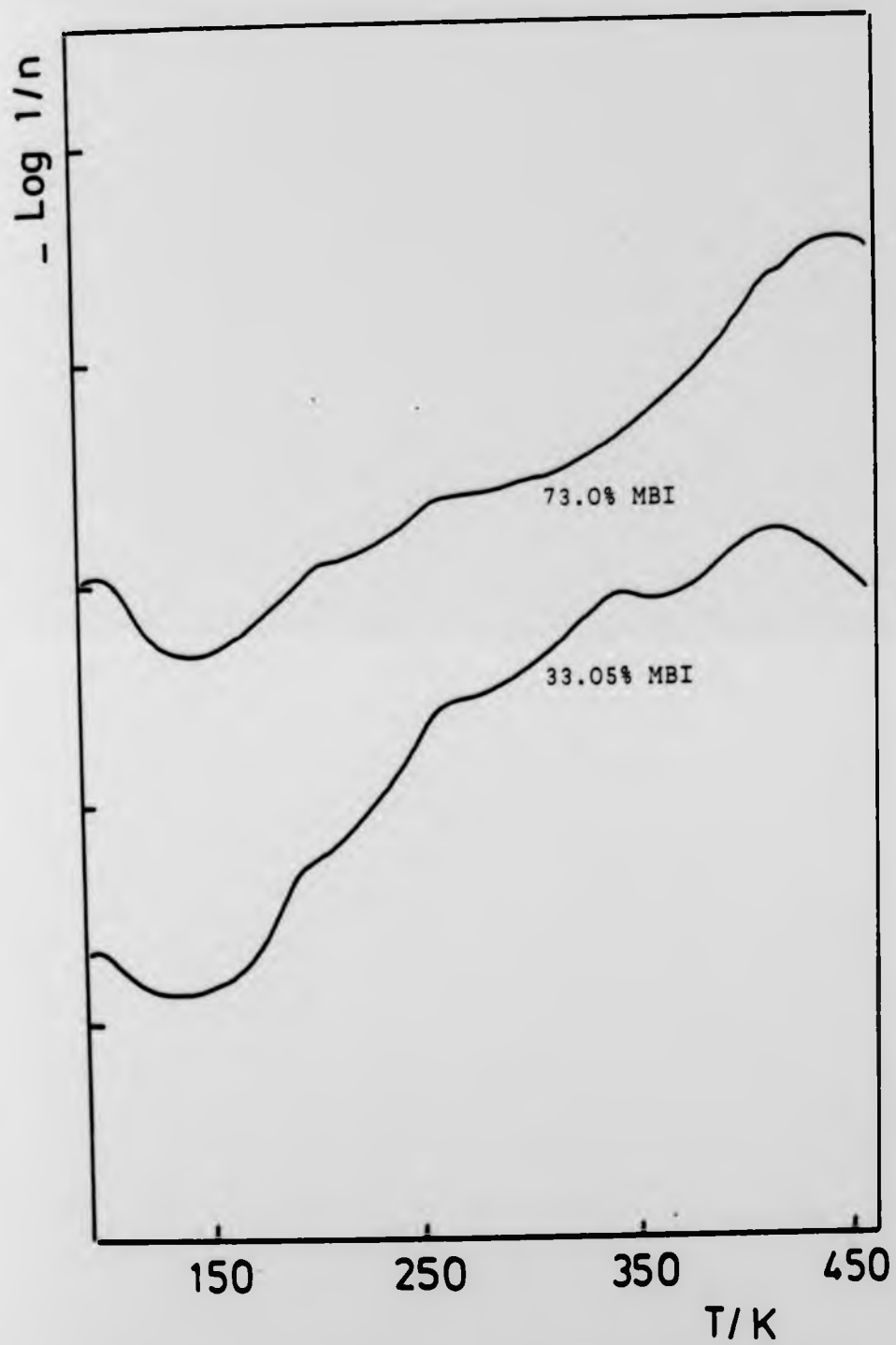


Fig. 7.5 TBA thermogram for poly(MBI+DBI) system.

TABLE 7.3 The glass transition temperatures of some poly(MBI+DBI) systems

Sample Number	Polymer	Mole % of MBI	Tg/K
10	poly(MBI+DBI)	33.05	340-345
11	poly(MBI+DBI)	73.0	408-414

7.4.3 Poly(MMI+DMI)

The TBA thermogram of this copolymer which contains 10.5 mole percentage of the monoester is shown in Figure 7.11. A glass transition temperature was recorded in the region 260-264K.

7.5 DISCUSSION

The transition regions are shown as maxima in the damping index. From Figure 7.4, four transition regions, indicated by maxima in the damping index, were observed. The first transition at ~95K is common to all samples and is caused by a molecular motion originating in the alkyl side chain, similar to that observed in poly(alkyl methacrylates)¹⁰⁷. This transition was observed in poly(mono-n-alkyl itaconates) only when the alkyl chain contained four or more atoms^{27,28}. The second transition is in the range 185-200K. It was suggested that this transition reflects cooperative motion of the complete alkyl side chain, but relaxations involving the

(COOH) group and possibly the water associated with it may also occur in this region. In the case of the poly(MBI+DBI) systems, the transition in the range 185-200K disappears as the mole percentage of the mono-n-butyl itaconate decreases, which suggested that this transition is associated with the presence of carboxyl group whilst in poly(MHpI+DHpI) systems the transition in the range 185-200K (first glass transition temperature) increases as the mole percentage of the mono-n-heptyl itaconate decreases. This may be due to the cooperative motion of the ester linkage, but absolute comparisons of peak intensities may not be accurate in the non-absolute torsional braid analysis technique. The transition (first glass transition temperature) which is seen in the range 185-200K does however appear to be a composite of two possible processes²⁸. The DSC thermogram shows this transition in the poly(MHpI+DHpI) systems and was indicated as the first glass transition temperature.

The third transition is the main glass transition temperature (the second glass transition temperature). It was confirmed that as the mole percentage of the monoester increases this glass transition temperature increases.

A fourth transition appears when the mole percentage of the monoester is more than 23.5 and this arises from the dehydration reaction (see section 8.3.2).

7.6 DSC RESULTS FOR THE MODIFIED POLYMERS

The DSC thermograms of modified poly(MHpI+DHpI), where the original mole percentages of the monoester are 0.29 and 4.93, are shown in Figures 7.6 and 7.7 respectively. These are similar in appearance to the DSC thermograms of the unmodified polymers of low monoester content. The glass transition temperatures and the original mole percentages of the monoester in the modified poly(MHpI+DHpI) are shown in Table 7.4.

TABLE 7.4 The glass transition temperatures of some modified polymers

Sample Number	Polymer	Mole % of TEPA	Tg ₁ (K)	Tg ₂ (K)
13	poly(MHpI+DHpI)/TEPA	0.29	173	240
14	poly(MHpI+DHpI)/TEPA	1.42	175	245
15	poly(MHpI+DHpI)/TEPA	3.12	176	249
16	poly(MHpI+DHpI)/TEPA	4.93	178	260

7.7 DISCUSSION

From Table 7.4, it can be seen that as the mole percentage of the side chain (TEPA) increases the main chain glass transition temperature Tg₂ (the second glass transition temperature) increases, whilst the relaxation of the side

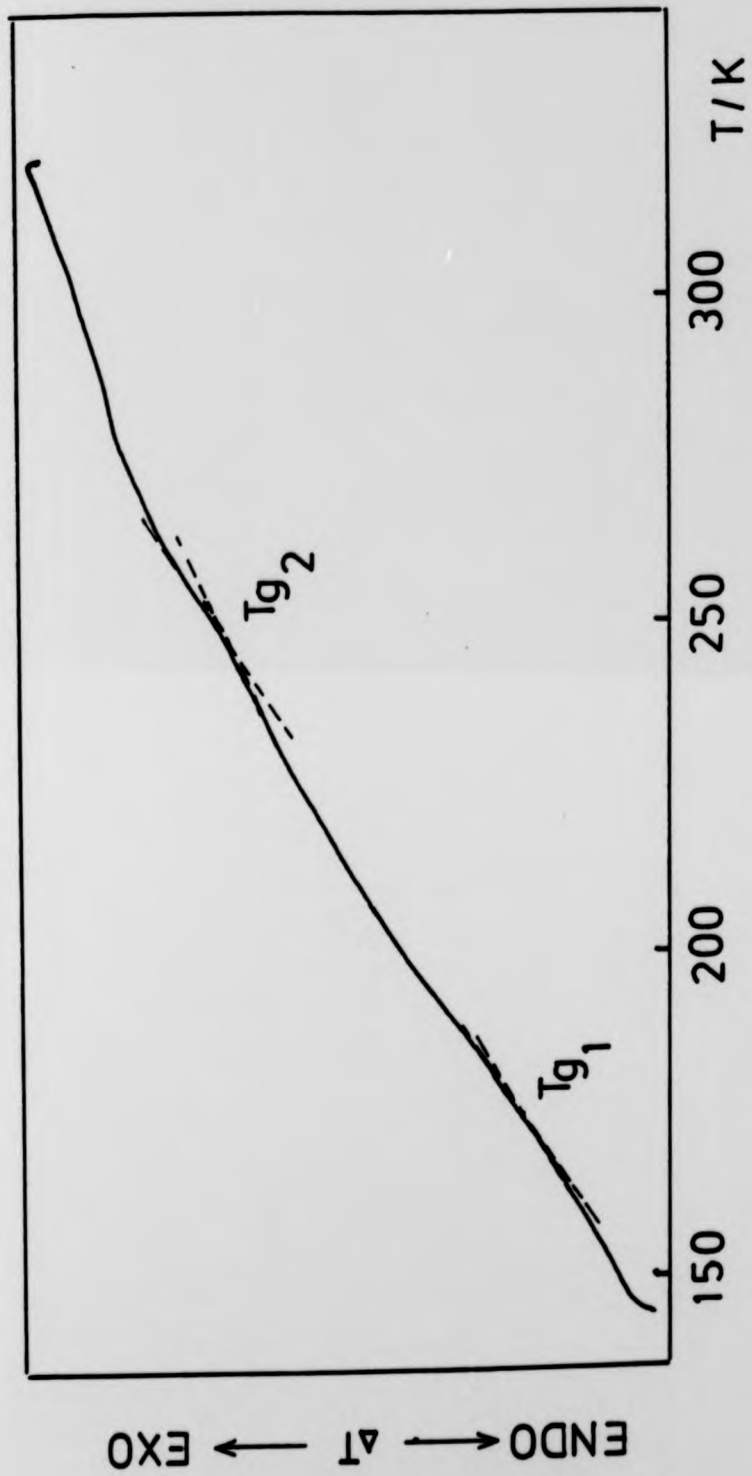


Fig. 7.6 DSC thermogram for poly(MHpI+DHPi)/TEPA, mole % of TEPA = 0.29.

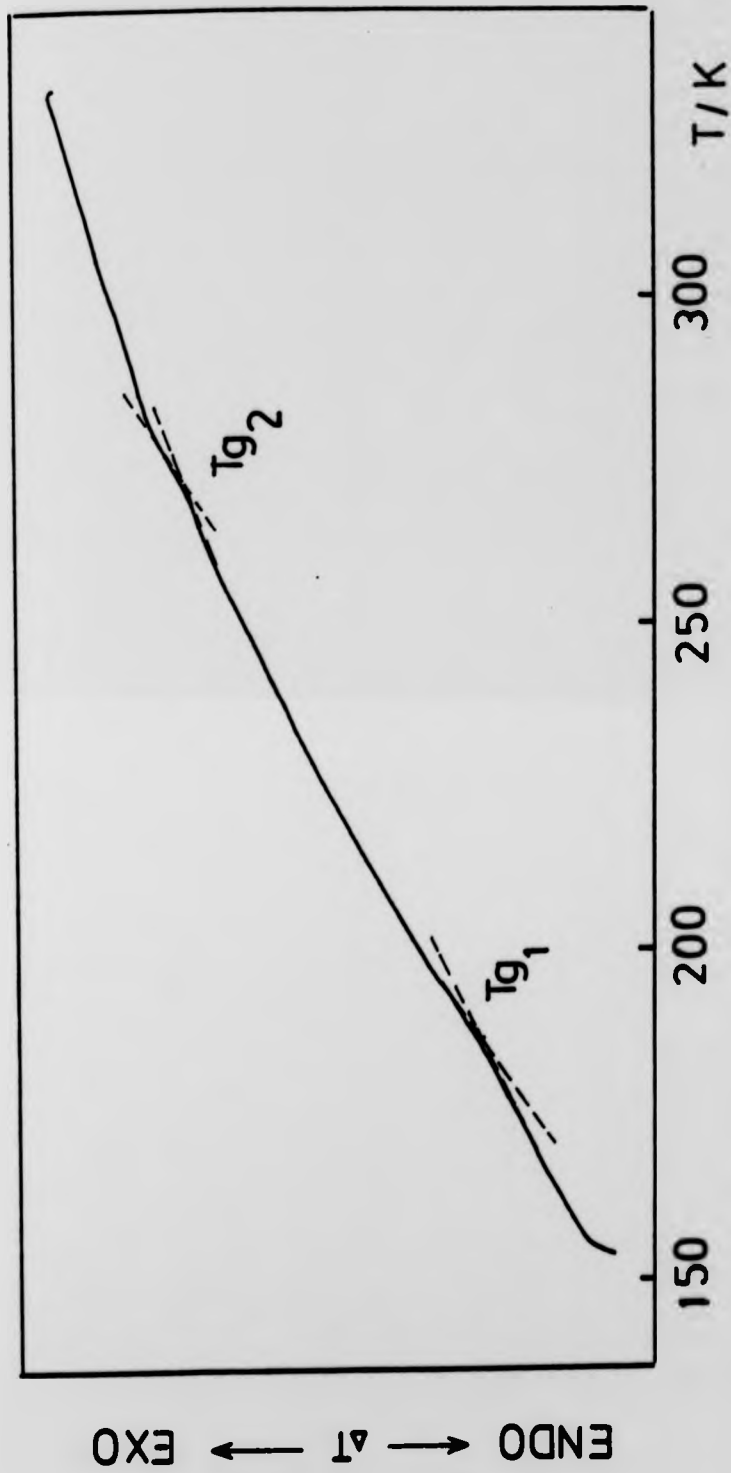


Fig. 7.7 DSC thermogram for poly(MHpI+DHpI)/TEPA, mole % of TEPA = 4.93.

chain, T_{g_1} (the first glass transition temperature) remain essentially constant. This is presumably because the degree of intermolecular interaction through the polar side chains increases. During the measurement of the glass transition temperature for the modified polymers which contained more than 6.3 mole percentage of the pendant ethylene imine groups; a sharp characteristic smell of heptanol was found on the head of the DSC instrument. The infrared spectrum confirmed that heptanol was evolved during the measurement (see section 8.3.2). The DSC thermogram for poly(MHpI+DHpI)/TEPA where the original mole percentage of the monoester is 50.05, is shown in Figure 7.8. The first run shows an exothermic peak in the region $\sim 400\text{K}$, whilst in the second run only a straight line was obtained, indicating that the chemical reaction causing the exotherm had gone to completion. The glass transition temperature was not detected. The DSC thermogram for poly(MMI+DMD/EN, where the original mole percentage of the monoester is 10.5, is shown in Figure 7.9. An exothermic peak in the region $\sim 400\text{K}$ was also observed in the first run, due to a chemical reaction. It was difficult to detect the glass transition temperature for these modified polymers because of the chemical reaction, occurring at $\sim 400\text{K}$, which changes the polymer structure.

The same results were obtained for the polymer-metal complexes, because of the higher degree of crosslinking, which resulted in the glass transition temperatures becoming broader and ill-defined.

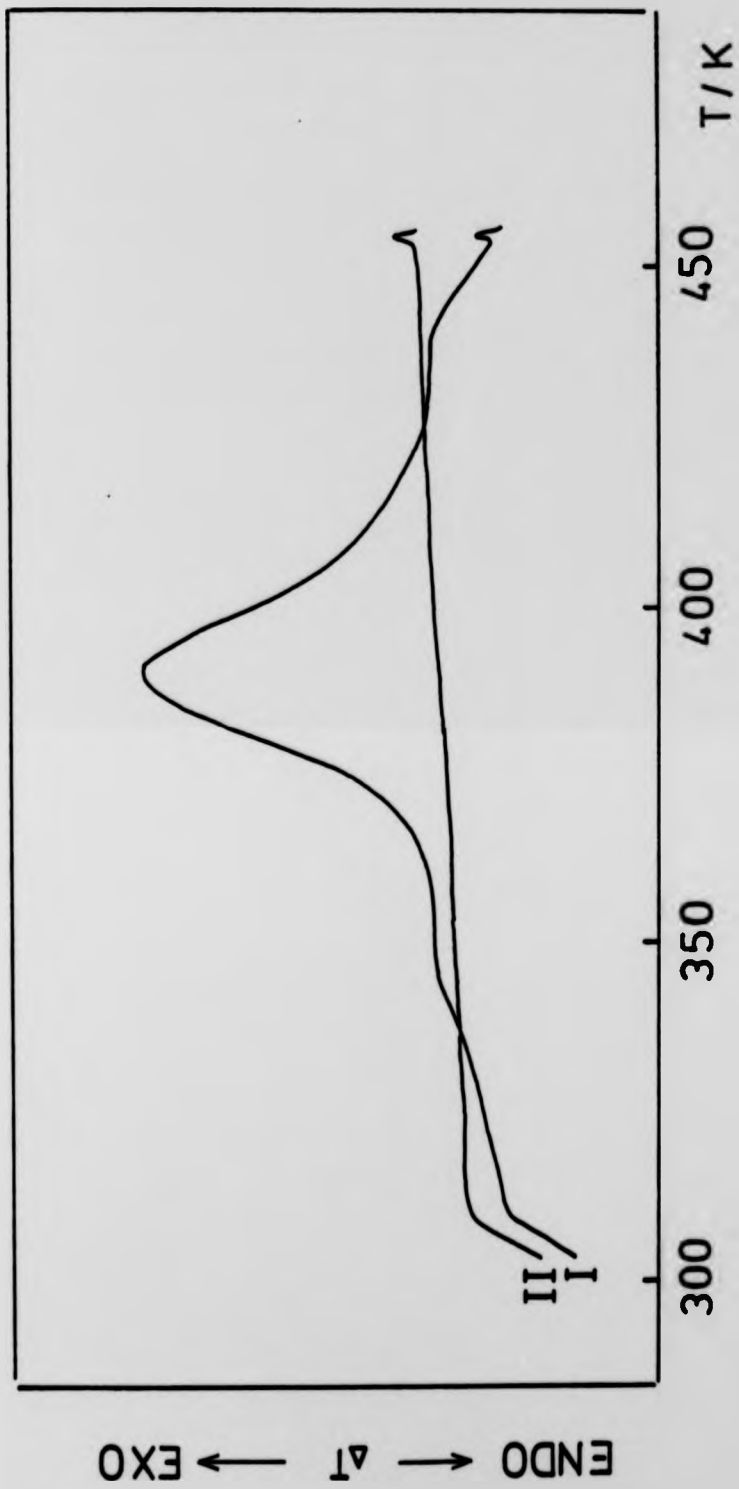


Fig. 7.8 DSC thermograms for poly(MMI+DMI)/TEPA, mole % of TEPA = 50.05.

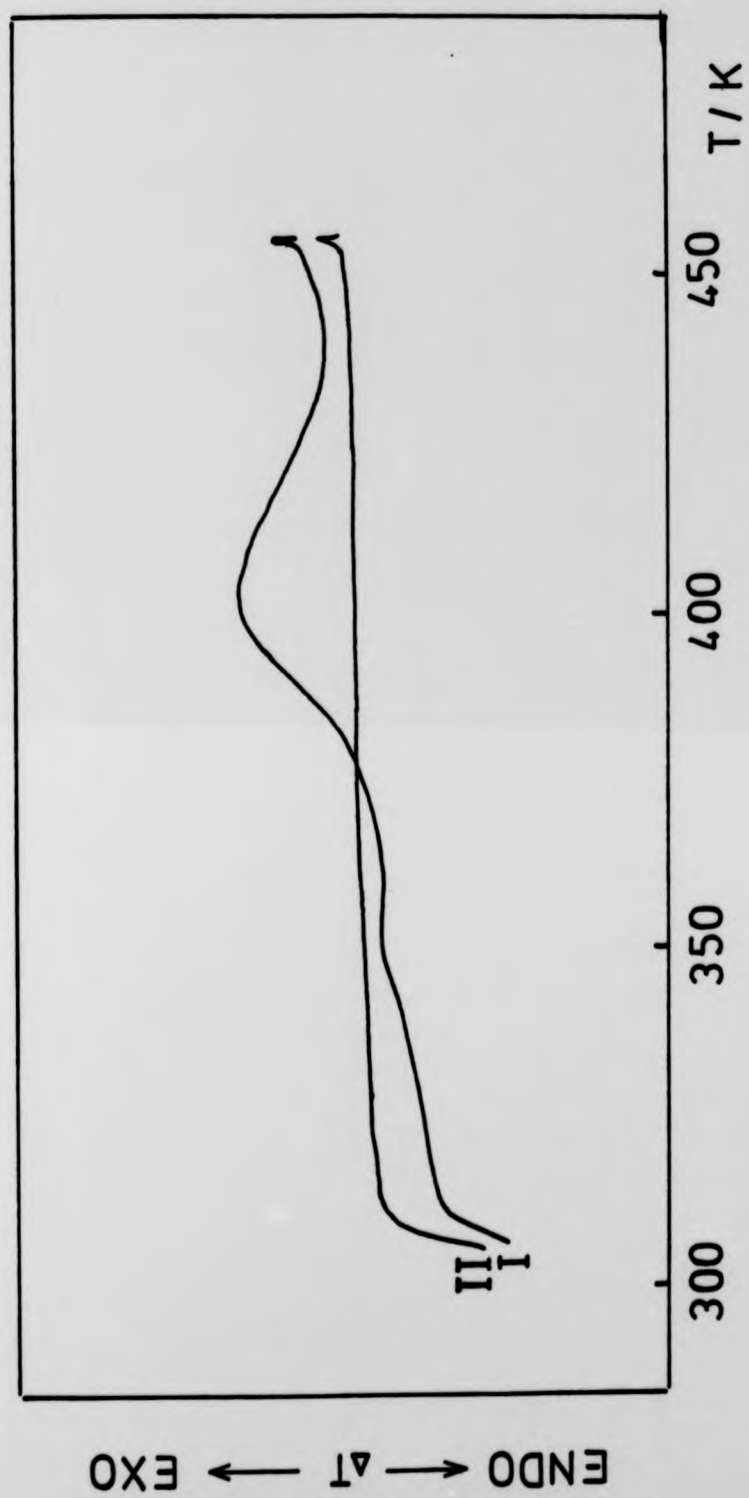


Fig. 7.9 DSC thermogram for poly(MHpI+DHpI)/EN, mole % of EN = 10.5.

7.8 TBA RESULTS FOR THE MODIFIED POLYMERS

The glass transition temperatures of some modified polymers containing pendant ethylene amine groups are shown in Table 7.5. The TBA thermograms are shown in Figures 7.10, 7.11, 7.12 and 7.13.

TABLE 7.5 The glass transition temperatures for some modified polymers

Sample Number	Polymer	Mole of side chains	Tg/K	Figure Number
21	poly(MHpI+DHpI)/EN	13.0	264-280	7.10
22	poly(MHpI+DHpI)/DETA	13.0	270-288	7.10
23	poly(MHpI+DHpI)/TETA	13.0	272-292	7.10
24	poly(MHpI+DHpI)/TEPA	13.0	273-294	7.10
45	poly(MMI+DMI)/EN	10.5		7.11
48	poly(MMI+DMI)/TEPA	10.5		7.11
29	poly(MHpI+DHpI)/EN	36.53	293-310	7.12
32	poly(MHpI+DHpI)/TEPA	36.53	304-320	7.12
33	poly(MHpI+DHpI)/EN	50.05		7.13
34	poly(MHpI+DHpI)/DETA	50.05		7.13
35	poly(MHpI+DHpI)/TETA	50.05		7.13
36	poly(MHpI+DHpI)/TEPA	50.05		7.13

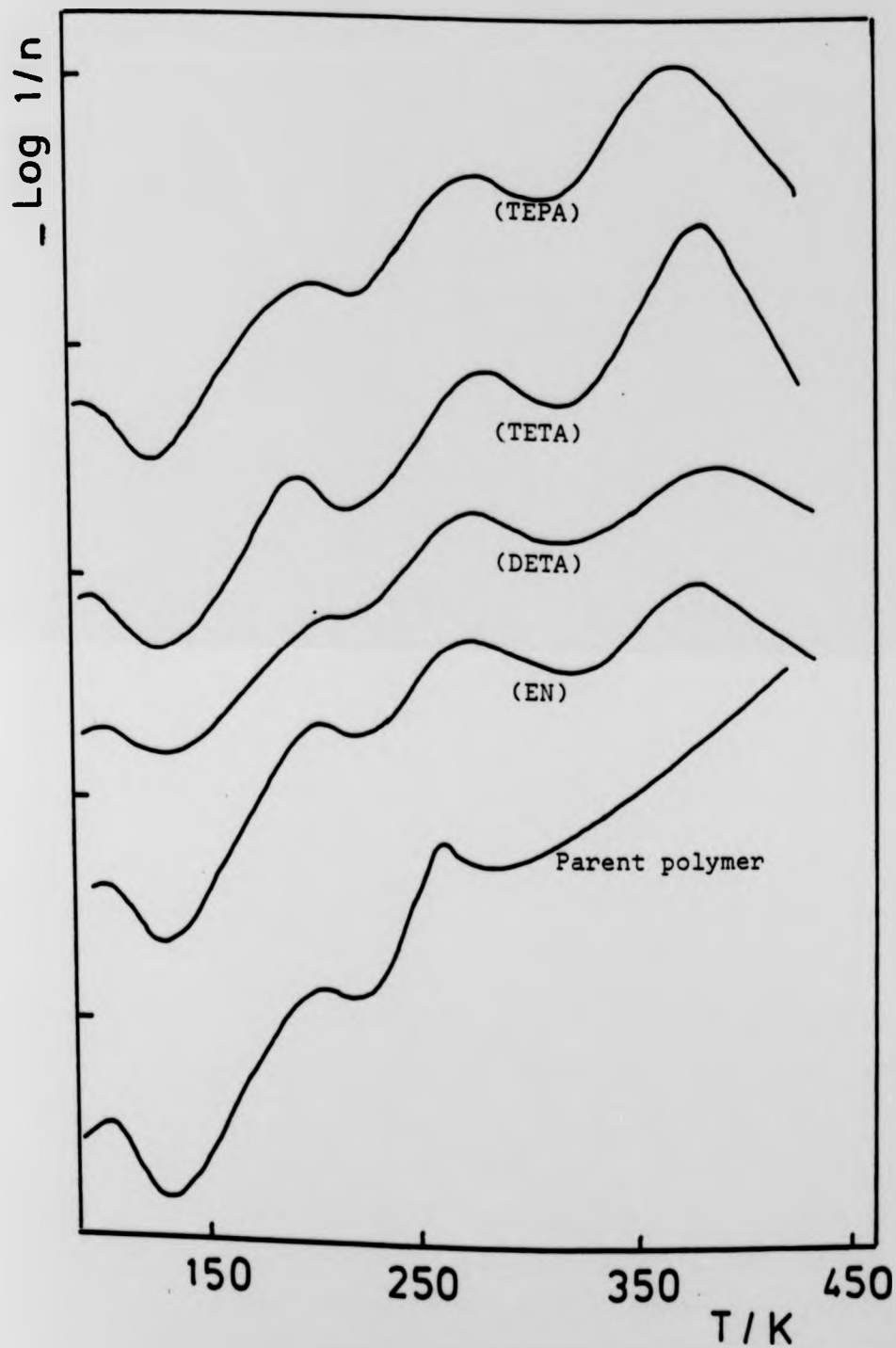


Fig. 7.10 TBA thermograms for modified poly(MHpI+DHpI),
mole % of side chain = 13.0.

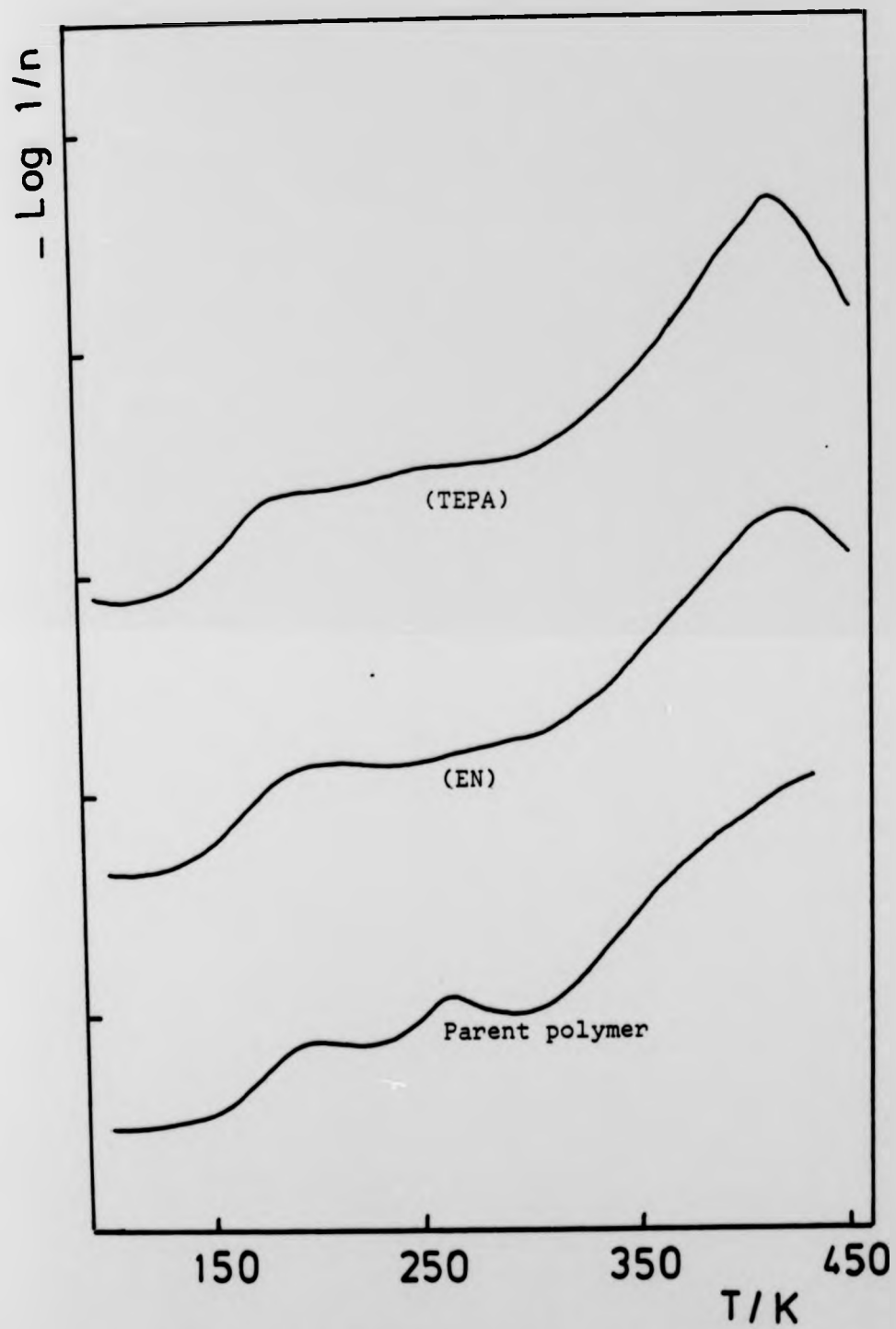


Fig 7.11 TBA thermograms for modified poly(MMI+DMI),
mole % of side chain = 10.5.

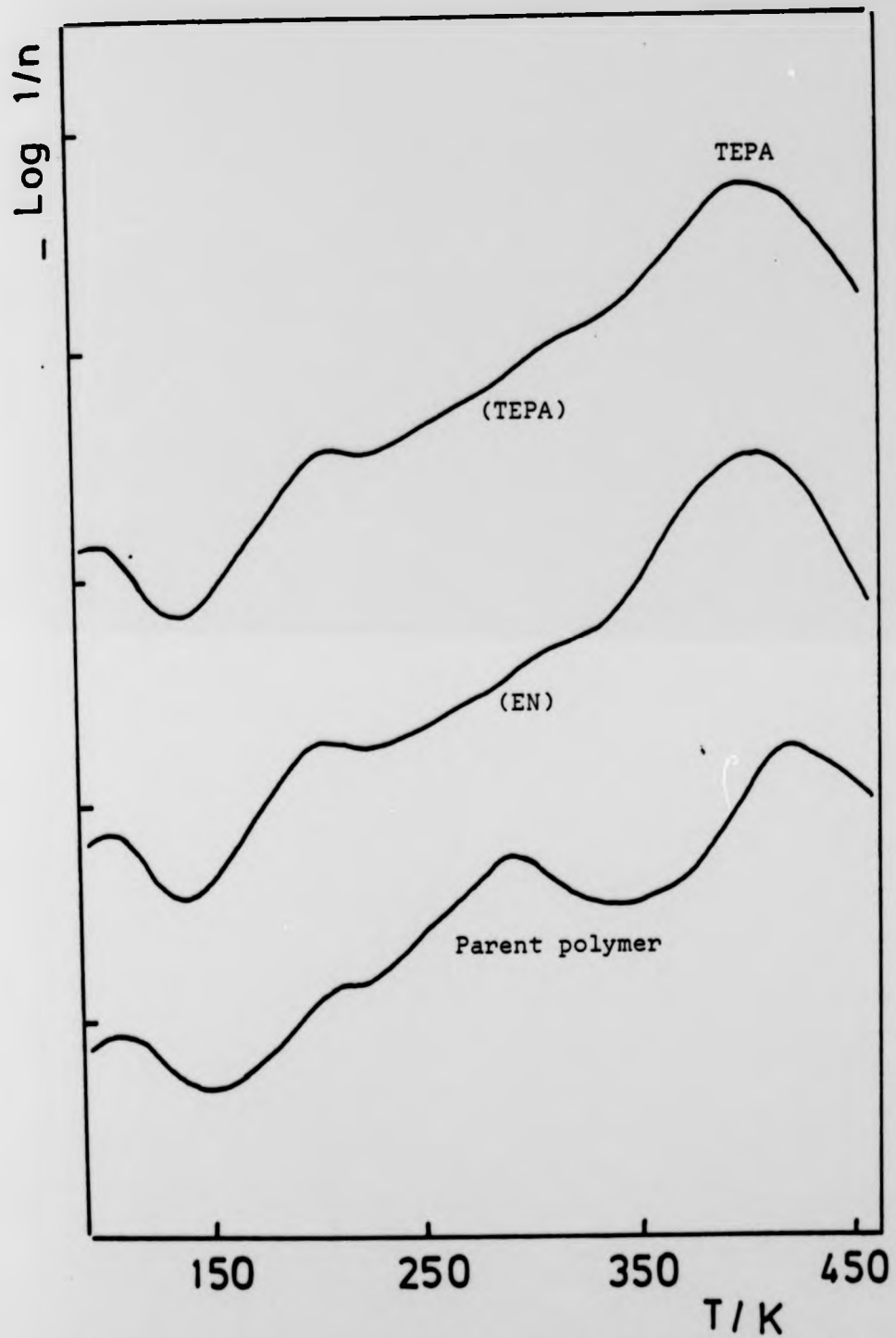


Fig. 7.12 TBA thermograms for modified poly(MHpI+DHpI),
mole % of side chain = 36.53.

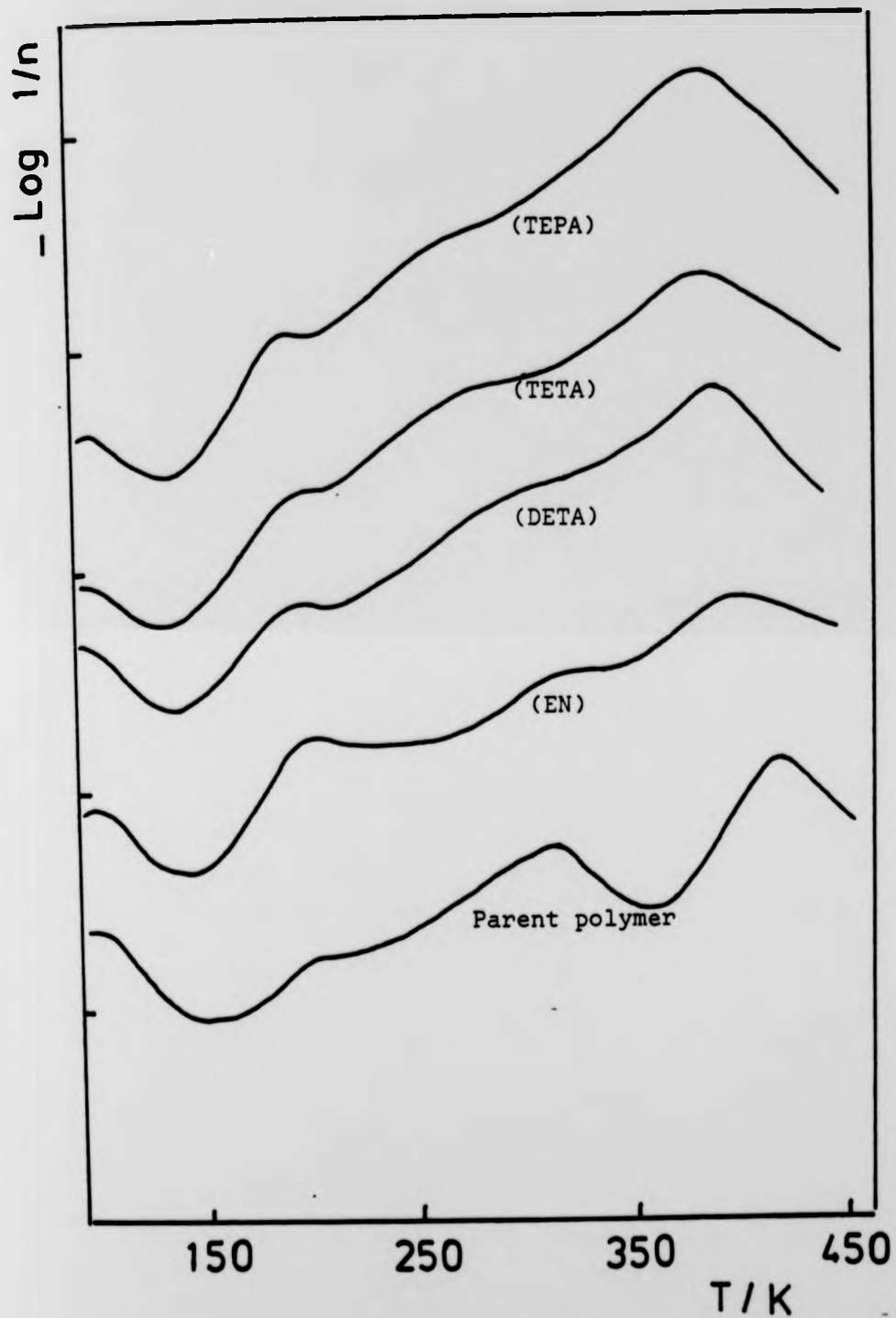


Fig. 7.13 TBA thermograms for modified poly(MHpI+DHpI), mole % of side chain = 50.05.

7.9 DISCUSSION

The TBA thermograms of the modified poly(MHpI+DHpI) systems, which contain originally 13.0 mole percentage of the monoester, together with that of the unmodified polymer, are shown in Figure 7.10. From Figure 7.10 it can be seen that the damping maxima associated with the upper (main chain) glass transition temperature becomes broader and shifts to a higher temperature with increasing side chain (the pendant ethylene imine group) length. This is due to an increase in the intermolecular hydrogen bonds which act as crosslinks, thereby tending to raise the glass transition temperature and causing the associated damping to become broad and ill-defined. The same results were obtained from the DSC thermograms of the modified poly(MHpI+DHpI) systems, the glass transition temperature increases as the mole percentage of the pendant ethylene amine group increases (see section 7.6). The lower (side chain) glass transition temperature appears in the range 180-200K, this is again due to the cooperative motion in the alkyl side chain (see section 7.5). The first damping maximum appearing at $\sim 95\text{K}$ was discussed in section 7.5. A fourth transition appears at $\sim 400\text{K}$ and is due to a chemical reaction. The thermal volatilization studies confirmed the formation of an imide structure and the elimination of ammonia and alcohol (see section 8.5). This peak does not appear in the TBA thermogram of the parent polymers, but when the mole percentage of the monoester

becomes more than 23.5, this transition appears, and is caused by the interaction between two adjacent acid groups to form the anhydride structure³⁷. To prove that this peak is due to a chemical reaction the poly(MHpI+DHpI)/EN was recycled and the TBA thermogram is shown in Figure 7.14. It can be seen that this transition disappears after recycling the sample. The glass transition temperature can be complicated, masked or even eliminated by a high degree of crosslinking¹⁰⁸ and as the mole percentage of the ethylene amine group increases, with a corresponding increase in the potential for hydrogen bond formation, so the glass transition temperature becomes less well defined.

In conclusion, it was very important to study the DSC and TBA thermograms of the parent polymers to compare and understand the behaviour of the modified polymers which contain pendant ethylene imine groups. The glass transition temperature was shifted to higher temperature, due to the tendency for crosslinks to form. The glass transition temperature becomes broad and ill-defined as the mole percentage of the pendant ethylene amine groups increases. An exothermic peak was observed in the DSC thermogram confirming the formation of an imide structure and the elimination of ammonia and alcohol.

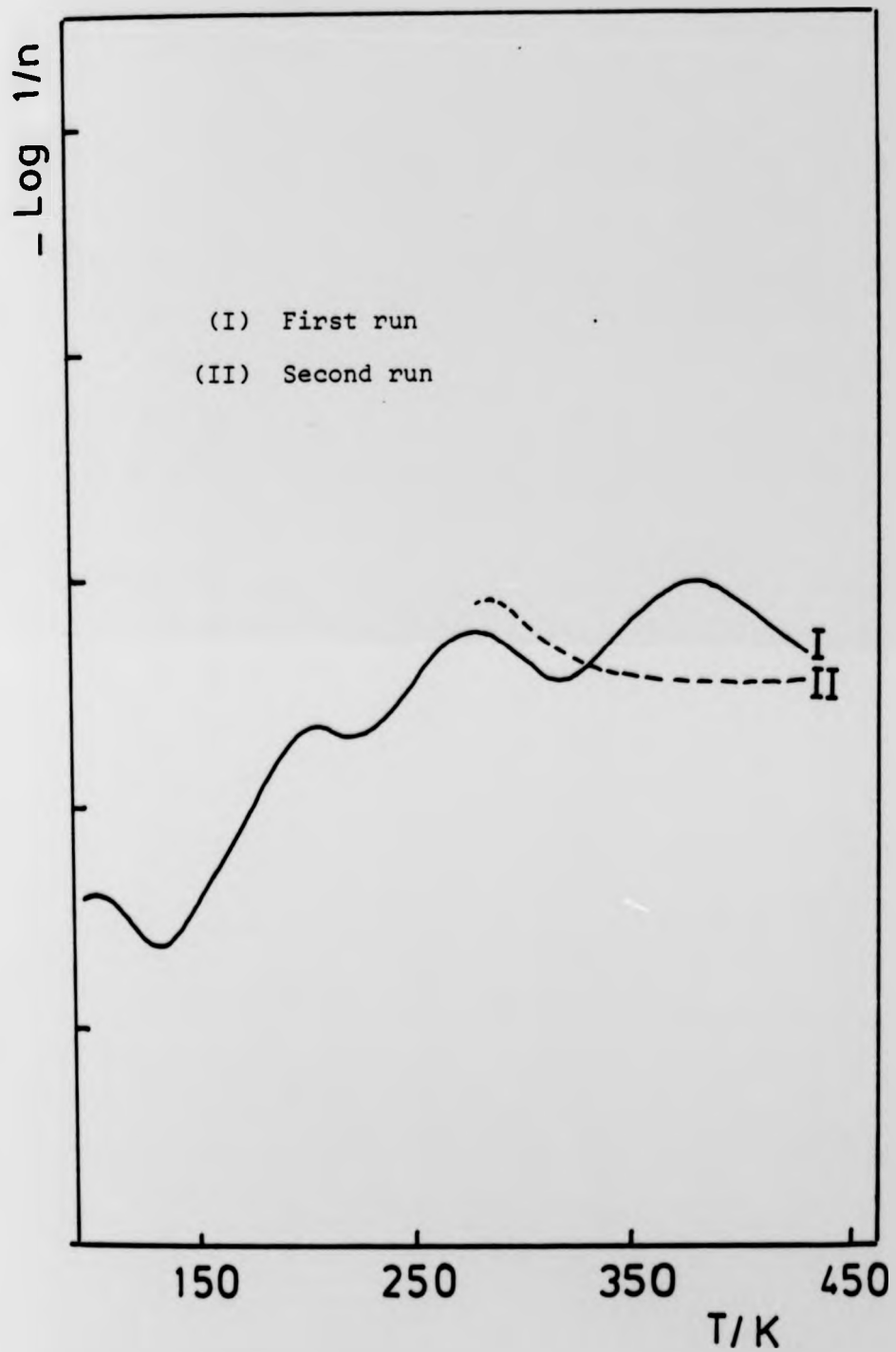


Fig. 7.14 TBA thermogram for poly(MHpI+DHpI)/EN, mole % of EN = 13.0.

7.10 VISCOELASTICITY

The viscoelastic response of the modified polymers and polymer-metal complexes as a function of temperature at a fixed frequency of 11 Hz using a Rheovibron was studied. The physical properties of the copolymers prepared in section 3.3, graduate from very sticky, tacky, viscous liquids to solid glassy-like materials and they are not always suitable for film formation. The modified polymers which contain EN, DETA, TETA or TEPA in the side chain and the polymer-metal complexes which contain cobalt as a metal ion show a tremendous change and as they can form good coherent films. The effect of the molecular weight and the mole percentage of the pendant ethylene amine groups on the behaviour of these modified polymers and polymer metal complexes has been studied.

7.11 THE VISCOELASTIC BEHAVIOUR OF THE MODIFIED POLYMERS

The viscoelastic behaviour of twelve modified polymers has been studied. The first four were poly(MHpI+DHpI)/TEPA, where the original mole percentages of the monoester are 0.29, 1.42, 3.12 and 4.93.

The average molecular weights of these modified polymers are shown in Table 7.6.

TABLE 7.6 The average molecular weights and the original mole percentages of some modified polymers

Sample Number	Polymer	Mole % of MHPi (equivalent to side chain concentration)	$\bar{M}_n/g \text{ mol}^{-1}$
13	poly(MHPi+DHPi)/TEPA	0.29	15.3×10^4
14	poly(MHPi+DHPi)/TEPA	1.42	16.1×10^4
15	poly(MHPi+DHPi)/TEPA	3.12	16.7×10^4
16	poly(MHPi+DHPi)/TEPA	4.93	17.1×10^4

The $\tan \delta$ against temperature curves for these modified polymers are shown in Figure 7.15. From this figure one maximum can be observed for each. A weak shoulder appears at $\sim 200\text{K}$ and corresponds to the so-called first glass transition temperature. This transition is due to relaxation of the alkyl side chains. This is confirmed from the DSC thermograms (see section 7.6). The second glass transition temperature is in the region 250-300K measured at 11 Hz and increases and becomes broader as the mole percentage of the side chain (TEPA) increases. Chemical crosslinking will increase the glass transition temperature and broaden the transition region. The resulting complex modulus (E^*) of these modified polymers was plotted against temperature as shown in Figure 7.16. From this figure it can be seen that as the mole percentage of the side chain (TEPA) increases there is a slight rise in the modulus in the rubbery region and an increase in the glass transition temperature, which can be taken as the mid point

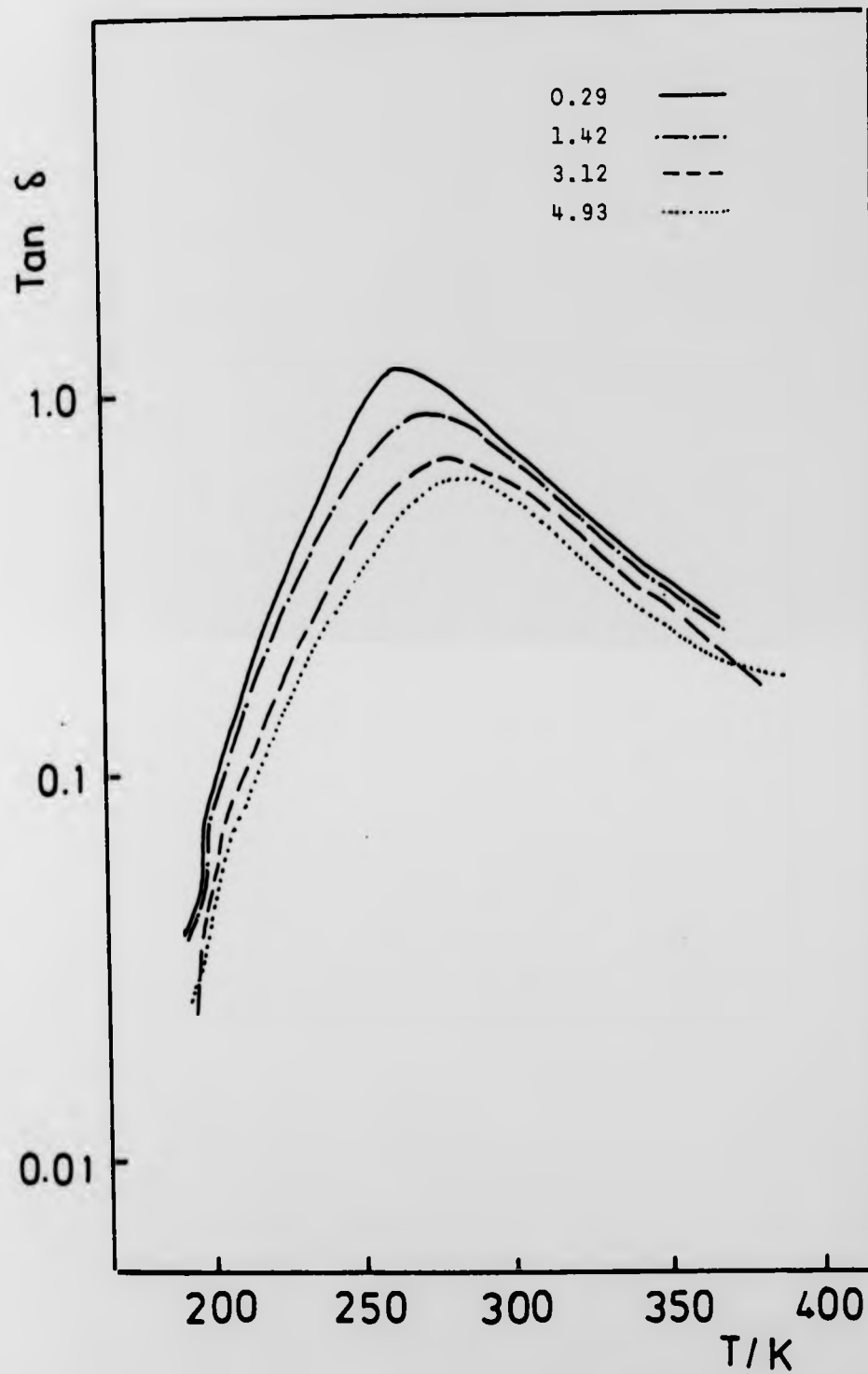


Fig. 7.15 RV tan δ curves for poly(MHpI+DHpI)/TEPA at indicate mole % of TEPA.

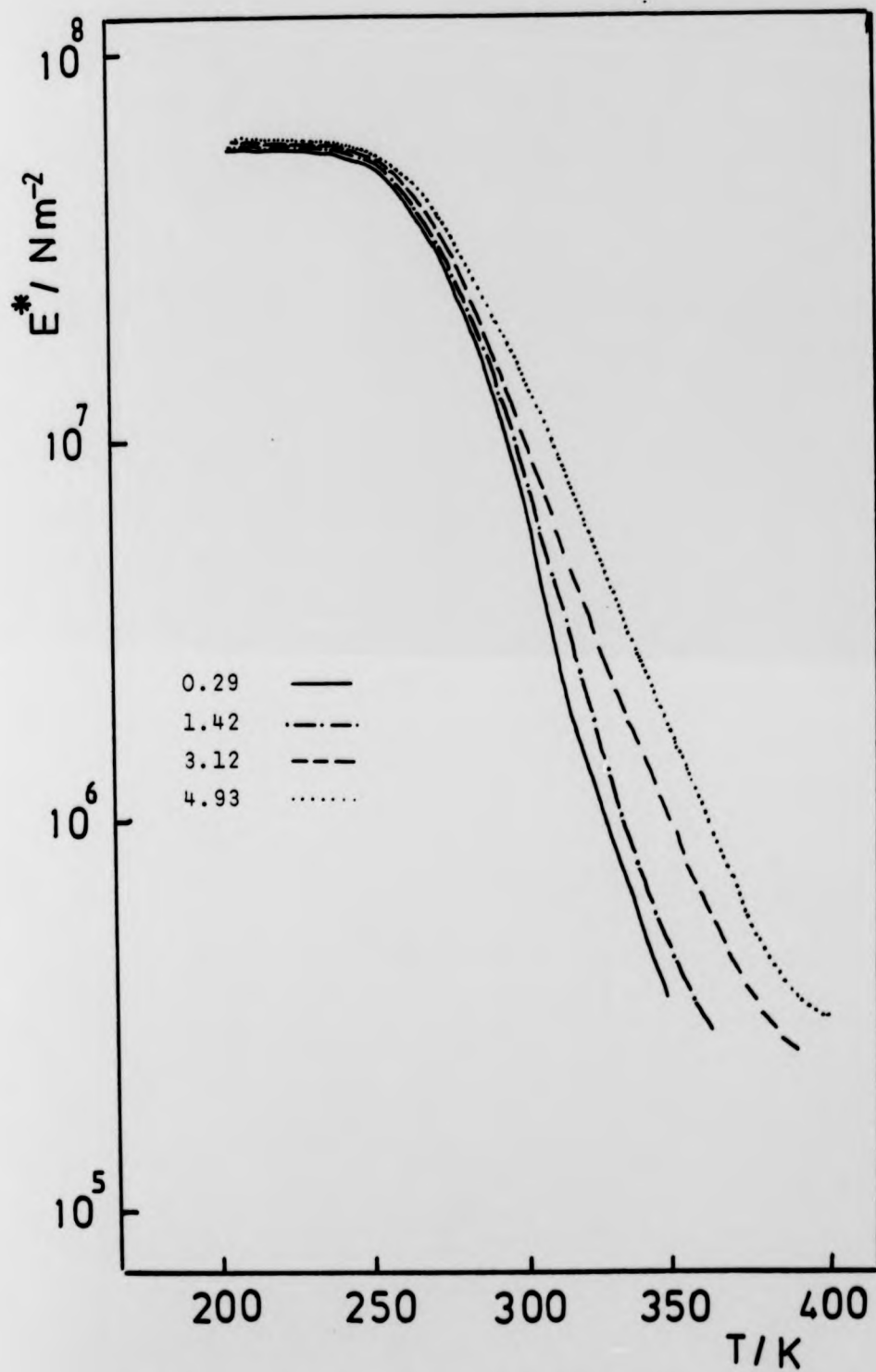


Fig. 7.16 RV modulus curves for poly(MHpI+DHpI)/TEPA at indicated mole% of TEPA.

in the modulus drop between $\sim 250\text{K}$ and $\sim 350\text{K}$. A modulus drop corresponding to the lower glass transition temperature is not evident.

7.11.1 Poly(MHpI+DHpI) with mole percentage of MHpI 6.3

The acid group in the mono-n-heptyl itaconate was reacted with EN, DETA, TETA or TEPA in the presence of DCC. The viscoelastic behaviour of these modified polymers is shown in Figures 7.17 and 7.18, and their molecular weights are shown in Table 7.7.

TABLE 7.7 The average molecular weights where the original mole percentage of monoester is 6.3

Sample Number	Polymer	$\bar{M}_n/\text{g.mol}^{-1}$
17	poly(MHpI+DHpI)/EN	87.6×10^3
18	poly(MHpI+DHpI)/DETA	88.5×10^3
19	poly(MHpI+DHpI)/TETA	89.8×10^3
20	poly(MHpI+DHpI)/TEPA	91.2×10^3

The $\tan \delta$ against temperature curves of these modified polymers are shown in Figure 7.17. No maxima could be resolved. The resulting complex modulus (E^*) of these modified polymers is shown in Figure 7.18. Their modulus fall quickly, but there was a slight increase in the modulus in the rubbery region when the side chain changed from EN to TEPA. The mechanical strength of a polymer depends on the size of the structural unit which is available to resist the

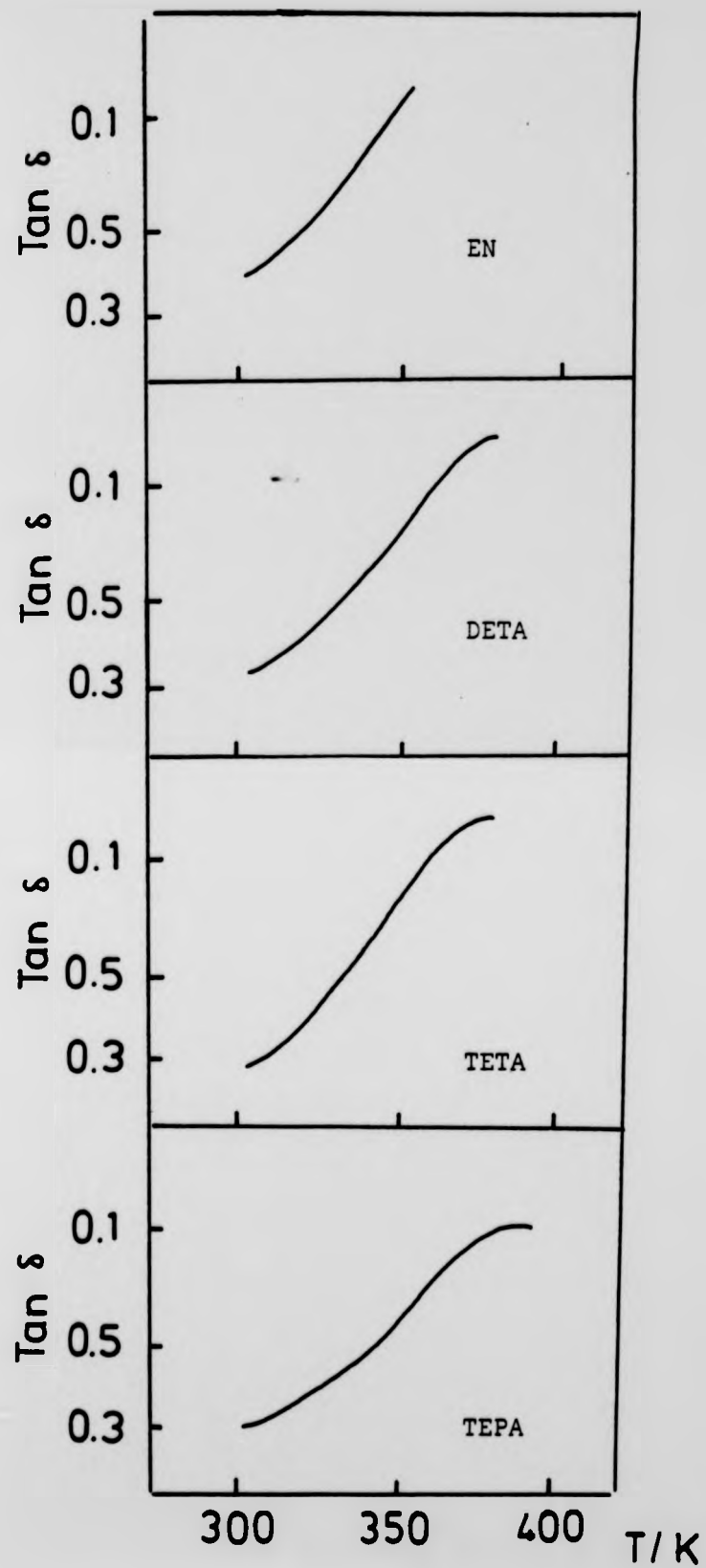


Fig. 7.17 RV $\tan \delta$ curves for modified poly(MHpI+DHpI), mole % of side chain = 6.3.

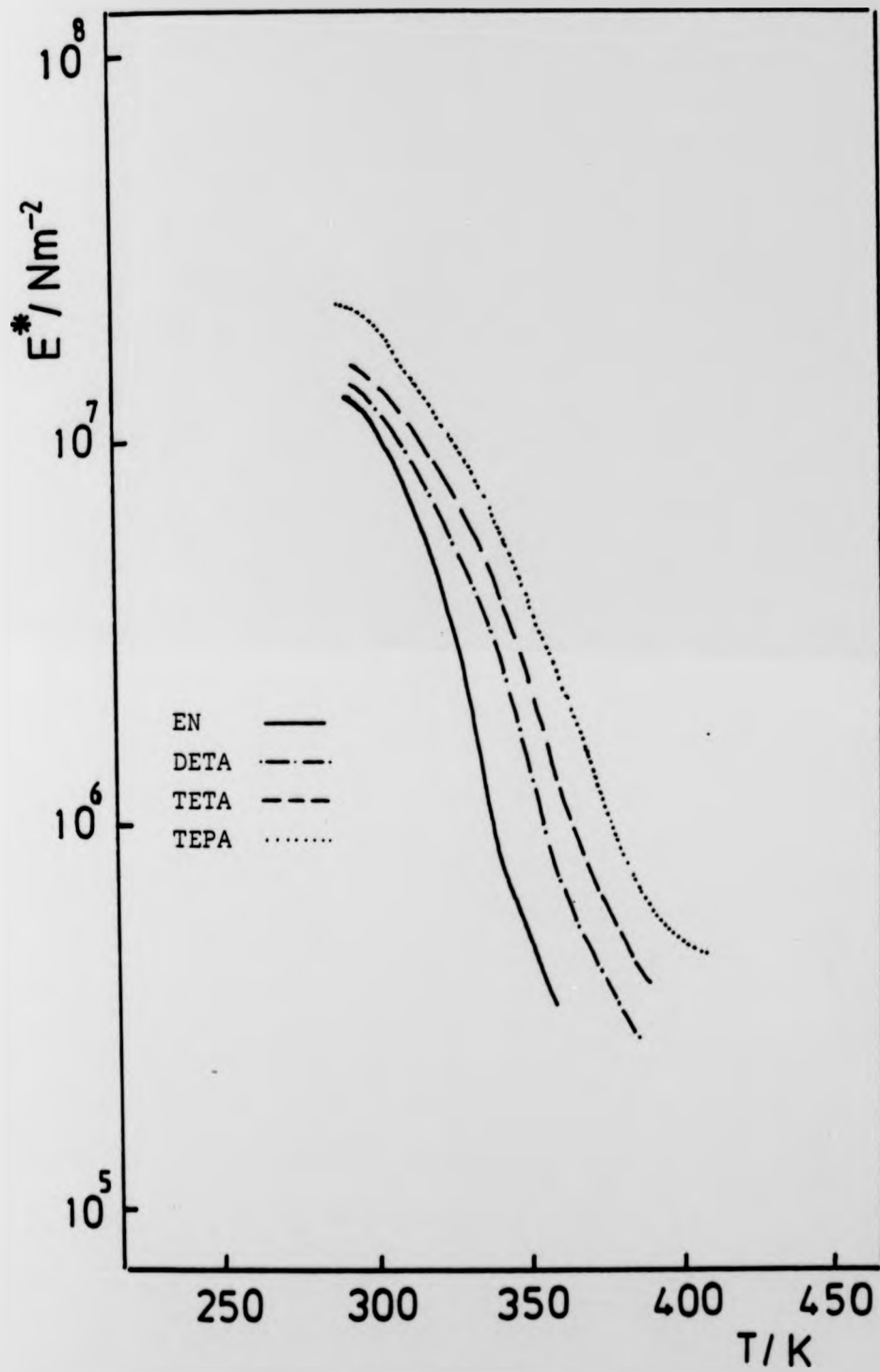


Fig. 7.18 RV modulus curves for modified poly(MHpI+DHpI), mole % of side chain = 6.3.

stress applied to it¹⁰⁹. This means that the mechanical strength increases with increase in the molecular weight of the modified polymer.

7.11.2 Poly(MHpI+DHpI) with mole percentage of MHpI 13.0

The average molecular weights of the modified polymers prepared from poly(MHpI+DHpI) where the original mole percentage of the monoester is 13.0 are shown in Table 7.8.

TABLE 7.8 The average molecular weights of modified poly(MHpI+DHpI)

Sample Number	Polymer	$\bar{M}_n/\text{g.mol}^{-1}$
21	poly(MHpI+DHpI)/EN	29.7×10^4
22	poly(MHpI+DHpI)/DETA	30.8×10^4
23	poly(MHpI+DHpI)/TETA	31.8×10^4
24	poly(MHpI+DHpI)/TETP	32.8×10^4

The $\tan \delta$ against temperature curves of these modified polymers are shown in Figure 7.19. Three well resolved peaks are observed, the first peak appears at $\sim 210\text{K}$ represents the first glass transition temperature, interpreted as being due to the independent cooperative relaxation of the side chain, the second peak at $\sim 310\text{K}$ is the second glass transition temperature and is due to the main chain relaxation resulting in the glass-rubber transition and the cooperative motion of the total molecule. The third peak at $\sim 400\text{K}$ is related to a chemical reaction. An

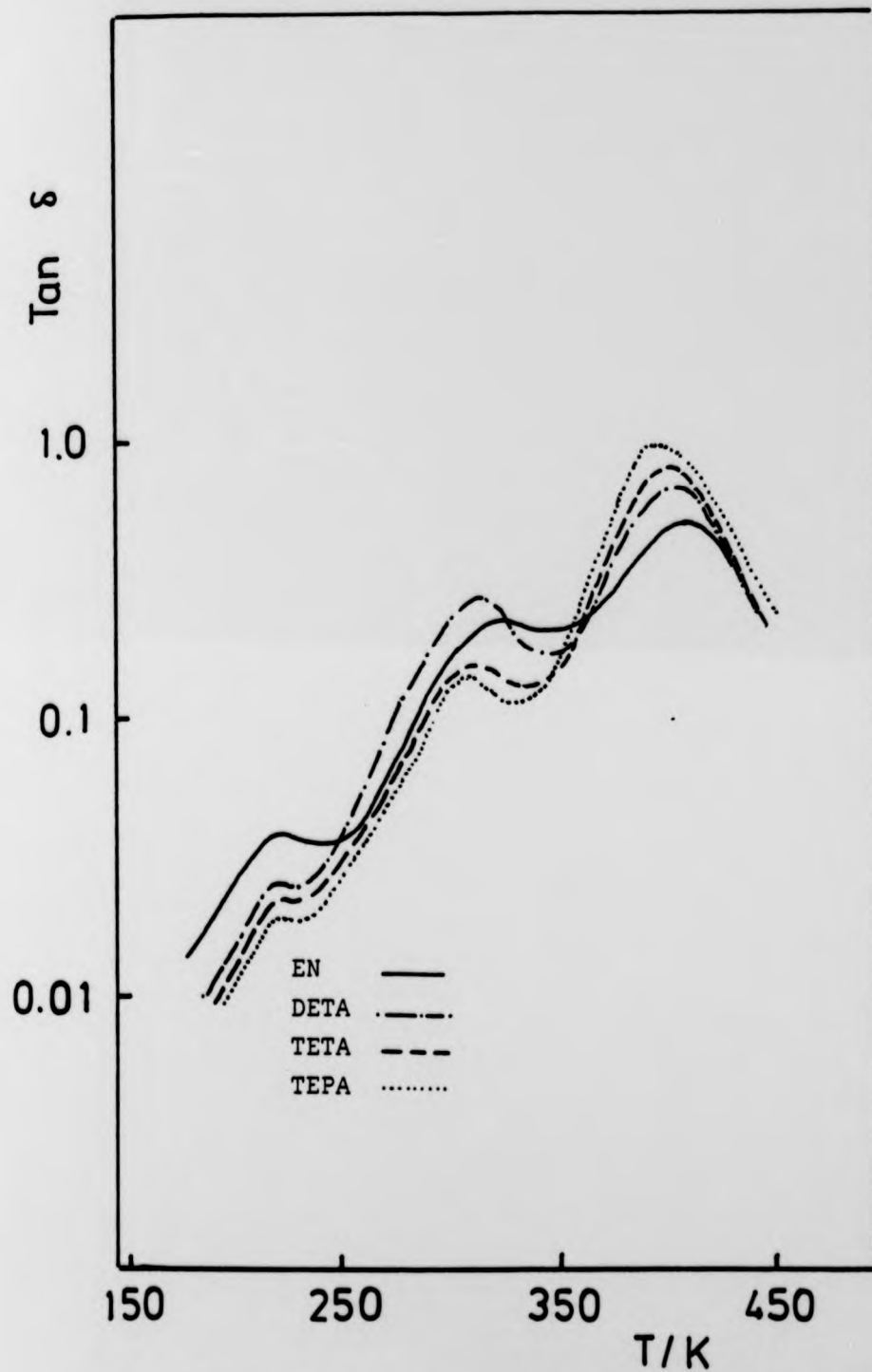


Fig. 7.19 RV tan δ curves for modified poly(MHpI+DHpI), mole % of side chain = 13.0.

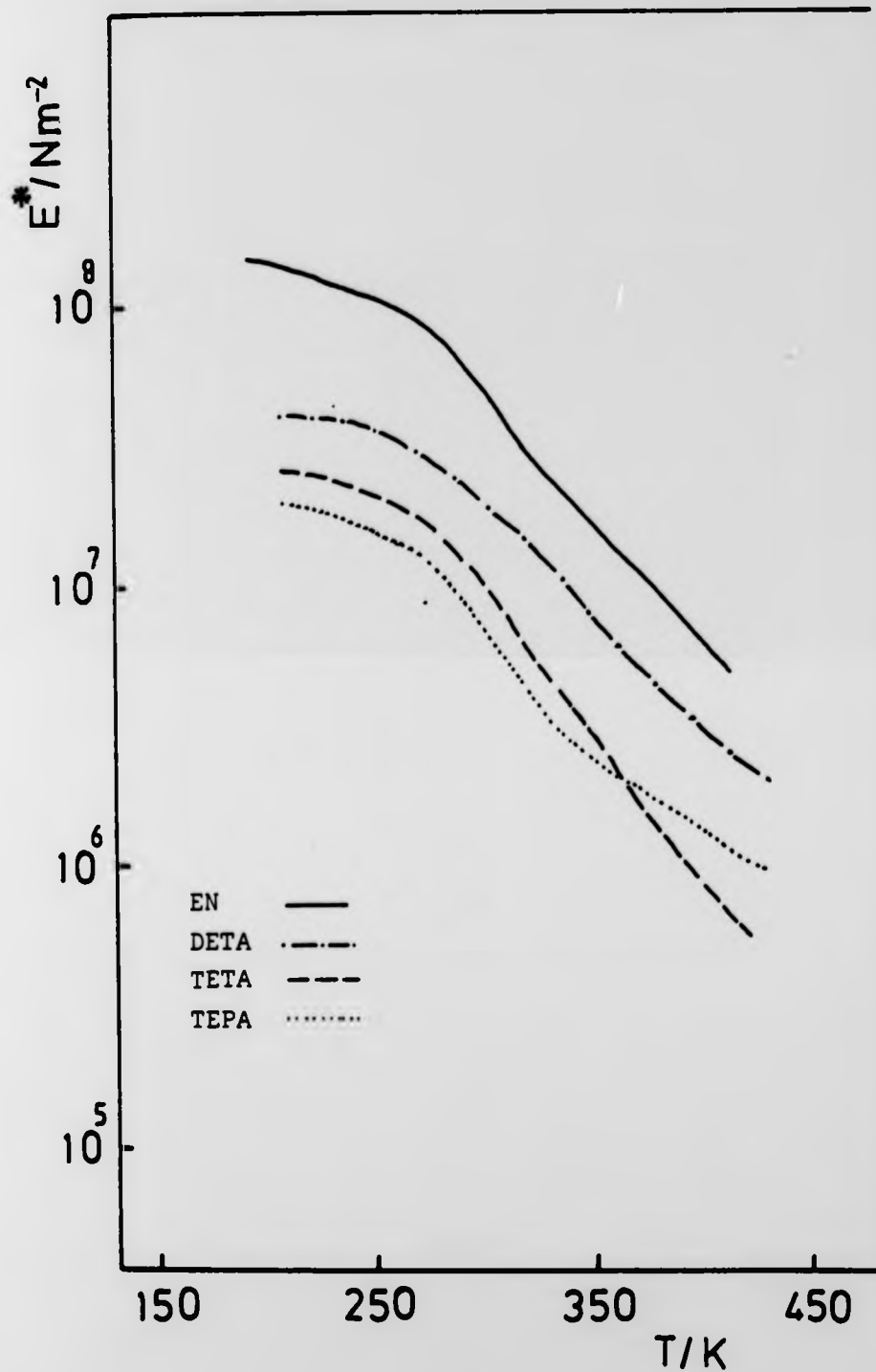


Fig. 7.20 RV modulus curves for modified poly(MHpI+DHpI), mole % of side chain = 13.0.

exothermic peak was observed in the DSC thermogram and confirmed as the formation of an imide structure (see section 7.6). The same peak was observed in the TBA thermogram which disappeared after recycling the sample (see section 7.8). Plots of the complex modulus (E^*) against temperature for the modified polymers are shown in Figure 7.20. The complex modulus (E^*) in the glassy region below $\sim 250\text{K}$ falls as the side chain changes from EN to TEPA. The polymer which contains TEPA in the side chain shows an increase in the modulus in the leathery region above $\sim 350\text{K}$, suggesting that increased polar interactions are coming into play as the length of the side chain increases, thereby enhancing the crosslinking in the sample. This is reflected in the modulus above the glass-transition.

7.12 DISCUSSION

The regions in the modulus-temperature curve depend upon the extent of the intermolecular interactions, which affect the ability of adjacent molecules to move past each other. Hydrogen bonding provides a large number of fairly strong intermolecular attractions between adjacent polymer molecules¹⁰⁹. The pendant ethylene amine groups increase the possibility of hydrogen bonding which will act as crosslinks and improves the modulus of the modified polymers. The changing of the parent polymers from a viscous liquid to

a material suitable for the formation of a film was noticeable. High molecular weight modified polymers with 13.0 mole percentage of the ethylene imine side chains exhibit some improvement of the modulus and an extension of the leathery region. Higher degrees of cross-linking restrict segmental motion raising the modulus in the rubbery region and convert the polymer to a leathery state.

7.13 THE VISCOELASTIC BEHAVIOUR OF POLYMER-METAL COMPLEXES

The viscoelastic behaviour of six polymer-metal complexes has been studied. The first four polymer-metal complexes show the effect of increasing the mole percentage of the metal ions. The $\tan \delta$ against temperature curves of these polymer-metal complexes, which contain (TEPA) in the side chain fully reacted with cobalt(II) chloride are shown in Figure 7.21. Two peaks are observed. The first peak at $\sim 220\text{K}$, which was not well resolved and looks like a shoulder could be the first glass transition temperature. The second in the region $300\text{-}320\text{K}$ is the second glass transition temperature which reflects the glass-rubber transition of the main chain backbone and the cooperative motion of the total molecule. As the mole percentage of the metal ion increases, the second peak shifts to a higher temperature. The curves of the complex modulus (E^*) against temperature for these polymer-metal complexes are

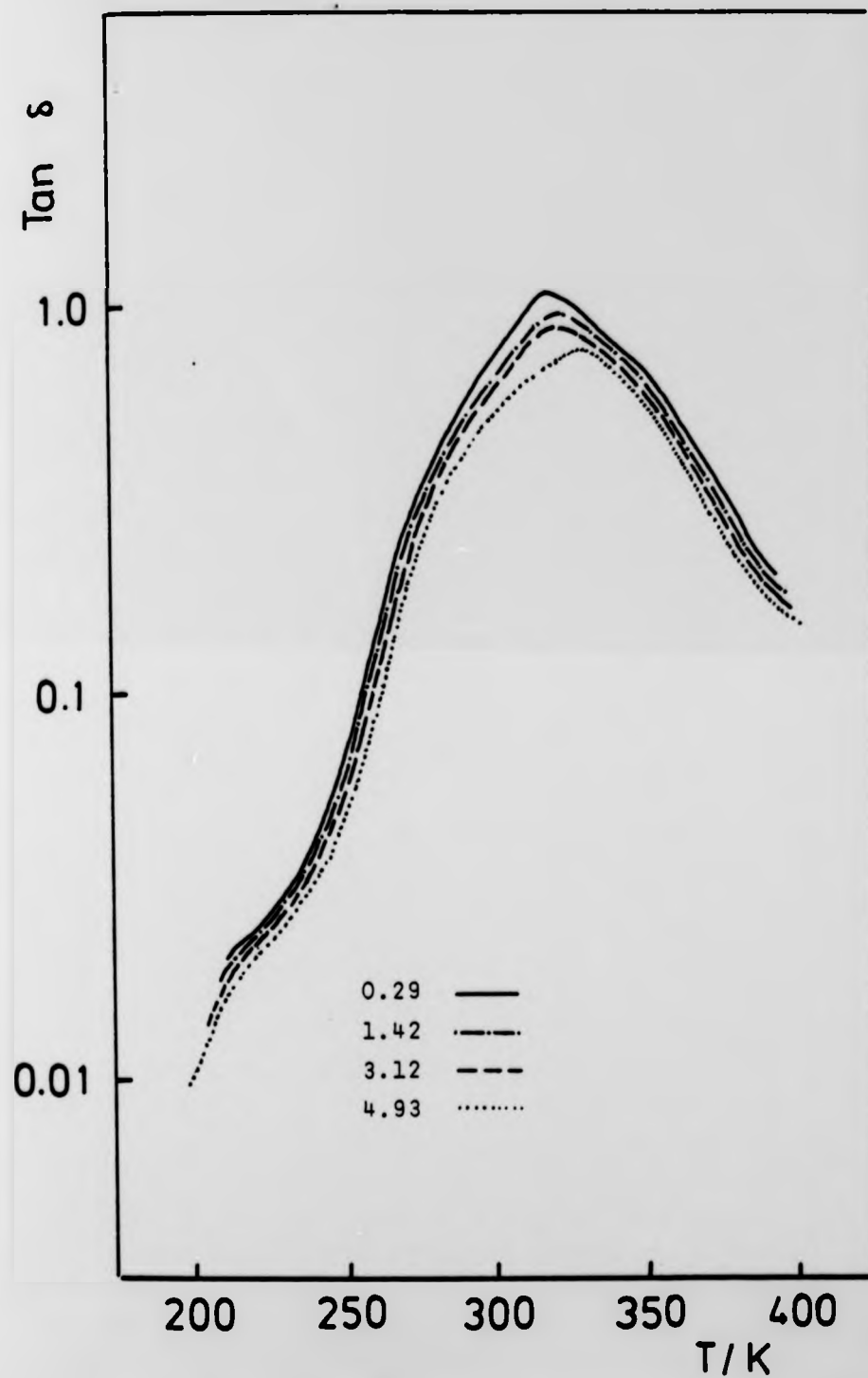


Fig. 7.21 RV tan δ curves for poly(MHpI+DHpI)/TEPA/CoCl₂ (fully reacted with CoCl₂) at indicated mole% of TEPA.

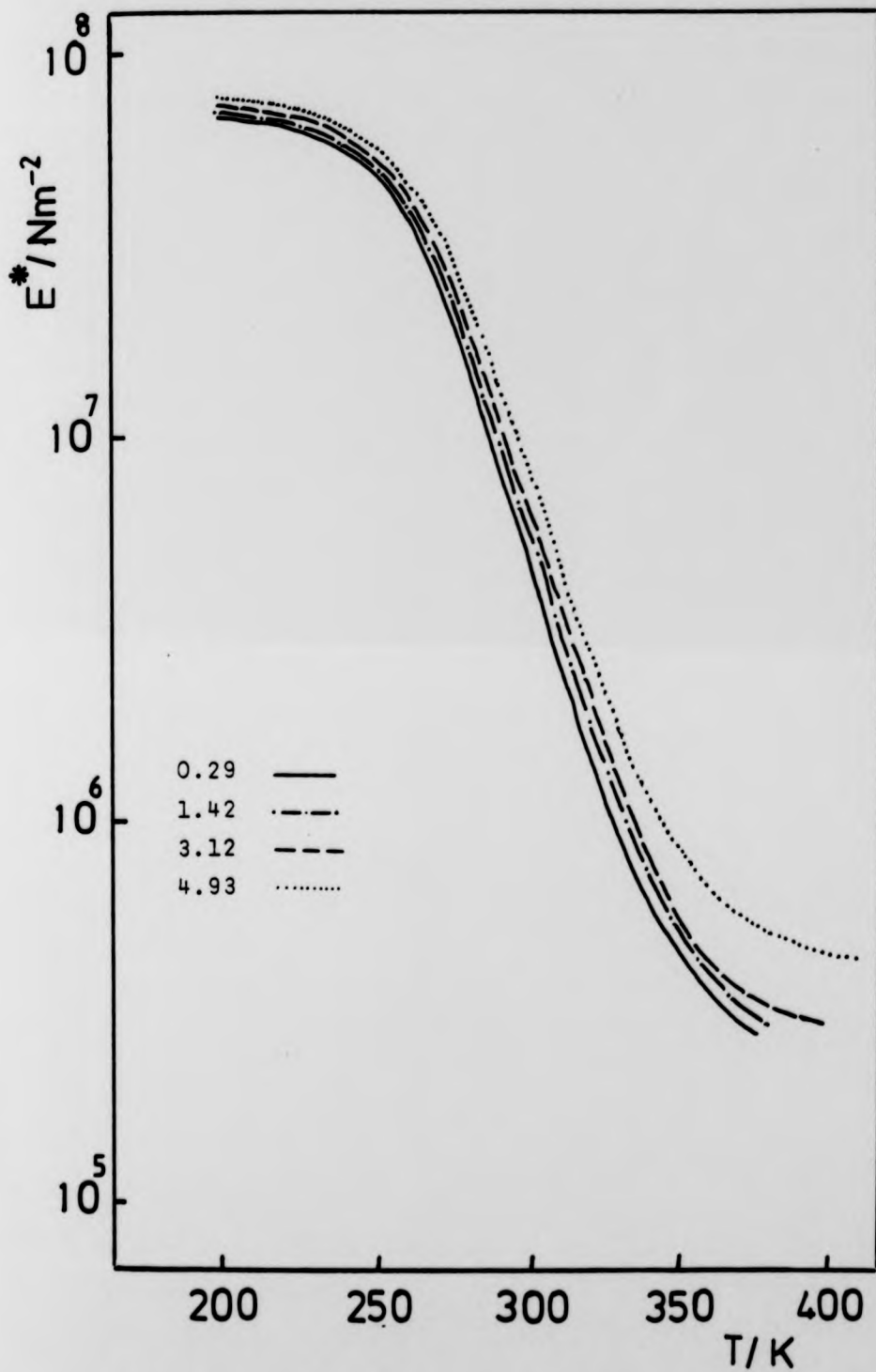


Fig. 7.22 RV modulus curves for poly(MHpI+DHpI)/TEPA/CoCl₂ (fully reacted with CoCl₂) at indicated mole % of TEPA.

shown in Figure 7.22 and it can be seen that the modulus of the rubbery region increases as the percentage of the metal ions increases.

A comparison between poly(MHpI+DHpI)/TEPA, where the mole percentage of the monoester is 6.3 and poly(MHpI+DHpI)/CoCl₂ (fully reacted with cobalt(II) chloride) is shown in Figure 7.23. Poly(MHpI+DHpI)/TEPA was mechanically weak (see section 7.11.1). The first and the second glass transition temperatures were observed in the case of polymer-metal complex and the modulus in the glassy region below ~250K was higher. Figure 7.24 shows the viscoelastic response of poly(MHpI+DHpI)/TEPA and poly(MHpI+DHpI)/TEPA/CoCl₂, where the original mole percentage of the monoester is 13.0. The complex modulus (E^*) against temperature curve of the polymer-metal complex shows an increase in the leathery region whilst the $\tan \delta$ curve shows that the transition due to the chemical reaction has shifted to higher temperatures.

7.14 DISCUSSION

Polymers crosslinked by coordination complexes may be considered as very similar to ionomers. These polymer-metal complexes were tougher than the parent polymers and they formed coloured films giving the characteristic colour of the metal after coordination (see section 5.2). At high metal ion concentrations the polymer-metal complexes were

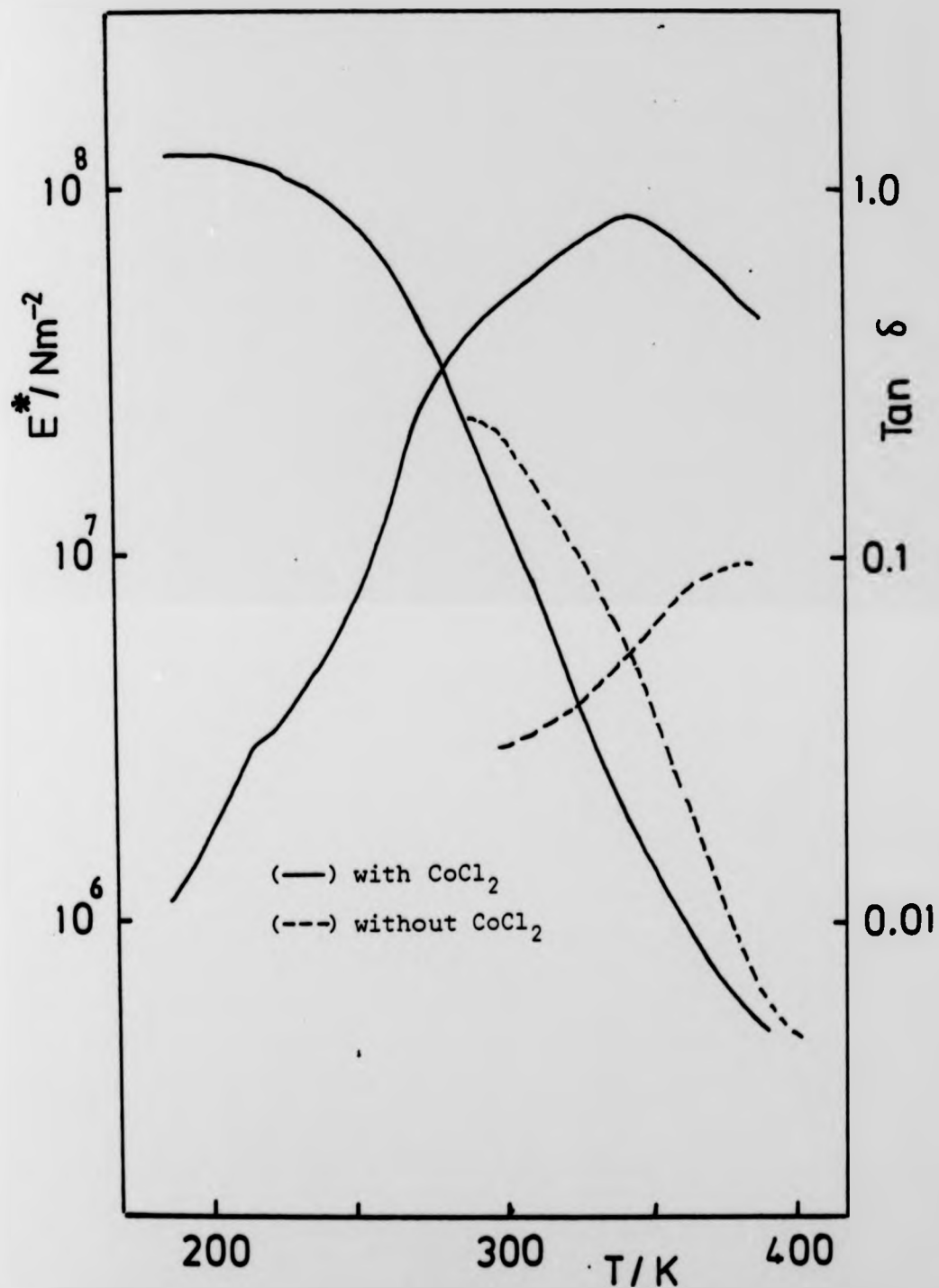


Fig. 7.23 RV thermograms for (---) poly(MHpI+DHpI)/TEPA mole % TEPA 6.3 and (—) poly(MHpI+DHpI)/TEPA/ $CoCl_2$.

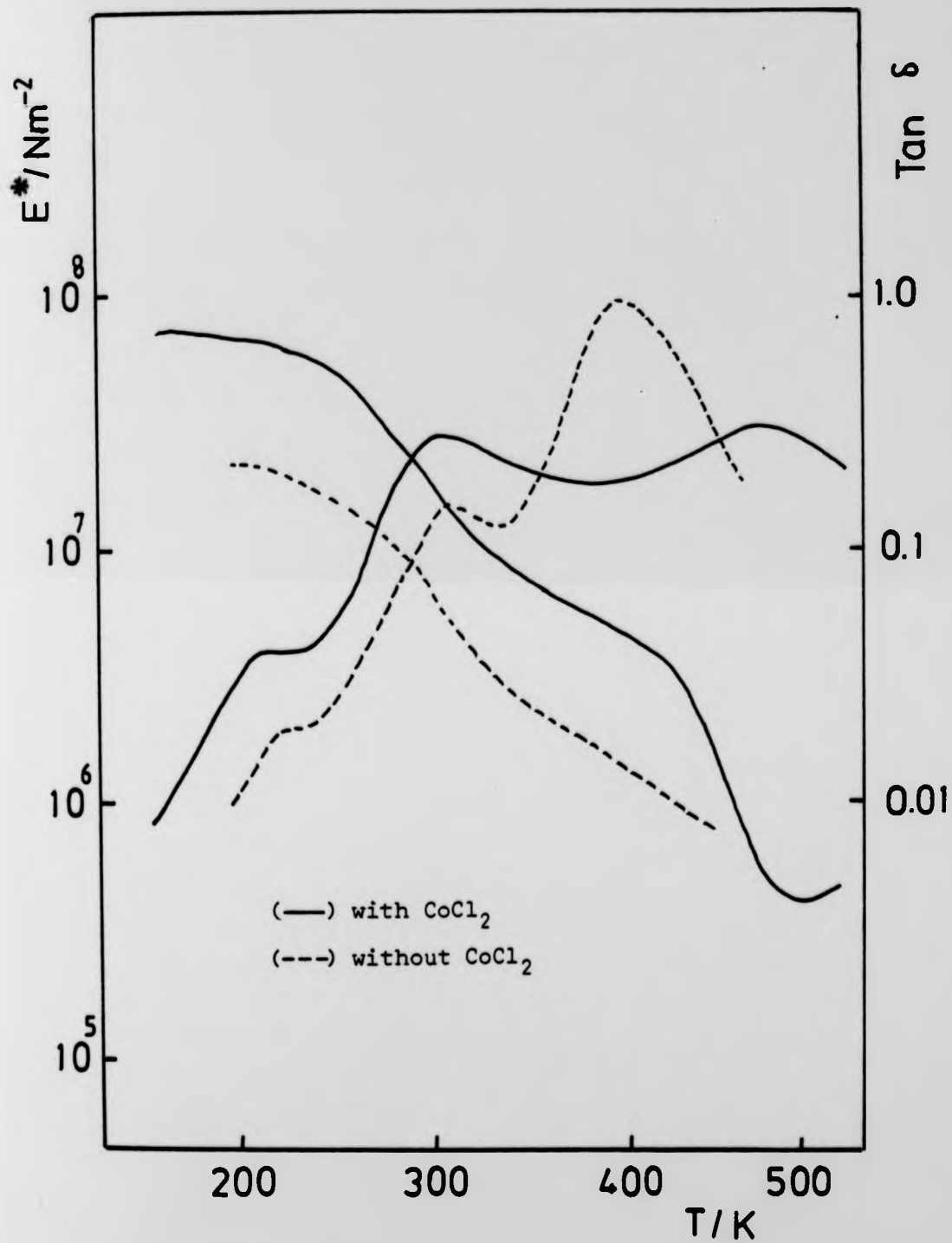


Fig. 7.24 RV thermograms for (---) poly(MHpI+DHpI)/TEPA, mole % TEPA 13.0 and (—) poly(MHpI+DHpI)/TEPA/ $CoCl_2$.

rigid glassy materials. The presence of a low degree of crosslinking in amorphous polymers will prevent liquid flow completely and extends the rubbery region up to the decomposition temperature. The glass transition temperature and the transition due to a chemical reaction were shifted to higher temperatures because of crosslinking. Presumably in the latter case this was because the nitrogen lone pairs are involved in complex formation and less available for reaction.

CHAPTER EIGHT
THERMAL STABILITY
RESULTS AND DISCUSSION

CHAPTER EIGHT
THERMAL STABILITY
RESULTS AND DISCUSSION

8.1 THERMAL STABILITY STUDIES

Thermogravimetric analysis (TGA) was combined with thermal volatilization analysis (TVA) to study the thermal degradation of the parent polymers, modified polymers and polymer-metal complexes. The thermal volatilization analyses of the following polymers, poly(MHpI+DHpI) with mole percentage of mono-n-heptyl itaconate = 13.0, poly(MHpI+DHpI)/EN, poly(MHpI+DHpI)/TEPA, poly(MHpI+DHpI)/TEPA/CoCl₂ and poly(MHpI+DHpI)/DETA, where the mole percentage of the original monoester is 50.05, have been carried out.

8.2 INTERPRETATION OF TVA TRACE

The pirani gauge response in the thermal volatilization analysis is non-linear with pressure, and its output is recorded as a function of temperature or time. The recorder trace shows one or more peaks corresponding to decomposition as the sample is heated, and these can be identified as the products of the thermal degradation of the polymers. The degradation products may or may not pass through all the pirani gauges, depending on their volatility⁸¹. In order to understand the behaviour of the pirani gauge, one must compare the response of the gauge following a trap at 275K with the behaviour of gauges in lines with lower trap

temperatures and this has been found to take three forms⁸¹.

- 1: The trace of a gauge in line with a lower trap temperature is coincident with that for the 273K trap. This means that no substance is trapped out at 273K.
- 2: The trace follows the base line. This means that the substance is fully condensed in the 273K trap and remains there.
- 3: The trace rises to a plateau and remains there for some time and eventually returns to the base line. This is termed a "limiting rate effect" which arises when a substance condenses in the initial trap but is also sufficiently volatile to distill slowly from the initial trap.

The area under the curve is a measure of the amount of material passing through the pirani gauge. During the thermal degradation, there are two types of product, involatile and volatile. The volatile products will be trapped off and identified by mass and infrared spectroscopy. The non-volatile products will condense at the furnace exit, giving rise to the so-called "cold ring fraction".

8.3 RESULT OF TVA STUDIES

8.3.1 Poly(MHpI+DHpI), mole percentage of MHpI 13.0

The TVA thermogram of this polymer is shown in Figure 8.1. Three peaks are present, but not resolved, at $\sim 580\text{K}$, $\sim 650\text{K}$ and $\sim 720\text{K}$. The initial weight loss and the initial evolution of volatile products at $\sim 450\text{K}$ are due to loss of water and heptanol to form anhydride structures. At $\sim 660\text{K}$ the TVA peak is most likely caused by a comparable breakdown of the anhydride polymer. At $\sim 720\text{K}$ thermal breakdown of the side chain occurs.

8.3.2 Discussion

Mass spectral and infrared analysis of the volatile products confirms the presence of carbon monoxide, carbon dioxide, water, heptanol and alkenes. Anhydride structures will be formed when water and heptanol are lost and the following mechanisms are proposed for the initial formation of anhydro-polymers³⁷ (see scheme I).

The distribution of the heptyl side chain in the copolymer is random, and an acid group adjacent to an ester linkage will form a relatively strained seven membered ring. Structure (II) could be formed if two adjacent acid groups interacted, and it has been found that during the course of preparation of these copolymers, heating under vacuum will often lead to the formation of anhydride structures. The infrared spectra confirm that

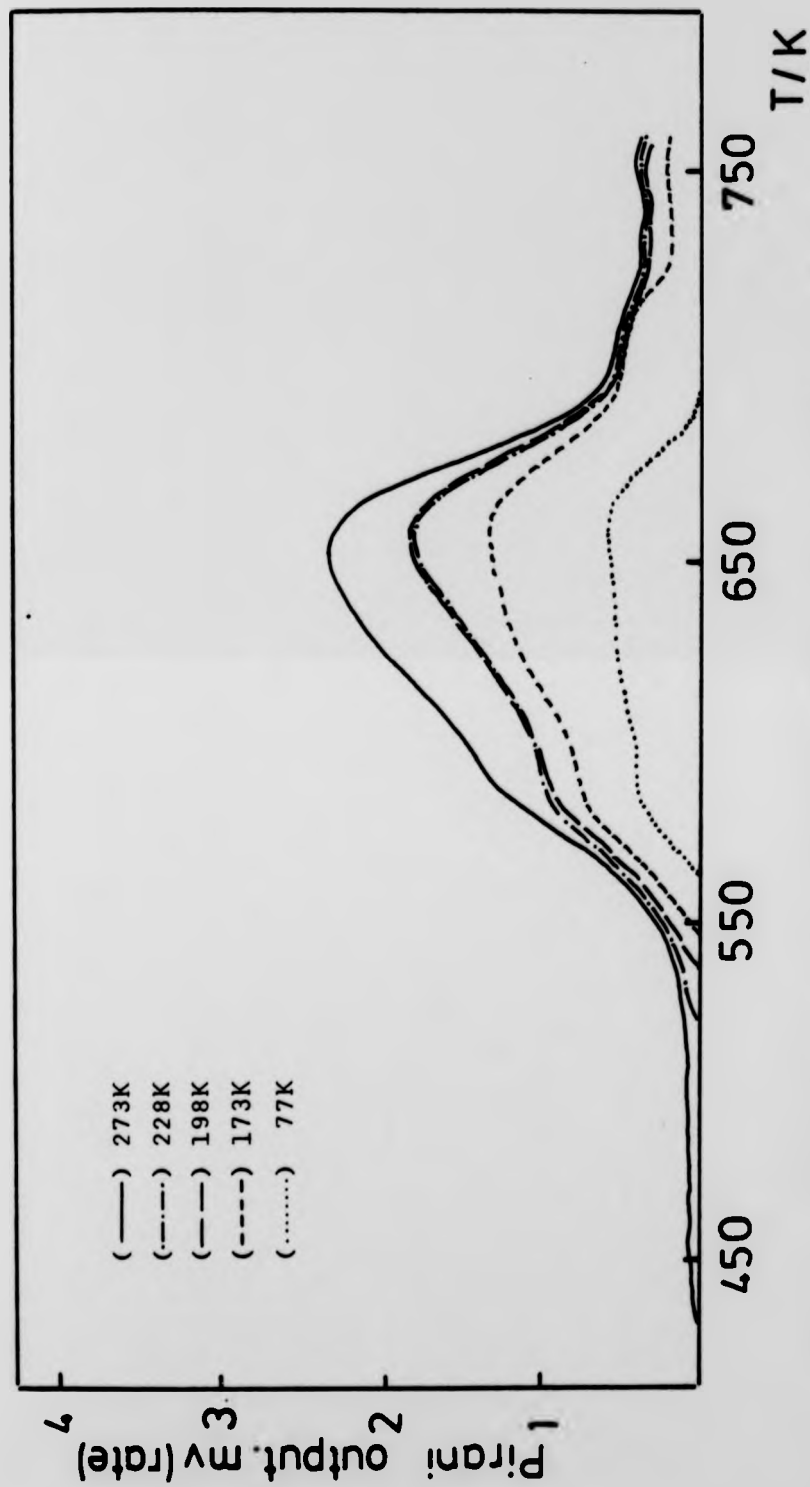
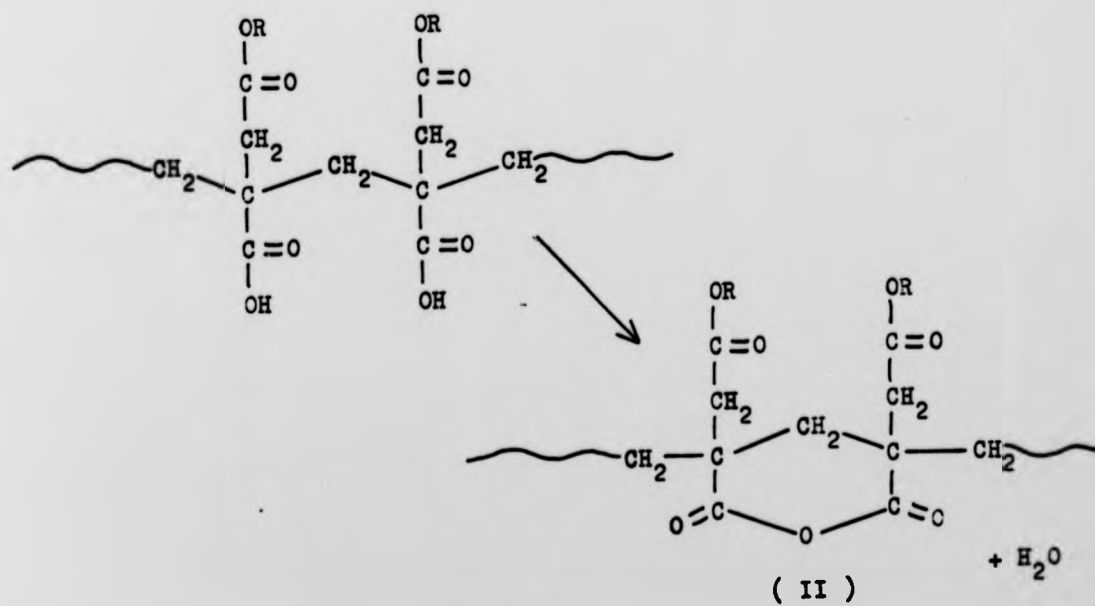
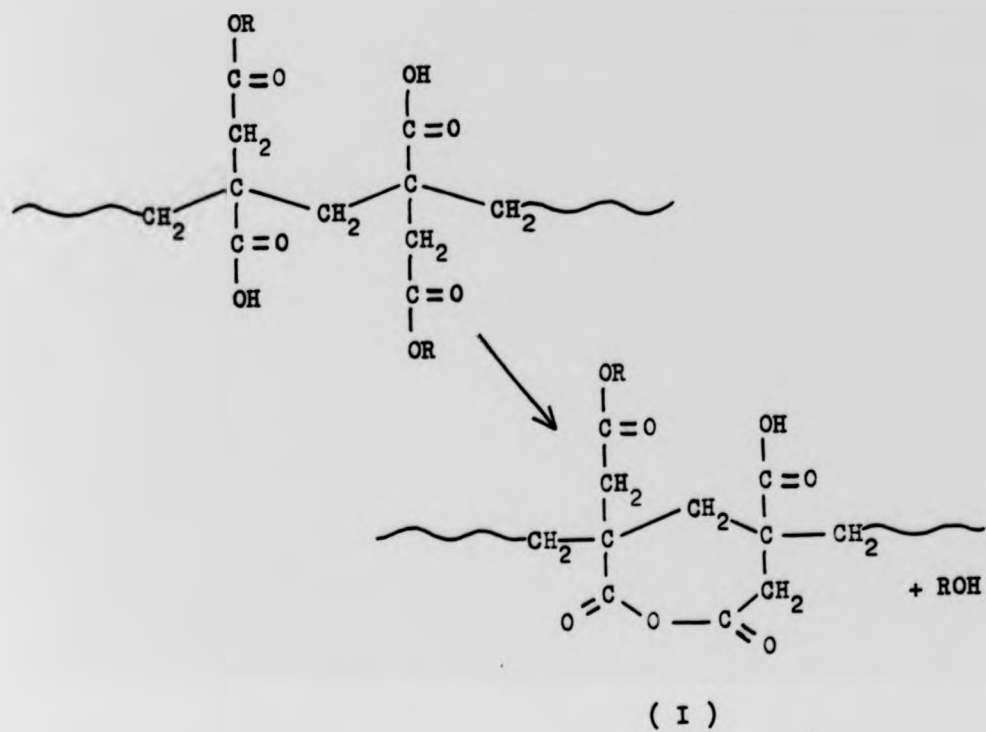


Fig. 8.1 TVA thermogram for poly(MHpI+DHpI), mole % of MHpI 13.0.



Scheme I

three additional absorptions are found at $\sim 1780 \text{ cm}^{-1}$, and 1855 cm^{-1} which are characteristic of anhydride structures. The highest TVA peak was at $\sim 660\text{K}$. At this temperature the anhydride polymer, which because of crosslinking is stable up to high temperatures, is broken down. The infrared spectrum of the cold ring fraction shows a carbonyl absorption but not monomer. From this information one can conclude that the thermal degradation occurs in a random manner.

8.4 RESULTS OF TVA OF MODIFIED POLYMERS

8.4.1 Poly(MHpI+DHpI)/EN

The TVA thermogram for poly(MHpI+DHpI)/EN where the original mole percentage of the monoester is 13.0, is shown in Figure 8.2. Three resolved peaks are observed in the TVA thermogram of this polymer. The first peak at $\sim 450\text{K}$ is due to loss of water, carbon monoxide, carbon dioxide and alcohol. At the second peak ($\sim 550\text{K}$) more water, carbon monoxide, carbon dioxide and alcohol were lost. From $\sim 560\text{K}$ to $\sim 600\text{K}$ little material was evolved, probably due to the formation of imide structures which will be discussed later. The highest temperature TVA peak was the third peak at $\sim 670\text{K}$ and most of the imide structure was destroyed at this temperature. The infrared spectrum shows the presence of ammonia, the elimination of which

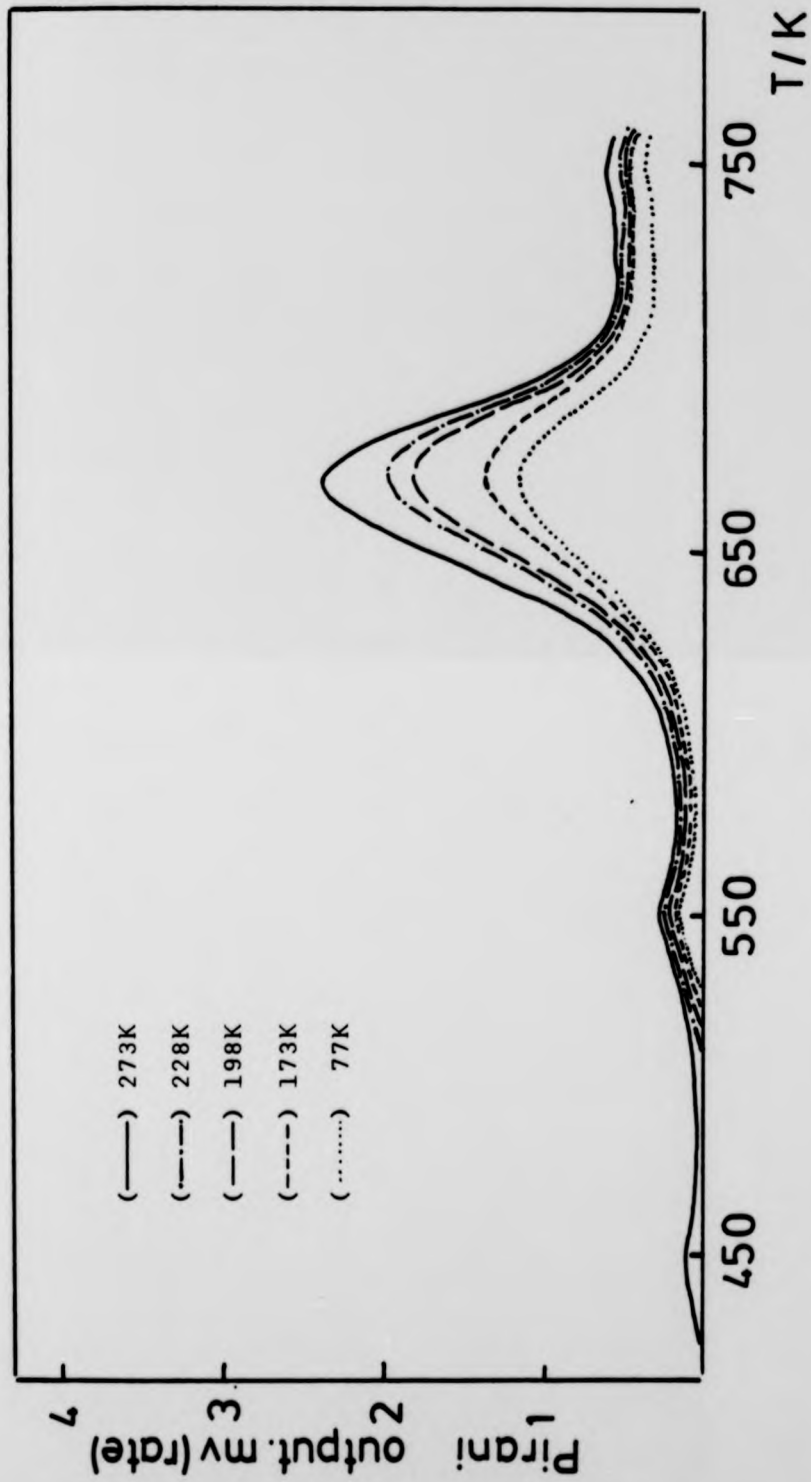


Fig. 8.2 TVA thermogram for poly(MHpI+DHpI)/EN, mole % of EN 13.0.

arises from the breakdown of the ethylene diamine side chains.

8.4.2 Poly(MHpI+DHpI)/DETA

The TVA thermogram of poly(MHpI+DHpI)/DETA, where the mole percentage of the original monoester is 50.05, is shown in Figure 8.3. Two peaks are present at ~500K and at ~660K. The peak in the region 720K was not resolved. The initial evolution products and weight losses at 450-550K are due to elimination of carbon monoxide carbon dioxide, water and heptanol. The highest temperature TVA peak is at ~660K, where a comparable breakdown of the imide structure occurs. Mass spectra confirm the elimination of carbon monoxide, carbon dioxide, water, heptanol, alkenes and ammonia. The infrared spectrum confirmed that ammonia was evolved.

8.4.3 Poly(MHpI+DHpI)/TEPA

Figure 8.4, shows the TVA thermogram of this polymeric ligand which contain originally 13.0 mole percentage of the monoester. Two resolved peaks are observed, at ~670K and at ~760K. Mass and infrared spectra confirmed the loss of carbon monoxide, carbon dioxide, water, heptanol, alkene and ammonia.

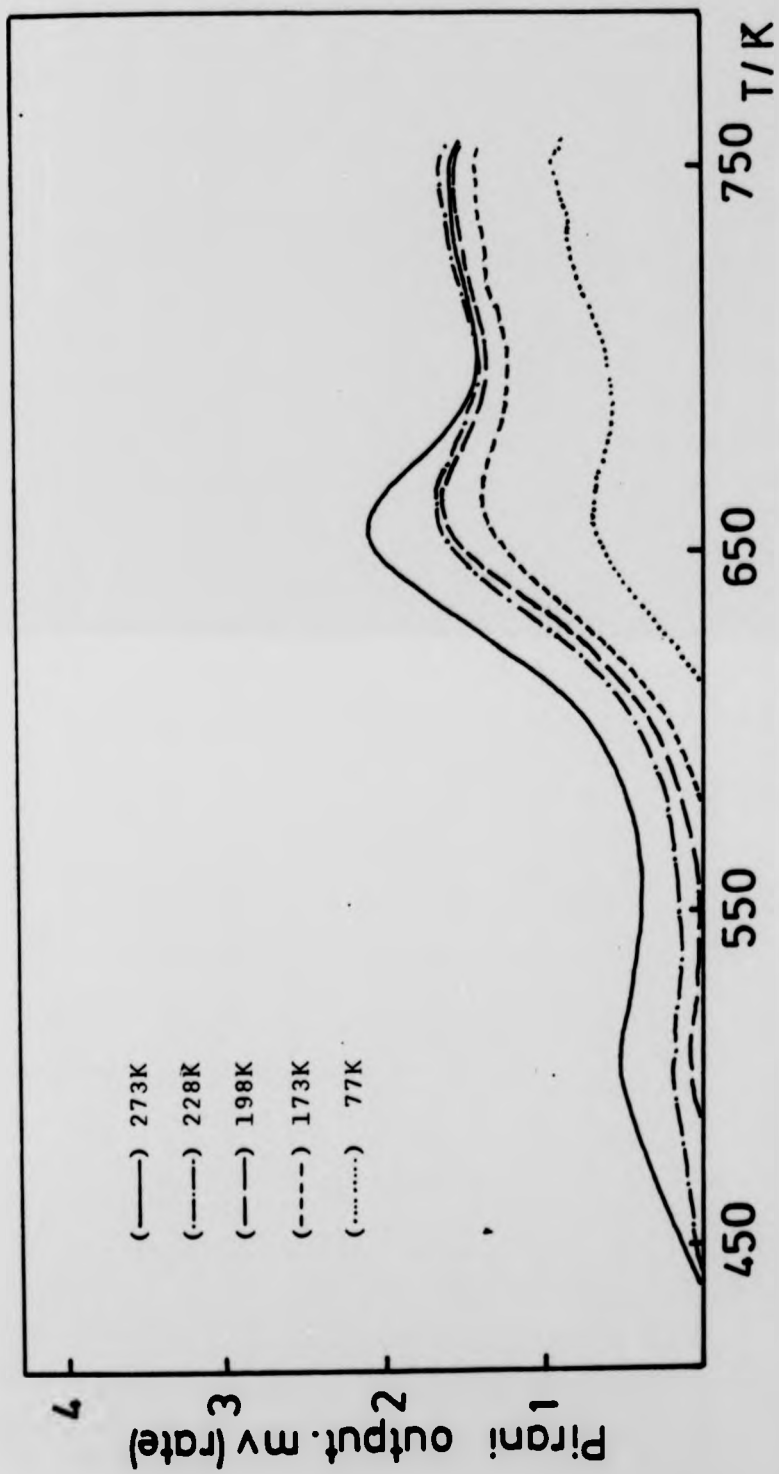


Fig 8.3 TVA thermogram for poly(MHpI+DHpI)/DETA, mole % of DETA 50.05.

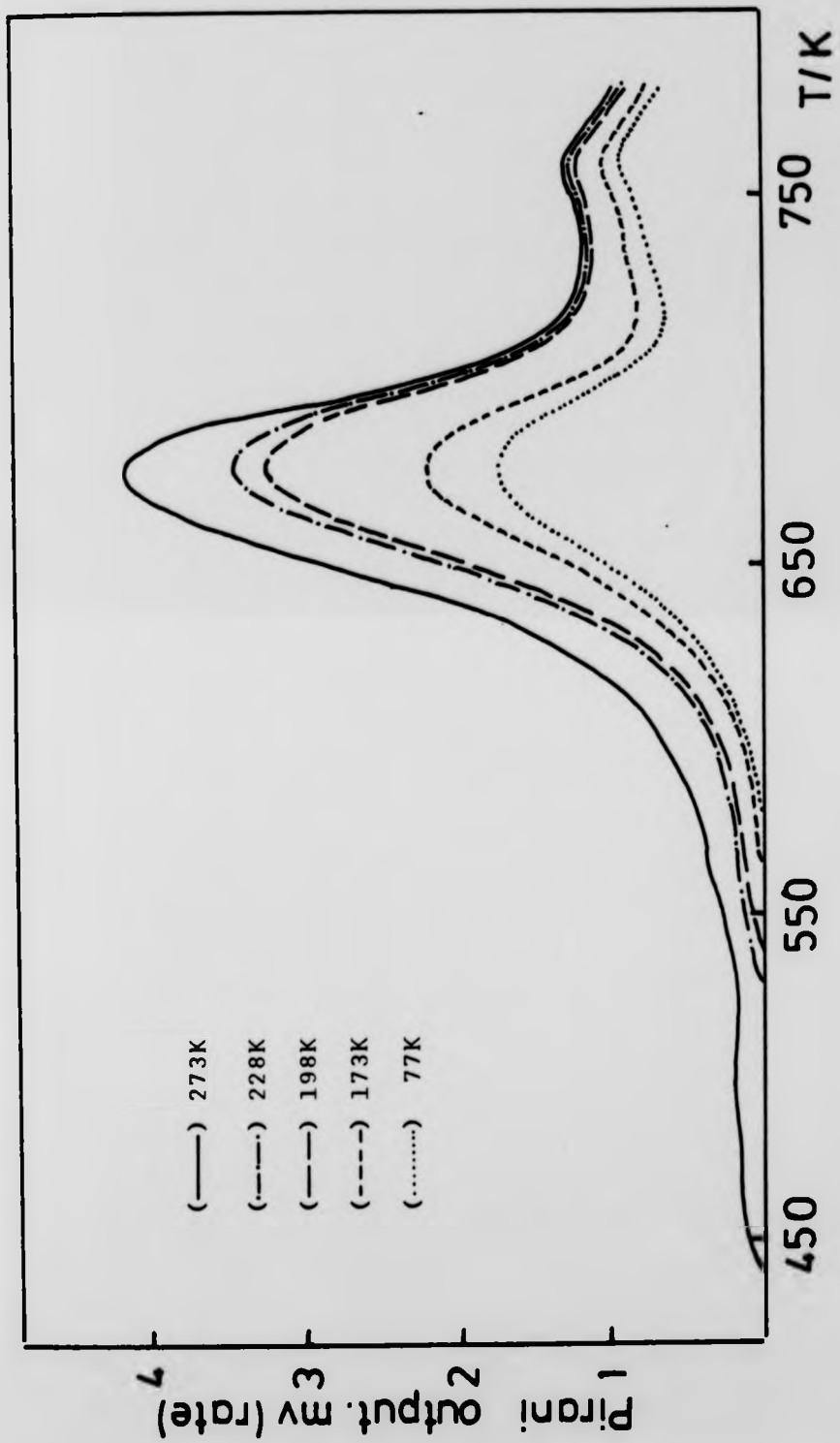
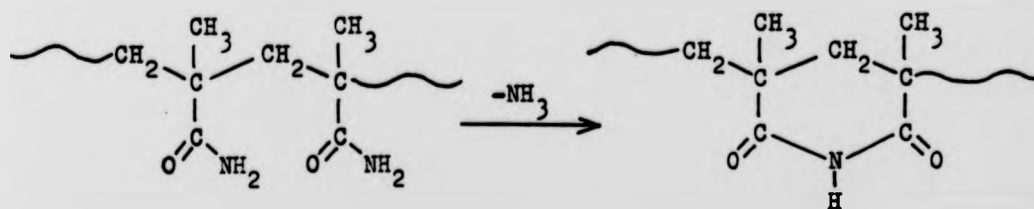


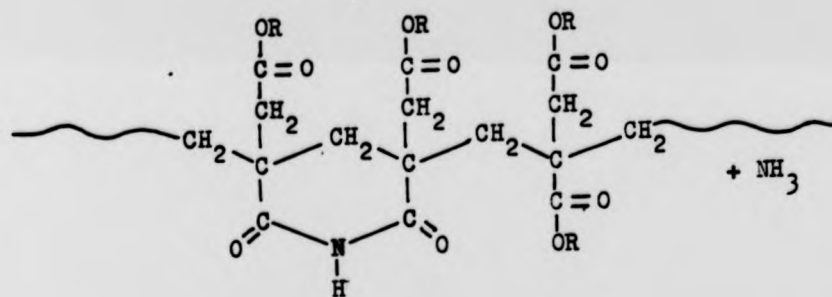
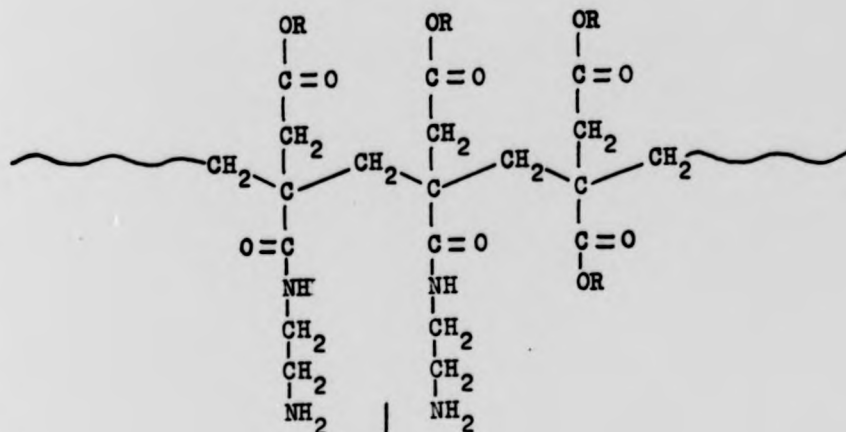
Fig. 8.4 TVA thermogram for poly(MHpI+DHpI)/TEPA, mole % of TEPA 13.0.

8.5 DISCUSSION

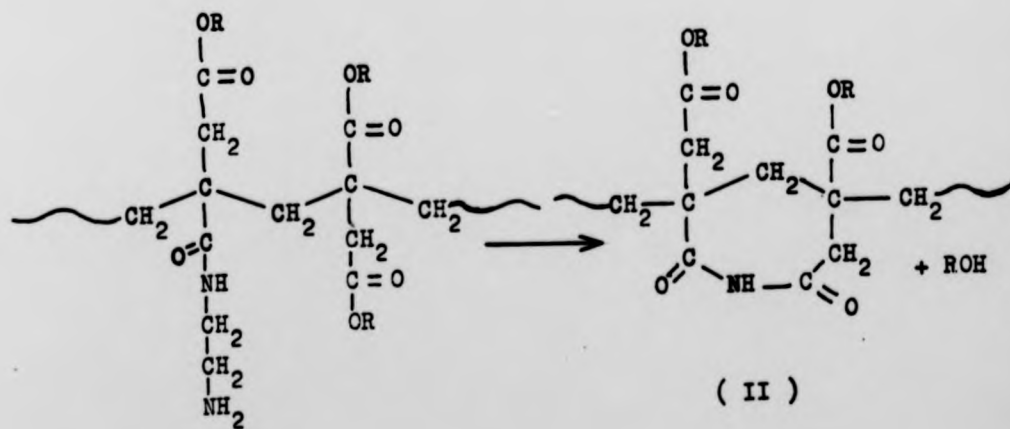
The TVA thermograms of the modified polymers (polymeric ligands) are shown in Figure 8.2, 8.3 and 8.4 confirming the loss of carbon monoxide, carbon dioxide, water, alcohol (heptanol), alkene and ammonia. It was found that as the mole percentage of the side chain (the pendant ethylene imine group) increases the amount of the ammonia evolved increases. The formation of imide structures and the elimination of ammonia during the thermal treatment of both polyacrylamide and polymethacrylamide have been reported¹¹⁰, as shown:



The following mechanism is proposed for the formation of imide structures.



(I)



(II)

Structure (I) will be formed when two adjacent ethylenediamine groups interact to form the imide structure. The formation of ammonia occurs through a radical reaction. Structure (II) will be formed if ethylenediamine interacts with an ester group.

A simple experiment was carried out to prove the evolution of ammonia from these modified polymers (polymeric ligands). Poly(MHpI+DHpI)/TEPA was left in a flask with 100 cm³ of distilled water. Using litmus paper the water was neutral, but when the water started to boil the colour of the litmus paper started to change to blue.

8.6 TVA RESULT FOR THE POLYMER-METAL COMPLEXE

8.6.1 Poly(MHpI+DHpI)/TEPA/CoCl₂

The TVA thermogram of this polymer-metal complex in which the original mole percentage of the monoester is 13.0 as shown in Figure 8.5. The initial weight loss starts at ~500K which proves that the polymer-metal complex is thermally more stable than the modified polymer. The highest temperature TVA peak is at ~670K and this is due to the breakdown of the complex. The infrared spectrum confirms the evolution of ammonia which could be due to the breakdown of the ligands.

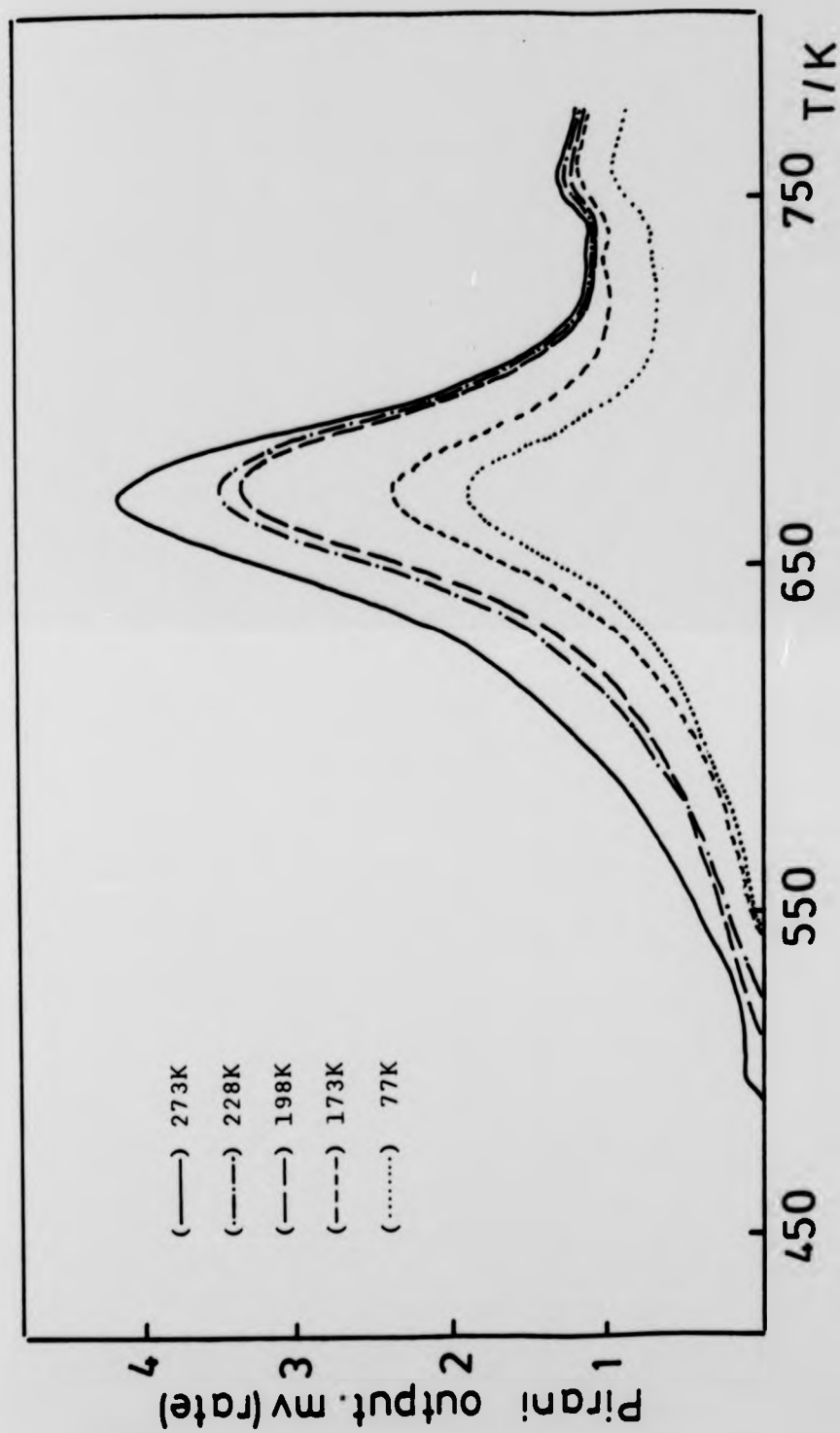


Fig. 8.5 TVA thermogram for poly(MHpI+DHpI)/TEPA/CoCl₂, mole % of TEPA 13.0.

8.7 THERMOGRAVIMETRIC ANALYSIS

The thermogravimetric analysis (TGA) of all the polymers prepared in this work has been carried out. These polymers were divided into three groups. The first contained the parent polymers, poly(MHpI+DHpI), poly(MBI+DBI) and poly(MMI+DMI); The second group contained the modified polymers with EN, DETA, TETA or TEPA in the side chain; the third group contained the polymer-metal complexes. The effect of the pendant ethylene imine group and the mole percentage of the side chain on the thermal stability has been studied. It is important to emphasise that all the measurements were performed under the same conditions and the effect of differences in sample weight or rate of heating were eliminated.

8.8 TGA RESULTS FOR THE PARENT POLYMERS

8.8.1 TGA results for poly(MHpI+DHpI)

The TGA thermograms of poly(MHpI+DHpI), where the mole percentage of the mono-n-heptyl itaconate increases from 0.29 to 4.93 are shown in Figure 8.6. From this figure it can be seen that as the mole percentage of the monoester increases the polymers become thermally less stable. The TGA thermograms of poly(MHpI+DHpI), where the mole percentages of the mono-n-heptyl itaconate are

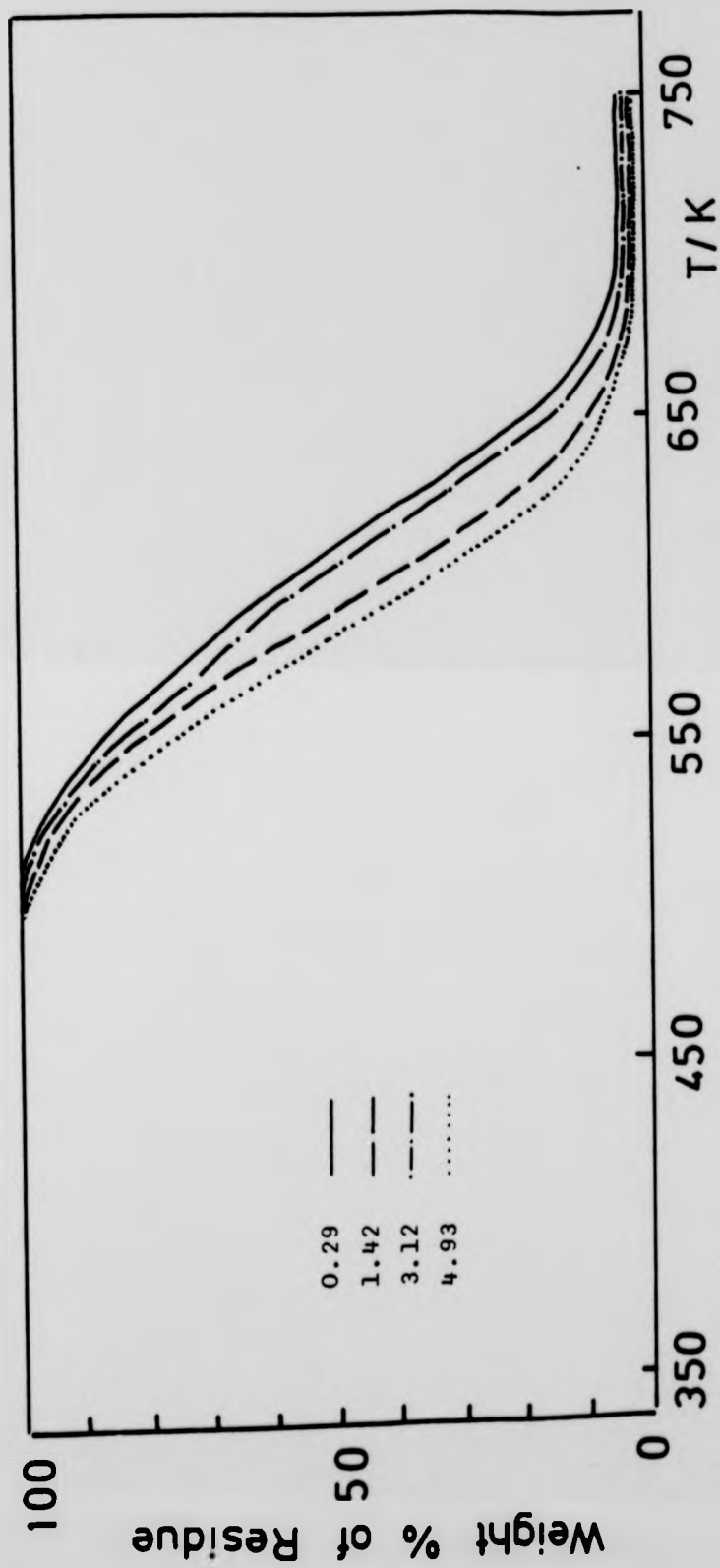


Fig. 8.6 TGA thermograms for poly(MHpI+DHpI) at indicated mole % of MHpI.

23.5, 36.53 and 50.05, are shown in Figure 8.7. The same result was obtained in that the thermal stability decreased with increase in the mole percentage of the monoester.

8.8.2 TGA result for poly(MBI+DBI)

The TGA thermograms for poly(MBI+DBI) systems are shown in Figure 8.8. From this figure it can be seen that the thermal stability is a function of the mole percentage of mono-n-butyl itaconate.

8.8.3 TGA result for poly(MMI+DMI)

The TGA thermogram of this polymer is shown also in Figure 8.8.

8.9 DISCUSSION

The TGA thermograms of these polymers show that the thermal stability of these polymers is a function of the mole percentage of the monoester in the copolymer. If the mole percentage of the monoester increases, the thermal stability decreases. It was found that poly di-n-alkyl itaconates were thermally more stable than poly mono-n-alkyl itaconates. This is because two adjacent carboxylic acid groups may interact to form the anhydride structure with loss in the weight (see section 8.3).

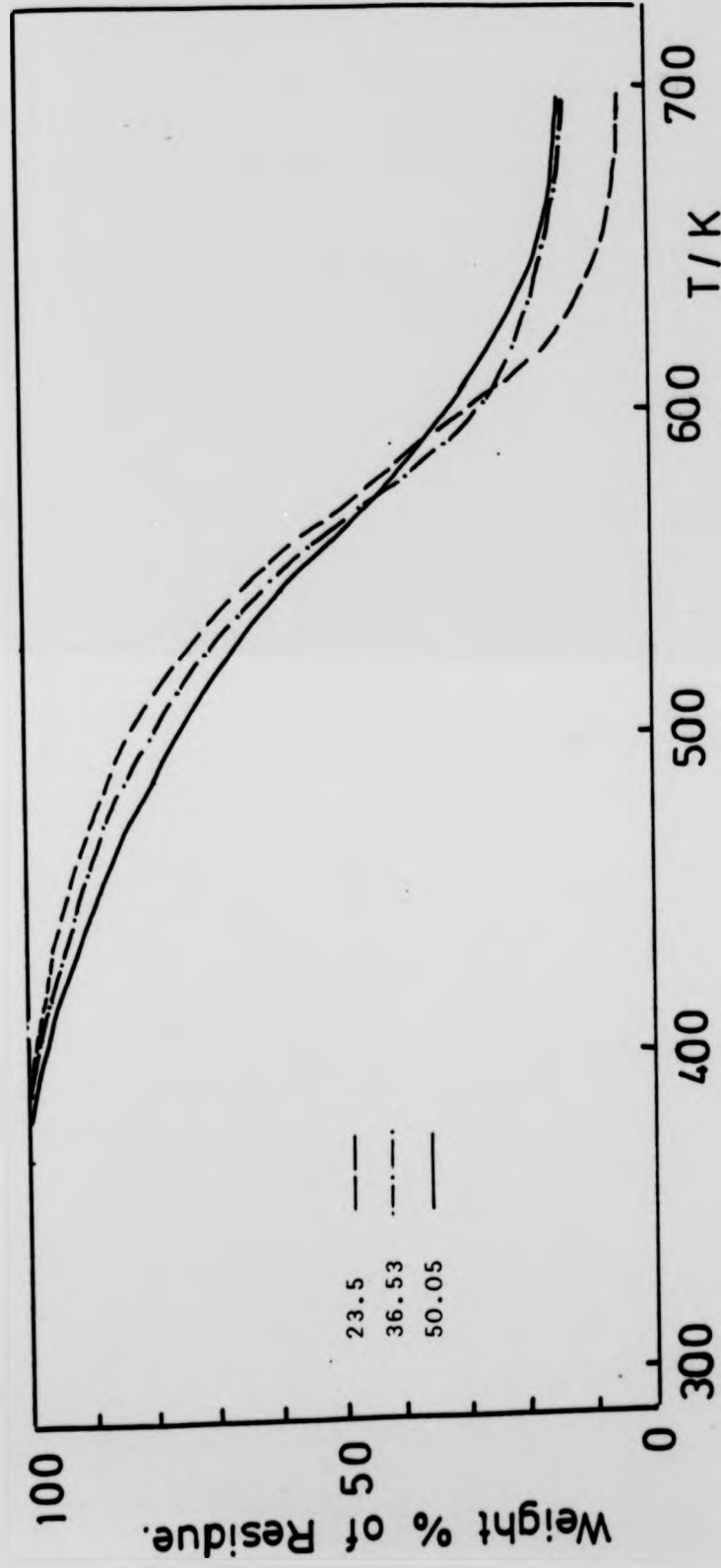


Fig. 8.7 TGA thermograms for poly(MHpI+DHpI) at indicated mole % of MHpI.

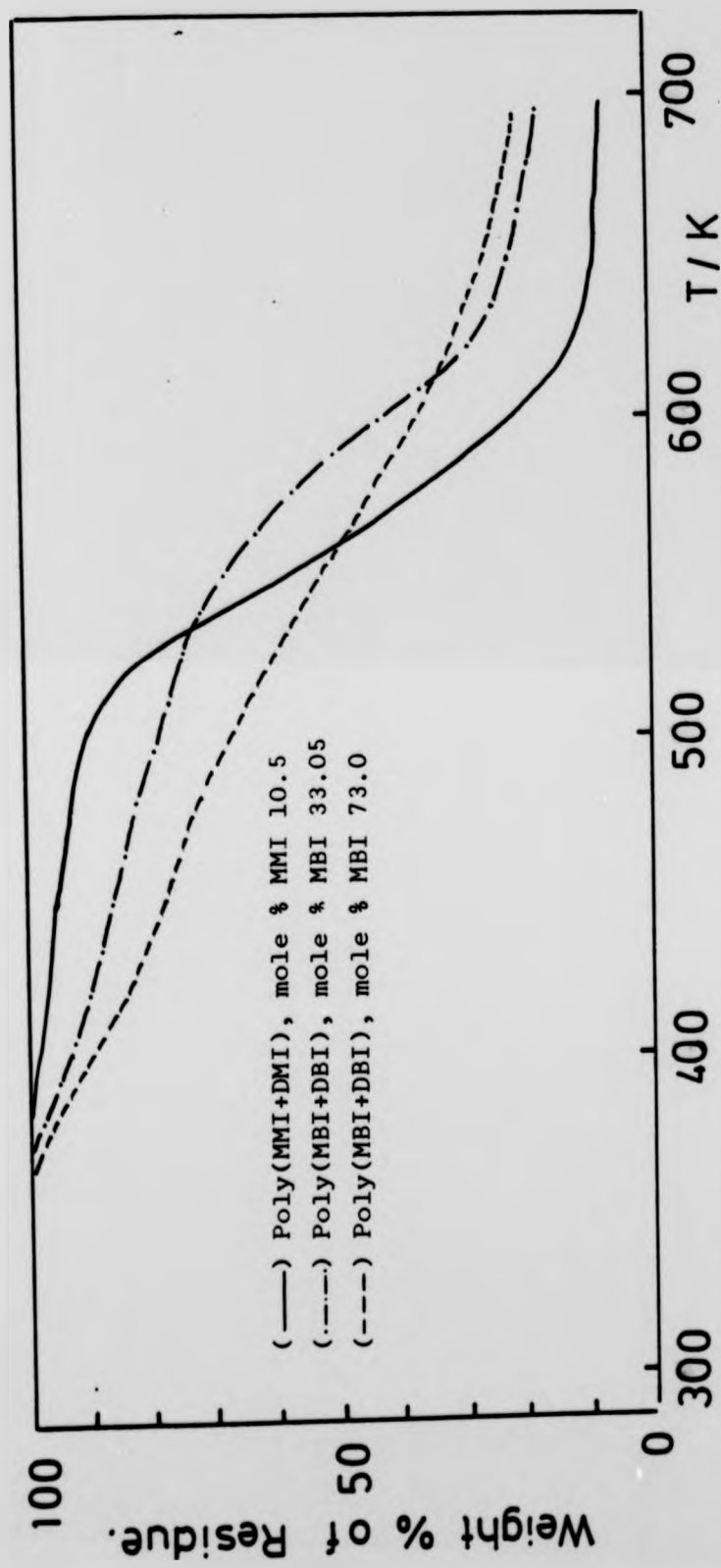


Fig. 8.8 TGA thermograms for the indicated copolymers.

8.10 TGA RESULTS OF THE MODIFIED POLYMERS

8.10.1 Modified poly(MHpI+DHpI)

The TGA thermograms of modified poly(MHpI+DHpI) which contain TEPA in the side chain are shown in Figure 8.9. This figure shows the effect of increasing the mole percentage of TEPA in the polymer on the thermal stability. The TGA thermograms of modified poly(MHpI+DHpI) which contain EN, DETA, TETA or TEPA in the side chain where the original mole percentages of the monoesters are 6.3, 13.0, 23.5, 36.53 and 50.05, are shown in Figures 8.10, 8.11, 8.12, 8.13 and 8.14 respectively. The modified polymers which contain EN, DETA, TETA or TEPA show an increase in the thermal stability over that of the parent unmodified polymers.

8.10.2 Modified poly(MBI+DBI)

The TGA thermograms of modified poly(MBI+DBI) which contain EN, DETA, TETA or TEPA in the side chain where the mole percentages of the original monoester are 33.0 and 73.0 are shown in Figures 8.15 and 8.16 respectively.

8.10.3 Modified poly(MMI+DMI)

Figure 8.17 shows the TGA thermograms of modified poly(MMI+DMI) containing EN, DETA, TETA or TEPA. The original mole percentage of the monoester is 10.5.

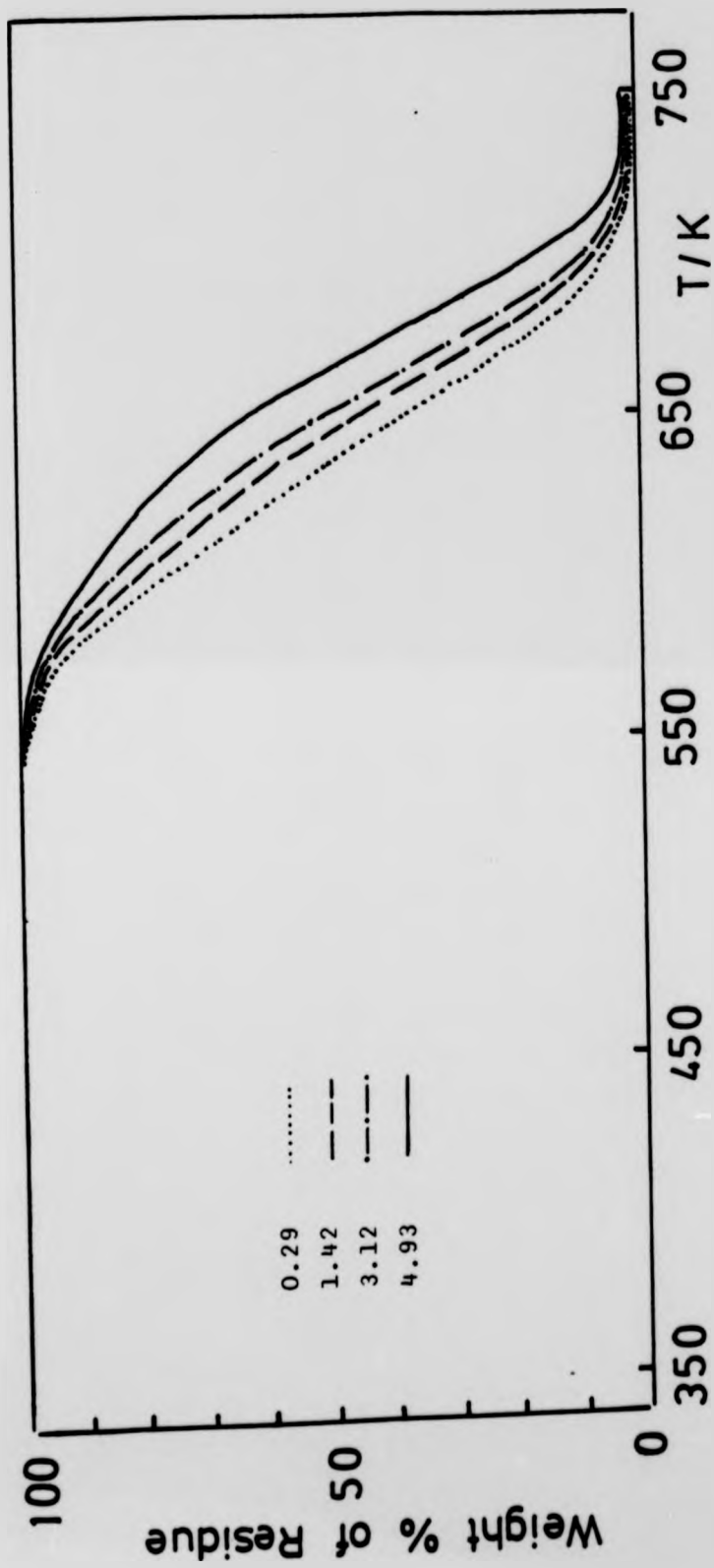


Fig. 8.9 TGA thermograms for poly(MHpI+DHPi)/TEPA at indicated mole% of TEPA.

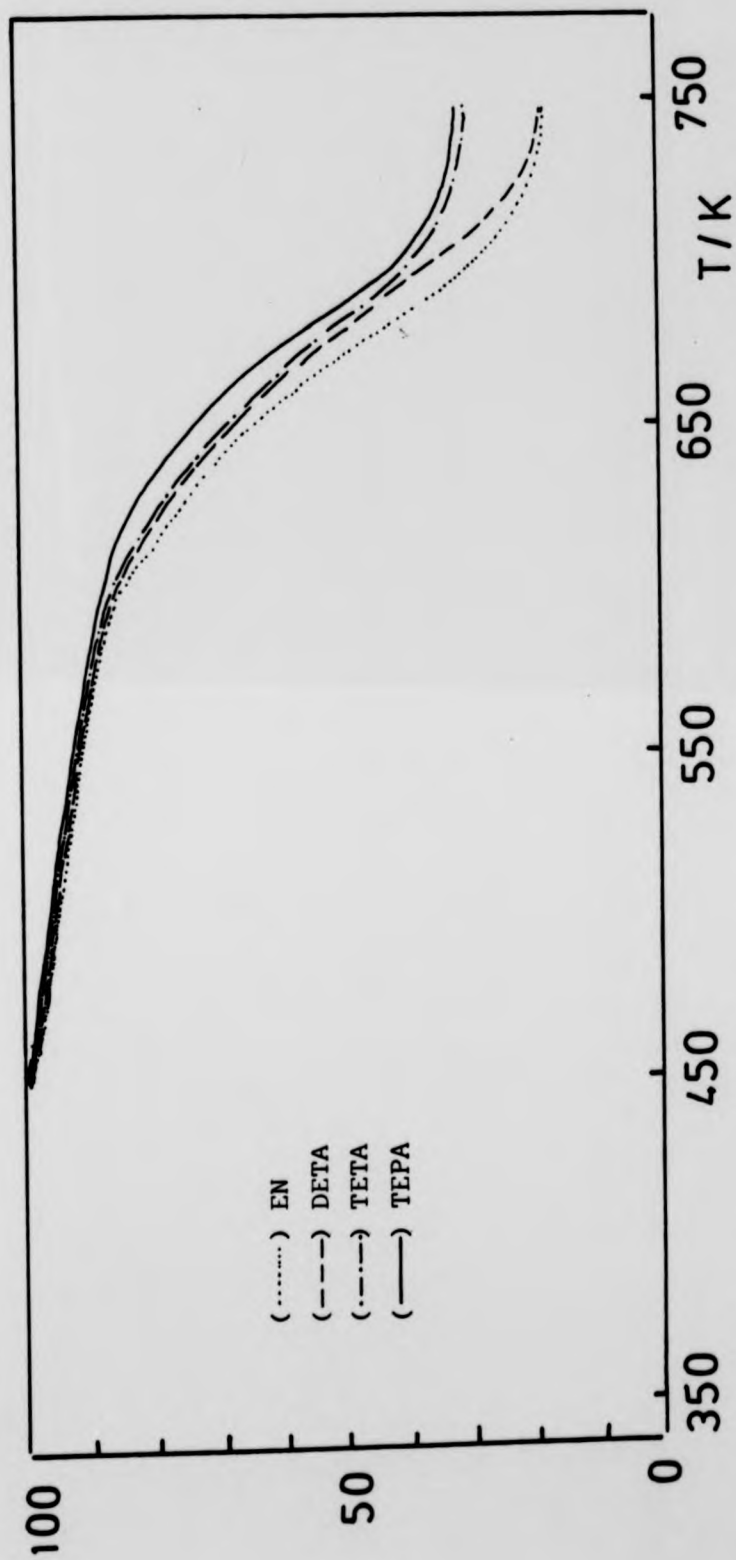


Fig. 8.10 TGA thermograms for modified poly(MHpI+DHpI) where the mole % of the side chain is 6.3.

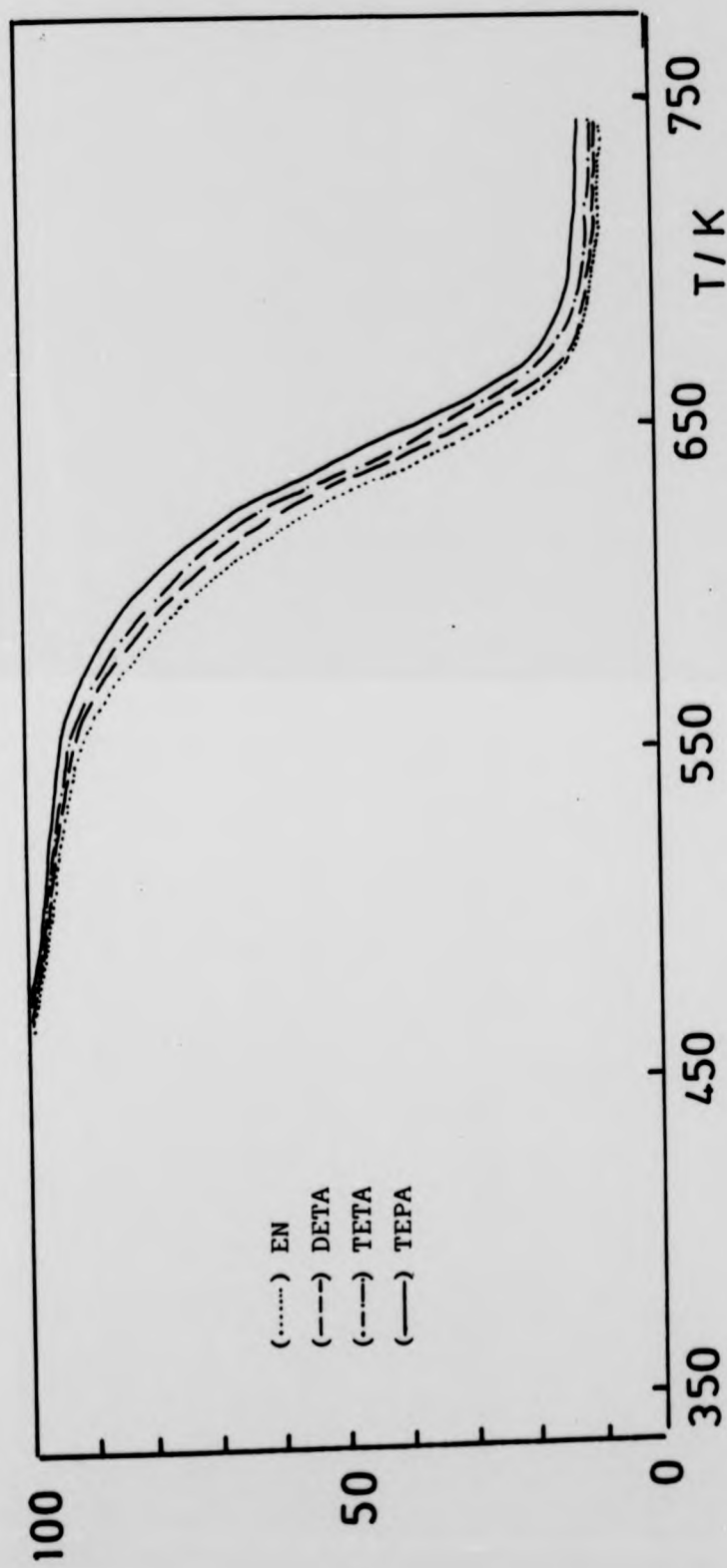


Fig. 8.11 TGA thermograms for modified poly(MHpI+DHpI) where the mole % of the side chain is 13.0.

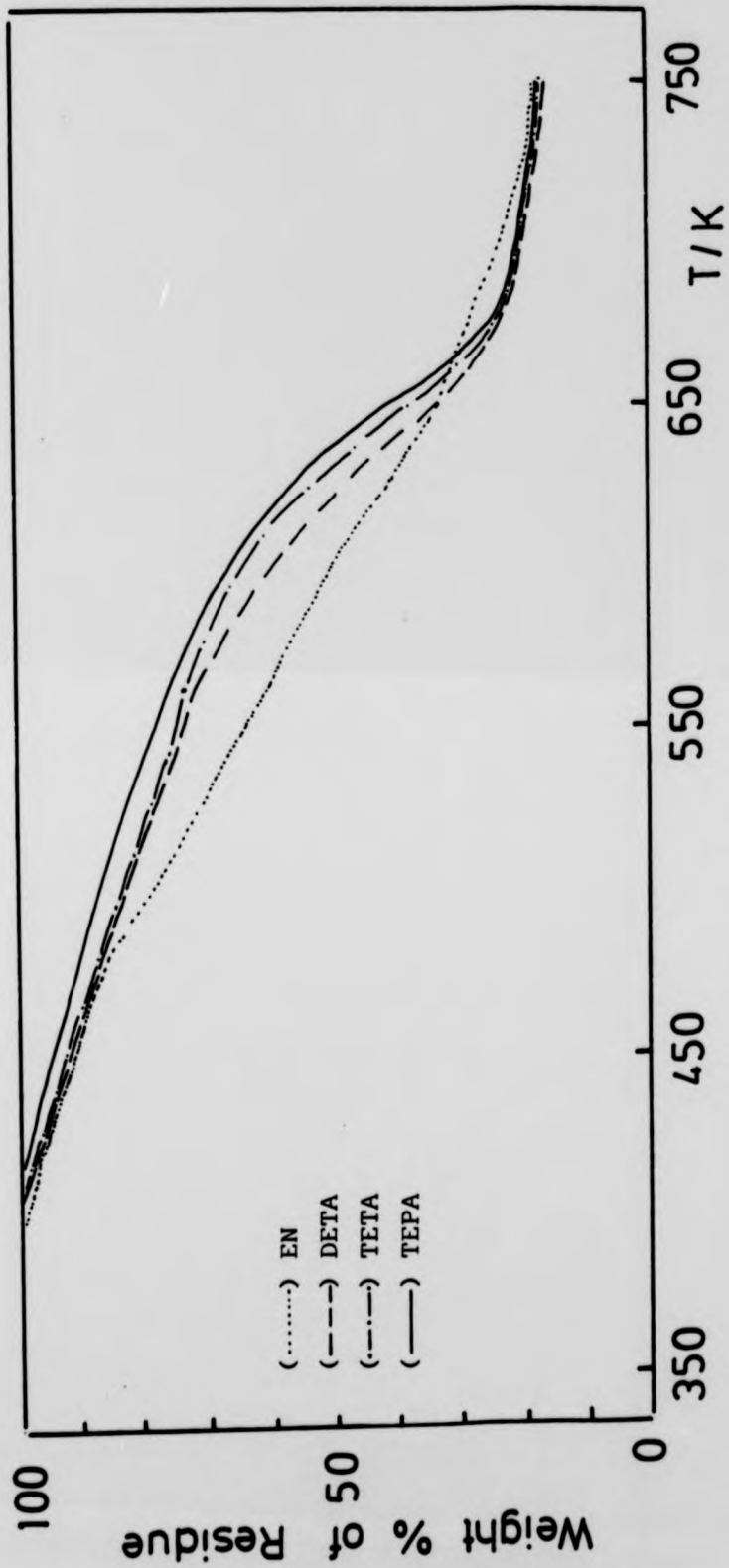


Fig. 8.12 TGA thermograms for modified poly(MHpI+DHpI) where the mole % of the side chain is 23.5.

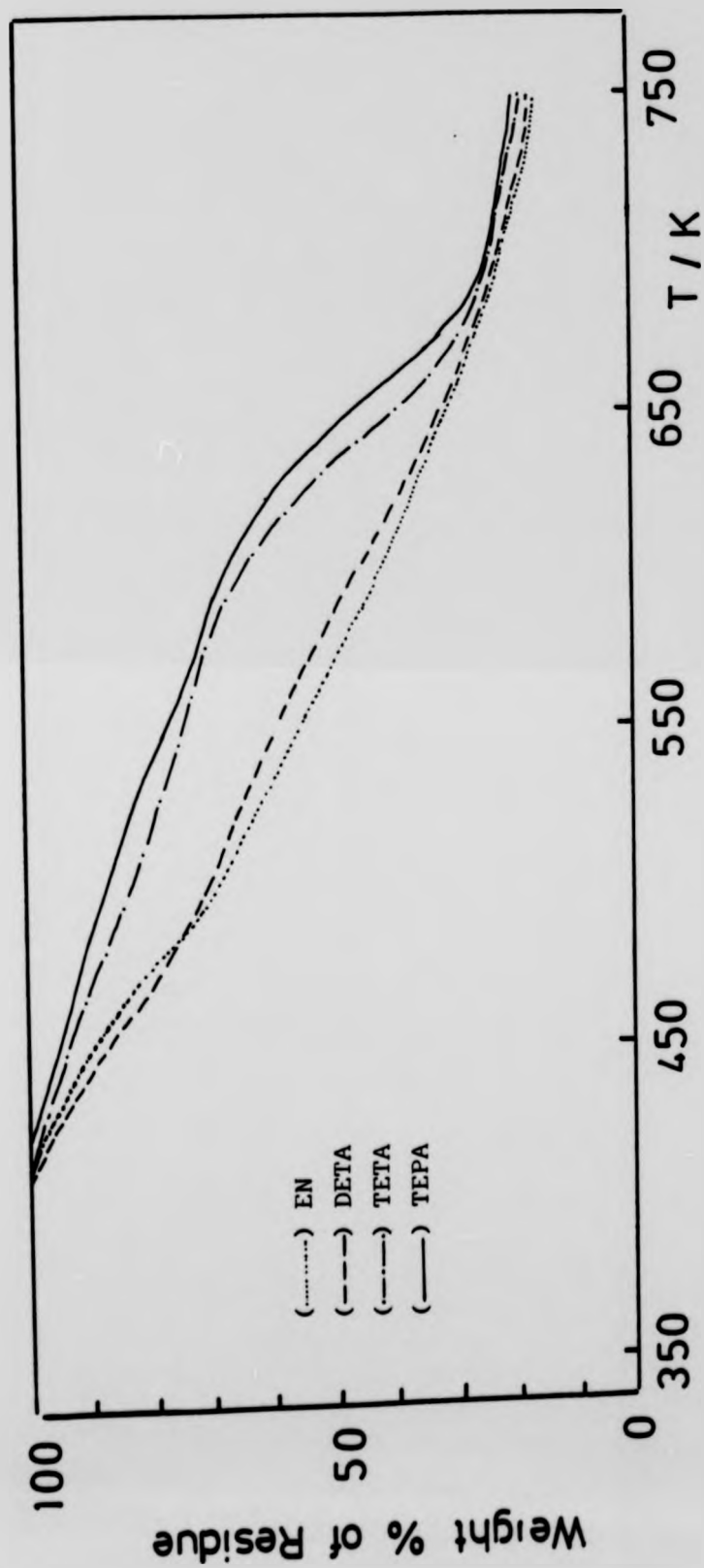


Fig. 8.13 TGA thermograms for modified poly(MHpI+DHpI) where the mole % of the side chain is 36.5.

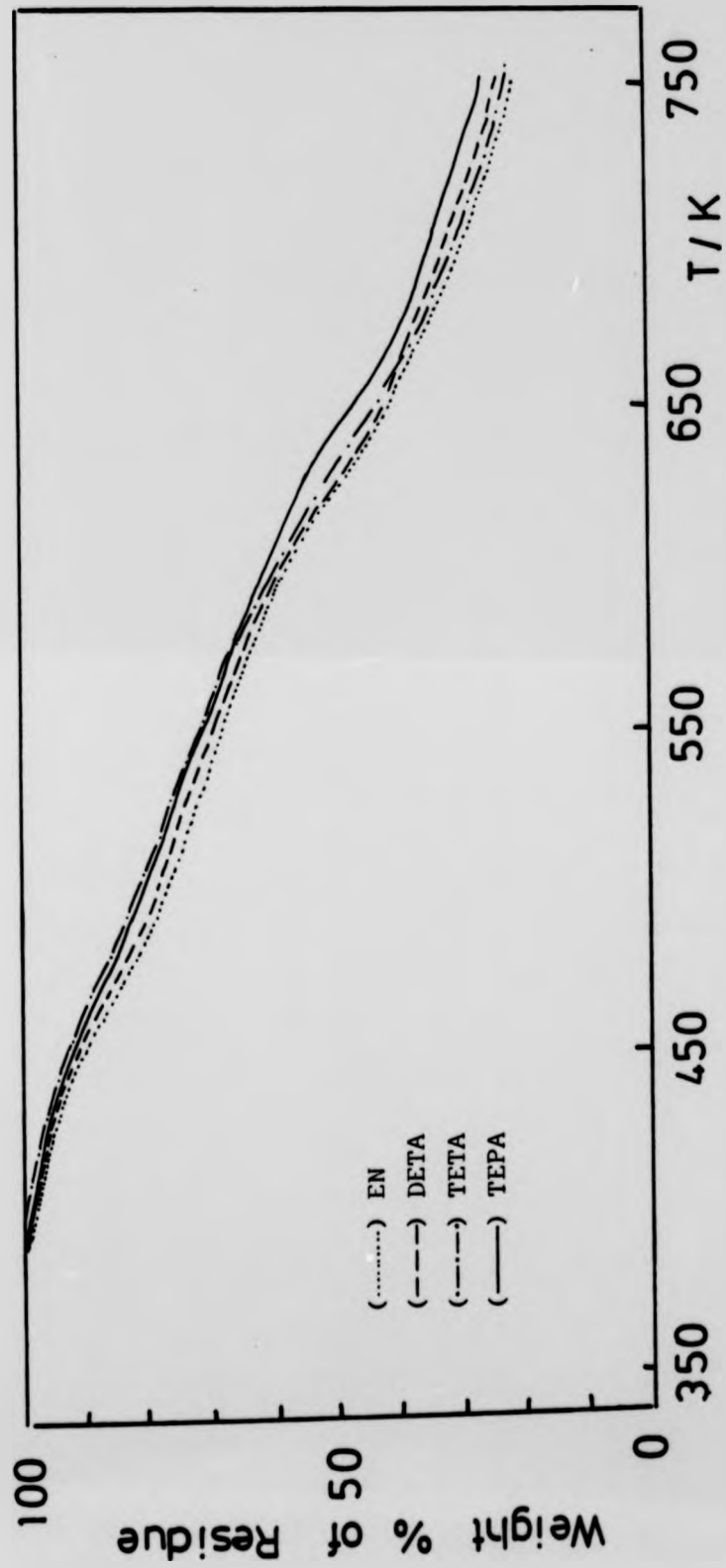


Fig. 8.14 TGA thermograms for modified poly(MHpI+DHpI) where the mole % of the side chain is 50.05.

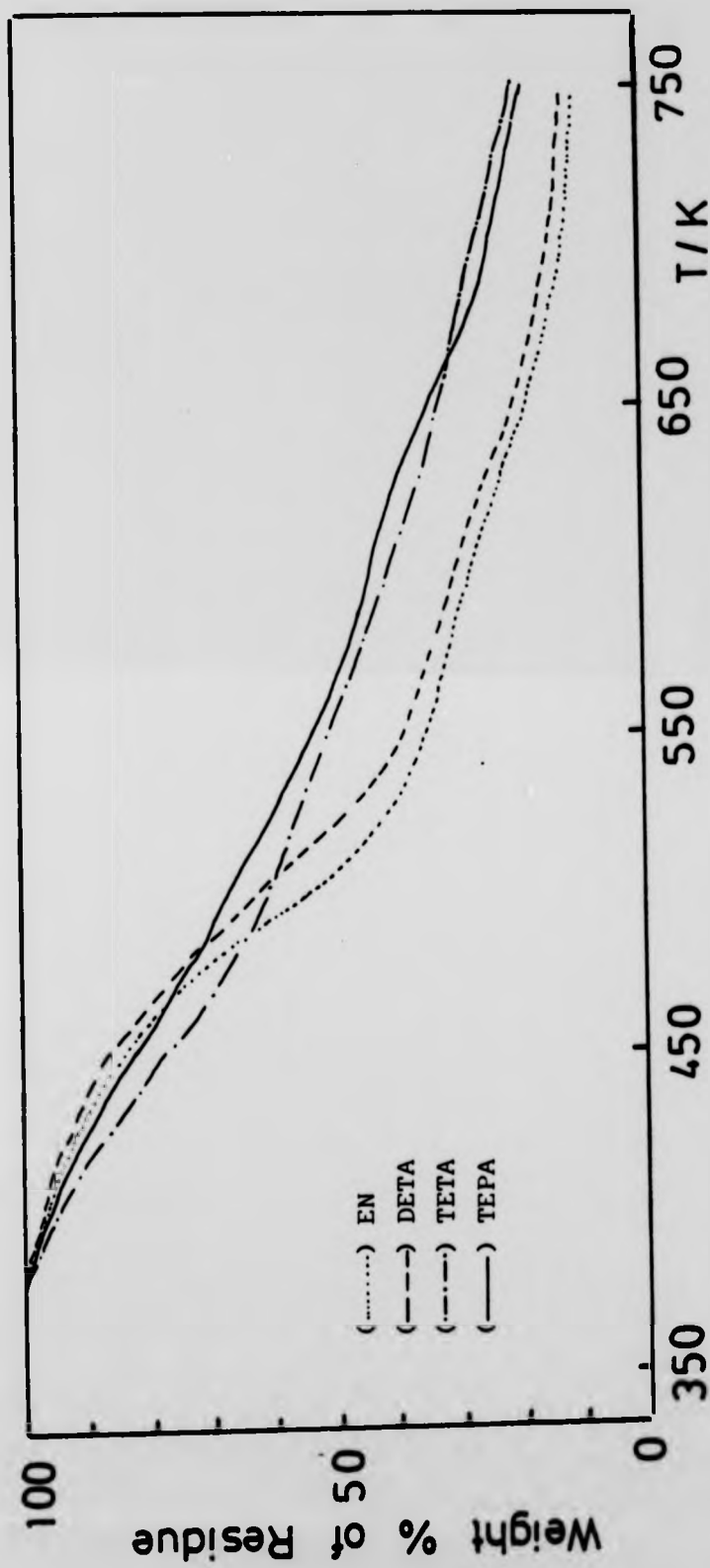


Fig. 8.15 TGA thermograms for modified poly(MBI+DBI) where the mole % of the side chain is 33.05.

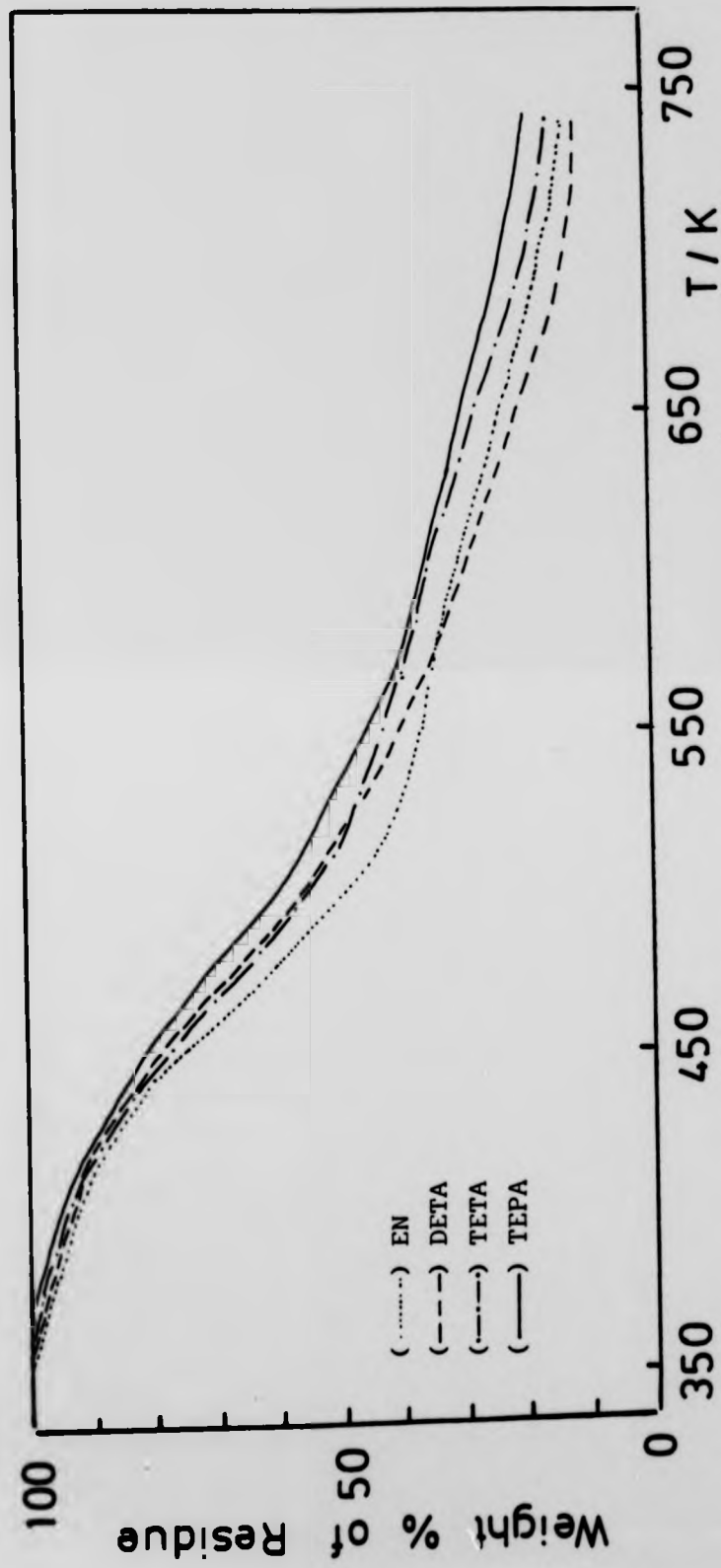


Fig. 8.16 TGA thermograms for modified poly(MBI+DBI) where the mole % of the side chain is 73.0.

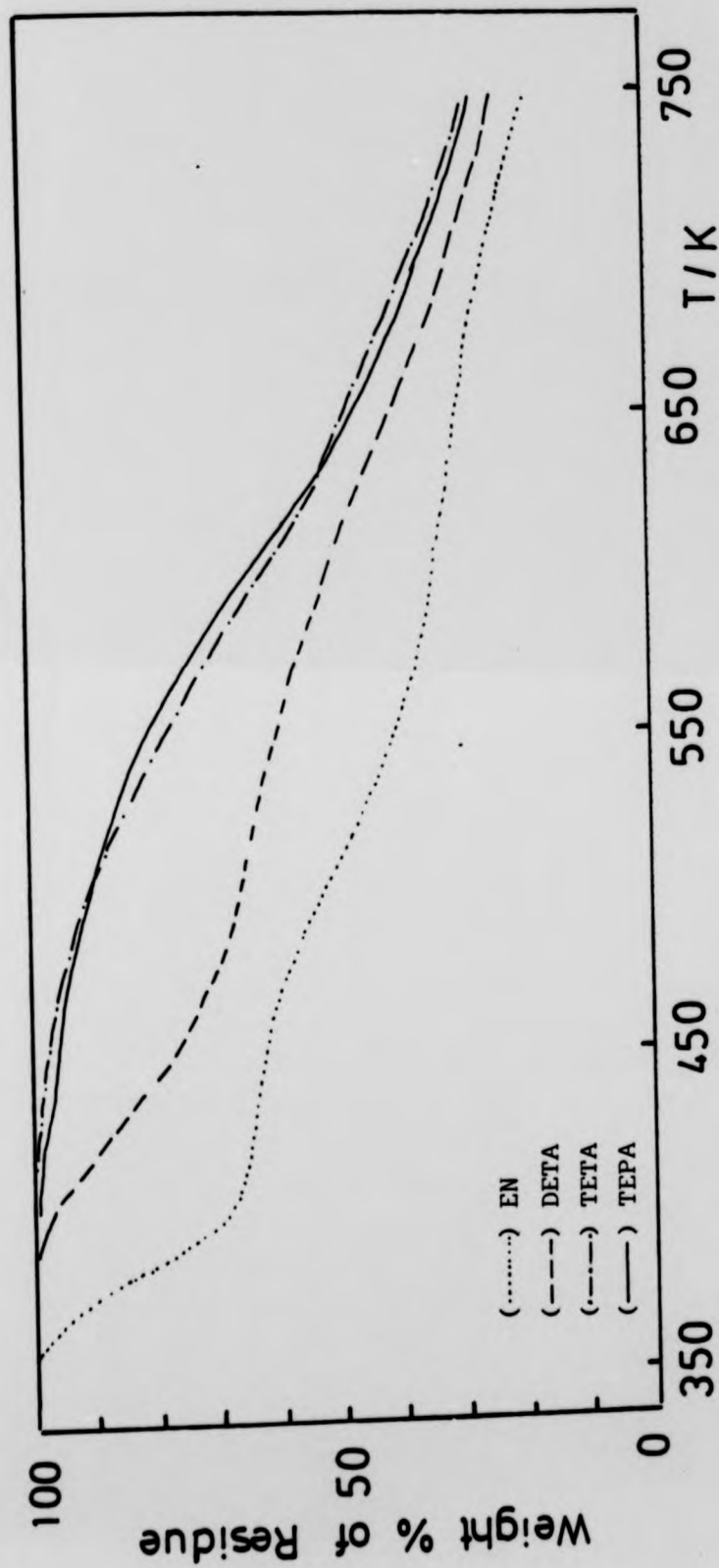


Fig. 8.17 TGA thermograms for modified poly(MMI+DMI) where the mole % of the side chain is 10.5.

8.11 DISCUSSION

When the pendant ethylene imine groups are introduced into the copolymer chain, the thermal stability improves. From the TGA thermograms of these modified polymers it can be seen that the thermal stability of those with TEPA in the side chain are slightly higher than those with EN in the side chain. These pendant ethylene imine groups increase the crosslinking tendency in the sample. The covalent bond between nitrogen and carbon is fairly strong and the nitrogen in these pendant ethylene amine group still has a lone pair of electrons which tend to enter into hydrogen bond formation.

8.12 TGA RESULTS FOR POLYMER-METAL COMPLEXES

The TGA thermograms for poly(MHpI+DHpI)/TEPA/CoCl₂ where the original mole percentages of the monoester are 0.29, 1.42, 3.12 and 4.93 are shown in Figure 8.18. The ligands (TEPA) were fully reacted with cobalt(II) chloride and these polymer-metal complexes are thermally more stable than the modified polymers (polymeric ligands). The TGA thermograms of polymer chelates of cobalt(II) chloride and copper(II) chloride, where the mole percentages of the original mole percentage of the monoester are 6.3, 13.0, 23.5, 36.53 and 50.05 are shown in Figures 8.19, 8.20, 8.21, 8.22 and 8.23 respectively.

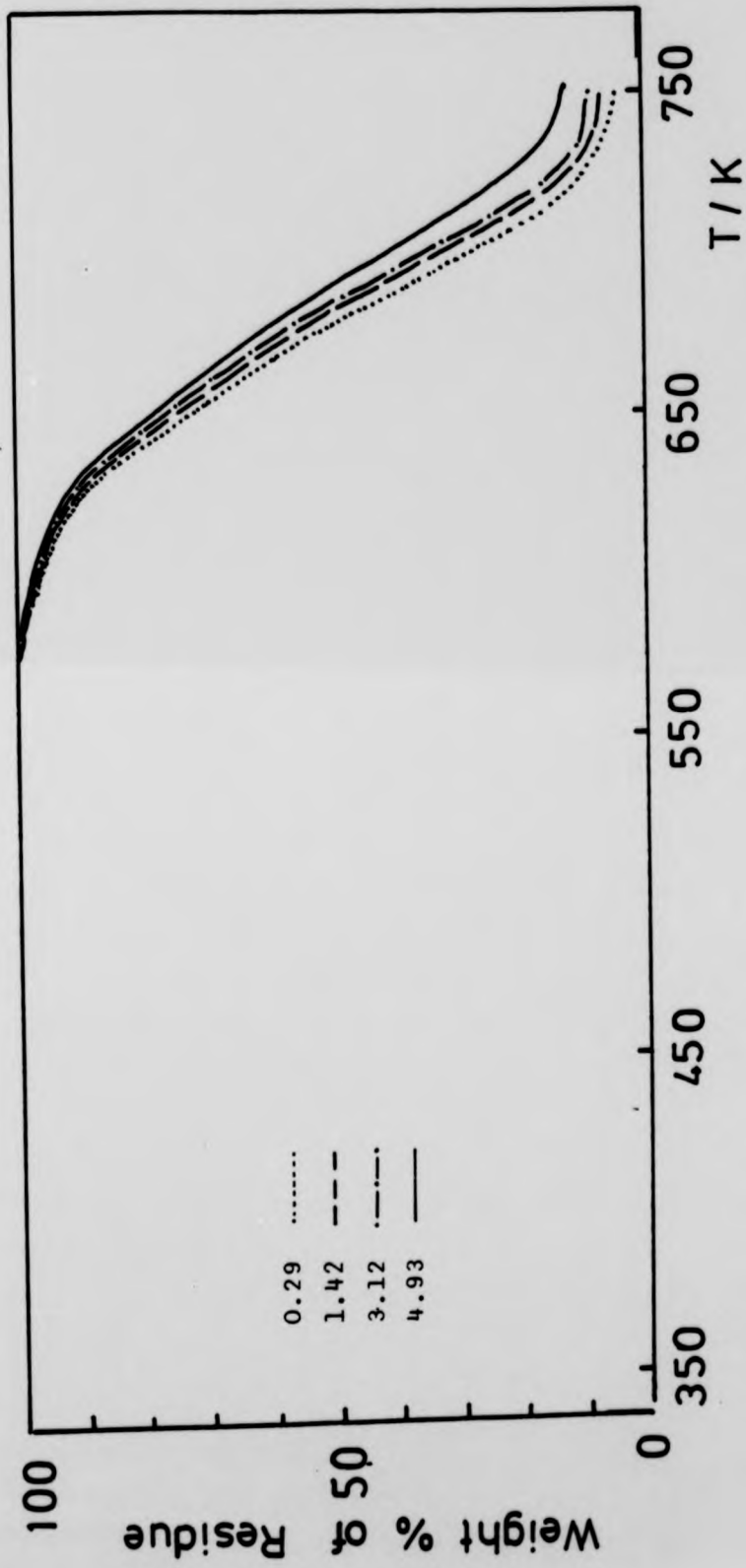


Fig. 8.18 TGA thermograms for poly(MHpI+DHpI)/TEPA/CoCl₂ (fully reacted with CoCl₂), at indicated mole % of TEPA.

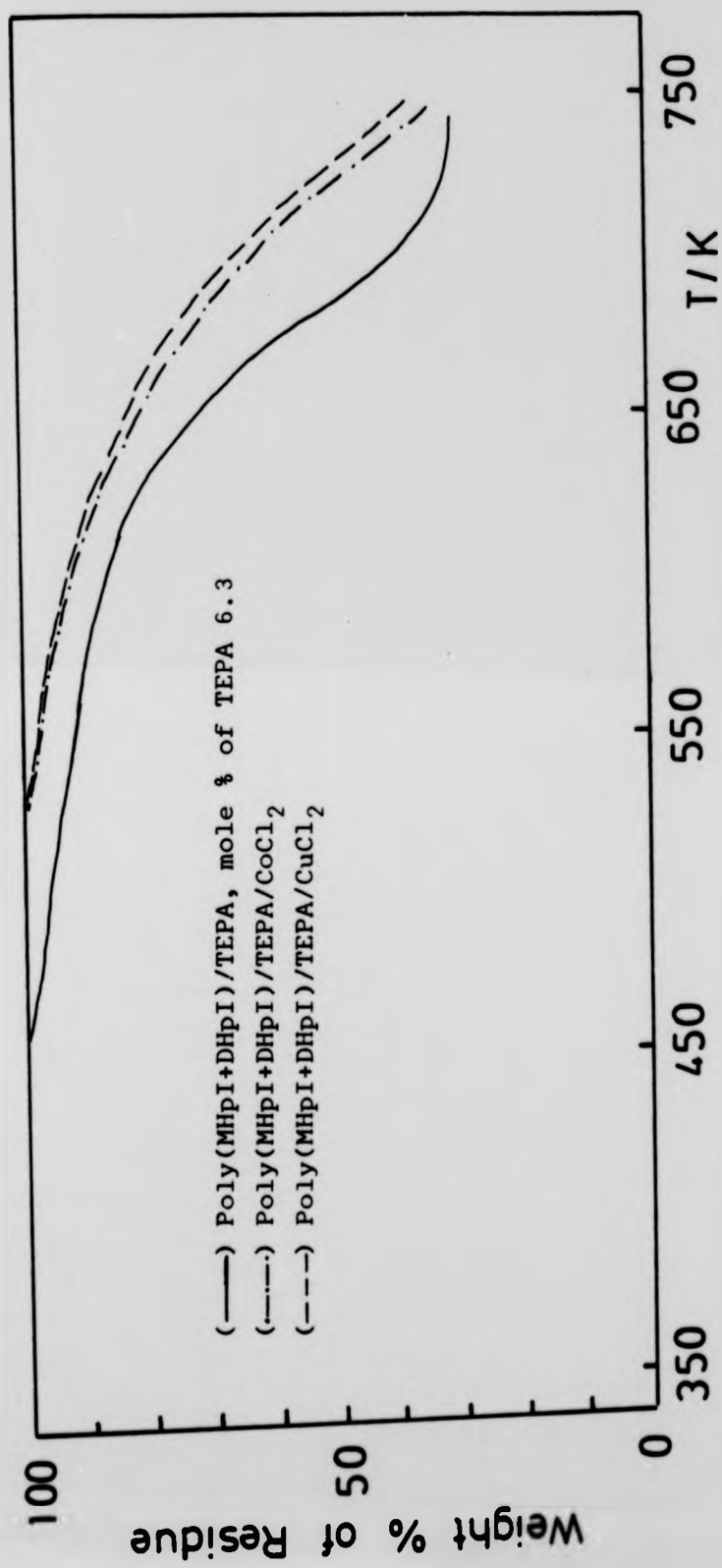


Fig. 8.19 TGA thermograms for indicated polymeric ligand and polymer metal complexes.

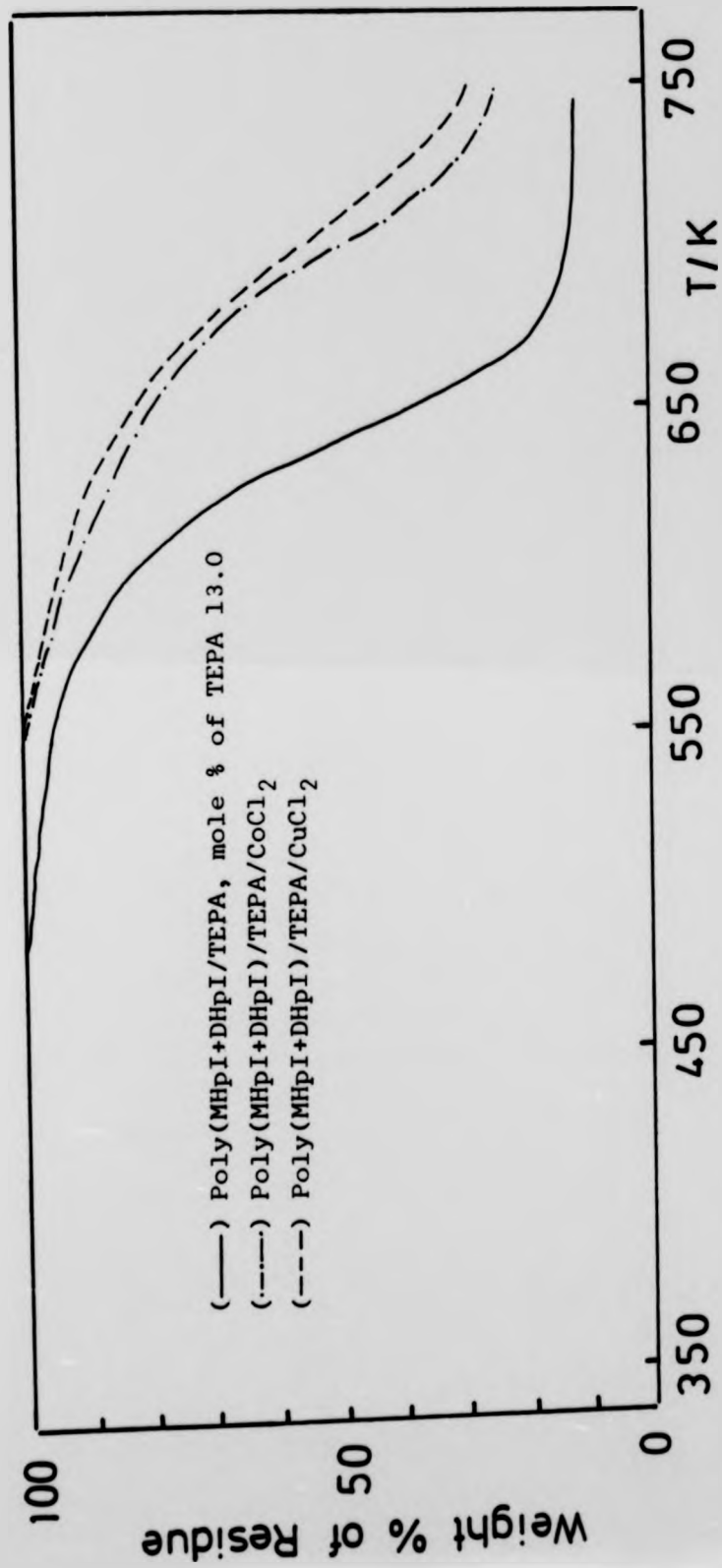


Fig. 8.20 TGA thermograms for the indicated polymeric ligand and polymer metal complexes.

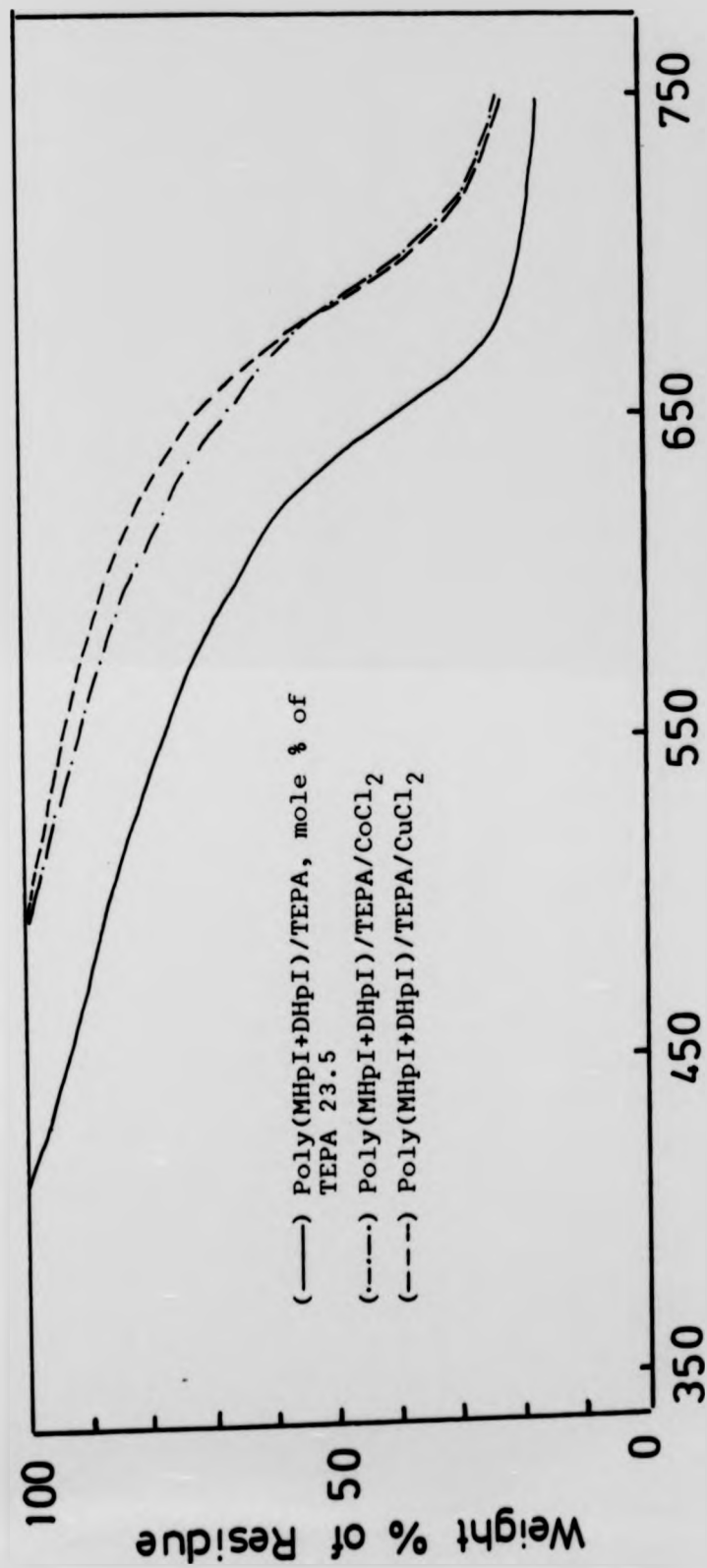


Fig. 8.21 TGA thermograms for indicated polymeric ligand and polymer metal complexes

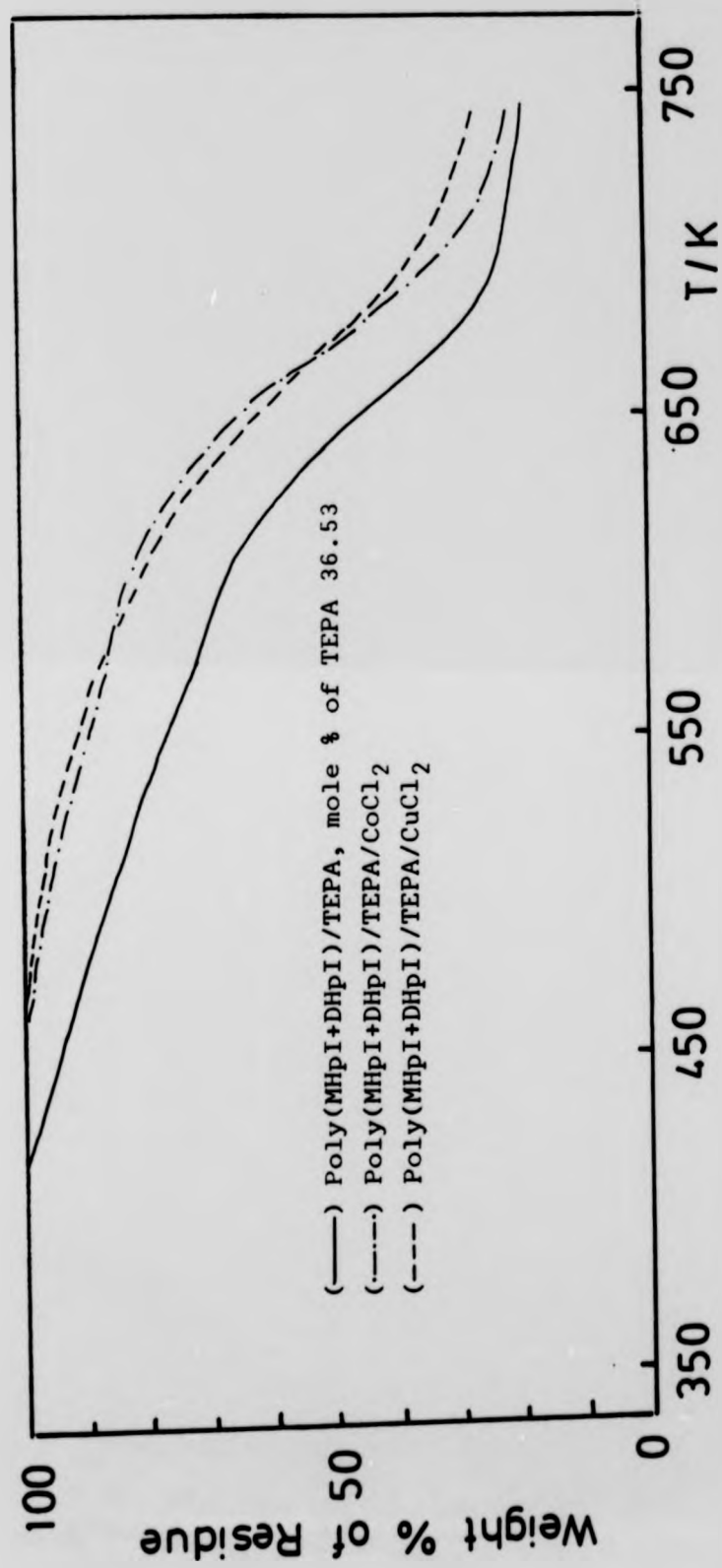


Fig. 8.22 TGA thermograms for indicated polymeric ligand and polymer metal complexes.

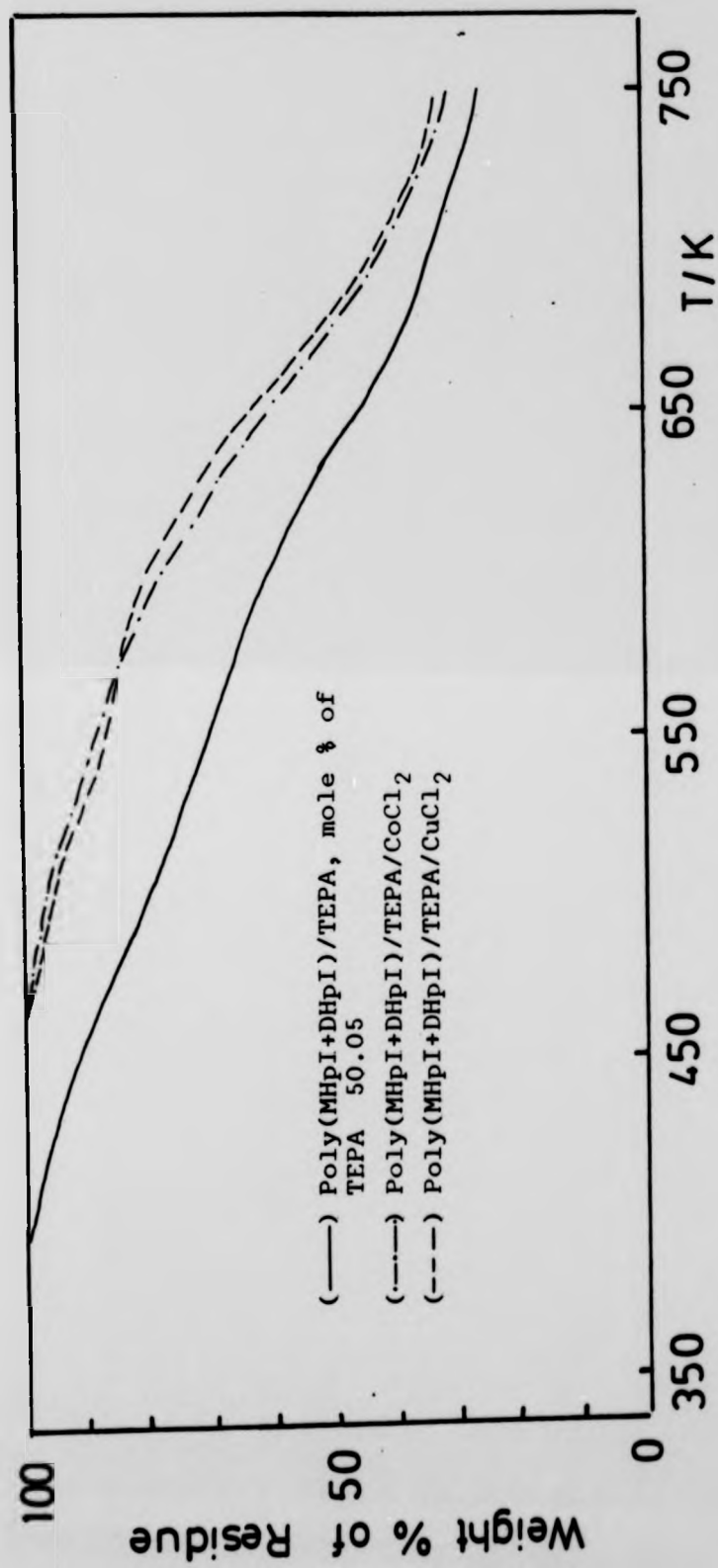


Fig. 8.23 TGA thermograms for the indicated polymeric ligand and polymer metal complexes.

The TGA thermograms for polymer chelates of cobalt(II) chloride or copper(II) chloride, prepared from poly(MBI+DBI)/TEPA, where the original mole percentages of the monoester are 33.05 and 77.0, are shown in Figure 8.24 and 8.25 respectively.

The TGA thermograms for polymer chelates of cobalt(II) chloride or copper(II) chloride, prepared from poly(MMI+DMI)/TEPA, where the original mole percentage of the monoester 10.5, is shown in Figure 8.26.

8.13 DISCUSSION

The thermal stability of the modified polymers which contain TEPA in the side chain, improved when this TEPA reacted with metal halides. The coordination bond between the metal ion and the ligand is stronger than the hydrogen bond, between the same ligand and the adjacent side group in the copolymer chain. The availability of the side chain to react with the adjacent group will be reduced, due to the complex formation.

In conclusion, the thermal degradation of the modified polymers and the polymer-metal complexes was a random chain scission. The thermal stability increased with change in the side chain from EN to TEPA. The reaction between the polymeric ligands and metal halides improved the thermal stability of these modified polymers.

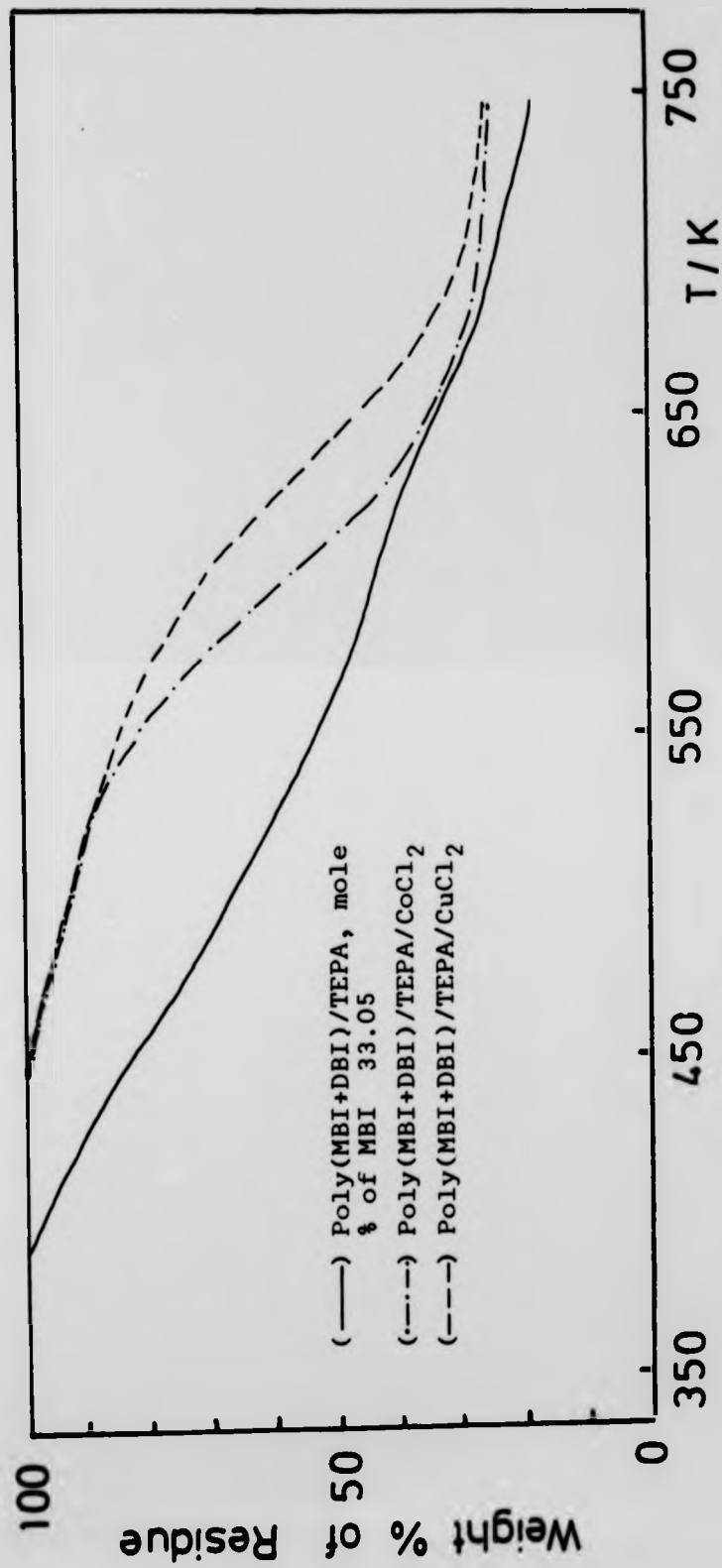


Fig. 8.24 TGA thermograms for the indicated polymeric ligand and polymer metal complexes.

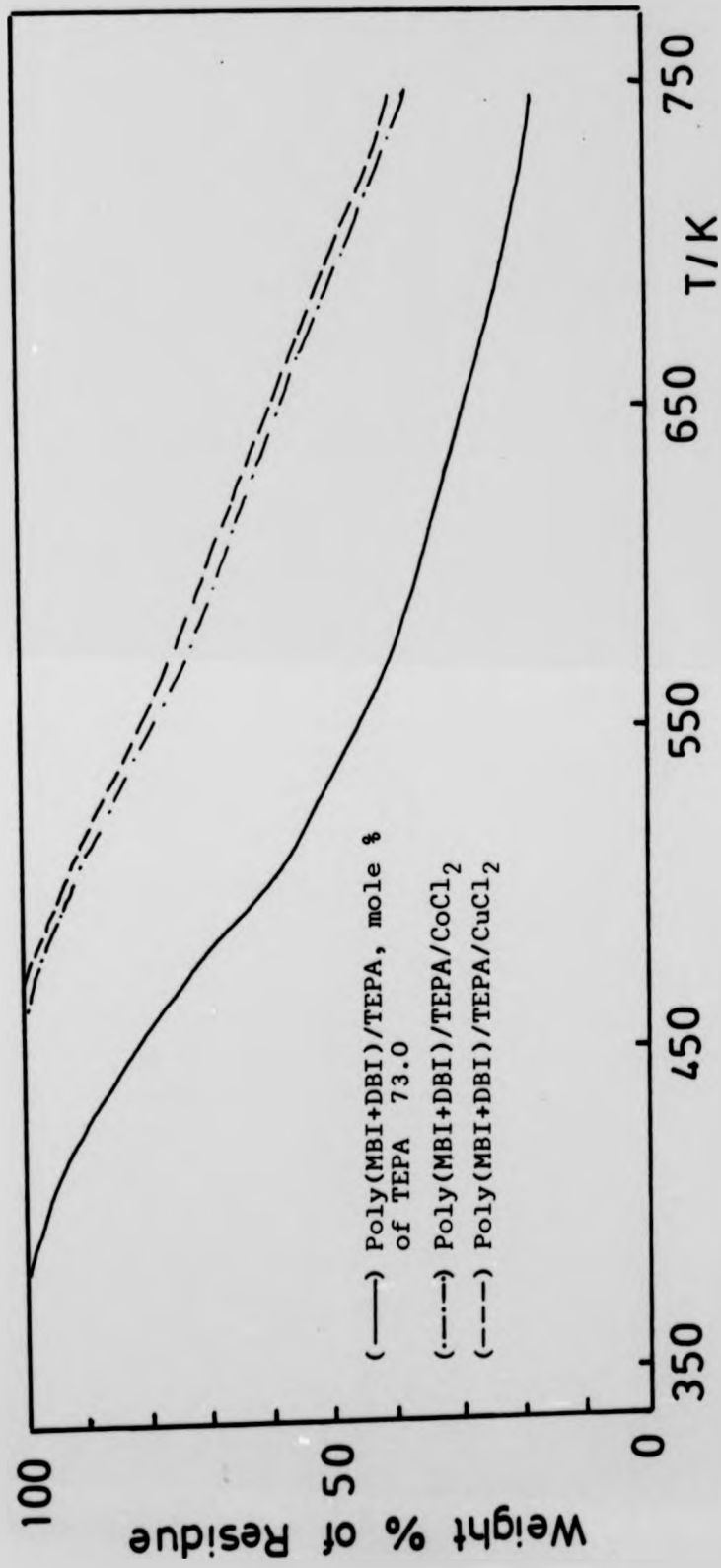


Fig. 8.25 TGA thermograms for the indicated polymeric ligand and polymer metal complexes.

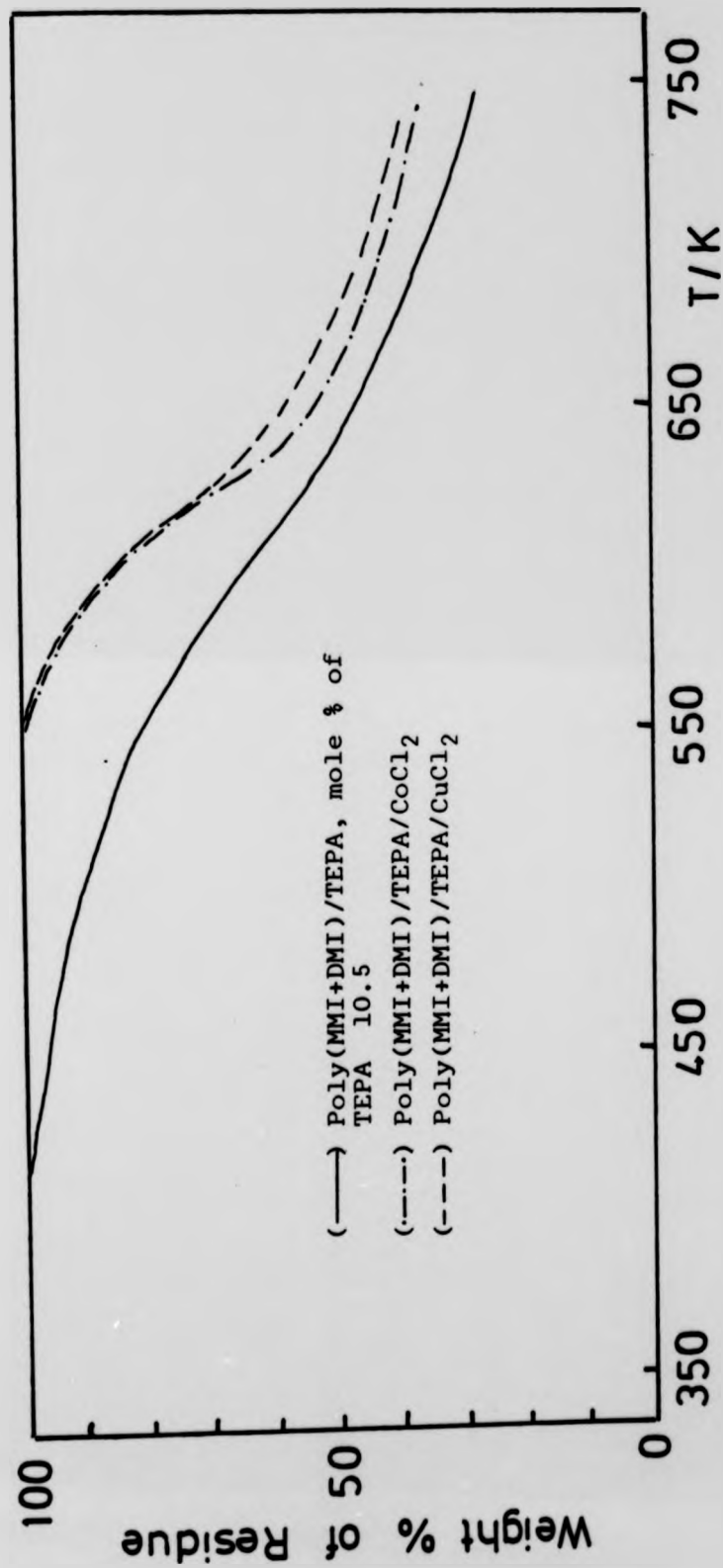


Fig. 8.26 TGA thermograms for the indicated polymeric ligand and polymer metal complexes.

CHAPTER NINE

GENERAL CONCLUSIONS

At times of rising oil prices, itaconic acid is an attractive and useful monomer because it is not an oil based product. The trifunctionality and the cheap cost of production leads to a wide versatility in application. Because itaconic acid is an organic acid with two carboxylic groups, most of its straight alkane chain, branch alkane chain, cyclo ring, phenyl ring, mono- and diesters have been prepared, characterized, homopolymerized and copolymerized with other unsaturated monomers. The preparation of monomer containing a pendant ethylene imine group was not successful because the amine tend to add across the vinyl double bond to give a cyclic product.

In this work three copolymers, poly(MHpI+DHpI), poly(MBI+DBI) and poly(MMI+DMI), with emphasis on the poly(MHpI+DHpI) system, were prepared by bulk copolymerization which proved to be easy, quick and to give satisfactory results. The conversion was kept below 15% to avoid composition drift. The copolymers were characterized by infrared spectroscopy and their composition was determined by two methods, titration of the acid group in non-aqueous media and microanalysis. A polymeranalogous reaction was used to prepare poly itaconate copolymers with pendant ethylene amine groups. Low concentrations of the copolymers were used and the acid groups in the monoesters were reacted with, ethylenediamine, diethylenetriamine, triethylenetetramine or tetraethylenepentamine in the presence of dicyclohexylcarbodiimide, which is a useful

reagent for peptide synthesis. Both amines and dicyclohexylcarbodiimide were used in excess. The modified polymers (polymeric ligands) which had ethylenediamine, diethylenetriamine, triethylenetetramine or tetraethylenepentamine in the side chain were characterised by infrared spectroscopy. The infrared spectra show two new absorptions, the first in the region $3200-3400\text{ cm}^{-1}$ due to the N-H stretch and the second in the region $1550-1635\text{ cm}^{-1}$, due to the N-H bending. Another method used to analyse the structure of the polymeric ligands was by complexation with metal halides to form polymer-metal complexes.

Two types of polymer-metal complexes have been prepared in this work. The first type includes polymer chelates of cobalt(II) chloride and copper(II) chloride and these were prepared in non-aqueous medium, because the polymeric ligands were not soluble in water. The second type includes pendant-type polymer-metal complexes and these were prepared by a substitution reaction of the weak ligand in a stable metal complex with a polymeric ligand. The reaction between the polymeric ligand which contains tetraethylenepentamine as ligand and copper(II) chloride or cobalt(II) chloride was followed by visible spectroscopy. Copper(II) chloride solution changes its colour from green to blue when it is reacted with the colourless polymeric ligand, whilst cobalt(II) chloride solution changes its colour from violet to red. This confirms a change in the substituent in the coordination sphere of the metal ion and

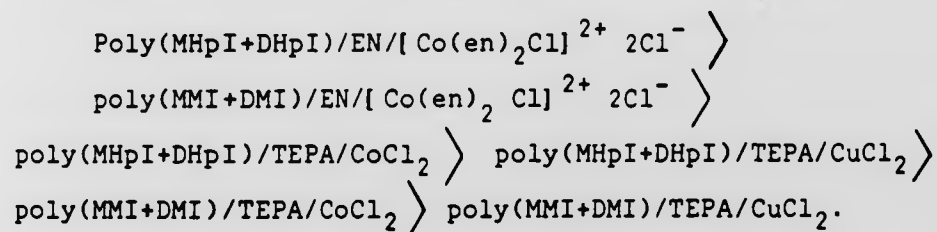
the formation of a metal complex with nitrogen donors. The chloride ion (Cl^-) can be either ionic chloride or coordinated chloride. The electron micrographs of the polymer-metal complexes show the metal ion clusters in the polymer matrix, and the size and number of these increases in proportion to the mole percentage of the metal ions.

The metal complex bound to the polymer backbone showed a specific type of catalytic behaviour. The catalytic activity of the polymeric ligands poly(MHpI+DHpI)/TEPA, poly(MHpI+DHpI)/EN, polymer chelates, poly(MHpI+DHpI)/TEPA/ CoCl_2 , poly(MHpI+DHpI)/TEPA/ CuCl_2 , poly(MMI+DMI)/TEPA/ CoCl_2 , poly(MMI+DMI)/TEPA/ CuCl_2 , and pendant-type polymer metal complexes poly(MMI+DMI)/EN/ $[\text{Co}(\text{en})_2\text{Cl}]^{2+} 2\text{Cl}^-$, poly(MHpI+DHpI)/EN/ $[\text{Co}(\text{en})_2\text{Cl}]^{2+} 2\text{Cl}^-$, on the decomposition of hydrogen peroxide at 313K was studied. The concentrations of the hydrogen peroxide and the metal ion were kept constant in order to compare the catalytic activity of these polymer-metal complexes. The residual hydrogen peroxide was determined by titrating aliquots of the reaction mixture with standardized potassium permanganate solution at intervals. This method was used because the experimental technique used to follow the reaction was easy and accurate. These polymer-metal complexes

are believed to show catalytic activity because:

- (a) They contain incomplete complexes due to the steric hindrance.
- (b) The coordination bond between the polymeric ligand and metal ion is relatively weak and this allows the substrate to coordinate.
- (c) There is an enhancement of the catalytic site.

Graphical and mathematical methods were used to determine and compare the catalytic activity of these polymer-metal complexes. It was found that the catalyst efficiencies were in the decreasing order of:



Again, it is thought that steric hindrance plays an important role. Catalysts prepared from poly(MHpI+DHpI) systems were more active than the corresponding poly(MMI+DMI) systems, suggesting that the longer ester side chain enhances the steric hindrance and so the catalytic activity.

Polymer-metal complexes which contain cobalt(II) or cobalt(III) ions had higher catalytic activity than those containing copper(II) ions. This is because the stability of the copper(II) complex in aqueous solution is stronger than that of the cobalt(II) or cobalt(III) complexes. The weaker the metal ion-nitrogen attraction the higher the

catalytic activity. It was difficult to suggest a mechanism for the decomposition of hydrogen peroxide in the presence of these polymer-metal complexes. The hydrogen peroxide in the initial step will form a transient intermediate and catalysis may proceed through chain decomposition or a free radical mechanism.

The thermal stability of the polymers prepared in this work was studied by both thermogravimetric analysis and thermal volatilization analysis techniques. It was found that the thermal stability of each parent polymer was decreased by increasing the mole percentage of the monoester. For the modified polymers, which contain pendant ethylene amine groups in the side chain, the thermal stability increases because of crosslinking. Thermal volatilization analysis confirms that the thermal degradation of these polymers was a random chain scission process. The thermal stability of the polymer-metal complexes was higher than that of the modified polymers (polymeric ligands). This is because there are coordinate bonds between the ligands in the polymer side chain and the metal ions.

The mechanical response of some modified polymers (polymeric ligands) and polymer-metal complexes was studied using a Rheovibron. It was found that when the mole percentage of the ligand (tetraethylenepentamine) in the side chain was less than 4.93, the rubbery region was increased, due to a light degree of crosslinking. When

catalytic activity. It was difficult to suggest a mechanism for the decomposition of hydrogen peroxide in the presence of these polymer-metal complexes. The hydrogen peroxide in the initial step will form a transient intermediate and catalysis may proceed through chain decomposition or a free radical mechanism.

The thermal stability of the polymers prepared in this work was studied by both thermogravimetric analysis and thermal volatilization analysis techniques. It was found that the thermal stability of each parent polymer was decreased by increasing the mole percentage of the monoester. For the modified polymers, which contain pendant ethylene amine groups in the side chain, the thermal stability increases because of crosslinking. Thermal volatilization analysis confirms that the thermal degradation of these polymers was a random chain scission process. The thermal stability of the polymer-metal complexes was higher than that of the modified polymers (polymeric ligands). This is because there are coordinate bonds between the ligands in the polymer side chain and the metal ions.

The mechanical response of some modified polymers (polymeric ligands) and polymer-metal complexes was studied using a Rheovibron. It was found that when the mole percentage of the ligand (tetraethylenepentamine) in the side chain was less than 4.93, the rubbery region was increased, due to a light degree of crosslinking. When

the mole percentage of the pendant ethylene amine group increases, the leathery region increases, due to a higher degree of crosslinking, but when the mole percentage becomes more than 14.0 the polymer becomes a glass-like material. The polymer-metal complexes with low degrees of crosslinking formed coloured films which showed an extended rubbery region. This is because crosslinks between the polymeric ligands and metal ions reduce the mobility and thus increase the modulus in the rubbery region. The torsional braid analysis of the modified polymers confirmed that the glass transition temperature was broad and shifted to a higher temperature, due to crosslinking. When the mole percentage of the pendant ethylene imine groups was more than 36.53, the glass transition temperature was difficult to detect. The differential scanning calorimeter study confirmed that the glass transition temperature was ill-defined and could not be detected, when the mole percentage of the pendant ethylene amine groups increased. An exothermic peak was observed at $\sim 400\text{K}$, due to a chemical reaction.

In conclusion the polymeranalogous reaction is a useful technique to prepare polymers which cannot be prepared from polymerization of a monomer. A polymeranalogous reaction can be used as a method to analyse the structure of the polymers. This was confirmed when the modified polymer (polymeric ligand) which contained tetraethylene-pentamine in the side chain reacted with a metal halide;

here, a polymer-metal complex was formed. These polymers, which contain pendant ethylene amine groups, are a very useful and attractive class of polymers. They could be used as supports for metal complexes and may catalyze different organic reactions. The preparation of high-temperature thermally stable polymers is another attractive feature of these polymers. The most attractive and useful application is as support for metal complexes. These polymer-metal complexes form heterogeneous catalysts in aqueous systems. The insolubility of these catalysts makes them easy to separate from the other components of the reaction mixture. This is a very attractive area in polymer science. Catalysts could be prepared for specific reactions, to reduce the cost of production of many materials. The mechanical response can be improved by introducing metal ions, and the rubbery region can be increased, making these materials useful for certain other applications.

In general, therefore, this study has shown that poly itaconate copolymers with pendant ethylene amine groups are a useful and interesting group of polymers, which can have many different applications.

here, a polymer-metal complex was formed. These polymers, which contain pendant ethylene amine groups, are a very useful and attractive class of polymers. They could be used as supports for metal complexes and may catalyze different organic reactions. The preparation of high-temperature thermally stable polymers is another attractive feature of these polymers. The most attractive and useful application is as support for metal complexes. These polymer-metal complexes form heterogeneous catalysts in aqueous systems. The insolubility of these catalysts makes them easy to separate from the other components of the reaction mixture. This is a very attractive area in polymer science. Catalysts could be prepared for specific reactions, to reduce the cost of production of many materials. The mechanical response can be improved by introducing metal ions, and the rubbery region can be increased, making these materials useful for certain other applications.

In general, therefore, this study has shown that poly itaconate copolymers with pendant ethylene amine groups are a useful and interesting group of polymers, which can have many different applications.

REFERENCES

1. Baup S, Ann.Chem., 19, 29 (1836).
2. Crasso G I, Ann.Chem., 34, 63 (1840).
3. Kinoshita K, J.Chem.Soc.Japan, 50, 583 (1929).
4. Smith G and Raistrick H, Biochem.J., 29, 606 (1935).
5. Calam C T, Oxford A E and Raistrick H, Biochem.J., 33, 1488 (1939).
6. Pfizer Chemicals, Pfizer Ltd, Kent, Production Information Sheet No 404.
7. Roberts E J, Ambler J A and Curl A L, US Pat. 2,488,831 (Sept. 7, 1948) (to the United States of America as represented by the Secy. of Agr.).
8. Swarts, F, Bull.Acad.Belg., 36, 69 (1973).
9. Messina G, De Pisapia N, Spano L, Maderno C and Condorelli E, U.S. Pat. 3,056,829 (1962).
10. Baker B R, Schaub R E and Williams J H, J.Org.Chem., 24, 116 (1952).
11. Vogel A I, "Practical Organic Chemistry", 3rd ed., Longmans Green & Co, London, 1956, page 381.
12. Marvel C S and Shepherd T H, J.Org.Chem., 24, 599 (1959).
13. Nagai S and Yoshida K, Kobunshi Kagaku, 17, 748 (1960).
14. Farbwerke Hoechst AG, British Pat. 1,102,273 (1968).
15. Yokota K, Hirabayashi T and Takashima T, Die Makromolek. Chem., 176, 1197 (1975).
16. Tate B E, Die Makromolek.Chem., 109, 176 (1967).
17. Nagai S, Polym.Lett., 7, 177 (1969).
18. Tate B E, in "Vinyl and Diene Monomers", ed. by Leonard E C, Wiley & Sons, London (1970) pp 205-261.

19. Stobbe H and Lippold A, J.Prakt.Chem., 90, 336 (1914).
20. Walden P, Z.Physik.Chem., 20, 382 (1869).
21. Knops C, Ann.Chem., 248, 175 (1888).
22. Nagai S and Yoshida K, Chem.High.Polym.Japan, 17, 82 (1960).
23. Tate B E, "The polymerization of itaconic acid and its esters", published by Pfizer Europe Chemicals, Kent, England.
24. Shinichi I and Shizuko S, J.Polym.Sci., Part A-1, 5, 689 (1967).
25. Velickovic J and Vasovic S, Die Makromolek.Chem., 153, 207 (1972).
26. Velickovic J, Filipovic J and Coseva S, Europ.Polym.J., 15, 521 (1979).
27. Cowie J M G and Haq Z, Brit.Polym.J., 9, 241 (1977).
28. Cowie J M G, Pure & Appl.Chem., 51, 2331 (1979).
29. Cowie J M G, Henshall S A E and McEwen I J, Polymer, 18, 612 (1977).
30. Cowie J M G, McEwen I J, Velickovic J and Haq Z, Polymer, 22, 327 (1981).
31. Cowie, J M G, McEwen I J and Haq Z, J.Polym.Sci., 17, 771 (1979).
32. Velickovic J and Plavsic M, Europ.Polym.J., 12, 151 (1976).
33. Cowie J M G and McEwen I J, Polymer, 16, 869 (1975).
34. Budevaska K, Bozhkova N and Panamski I, Angew Makromol. Chem., 28, 121 (1973).
35. Bekiturov Y A, Bimendina L A, Rogonov V V and Rafikov S R, Vysokmol Soyed., Part A14, No 2, 343 (1972).

36. Cowie J M G and Haq Z, *Europ.Polym.J.*, 13, 745 (1977).
37. Cowie J M G and Haq Z, *Brit.Polym.J.*, 9, 246 (1977).
38. Cowie J M G and Haq Z, *Polymer*, 19, 1052 (1978).
39. Akashi H, *Kogyo Kagaku Zasshi.*, 61, 1586 (1958).
40. Fettes E M, "Chemical Reaction of Polymers", Wiley and Sons New York (1964).
41. Duck F W, "Plastic and Rubbers", Butterworths, London (1971).
42. Rempp P, *Pure & Appl.Chem.*, 46, 9 (1976).
43. Cameron G G in "Reaction of Polymers: Polymer Modification", A specialist periodical report, *Macromolecular Chemistry*, Vol. 1, published by The Royal Society of Chemistry, London (1980).
44. Schulz R C and Aydin O, *J.Polym.Sci: Symposium No 50*, 497 (1975).
45. Flory P J, *J.Am.Chem.Soc.*, 61, 3334 (1939).
46. Sakurada I, *Kobunshi.*, 17, 207 (1968).
47. Odian G, "Principles of Polymerization", Chap. 9, Wiley & Sons, New York (1981).
48. Plate N A and Noah O V, *Adv.Polym.Sci.*, 31, 133 (1979).
49. Plate N E, *Pure & Appl.Chem.*, 46, 49 (1976).
50. Vogl O, *Pure & Appl.Chem.*, 51, 2409 (1979).
51. Geckeler K, Lange G, Eberhardt H and Bayer E, *Pure & Appl.Chem.*, 52, 1883 (1980).
52. Tazuke S and Okamura S, *J.Polym.Sci.*, A1, 4, 2461 (1966).
53. Hatano M, Nozawa T, Yamamoto T and Kambara S, *Die Makromolek.Chem.*, 115, 10 (1968).

54. Tsuchida E and Nishide H, Adv.Polym.Sci., 24, 1 (1977).
55. Teyssie P H, Decoere C and Teyssie M T, Makromol.Chem., 84, 51 (1965).
56. Kurimura Y, Tsuchida E and Kaneko M, J.Polym.Sci., Part 1A, 9, 3511 (1971).
57. Tsuchida E and Nishide H, in "Polymeric Amines and Ammonium Salts", Page 271, ed. by Goethals E J, (I.U.P.A.), Pergamon Press (1980).
58. Kurimura Y, Sekine I, Tsuchida E and Karinc Y, Bull.Chem.Soc.Japan, 47, 1823 (1974).
59. Nose Y, Hatano M and Kambara S, Die Makromolek.Chem., 98, 136 (1966).
60. Meinders H G and Challa G, in "Polymeric Amines and Ammonium Salts", page 255, ed. by Goethals E J (I.U.P.A.) Pergamon Press (1980).
61. Aklonis J J, MacKnight W J and Shen M, "Introduction to Polymer Viscoelasticity", Wiley & Sone, London (1972).
62. Cowie J M G, "Polymer Chemistry and Physics of Modern Materials", Wiley & Sons, London (1973).
63. Conley R T, "Thermal Stability of Polymers", Vol. 1, Marcel Dekker Inc., New York (1970).
64. McCaffery E M, "Laboratory Preparation for Macromolecular Chemistry", McGraw-Hill, London (1970).
65. Rodriguez F, "Principles of Polymer Systems", McGraw-Hill New York(1970).
66. Fieser L F and Fieser M, "Reagents for Organic Synthesis", Wiley & Sons, London (1967).

67. Rose J, "Advance Physico-Chemical Experiments", Pitman & Sons, London (1964).
68. Rabek J F, "Experimental Methods in Polymer Chemistry", Wiley & Sons, New York (1980).
69. Elias H G, "Macromolecules. 1 Structure and Properties", Wiley & Sons, London (1977).
70. Watson E S, O'Neill M J, Justin J and Brenner N, Anal.Chem., 36, 1233 (1964).
71. O'Neill M J, Anal.Chem., 36, 1238 (1964).
72. Wunderlich B, "Physical Method of Chemistry", Vol 1, Chap. VIII, of a Weissberger ed. Technique of Chemistry Part 5, Wiley & Sons, New York (1971).
73. Muragama T, "Dynamic Mechanical Analysis of Polymeric Material", Elsevier Scientific Publishing Co. (1978).
74. Collins E A, Bares J and Bellmeyer J R, "Experiments in Polymer Science", Wiley & Sons, U.S.A. (1973).
75. Rheovibron, "Direct Reading Dynamic Viscoelastometer Model DDV-II-C", Instruction Manual No 68 (1973).
76. Gillham J K, AIChE.J, No 6, 20, 1066 (1974).
77. Slade P E and Jenkins L T "Thermal Characterization Techniques", Marcel Dekker Inc., New York (1970).
78. Henshall S A E, PhD Thesis (1974). Dept. of Chemistry, University of Stirling.
79. Weast R C and Selby, S M "Handbook of Chemistry and Physics", 48th ed. The Chemical Rubber Co. (1967).
80. Honda K, Sci.Rept., Tohoku Uni., 4, 97 (1915).
81. McNeill I C, Europ.Polym.J., 6, 373 (1970).
82. McNeill I C, Ackerman L, Gupta S N, Zulfiqar M and Zulfiqar S, J.Polym.Sci., 15, 2381 (1977).

83. Grassie N, Johnston A and Scotney A, *Europ.Polym.J.*, 17, 589 (1981).
84. Hilgetag G and Martini A, "Preparative Organic Chemistry", Wiley & Sons, New Yor, (1972).
85. Haq Z, PhD Thesis (1976). Department of Chemistry, University of Stirling.
86. Klesper E, Strasilla D and Berg M C, *Europ.Polym.J.*, 15, 587 (1979).
87. Klesper E, Strasilla D and Berg M C, *Europ.Polym.J.*, 15, 593 (1979).
88. Solomos T W G, "Organic Chemistry", Wiley & Sons, London (1976).
89. Kurzer F and Douraghi-Zaheh K, *Chemical Reviews*, No 2, 67, 107 (1967).
90. Pavia D L, Lampman G M and Kriz G S, "Introduction to Spectroscopy", W B Saunders Co, London (1979).
91. Elliott A, "Infrared Spectra and Structure of Organic Long-Chain Polymers", Edward Arnold Ltd, London (1969).
92. Snow M R, Buckingham D A, Marzilli P A and Sargeson A M, *J.Chem.Soc., Chem.Comm.*, 891 (1969).
93. Antonelli M L, Bucci R I, Carunchio V and Enrico C, *Polym. Lett.*, 18, 179 (1980).
94. Basolo F and Johnson R C, "Coordination Chemistry", W A Benjamin, Inc., California (1964).
95. Tsuchida E, Nishide H and Takeshita M, *Die Makromolek. Chem.*, 175, 2293 (1974).
96. Bedetti R, Carunchio V and Cernia E, *Polym.Lett.*, 13, 329 (1975).
97. Vogel's "Textbook of Quantitative Inorganic Analysis", Longman, London (1978).

98. Pineri M, Meyer C and Bourret A, J.Polym.Sci., A-2 13, 1881 (1972).
99. Bertalan V, Z.Physik.Chem., 95, 328 (1920).
100. Bohanson V L and Robertson A C, J.Am.Chem.Soc., 45, 2493 (1923).
101. Haber F and Weiss J, Proc.Roy.Soc. London, A147, 332 (1934).
102. Huheey J E, "Inorganic Chemistry", Harper & Row, London (1975).
103. Sasaki T and Matsunaga F, Bull.Chem.Soc.Japan, 41, 2440 (1968).
104. Ashmore P G, "Catalysis and Inhibition of Chemical Reactions", Butterworths, London (1963).
105. Barrow G M, "Physical Chemistry". McGraw-Hill, London (1973).
106. Stevens B, "Chemical Kinetics", Chapman and Hall Ltd., U.S.A. (1970).
107. Hoff E A W, Robinson D W and Willbourn A H, J.Polym.Sci., 18, 161 (1955).
108. Ward I M, "Mechanical Properties of Solid Polymers", Wiley & Sons, New York (1979).
109. Deanin R D, "Polymer Structure, Properties and Applications", Cahners Publishing Co. U.S.A. (1972).
110. Grassie N, McNeill I C and Samson J N R, Europ.Polym.J. 14, 931 (1978).

A P P E N D I X

Decomposition of hydrogen peroxide in the presence of
CoCl₂ solution.

Time hr	KMnO ₄ ml	Residual H ₂ O ₂ %	Log(a-x)	Cal.
0.00	8.08	100.00	0.9074	0.9060
1.00	8.04	99.50	0.9052	0.9044
2.00	7.98	98.76	0.9020	0.9029
3.00	7.94	98.26	0.8998	0.9013
4.00	7.92	98.01	0.8987	0.8998
5.00	7.92	98.01	0.8987	0.8982
6.00	7.88	97.52	0.8965	0.8966
7.00	7.86	97.27	0.8954	0.8951
8.00	7.84	97.02	0.8943	0.8935
9.00	7.80	96.53	0.8920	0.8920

Decomposition of hydrogen peroxide in the presence of
CuCl₂ solution.

Time hr	KMnO ₄ ml	Residual H ₂ O ₂ %	Log(a-x)	Cal.
0.00	8.08	100.00	0.9074	0.9056
1.00	8.04	99.50	0.9052	0.9046
2.00	8.00	99.00	0.9030	0.9035
3.00	7.96	98.51	0.9009	0.9024
4.00	7.94	98.26	0.8998	0.9013
5.00	7.94	98.26	0.8998	0.9002
6.00	7.92	98.01	0.8987	0.8991
7.00	7.92	98.01	0.8987	0.8980
8.00	7.90	97.77	0.8976	0.8969
9.00	7.88	97.52	0.8965	0.8958

Decomposition of hydrogen peroxide in the presence of
trans[Co(en)₂Cl₂]Cl.

Time hr	KMnO ₄ ml	Residual H ₂ O ₂ %	Log(a-x)	Cal.
0.00	8.06	100.00	0.9063	0.8986
1.00	7.86	97.51	0.8954	0.8923
2.00	7.66	95.03	0.8842	0.8860
3.00	7.52	93.30	0.8762	0.8796
4.00	7.34	91.06	0.8656	0.8733
5.00	7.30	90.57	0.8633	0.8670
6.00	7.22	89.57	0.8585	0.8607
7.00	7.12	88.33	0.8524	0.8544
8.00	7.10	88.08	0.8512	0.8481
9.00	7.06	87.59	0.8488	0.8418

Decomposition of hydrogen peroxide in the presence of
 poly(MHpI+DHpI)/TEPA.

Time hr	KMnO ₄ ml	Residual H ₂ O ₂ %	Log(a-x)	Cal.
0.00	8.06	100.00	0.9063	0.9067
1.00	8.06	100.00	0.9063	0.9063
2.00	8.05	99.87	0.9057	0.9059
3.00	8.05	99.87	0.9057	0.9054
4.00	8.04	99.75	0.9052	0.9050
5.00	8.04	99.75	0.9052	0.9046
6.00	8.02	99.50	0.9041	0.9042
7.00	8.01	99.37	0.9036	0.9038
8.00	8.00	99.25	0.9030	0.9034
9.00	8.00	99.25	0.9030	0.9030

Decomposition of hydrogen peroxide in the presence of
poly(MHpI+DHpI)/EN.

Time hr	KMnO ₄ ml	Residual H ₂ O ₂ %	Log(a-x)	Cal.
0.00	8.06	100.00	0.9063	0.9067
1.00	8.06	100.00	0.9063	0.9063
2.00	8.05	99.87	0.9057	0.9059
3.00	8.05	99.87	0.9057	0.9054
4.00	8.04	99.75	0.9052	0.9050
5.00	8.04	99.75	0.9052	0.9046
6.00	8.02	99.50	0.9041	0.9042
7.00	8.01	99.37	0.9036	0.9038
8.00	8.00	99.25	0.9030	0.9034
9.00	8.00	99.25	0.9030	0.9030

Decomposition of hydrogen peroxide alone.

Time hr	KMnO ₄ ml	Residual H ₂ O ₂ %	Log(a-x)	Cal.
0.00	8.06	100.00	0.9063	0.9067
1.00	8.06	100.00	0.9063	0.9063
2.00	8.05	99.87	0.9057	0.9059
3.00	8.05	99.87	0.9057	0.9054
4.00	8.04	99.75	0.9052	0.9050
5.00	8.04	99.75	0.9052	0.9046
6.00	8.02	99.50	0.9041	0.9042
7.00	8.01	99.37	0.9036	0.9038
8.00	8.00	99.25	0.9030	0.9034
9.00	8.00	99.25	0.9030	0.9030

Decomposition of hydrogen peroxide in the presence of poly(MMI+DMI)/TEPA/CoCl₂.

Time hr	KMnO ₄ ml	Residual % H ₂ O ₂	Log(a-x)	Cal.
0.00	8.08	100.00	0.9074	0.9053
1.00	8.00	99.00	0.9030	0.9024
2.00	7.92	98.01	0.8987	0.8995
3.00	7.88	97.52	0.8965	0.8966
4.00	7.80	96.53	0.8920	0.8937
5.00	7.76	96.03	0.8898	0.8908
6.00	7.70	95.29	0.8864	0.8879
7.00	7.68	95.04	0.8853	0.8850
8.00	7.64	94.55	0.8830	0.8821
9.00	7.60	94.05	0.8808	0.8792

Decomposition of hydrogen peroxide in the presence of poly(MMI+DMI)/TEPA/CuCl₂.

Time hr	KMnO ₄ ml	Residual % H ₂ O ₂	Log(a-x)	Cal.
0.00	8.08	100.00	0.9074	0.9062
1.00	8.04	99.50	0.9052	0.9036
2.00	7.96	98.51	0.9009	0.9011
3.00	7.90	97.77	0.8976	0.8985
4.00	7.86	97.27	0.8954	0.8959
5.00	7.78	96.28	0.8909	0.8934
6.00	7.76	96.03	0.8898	0.8908
7.00	7.72	95.54	0.8876	0.8882
8.00	7.70	95.29	0.8864	0.8856
9.00	7.68	95.04	0.8853	0.8831

Decomposition of hydrogen peroxide in the presence of poly(MMI+DMI)/TEPA/CoCl₂.

Time hr	KMnO ₄ ml	Residual H ₂ O ₂ %	Log(a-x)	Cal.
0.00	8.08	100.00	0.9074	0.9053
1.00	8.00	99.00	0.9030	0.9024
2.00	7.92	98.01	0.8987	0.8995
3.00	7.88	97.52	0.8965	0.8966
4.00	7.80	96.53	0.8920	0.8937
5.00	7.76	96.03	0.8898	0.8908
6.00	7.70	95.29	0.8864	0.8879
7.00	7.68	95.04	0.8853	0.8850
8.00	7.64	94.55	0.8830	0.8821
9.00	7.60	94.05	0.8808	0.8792

Decomposition of hydrogen peroxide in the presence of poly(MMI+DMI)/TEPA/CuCl₂.

Time hr	KMnO ₄ ml	Residual H ₂ O ₂ %	Log(a-x)	Cal.
0.00	8.08	100.00	0.9074	0.9062
1.00	8.04	99.50	0.9052	0.9036
2.00	7.96	98.51	0.9009	0.9011
3.00	7.90	97.77	0.8976	0.8985
4.00	7.86	97.27	0.8954	0.8959
5.00	7.78	96.28	0.8909	0.8934
6.00	7.76	96.03	0.8898	0.8908
7.00	7.72	95.54	0.8876	0.8882
8.00	7.70	95.29	0.8864	0.8856
9.00	7.68	95.04	0.8853	0.8831

Decomposition of hydrogen peroxide in the presence of
poly(MHpI+DHpI)/TEPA/CoCl₂.

Time hr	KMnO ₄ ml	Residual H ₂ O ₂ %	Log(a-x)	Cal.
0.00	8.08	100.00	0.9074	0.9034
1.00	7.92	98.1	0.8987	0.8995
2.00	7.88	97.52	0.8865	0.8957
3.00	7.76	96.03	0.8898	0.8918
4.00	7.68	95.04	0.8853	0.8880
5.00	7.64	94.55	0.8830	0.8841
6.00	7.56	93.56	0.8785	0.8803
7.00	7.52	93.06	0.8762	0.8765
8.00	7.48	92.57	0.8739	0.8726
9.00	7.44	92.07	0.8715	0.8688

Decomposition of hydrogen peroxide in the presence of
poly(MHpI+DHpI)/TEPA/CuCl₂.

Time hr	KMnO ₄ ml	Residual H ₂ O ₂ %	Log(a-x)	Cal.
0.00	8.08	100.00	0.9074	0.9041
1.00	8.02	99.25	0.9041	0.9005
2.00	7.86	97.27	0.8954	0.8969
3.00	7.78	96.28	0.8909	0.8934
4.00	7.72	95.54	0.8876	0.8898
5.00	7.62	94.30	0.8819	0.8862
6.00	7.60	94.05	0.8808	0.8826
7.00	7.56	93.56	0.8785	0.8755
8.00	7.54	93.31	0.8773	0.8755
9.00	7.52	93.06	0.8762	0.8719

Decomposition of hydrogen peroxide in the presence of
poly(MMI+DMI)/EN/[Co(en)₂Cl]²⁺ 2Cl⁻.

Time hr	KMnO ₄ ml	Residual % H ₂ O ₂	Log(a-x)	Cal.
0.00	8.06	100.00	0.9063	0.8972
1.00	7.78	96.52	0.8909	0.8892
2.00	7.58	93.30	0.8796	0.8812
3.00	7.40	91.81	0.8692	0.8732
4.00	7.24	89.82	0.8597	0.8651
5.00	7.10	88.08	0.8512	0.8571
6.00	7.00	86.84	0.8450	0.8491
7.00	6.94	86.10	0.8413	0.8411
8.00	6.85	84.98	0.8356	0.8331
9.00	6.80	84.36	0.8325	0.8250

Decomposition of hydrogen peroxide in the presence of
poly(MHpI+DHpI)/EN/[Co(en)₂Cl]²⁺ 2Cl⁻.

Time hr	KMnO ₄ ml	Residual % H ₂ O ₂	Log(a-x)	Cal.
0.00	8.06	100.00	0.9063	0.9007
1.00	7.82	97.02	0.8920	0.8899
2.00	7.58	94.04	0.8796	0.8790
3.00	7.32	90.81	0.8645	0.8682
4.00	7.14	88.58	0.8536	0.8574
5.00	6.92	85.85	0.8401	0.8466
6.00	6.80	84.36	0.8325	0.8358
7.00	6.64	82.38	0.8221	0.8250
8.00	6.56	81.38	0.8169	0.8142
9.00	6.48	80.39	0.8115	0.8034

Decomposition of hydrogen peroxide in the presence of
poly(MMI+DMI)/EN/[Co(en)₂Cl]²⁺ 2Cl⁻.

Time hr	KMnO ₄ ml	Residual H ₂ O ₂ %	Log(a-x)	Cal.
0.00	8.06	100.00	0.9063	0.8972
1.00	7.78	96.52	0.8909	0.8892
2.00	7.58	93.30	0.8796	0.8812
3.00	7.40	91.81	0.8692	0.8732
4.00	7.24	89.82	0.8597	0.8651
5.00	7.10	88.08	0.8512	0.8571
6.00	7.00	86.84	0.8450	0.8491
7.00	6.94	86.10	0.8413	0.8411
8.00	6.85	84.98	0.8356	0.8331
9.00	6.80	84.36	0.8325	0.8250

Decomposition of hydrogen peroxide in the presence of
poly(MHpI+DHpI)/EN/[Co(en)₂Cl]²⁺ 2Cl⁻.

Time hr	KMnO ₄ ml	Residual H ₂ O ₂ %	Log(a-x)	Cal.
0.00	8.06	100.00	0.9063	0.9007
1.00	7.82	97.02	0.8920	0.8899
2.00	7.58	94.04	0.8796	0.8790
3.00	7.32	90.81	0.8645	0.8682
4.00	7.14	88.58	0.8536	0.8574
5.00	6.92	85.85	0.8401	0.8466
6.00	6.80	84.36	0.8325	0.8358
7.00	6.64	82.38	0.8221	0.8250
8.00	6.56	81.38	0.8169	0.8142
9.00	6.48	80.39	0.8115	0.8034

Attention is drawn to the fact that the copyright of this thesis rests with its author.

This copy of the thesis has been supplied on condition that anyone who consults it is understood to recognise that its copyright rests with its author and that no quotation from the thesis and no information derived from it may be published without the author's prior written consent.

II